

## STATUS OF THESIS

Title of thesis

INTELLIGENT OPTIMIZATION OF INTERLINE POWER  
FLOW CONTROLLER IN TRANSMISSION SYSTEM

I KHALID HAROUN MOHAMED ABDELGADIR

hereby allow my thesis to be placed at the Information Resource Center (IRC) of  
University Teknologi PETRONAS (UTP) with the following conditions:

1. The thesis becomes the property of UTP
2. The IRC of UTP may make copies of the thesis for academic purposes only.
3. This thesis is classified as

☐

Confidential

☒

Non-confidential

If this thesis is confidential, please state the reason:

---

---

---

The content of the thesis will remain confidential for \_\_\_\_ years.

Remarks on disclosure:

---

---

---

Endorsed by

\_\_\_\_\_  
Signature of Author

Permanent address:

El-Azhari Block No. 11/528\_

Khartoum / Sudan

Date: \_\_\_\_\_

\_\_\_\_\_  
Signature of Supervisor

Assoc.Prof. Dr. K. S. Rama Rao

Electrical and Electronic Department

Universiti Teknologi PETRONAS

Tronoh, Bandar Seriskandar, Perak

Date: \_\_\_\_\_

UNIVERSITI TEKNOLOGI PETRONAS

INTELLIGENT OPTIMIZATION OF INTERLINE POWER FLOW CONTROLLER  
IN TRANSMISSION SYSTEM

by

KHALID HAROUN MOHAMED ABDELGADIR

The undersigned certify that they have read, and recommend to the Postgraduate Studies Programme for acceptance this thesis for the fulfilment of the requirements for the degree stated.

Signature:

\_\_\_\_\_

Main Supervisor:

Assoc.Prof. Dr. K. S. Rama Rao

Signature:

\_\_\_\_\_

Head of Department:

Dr. Nor Hisham Bn Hamid

Date:

\_\_\_\_\_

INTELLIGENT OPTIMIZATION OF INTERLINE POWER FLOW CONTROLLER  
IN TRANSMISSION SYSTEM

by

KHALID HAROUN MOHAMED ABDELGADIR

A Thesis

Submitted to the Postgraduate Studies Programme

as a Requirement for the Degree of

MASTER OF SCIENCE

DEPARTMENT OF ELECTRICAL AND ELECTRONIC ENGINEERING

UNIVERSITI TEKNOLOGI PETRONAS

BANDAR SERI ISKANDAR,

PERAK

AUGUST 2010

## DECLARATION OF THESIS

Title of thesis

|   |
|---|
| INTELLIGENT OPTIMIZATION OF INTERLINE POWER<br>FLOW CONTROLLER IN TRANSMISSION SYSTEM |
|---|

I KHALID HAROUN MOHAMED ABDELGADIR

hereby declare that the thesis is based on my original work except for quotations and citations which have been duly acknowledged. I also declare that it has not been previously or concurrently submitted for any other degree at UTP or other institutions.

Witnessed by

\_\_\_\_\_  
Signature of Author

\_\_\_\_\_  
Signature of Supervisor

Permanent address:

El-Azhari Block No. 11/528

Khartoum / Sudan

Date: \_\_\_\_\_

Assoc.Prof. Dr. K. S. Rama Rao

Electrical and Electronic Department

Universiti Teknologi PETRONAS

Tronoh, Bandar Seriskandar, Perak

Date: \_\_\_\_\_

*To my family*

## ACKNOWLEDGEMENTS

First and foremost, I would like to thank God the Almighty, for without His consent, it would be impossible to achieve what has been done in this work , for giving me the strength and persistence to keep going without losing hope in scientific research even during the most difficult moments. May Allah accept this work, count it as a good deed and make it useful. And I would like to thank my parents and all of my family, relative members for their love and support from a distance, to go on with this work.

I would like to express my total appreciation and gratitude to my supervisor Associate Professor, Dr. K. S. Rama Rao for his invaluable time and guidance throughout this work.

I express my sincere appreciation to my co-supervisor Ms. Khairul Nisak Bt Md. Hasan, for her understanding and support.

I wish to express my thanks to the Head and members of the Electrical and Electronic Engineering Department for their support. I also extend my appreciation to the members of the Postgraduate Studies Office for their invaluable help.

Last but not least, my special thanks are given to my colleagues and friends, who supported and comforted me through the good and bad times, and for giving me a lot of unforgettable moments.

## ABSTRACT

Flexible AC Transmission system (FACTS) controllers are widely accepted worldwide to provide benefits in increasing power transfer capability and maximizing the use of the existing transmission networks. A new generation of FACTS controllers, particularly the Interline Power Flow Controller (IPFC) based on voltage source converter (VSC) provides fast power flow control flexibility. The IPFC with its unique capability of power flow management is significantly extended to control power flows of multi-lines or a sub network. Generally IPFC employs two or more VSCs connected together with DC links and each converter provides series compensation for the selected line of the transmission system. Optimal power flow is an important factor in power system operation, planning and control. In this thesis, the mathematical model of IPFC together with the modified Newton-Raphson method for power flow is used to derive the optimal parameters (the magnitude and voltage angles) of VSCs of IPFC. The optimal parameters are derived to minimize the transmission line losses using three intelligent optimization techniques, namely Particle Swarm Optimization (PSO), Genetic Algorithm (GA) and Simulated Annealing (SA). The proposed methods are applied using MATLAB 7.6 and tested on IEEE 14-bus and 30-bus bench mark power systems. The optimal parameters of IPFC, the voltage profile and the transmission line losses of the bench mark power systems are derived from the simulations. The simulation results obtained with PSO technique are compared with those obtained by other two optimization techniques. The thesis also covers the basic principles and operation of IPFC, the modified Newton-Raphson power flow method and an overview of the three intelligent optimization techniques used in this thesis. The results prove the efficacy of the three intelligent methods for the optimization of IPFC parameters and minimization of transmission line losses.

## ABSTRAK

Flexible AC Transmission System (FACTS) diterima di seluruh dunia secara meluas kerana memberikan manfaat kepada peningkatan kemampuan pemindahan kuasa dan memaksimumkan penggunaan rangkaian transmisi yang sedia ada. Sebuah generasi baru kawalan FACTS, khususnya Interline Power Flow Controller (IPFC) berdasarkan Voltage Source Converter (VSC) memberikan fleksibiliti kawalan aliran kuasa elektrik yang cepat. IPFC dengan kemampuan unik dalam pengurusan aliran kuasa elektrik secara signifikan diperluas untuk mengawal aliran kuasa pelbagai talian atau sub rangkaian. Umumnya, IPFC terdiri daripada dua atau lebih VSC disambungkan bersama-sama dengan pautan konverter DC dan setiap konverter menyediakan penggantian siri untuk talian yang dipilih daripada sistem transmisi. Aliran kuasa yang optimum merupakan faktor penting dalam operasi sistem tenaga, perancangan dan kawalan. Dalam tesis ini, model matematik dari IPFC dan kaedah Newton-Raphson yang telah diubahsuai diselidik untuk menguraikan parameter optimum untuk VSC di dalam IPFC. Parameter optimum dikeluarkan untuk mengurangkan kerugian saluran transmisi menggunakan tiga teknik optimasi yang cerdas, iaitu, Particle Swarm Optimization (PSO), Algoritma Genetik (GA) dan Simulated Annealing (SA). Kaedah yang dicadangkan dilaksanakan menggunakan MATLAB 7.6 dan diuji pada sistem tanda aras IEEE 14-bus and 30-bus. Parameter optimum IPFC, profil voltan dan kerugian untuk tanda aras saluran transmisi daripada sistem kuasa diperolehi daripada simulasi. Keputusan simulasi yang diperolehi daripada teknik PSO dibandingkan dengan yang diperolehi oleh dua teknik optimasi yang lain. Tesis ini juga merangkumi prinsip-prinsip asas dan operasi IPFC, kaedah aliran kuasa Newton Raphson yang telah diubahsuai dan gambaran kasar untuk tiga teknik optimasi cerdas yang digunakan dalam tesis ini. Keputusan membuktikan keberkesanan tiga kaedah cerdas untuk pengoptimuman parameter IPFC dan meminimumkan kerugian transmisi kuasa.



In compliance with the terms of the Copyright Act 1987 and the IP Policy of the university, the copyright of this thesis has been reassigned by the author to the legal entity of the university,

Institute of Technology PETRONAS Sdn Bhd.

Due acknowledgement shall always be made of the use of any material contained in, or derived from, this thesis.

© Khalid Haroun Mohamed Abdelgadir, 2010

Institute of Technology PETRONAS Sdn Bhd

All rights reserved.

## TABLE OF CONTENTS

|                        |      |
|------------------------|------|
| Status of Thesis.....  | i    |
| Approval Page.....     | ii   |
| Title of Thesis.....   | iii  |
| Declaration .....      | iv   |
| Dedication.....        | v    |
| Acknowledgments.....   | vi   |
| Abstract.....          | vii  |
| Abstrak.....           | viii |
| Copyright Page.....    | ix   |
| Table of Contents..... | x    |
| List of Tables.....    | xiv  |
| List of Figures.....   | xv   |
| Nomenclature.....      | xix  |
| Abbreviations.....     | xxii |

|                                       |          |
|---------------------------------------|----------|
| <b>CHAPTER 1 INTRODUCTION.....</b>    | <b>1</b> |
| 1.1 Background .....                  | 1        |
| 1.1.1 Optimal Power Flow Problem..... | 2        |
| 1.1.2 Objective Function .....        | 3        |
| 1.2 Problem Statement.....            | 5        |
| 1.3 Objectives of Thesis .....        | 6        |
| 1.4 Scope of Study.....               | 7        |
| 1.5 Organization of Thesis.....       | 7        |

|  |          |
|--|----------|
| <b>CHAPTER 2 LITERTURE REVIEW AND POWER FLOW STUDIES<br/>USING IPFC.....</b> | <b>9</b> |
| 2.1 Introduction .....   | 9        |
| 2.2 Flexible AC Transmission Systems (FACTS) Controllers .....               | 9        |

|  |           |
|--|-----------|
| 2.3 Types of FACTS Controllers .....                               | 11        |
| 2.3.1 Thyristor-Based FACTS Controllers .....                      | 12        |
| 2.3.1.1 Static Var Compensator (SVC) .....                         | 12        |
| 2.3.1.2 Thyristor Controlled Series Capacitor (TCSC) .....         | 13        |
| 2.3.1.3 Thyristor Controlled Series Reactor (TCSR) .....           | 14        |
| 2.3.1.4 Thyristor Switched Series Capacitor (TSSC) .....           | 15        |
| 2.3.2 Voltage Source Converter-Based FACTS Controllers .....       | 15        |
| 2.3.2.1 Mathematical Model of Voltage Source Converter (VSC) ..... | 16        |
| 2.3.2.2 Static Synchronous Compensator (SSC) or STATCOM .....      | 20        |
| 2.3.2.3 Static Synchronous Series Compensator (SSSC) or S3C .....  | 21        |
| 2.3.2.4 Interphase Power Controller (IPC) .....                    | 21        |
| 2.3.2.5 Unified Power Flow Controller (UPFC) .....                 | 22        |
| 2.3.2.6 Interline Power Flow Controller (IPFC) .....               | 24        |
| 2.4 FACTS Controllers and Their Potential .....                    | 25        |
| 2.5 Power Flow Representation in a Power System .....              | 27        |
| 2.5.1 Power Flow Representation with IPFC .....                    | 28        |
| 2.5.2 General Power Flow Expressions with IPFC .....               | 32        |
| 2.5.3 Operating Modes of IPFC .....                                | 33        |
| 2.5.4 Transmission Line Loss .....                                 | 34        |
| 2.6 Modified Newton Raphson Power Flow Algorithm .....             | 35        |
| 2.7 Summary .....  | 36        |
| <br><b>CHAPTER 3 RESEARCH METHODOLOGY .....</b>                    | <b>37</b> |
| 3.1 Introduction .....   | 37        |
| 3.2 Particle Swarm Optimization (PSO) Technique .....              | 38        |
| 3.2.1 Element of the Particle Swarm Optimization .....             | 41        |
| 3.2.1.1 Swarm Size .....   | 41        |
| 3.2.1.2 Velocity of the Particle .....                             | 41        |
| 3.2.1.3 Particle's Position .....                                  | 41        |
| 3.2.1.4 Inertia Weight Approach PSO (IWAPSO) .....                 | 42        |
| 3.2.1.5 Weighting Factors C1 and C2 .....                          | 43        |
| 3.2.1.6 Best Particle's Position .....                             | 43        |
| 3.2.1.7 Global Best Position .....                                 | 43        |

|  |           |
|--|-----------|
| 3.2.1.8 Stopping Criteria .....  | 43        |
| 3.2.2 Parameter Selection for Particle Swarm Optimization.....                 | 43        |
| 3.2.3 Variants of PSO.....   | 44        |
| 3.2.3.1 Constriction Factor Approach Particle Swarm Optimization (CFAPSO)..... | 45        |
| 3.2.4 The Proposed PSO for Optimal Parameters of the VSCs of IPFC .....        | 46        |
| 3.2.5 Advantages of Particle Swarm Optimization.....                           | 48        |
| 3.2.6 Applications of PSO to Power System.....                                 | 48        |
| 3.3 Genetic Algorithm (GA) Technique.....                                      | 49        |
| 3.3.1 Genetic Algorithm Operators.....   | 51        |
| 3.3.2 Selection Process .....  | 51        |
| 3.3.2.1 Mate Selection .....   | 51        |
| 3.3.2.2 Roulette Wheel Selection .....   | 51        |
| 3.3.2.3 Tournament Selection .....   | 52        |
| 3.3.3 Crossover .....  | 53        |
| 3.3.4 Mutation.....  | 54        |
| 3.3.5 Termination Criteria .....   | 54        |
| 3.3.6 Implementation of GA Technique for Optimal Parameters of IPFC .....      | 55        |
| 3.3.7 Comparison Between GA and Traditional Search Algorithms.....             | 57        |
| 3.4 Simulated Annealing (SA) Technique.....                                    | 57        |
| 3.4.1 Simulated Annealing Physical Concepts .....                              | 58        |
| 3.4.2 SA Techniques Factors.....   | 59        |
| 3.4.2.1 Initialization.....  | 59        |
| 3.4.2.2 Markov Length.....   | 59        |
| 3.4.2.3 Step Size .....  | 59        |
| 3.4.2.4 Termination Criterion.....   | 59        |
| 3.4.3 An implementation of SA Technique for Optimal Parameters of IPFC .....   | 60        |
| 3.5 Global Optimization Toolbox in MATLAB .....                                | 62        |
| 3.5.1 GA Solver .....  | 62        |
| 3.5.2 SA Solver .....  | 66        |
| 3.6 Summary .....  | 68        |
| <br><b>CHAPTER 4 RESULTS OF SIMULATION AND DISCUSSION.....</b>                 | <b>69</b> |
| 4.1 Introduction .....   | 69        |

|   |            |
|---|------------|
| 4.2 Case 1 Standard IEEE 14-bus power system .....  | 69         |
| 4.2.1 Power Flow Analysis of IEEE 14-bus Power System without IPFC .....                                  | 70         |
| 4.2.2 Power Flow Analysis of IEEE 14-bus Power System with IPFC .....                                     | 71         |
| 4.2.3 Power Flow Analysis of IEEE 14-bus Power System with IPFC and using<br>PSO73                        |            |
| 4.2.4 Power Flow Analysis of IEEE 14-bus Power System with IPFC using GA 79                               |            |
| 4.2.5 Power Flow Analysis of IEEE 14-bus Power System with IPFC using SA 85                               |            |
| 4.2.6 Comparison of Simulation Results with PSO, GA and SA Techniques of<br>IEEE 14-bus Power System..... | 91         |
| 4.3 Case 2 Standard IEEE 30-bus Power System .....  | 94         |
| 4.3.1 Power Flow Analysis of IEEE 30-bus Power System without IPFC .....                                  | 94         |
| 4.3.2 Power Flow Analysis of IEEE 30-bus Power System with IPFC .....                                     | 95         |
| 4.3.3 Power Flow Analysis of IEEE 30-bus Power System with IPFC and using<br>PSO.....                     | 97         |
| 4.3.4 Power Flow Analysis of IEEE 30-bus Power System with IPFC using GA100                               |            |
| 4.3.5 Power Flow Analysis of IEEE 30-bus Power System with IPFC using SA106                               |            |
| 4.3.6 Comparison of Simulation Results with PSO, GA and SA Techniques of<br>IEEE 30-bus Power System..... | 112        |
| 4.4 Summary .....   | 115        |
| <br><b>CHAPTER 5 CONCLUSIONS AND RECOMMENDATIONS.....</b>   | <b>116</b> |
| 5.1 Conclusions.....  | 116        |
| 5.2 Significat Contributions.....   | 117        |
| 5.3 Recommendations for Future Work.....  | 117        |
| <b>REFERENCES:.....</b>   | <b>162</b> |
| <b>LIST OF PUPPLICATIONS:.....</b>  | <b>162</b> |
| <b>APPENDICES:.....</b>   | <b>162</b> |
| Appendix A:.....  | 162        |
| Appendix B:.....  | 162        |
| Appendix C:.....  | 162        |
| Appendix D:.....  | 162        |
| Appendix E:.....  | 162        |

## LIST OF TABLES

|   |    |
|---|----|
| Table 2.1: FACTS Devices and their Controller.....  | 26 |
| Table 3.1: Some papers related with PSO, GA and SA optimization techniques.....                       | 37 |
| Table 3.2: PSO parameters .....   | 44 |
| Table 3.3: Application of PSO .....   | 49 |
| Table 4.1: Voltages of generator buses of the IEEE 14-bus power system.....                           | 70 |
| Table 4.2: Transmission line losses of the IEEE 14-bus power system without IPFC                      | 70 |
| Table 4.3: The control parameters of the IPFC and the system losses of IEEE 14-bus power system ..... | 72 |
| Table 4.4: PSO control Parameters .....   | 73 |
| Table 4.5: The control parameters of IPFC and the system losses of IEEE 14-bus power system .....     | 74 |
| Table 4.6: GA control parameters .....  | 79 |
| Table 4.7: Optimal parameters of IPFC and the system line losses with GA.....                         | 80 |
| Table 4.8: SA control parameters.....   | 85 |
| Table 4.9: The control parameter and the system losses .....  | 86 |
| Table 4.10: The IPFC parameters and the transmission line active power losses .....                   | 91 |
| Table 4.11: Comparison between optimization methods .....   | 92 |
| Table 4.12: The voltages of generator buses .....   | 94 |
| Table 4.13: Transmission line losses of IEEE 30-bus power system without IPFC...                      | 95 |
| Table 4.14: The control parameter and the system losses of IEEE 30-bus power system with IPFC .....   | 96 |
| Table 4.15: PSO control parameters.....   | 97 |

|  |     |
|--|-----|
| Table 4.16: The control parameter of IPFC and the system losses of IEEE 30-bus power system..... | 98  |
| Table 4.17: GA control parameters .....  | 100 |
| Table 4.18: Optimal parameters of IPFC and the system losses .....                               | 101 |
| Table 4.19: SA control parameters .....  | 106 |
| Table 4.20: The control parameter and the system losses .....                                    | 107 |
| Table 4.21: The IPFC parameters and the transmission line active power losses ....               | 112 |
| Table 4.22: Comparison between optimization methods.....   | 113 |

## LIST OF FIGURES

|   |    |
|---|----|
| Figure 2.1: Schematic diagram of an SVC .....                                     | 13 |
| Figure 2.2: Thyristor Controlled Series Capacitor .....                           | 14 |
| Figure 2.3: A TCSR schematic .....  | 14 |
| Figure 2.4: A schematic of TSSC.....  | 15 |
| Figure 2.5: Circuit set up of a 6-pluse VSC.....                                  | 17 |
| Figure 2.6: Gate pulse signal for 6-pulse VSC .....                               | 17 |
| Figure 2.7: A Schematic of STATCOM.....   | 20 |
| Figure 2.8: A Schematic of SSSC .....   | 21 |
| Figure 2.9: A Schematic of IPC .....  | 22 |
| Figure 2.10: A Schematic diagram of UPFC .....                                    | 23 |
| Figure 2.11: A schematic diagram of IPFC with two VSC converters .....            | 25 |
| Figure 2.12: Equivalent circuit of the IPFC with two converters .....             | 28 |
| Figure 2.13: Modified Newton Raphson method.....                                  | 35 |
| Figure 3.1: Modification of current position by PSO.....                          | 39 |
| Figure 3.2: Particles in a solution space .....                                   | 40 |
| Figure 3.3: Proposed algorithm flowchart of PSO.....                              | 47 |
| Figure 3.4: Gene string and chromosome.....                                       | 50 |
| Figure 3.5: Roulette wheel probabilities for four parents in the mating pool..... | 52 |
| Figure 3.6: Tournament selection.....   | 53 |
| Figure 3.7: Crossover operation.....  | 53 |
| Figure 3.8: Mutation operation .....  | 54 |



|   |    |
|---|----|
| Figure 3.9: Flowchart of GA technique .....   | 56 |
| Figure 3.10: Flow chart of a SA.....  | 61 |
| Figure 3.11: GA solver .....  | 62 |
| Figure 3.12: SA solver.....   | 66 |
| Figure 4.1: The voltage profile of IEEE 14-bus power system without IPFC.....   | 70 |
| Figure 4.2: The voltage profile of IEEE 14-bus power system with IPFC.....  | 72 |
| Figure 4.3: The voltage profile of IEEE 14-bus power system without and with IPFC<br>.....                            | 73 |
| Figure 4.4: Variation of total line losses with the change in iterations by BPSO .....                                | 75 |
| Figure 4.5: Variation of total line losses with the change in iterations by IWAPSO..                                  | 75 |
| Figure 4.6: Variation of total line losses with the change in iterations by CFAPSO ..                                 | 76 |
| Figure 4.7: The voltage profile of IEEE 14-bus power system with IPFC and BPSO  | 76 |
| Figure 4.8: The voltage profile of IEEE 14-bus power system with IPFC and<br>IWAPSO .....                             | 77 |
| Figure 4.9: The voltage profile of IEEE 14-bus power system with IPFC and CFAPSO<br>.....                             | 77 |
| Figure 4.10: The voltage profile of IEEE 14-bus power system with IPFC and BPSO,<br>IWAPSO and CFAPSO techniques..... | 78 |
| Figure 4.11: The voltage profile of IEEE 14-bus power system with IPFC and<br>with IPFC using PSO.....                | 78 |
| Figure 4.12: The voltage profile of IEEE 14-bus power system without IPFC,<br>with IPFC and with IPFC using PSO ..... | 79 |
| Figure 4.13: Current best individual of the optimal parameters .....  | 81 |
| Figure 4.14: Fitness of each individual.....  | 81 |
| Figure 4.15: Average distance value with the change in number of generation of GA<br>.....                            | 82 |

|  |    |
|--|----|
| Figure 4.16: Variation of best function value with the change in number of generation of GA.....   | 82 |
| Figure 4.17: stopping criteria percentages.....  | 83 |
| Figure 4.18: The voltage profile of IEEE 14-bus power system with IPFC using GA83  |    |
| Figure 4.19: The voltage profile of IEEE 14-bus power system with IPFC and with IPFC using GA.....   | 84 |
| Figure 4.20: The voltage profile of IEEE 14-bus power system without IPFC, with IPFC and with IPFC using GA.....                                 | 84 |
| Figure 4.21: current points of the optimal parameters .....  | 86 |
| Figure 4.22: best point of the optimal parameters.....   | 87 |
| Figure 4.23: Temperatures of the optimal parameters.....   | 87 |
| Figure 4.24: The variation of the current objective function value with the change in iterations by SA .....                                     | 88 |
| Figure 4.25: Variation of best objective function value with the change in iterations by SA.....   | 88 |
| Figure 4.26: The stopping criteria .....   | 89 |
| Figure 4.27: The voltage profile of IEEE 14-bus power system with IPFC using SA  | 89 |
| Figure 4.28: The voltage profile of IEEE 14-bus power system with IPFC and with IPFC using SA .....  | 90 |
| Figure 4.29: The voltage profile of IEEE 14-bus power system without IPFC, with IPFC, and with IPFC using SA .....                               | 90 |
| Figure 4.30: Variation of objective function with the change in iterations .....   | 92 |
| Figure 4.31: The voltage profile of IEEE 14-bus power power system with IPFC together with PSO or GA or SA technique.....                        | 93 |
| Figure 4.32: The voltage profile of IEEE 14-bus power system without IPFC, with IPFC and with IPFC together with PSO or GA or SA technique ..... | 93 |
| Figure 4.33: The voltage profile of IEEE 30-bus power system without IPFC.....   | 95 |
| Figure 4.34: The voltage profile of IEEE 30-bus power system with IPFC.....  | 96 |

|  |     |
|--|-----|
| Figure 4.35: The voltage profile of IEEE 30-bus power system without and with IPFC .....                           | 97  |
| Figure 4.36: Variation of total line losses with the change in iterations by PSO .....                             | 99  |
| Figure 4.37: The voltage profile of IEEE 30-bus power system with IPFC and PSO                                     | 99  |
| Figure 4.38: The voltage profile of IEEE 30-bus power system without IPFC, with IPFC and with IPFC using PSO ..... | 100 |
| Figure 4.39: current points of the optimal parameters.....   | 102 |
| Figure 4.40: Fitness of each individual.....   | 102 |
| Figure 4.41: Average distance value with the change in number of generation of GA .....                            | 103 |
| Figure 4.42: Variation of best function value with the change in number of generations of GA .....                 | 103 |
| Figure 4.43: stopping criteria percentages .....   | 104 |
| Figure 4.44: The voltage profile of IEEE 30-bus power system with IPFC using GA .....                              | 104 |
| Figure 4.45: The voltage profile of IEEE 30-bus power system with IPFC and with IPFC using GA.....                 | 105 |
| Figure 4.46: The voltage profile of IEEE 30-bus power system without IPFC, with IPFC and with IPFC using GA.....   | 105 |
| Figure 4.47: Current points of the optimal parameters.....   | 107 |
| Figure 4.48: Best point of the optimal parameters .....  | 108 |
| Figure 4.49: Current temperatures of the optimal parameters .....  | 108 |
| Figure 4.50: The variation of the current objective function value with the change in iterations by SA .....       | 109 |
| Figure 4.51: Variation of best objective function value with the change in iterations by SA.....                   | 109 |
| Figure 4.52: The stopping criteria .....   | 110 |

|  |     |
|--|-----|
| Figure 4.53: The voltage profile of IEEE 30-bus power system with IPFC using SA .....  | 110 |
| Figure 4.54: The voltage profile of IEEE 30-bus power system with IPFC and with IPFC using SA .....  | 111 |
| Figure 4.55: The voltage profile of IEEE 30- bus system without IPFC, with IPFC, and with IPFC using SA .....                                    | 111 |
| Figure 4.56: Variation of objective function with the change in iterations .....   | 113 |
| Figure 4.57: The voltage profile of IEEE 30-bus power system with IPFC together with and PSO or GA or SA technique.....                          | 114 |
| Figure 4.58: The voltage profile of IEEE 30-bus power system without IPFC, with IPFC and with IPFC together with PSO or GA or SA technique. .... | 114 |

## NOMENCLATURE

| Nomenclature | Description                                 |
|--------------|---|
| $F, f$       | Objective function                          |
| $g$          | Equality constrains                         |
| $h$          | Inequality constrains                       |
| $x$          | State variables                             |
| $u$          | Set of control variable                     |
| $P_S$        | Slack bus active power                      |
| $P_G$        | Generator real power                        |
| $Q_G$        | Generator reactive power                    |
| $N$          | Number of transmission lines                |
| $V_l$        | Voltage at bus l                            |
| $V_k$        | Voltage at bus k                            |
| $G_{lk}$     | Transfer conductance between lines l and k  |
| $B_{lk}$     | Transfer susceptance between lines l and k  |
| $P_k^{cal}$  | Calculated active power at node k           |
| $Q_k^{cal}$  | Calculated reactive power at node k         |
| $P_k^{net}$  | Net scheduled active power at node k        |
| $Q_k^{net}$  | Net scheduled reactive power at node k      |
| $P_k^{gen}$  | Active power generated at node k            |
| $Q_k^{gen}$  | Reactive power generated at node k          |
| $P_k^{load}$ | Active power consumed by the load at node k |

|                |   |
|----------------|---|
| $Q_k^{load}$   | Reactive power consumed by the load at node k                                     |
| $V_{di}$       | Load bus voltage  |
| $S_i$          | Transmission line loading   |
| $V_{slk}$      | Series injected voltage source magnitude  |
| $\theta_{slk}$ | Series injected voltage angle   |
| $I_{lk}$       | Line current magnitude  |
| $S_{slk}$      | Power injected in to the line by series VSCs                                      |
| $P_{slk}$      | Circulated real power   |
| $V_{sa}$       | Instantaneous phase a voltage of AC power system                                  |
| $V_{sb}$       | Instantaneous phase b voltage of AC power system                                  |
| $V_{sc}$       | Instantaneous phase c voltage of AC power system                                  |
| $V_{ca}$       | Instantaneous phase a voltage of AC side of the converter                         |
| $V_{cb}$       | Instantaneous phase b voltage of AC side of the converter                         |
| $V_{cc}$       | Instantaneous phase c voltage of AC side of the converter                         |
| $L$            | Inductance value of the reactor   |
| $R$            | The equivalent resistance value of the converter and transformer loss             |
| $d-q$          | Synchronous d-q reference frame   |
| $\alpha-\beta$ | $\alpha-\beta$ reference frame  |
| $\omega$       | The angular speed of the rotating d-q reference frame                             |
| $C$            | DC capacitor  |
| $V_{dc}$       | Instantaneous voltage of the DC side of the converter                             |
| $i_{dc}$       | Instantaneous current injected in to the converter                                |
| $i_{dl}$       | Instantaneous current from the DC network into the converter and the DC capacitor |

|                  |  |
|------------------|--|
| $P_l$            | Net active power at bus l  |
| $Q_l$            | Net reactive power at bus l  |
| $I_l$            | Net current injected into the network at bus l                       |
| $V_{slm}$        | The injected voltage source at branch l-m                            |
| $V_{sln}$        | The injected voltage source at branch l-n                            |
| $P_{se1}$        | Active power exchange through the DC link by VSC <sub>1</sub>        |
| $P_{se2}$        | Active power exchange through the DC link by VSC <sub>2</sub>        |
| $P_{lk}$         | Active power flow injection at node l                                |
| $Q_{lk}$         | Reactive power flow injection at node l                              |
| $P_{kl}$         | Active power flow injection at node k                                |
| $Q_{kl}$         | Ractive power flow injection at node k                               |
| $S_{lk}$         | The complex power from bus l to k                                    |
| $S_{kl}$         | The complex power from bus k to l                                    |
| $S_{losslk}$     | The power loss in line l-k   |
| $P_{losslk}$     | The active power loss in line l-k                                    |
| $Q_{losslk}$     | The reactive power loss in line l-k                                  |
| $V_i^k$          | The current velocity of particle i at k <sup>th</sup> iteration      |
| $V_i^{k+1}$      | The modified velocity of particle i at (k+1) <sup>th</sup> iteration |
| $W$              | The inertia weight factor  |
| $rand_1, rand_2$ | The random numbers between 0 and 1                                   |
| $Pbest_i^k$      | The best value found by particle i at k <sup>th</sup> iteration      |
| $Gbest_i^k$      | The best particle found in the group until iteration k.              |

|                           |   |
|---------------------------|---|
| $X_i^k$                   | The current position of the particle i at $k^{\text{th}}$ iteration     |
| $X_i^{k+1}$               | The current position of the particle i at $(k+1)^{\text{th}}$ iteration |
| $W_{max}$                 | The initial value of the inertia weight                                 |
| $W_{min}$                 | The final value of the inertia weight                                   |
| $iter_{max}$              | The maximum iteration number  |
| $iter$                    | The current iteration number  |
| $C_1, C_2$                | The weighting factors   |
| $K$                       | The construction factor   |
| $\phi$                    | Constant used to control the convergence characteristic of system       |
| $P_{con}$                 | Probability of specific configuration                                   |
| $E_{con}$                 | The energy of the given configuration                                   |
| $E_c, E_t$                | The energy level of the current and trial configuration                 |
| $T$                       | The control parameter of the cooling schedule                           |
| $Z_{lk}$                  | The line impedance between bus l-k                                      |
| $R_{lk}, R_{slk}$         | The transmission line and series voltage source resistance              |
| $X_{lk}, X_{slk}$         | The transmission line and series voltage source reactances              |
| $\Delta P, \Delta Q$      | The active and reactive power mismatch                                  |
| $\Delta V, \Delta \delta$ | The voltage and power angle change                                      |
| $J_1, J_2, J_3, J_4$      | The elements of Jacobian matrix   |



## **ABBREVIATION**

| <b>Abbreviation</b> | <b>Description</b>                                       |
|---------------------|--|
| BPSO                | Basic Particle Swarm Optimization                        |
| CFA                 | Construction Factor Approach                             |
| CFAPSO              | Construction Factor Approach Particle Swarm Optimization |
| FACTS               | Flexible AC Transmission System                          |
| GA                  | Genetic Algorithm  |
| GTO                 | Gate Turn-off Thyristor                                  |
| IGBT                | Insulated Gate Bipolar Transistor                        |
| IGCT                | Insulated Gate Commutated Turn-off                       |
| IPC                 | Interphase Power Controller                              |
| IPFC                | Interline Power Flow Controller                          |
| IWAPSO              | Inertia Wight Approach Particle Swarm Optimization       |
| OPF                 | Optimal Power Flow                                       |
| PMW                 | Pulse width Modulation                                   |
| PSO                 | Particle Swarm Optimization                              |
| PWM                 | Plus Width Modulation                                    |
| SA                  | Simulated Annealing                                      |
| SSSC                | Static Synchronous Series Compensator                    |
| STATCOM             | Static Synchronous Compensator                           |
| SVC                 | Static Var Compensator                                   |
| TCSC                | Thyristor Control Series Capacitor                       |
| TCSR                | Thyristor Control Series Reactor                         |

|      |                                     |
|------|-------------------------------------|
| TSSC | Thyristor Switched Series Capacitor |
| UPFC | Unified Power Flow Controller       |
| VSC  | Voltages Source Converter           |

# **CHAPTER 1**

## **INTRODUCTION**

### **1.1 Background**

The recent generation of Flexible AC Transmission System (FACTS) controllers using Voltage Source Converter (VSC) are usually employed as shunt reactive compensator Static Synchronous Compensator (STATCOM), series active or reactive compensator Static Synchronous Series Compensator (SSSC) and combination of series and shunt United Power Flow Controller (UPFC) or the latest one series-series Interline Power Flow Controller (IPFC) [1]-[2]-[3]. The UPFC is used to control both active and reactive power flow, and thus provides the maximization of real power transfer at minimum losses, in individual transmission line. As compared with the UPFC and SSSC, the IPFC has much more flexible topologies, consisting of at least two or more VSCs, and can be used to control power flow of multi-line transmission system. The IPFC concept provides a solution to control power flows in multi-line transmission system at a given substation. The converters within the IPFC are able to transfer the active power to each other through the DC-links and thereby facilitate active power transfer among the lines, together with independently controllable reactive compensation of each individual transmission line [4, 5].

Generally, with the FACTS devices it is possible to control voltage magnitude and phase angle at selected buses and line impedance of a transmission line system. But the existing conventional Optimal Power Flow (OPF) algorithms have to be modified such that power system analysis is possible for modern power system with FACTS devices [6]. In the very recent years, researchers have developed efficient algorithms to solve optimal power flow incorporating FACTS devices.

The problem of power system operation, planning and analysis can be considered to be a combinatorial optimization problem. Earlier researchers have developed many

conventional optimization techniques and applied to solve the optimal power flow (OPF) problem. These techniques have some disadvantages such as: (i) Nonlinear programming techniques are prone to insecure convergence properties and algorithmic complexity. (ii) Linear programming methods which are fast and reliable have certain disadvantages associated with piecewise linear objective-function approximation. (iii) Quadratic programming based techniques find problems with piecewise quadratic objective function approximation. (iv) The interior point methods are reported to be computationally efficient, but if the step size is not chosen properly, the sub-linear problem may have a solution that is infeasible in the original non-linear domain [7, 8].

Thus the above optimization techniques sometimes fails to find the global optimum for OPF whose objective function is non-convex, non-smooth and non-differentiable. Heuristic algorithms i.e. Genetic Algorithms (GA) and other evolutionary techniques are developed as an alternative to the conventional methods. However, the optimal values obtained with these methods are not true global optimums but near to global optimum values [8]. The application of intelligent optimization techniques in power systems is recently gaining interest. However the investigation of optimal parameters of an IPFC minimizing transmission line losses of a bench mark power system using these intelligent optimization methods is not reported in the published literature.

### 1.1.1 Optimal Power Flow Problem

The steady state performance of a power system is optimized by the optimal power flow problem method. The active power losses considered as the objective function is subjected to a number of equality and inequality constraints.

The OPF problem is stated mathematically as follows:

$$\text{Minimize } f(x, u) \quad (1.1)$$

Subjected to the constraints

$$g(x, u) = 0 \quad (1.2)$$

$$h(x, u) \leq 0 \quad (1.3)$$

where  $f$  is the objective function to be minimized,  $g$  are the equality constraints,  $h$  are the inequality constraints,  $x$  is the set of state variables such as slack bus power, PS, load bus voltage,  $V_l$ , generator reactive power,  $Q_G$ , and,  $u$  is a set of control variables such as generator voltages,  $V_G$ , generator real powers,  $P_G$ , except the slack bus power output.

### 1.1.2 Objective Function

The OPF in this study has the main objective to minimize the transmission line losses and to keep the voltage profile within the acceptable limits [9] which can be formulated as in (1.4).

$$\text{Minimize } F = \sum_{k=(m,n)}^N P_{loss} \quad (1.4a)$$

or:

$$\begin{aligned} P_{loss} = & (|V_l|^2 G_{lk} - |V_l||V_k|[G_{lk} \cos \theta_{lk} + B_{lk} \sin \theta_{lk}] - \\ & |V_l||V_{slk}][G_{lk} \cos \theta_{lslk} + B_{lk} \sin \theta_{lslk}]) + (|V_k|^2 G_{lk} - \\ & |V_k||V_l|[G_{lk} \cos \theta_{kl} + B_{lk} \sin \theta_{kl}] + |V_k||V_{slk}][G_{lk} \cos \theta_{kslk} \\ & + B_{lk} \sin \theta_{kslk}]) \end{aligned} \quad (1.4b)$$

where  $F$  is the objective function,  $N$  is the number of transmission lines,  $V_l = |V_l| \angle \theta_l$  and  $V_k = |V_k| \angle \theta_k$  are the voltages at the end buses  $l$  and  $k$  ( $k = m, n$ ),  $V_{slk} = |V_{slk}| \angle \theta_{slk}$  ( $k = m, n$ ) is the series injected voltage source of  $k$ th line,  $G_{lk}$  and  $B_{lk}$  are the transfer conductance and susceptance between buses  $l$  and  $k$  ( $k = m, n$ ) respectively. The magnitude and phase angle of the series injected voltage of VSC of IPFC will be determined optimally.

The equality constraints represent the typical load flow equations which are formulated as in (1.5) and (1.6).

$$P_k^{net} - P_k^{cal} = 0 \quad (k = m, n) \quad (1.5)$$

$$Q_k^{net} - Q_k^{cal} = 0 \quad (k = m, n) \quad (1.6)$$

$P_k^{cal}$  and  $Q_k^{cal}$  are the calculated active and reactive powers at node  $k$  which are formulated as in (1.7) and (1.8).

$$P_k^{cal} = |V_k|^2 G_{lk} - |V_k| |V_l| [G_{lk} \cos \theta_{lk} + B_{lk} \sin \theta_{lk}] + |V_k| |V_{slk}| [G_{lk} \cos \theta_{kslk} + B_{lk} \sin \theta_{kslk}] \quad (1.7)$$

$$Q_k^{cal} = -|V_k|^2 B_{lk} - |V_k| |V_l| [G_{lk} \sin \theta_{lk} - B_{lk} \cos \theta_{lk}] + |V_k| |V_{slk}| [G_{lk} \sin \theta_{kslk} - B_{lk} \cos \theta_{kslk}] \quad (1.8)$$

where  $P_k^{net} = P_k^{gen} - P_k^{load}$  is the net scheduled active power at node  $k$ .  $Q_k^{net} = Q_k^{gen} - Q_k^{load}$  is the net scheduled reactive power at node  $k$ ,  $P_k^{gen}$  and  $Q_k^{gen}$  are the active and reactive powers generated at node  $k$ ,  $P_k^{load}$  and  $Q_k^{load}$  are the active and reactive powers consumed by the load at node  $k$ . From the operating principle of the IPFC, active power supplied to one converter is equal to the active power demanded by the other [10, 11] and therefore this condition is formulated as in (1.9) and (1.10).

$$real(V_{slm} I_{lm}^* + V_{sln} I_{ln}^*) = 0 \quad (1.9)$$

or:

$$\sum_{k=m,n} (|V_{slk}|^2 G_{lk} - |V_l| |V_{slk}| [G_{lk} \cos \theta_{lslk} - B_{lk} \sin \theta_{lslk}] + |V_k| |V_{slk}| [G_{lk} \cos \theta_{kslk} - B_{lk} \sin \theta_{kslk}]) = 0 \quad (1.10)$$

The inequality constraints of the OPF problem represent the state variable limit and control variable limit or the operation limit of the system. The operation constraints of the system consist of the upper and lower limits of active power generation of slack bus, reactive power generations of generators, load bus voltage and transmission line loading which are described by.

$$P_{Gs}^{\min} \leq P_{Gs} \leq P_{Gs}^{\max} \quad (s = slack) \quad (1.11)$$

$$Q_{Gi}^{\min} \leq Q_{Gi} \leq Q_{Gi}^{\max} \quad (i = 1, \dots, N_G) \quad (1.12)$$

$$V_{di}^{\min} \leq V_{di} \leq V_{di}^{\max} \quad (i = 1, \dots, N_B) \quad (1.13)$$

$$S_i \leq S_i^{\max} \quad (i = 1, \dots, N_i) \quad (1.14)$$

Considering the control variables, real power outputs and generators voltage, are bounded by (1.15) and (1.16).

$$P_{Gi}^{\min} \leq P_{Gi} \leq P_{Gi}^{\max} \quad (i = 1, \dots, N_G) \quad (1.15)$$

$$V_{Gi}^{\min} \leq V_{Gi} \leq V_{Gi}^{\max} \quad (i = 1, \dots, N_G) \quad (1.16)$$

For the series injected voltage source converter of an IPFC, the operating constraint limits are described as in (1.17) to (1.21) [12].

- Injected voltage with controllable magnitude,  $V_{slk}$ , and angle,  $\theta_{slk}$ .

$$V_{slk}^{\min} \leq V_{slk} \leq V_{slk}^{\max} \quad (k = m, n) \quad (1.17)$$

$$\theta_{slk}^{\min} \leq \theta_{slk} \leq \theta_{slk}^{\max} \quad (k = m, n) \quad (1.18)$$

- Line current magnitude through the series, VSC

$$I_{lk}^{\min} \leq I_{lk} \leq I_{lk}^{\max} \quad (k = m, n) \quad (1.19)$$

- Power injected by VSC

$$|S_{slk}| \leq S_{slk}^{\max} \quad (k = m, n) \quad (1.20)$$

where  $S_{slk}$  is the complex power injected in to the line by the series VSC.

- The circulated real power,  $P_{slk}$ .

$$|P_{slk}| \leq P_{slk}^{\max} \quad (k = m, n) \quad (1.21)$$

## 1.2 Problem Statement

In 2006 El-Zonkoly [13] used PSO technique to find the optimal parameters of SSSC based on steady-state models of FACTS devices. The sizing of SSSC controllers in a

transmission network is formulated as an optimization problem. The objective of the problem is reduction of the transmission line losses in the network. The modified Newton-Raphson load flow algorithm is used to consider the insertion of the SSSC devices in the network.

The OPF program used to optimize a single or multiple objective functions such as the active power loss in a power network is considered as a common optimization goal because it is closely related with the cost [14].

The application of intelligent optimization techniques such as Particle Swarm Optimization (PSO), Genetic Algorithm (GA) and Simulated Annealing (SA) in power systems is recently gaining interest. However, the investigation of optimal parameters of an IPFC to minimize the transmission line losses of a bench mark power system using the above intelligent optimization techniques is not reported in the published literature.

In this thesis, the problem of obtaining the parameters of VSCs of IPFC is formulated as an optimization problem, with the objective of minimizing the transmission line losses in a network. In order to compute the active power losses and to check the system operating constraints such as voltage profile, a load flow model is developed. A modified load flow model, based on the existing Newton-Raphson load flow algorithm, is introduced to include the IPFC devices into the network.

### **1.3 Objectives of Thesis**

- To develop a mathematical model of an IPFC system with two VSCs to compensate the transmission line impedance.
- To develop some intelligent optimization techniques such as PSO, GA and SA for finding the optimal parameter of VSCs of IPFC.
- To implement the model of IPFC in software environment such as MATLAB and to compare the performances of these intelligent optimization techniques in terms of loss minimization, voltage improvement and execution running time.



## **1.4 Scope of Study**

To fulfill the objectives of this study:

- The optimal power flow problem using intelligent optimization techniques in multi-terminal transmission line system adopting IPFC will be reported in this thesis.
- To simulate the power flow using a modified Newton-Raphson load flow method including the VSCs of the IPFC.
- To demonstrate the effectiveness and accuracy of the optimal parameters of the IPFC and minimization of transmission line losses of standard IEEE 14-bus and 30-bus bench mark power systems by the proposed intelligent optimization techniques.

## **1.5 Organization of Thesis**

The main aspects of this thesis are structured into five chapters. Chapter one is referred to as the introduction chapter, section 1.1 provides a brief background needed for FACTS devices especially the FACTS devices based on VSCs, the need for OPF in power system network and optimization techniques. Section 1.2 shows the problem statement. The objective and scope of the thesis are presented in sections 1.3 and 1.4 respectively. Sections 1.5 present the outline of the thesis.

Chapter two introduces the basic concepts and terminology of Flexible AC Transmission System (FACTS) and some of the work from literature that is relevant to this thesis has been reviewed. In section 2.2, the objective of such FACTS devices, the benefits of FACTS controllers, have been discussed. In section 2.3 the types of FACTS Controllers are discussed. Section 2.4 has presented FACTS controller and their potential. In section 2.5, general power flow representation in a power system is presented. The Interline Power Flow Controller (IPFC) equivalent circuit and power flow equations using IPFC are discussed in section 2.5.1. General power flow expressions with IPFC and operating modes of IPFC have been discussed in section 2.5.2 and 2.5.3 respectively. Finally the chapter summary is presented.

Chapter three discusses the methods of optimization techniques used in this thesis. Section 3.1 provides an introduction to this chapter. Section 3.2 present more details about the PSO technique, the elements of PSO, parameter selection for PSO, variants of PSO, proposed PSO for optimal parameters of VSC of IPFC, advantages of PSO and application of PSO to power system. Section 3.3 presents an overview of GA, GA operator, selection process, crossover, mutation, termination criteria, GA implementation and comparison between GA and traditional search algorithm. Section 3.4 presents the SA technique, physical concepts, control factors and implementation of SA. Section 3.5 presents the global optimization tool box in MATLAB 7.6, GA solver and SA solver. The chapter is summarized in the last section.

Chapter four presents the simulation results and discussions. Section 4.1 presents an introduction of this chapter, Newton-Raphson power flow method and Newton-Raphson power flow method using IPFC. Section 4.2 provides simulation results and discussion for case-1 standard IEEE 14-bus system, power flow analysis for IEEE 14-bus system without IPFC, with IPFC, with IPFC and using PSO technique, with IPFC and using GA technique, and finally with IPFC and using SA technique. Section 4.3 presents simulation results and discussion for case-2 standard IEEE 30-bus power system, power flow analysis of IEEE 30-bus power system without IPFC, with IPFC, with IPFC and using PSO technique, with IPFC and using GA technique , and finally with IPFC and using SA technique. The last section summaries this chapter.

Chapter five discusses the entire study and summarizes the important findings and also lays directions for future work in this area.

## **CHAPTER 2**

### **LITERATURE REVIEW AND POWER FLOW STUDIES USING IPFC**

#### **2.1 Introduction**

This chapter introduces and discusses the essential information to understand this work and provides the background information on Flexible AC Transmission Systems (FACTS) controllers in general and Interline Power Flow Controller (IPFC) in particular.

#### **2.2 Flexible AC Transmission Systems (FACTS) Controllers**

Globally, power system networks are becoming complex encompassing a huge number of generators and buses. Hence, the requirements for providing stability, security, controllability, economic considerations, power quality and so on, in the deregulated electrical power supply environment are becoming important. Installations of new equipment on power system and facilities are basically determined based on environmental and economic considerations. In addition, a new transmission line is expensive and takes considerable amount of time to build. Based on this condition, in order to meet the ever-increasing power demands, electric utilities must rely on power export/import arrangements through existing transmission systems. This condition has resulted in an increased potential of transient, oscillatory and voltage instability, which are now brought into concerns in many utilities, especially in planning and operation. Furthermore, the trend of the re-regulated power system operation has caused some problems, such as over loading of transmission line corridors.

FACTS, which is an acronym for Flexible AC Transmission System, that involved the application of high power electronic controllers in AC transmission

networks was proposed by Hingorani [15, 16]. It has been reported that FACTS devices enable fast and reliable control of power flows and voltages. Basically FACTS do not indicate a particular controller but a host of controllers which the system planner can choose, based on cost benefit analysis [17].

The quick developments of FACTS controllers have led to many applications in electric power transmission systems. They are useful tools not only in improving the stability of existing power system network but also in providing flexibility of operation to the power system. In addition, they help utilities meet both the growing demand of electric power, and the emerging challenges of open transmission access. These new devices, coupled with better computer and communications technology, offer the potential for enhanced system control both during the steady state operation and especially following system disturbance.

IEEE FACTS Working Group defines FACTS and FACTS Controllers by “Alternating current transmission system incorporating power electronic-based and other static controllers to enhance controllability and increase power transfer capability”. And “A power electronic-based system and other static equipment that offer control of single or further AC transmission system parameters” [18] respectively. From these definitions, as summarized, the objectives of such FACTS devices [19] are:

- To improve the system transient stability limit.
- To enhance system damping of oscillations.
- To mitigate the sub synchronous resonance.
- To limit the short circuit currents.
- To improve the High Voltage Direct Current (HVDC) converter terminal performance.
- To enhance the power transfer capability of the transmission networks
- To control the power flow in the transmission line.

Basically, FACTS controllers can provide voltage support at critical buses in an electric system, and regulate power flow in critical lines. FACTS controllers such as unified power flow controller (UPFC) is used for both voltage and power flow control. The power electronic controller is quite fast, and this enables voltage and

power regulations both under steady state and dynamic conditions. The benefits of FACTS controllers are listed [20] as follows:

- They contribute to the optimal operation of the system by reducing power losses and improving voltage profile.
- The power flow in critical lines can be improved as the operating margins can be reduced due to fast controllability. In general, the power carrying capacity of lines can be increased to values up to the thermal limits (imposed by current carrying capacity of the conductors).
- The transient stability limit is increased thereby improving dynamic security of the system, and reducing the incidence of blackouts caused by cascading outages.
- The steady state or small signal stability region can be improved by providing auxiliary stabilizing controllers to damp low frequency oscillations.
- FACTS controllers such as Thyristor Control Series Capacitor (TCSC) can counter the problem of Sub-Synchronous Resonance (SSR) experienced with fixed series capacitors connected in lines evacuating power from thermal power stations (with turbo-generators).
- The problem of voltage fluctuations and in particular, dynamic over voltages can be overcome by FACTS controllers.

### **2.3 Types of FACTS Controllers**

The rapid development of power electronics has simplified the FACTS technology. As a result, different FACTS controllers have been initiated which are classified into two categories: Thyristor-based FACTS controllers and Voltage Source Converter (VSC) based FACTS controllers. It is better known that VSC-based FACTS controllers illustrate the new technology for AC transmission system compensation and power flow control with operating features, functional performance and application flexibility impossible by the Thyristor-based FACTS controllers [21]. VSC-based FACTS controllers include the Static Synchronous Series Compensator (SSSC) for series reactive power compensation, Static Synchronous Compensator (STATCOM) for shunt reactive power compensation, the unified power flow controller (UPFC) with the unique capability of independently controlling both the

active and reactive power flow in the line, and the Interline Power Flow Controller (IPFC) is the main topic of the present research. An IPFC optimizes both active and reactive power flow among multi-lines, transfer power from overloaded to under loaded lines.

### **2.3.1 Thyristor-Based FACTS Controllers**

There are various types of thyristor-based FACTS controllers, and some of them are listed as follows:

- Static Var Compensator (SVC)
- Thyristor Controlled Series Capacitor (TCSC)
- Thyristor Controlled Series Reactor (TCSR)
- Thyristor Switched Series Capacitor (TSSC)

The brief descriptions and operation principles of these FACTS controllers are presented as follows.

#### **2.3.1.1 Static Var Compensator (SVC)**

IEEE FACTS Working Group defines Static Var Compensator (SVC) as “Shunt-connected Static Var generator or absorber whose output is adjusted to exchange capacitive or inductive current so as to maintain or control specific parameters of the electrical power system (typically bus voltage)” [18].

Static Var system is capable of controlling individual phase voltages; therefore, Static Var can be used for controlling the negative sequence as well as positive sequence voltage deviations. A typical static Var compensator as shown in Figure 2.1 consists of a thyristor controlled reactor (TCR), a couple of thyristor-switched capacitors (TSCs) and harmonic filters. The harmonic filters behave like capacitor and generate some of the reactive power requirement at the power frequency [22]. Also, it is composed of mechanically switched shunt capacitors, and hence the term Static Var system is used.

The TCR is typically larger than the TSC blocks so that continuous control is realized. Other possibilities are fixed capacitors (FCs), and thyristor switched reactors (TSRs). A transformer is often used with the compensator equipment at medium

voltage power system network. The transmission side voltage is controlled, and the Mvar ratings are referred to the transmission side [23].

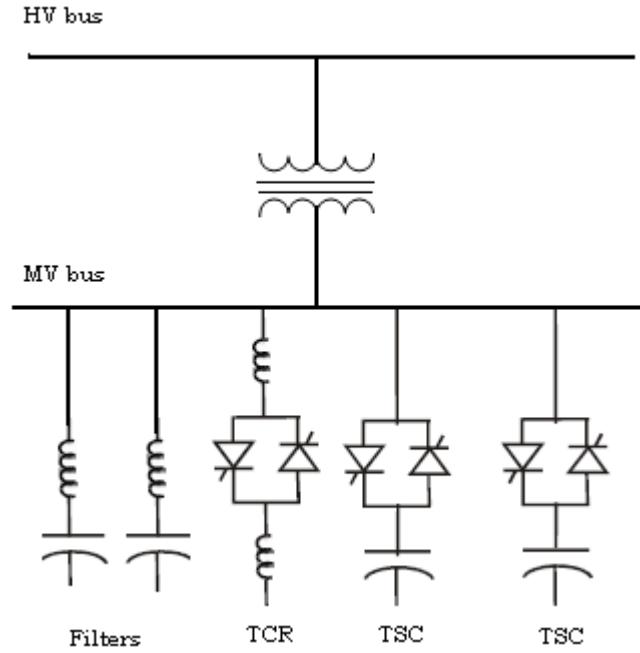


Figure 2.1: Schematic diagram of an SVC

### 2.3.1.2 Thyristor Controlled Series Capacitor (TCSC)

IEEE FACTS Working Group defines thyristor controlled series capacitor (TCSC) as “A capacitive reactance compensator which consists of a series capacitor bank shunted by thyristor controlled reactor in order to provide a smoothly variable series capacitive reactance” [18]. A TCSC Model developed mainly for use in steady state conditions consists of a fixed number of discrete values. As shown in Figure 2.2, a TCSC is connected in series with a transmission line. The effect of TCSC on a network can be seen as a controllable reactance inserted in a transmission line that compensates reactance of the line. It has one of the two possible characteristics: capacitive or inductive to increase or decrease the reactance of the line,  $X_L$  respectively [24].

The TCSC is the first generation of FACTS controllers. The major benefits of TCSC are their abilities to schedule power flows along desired lines and rapidly modulate the effective impedance in response to power system dynamics. The largest

TCSC in the world has been installed at the Slatt substation in USA and has been operating since 1993 [25].

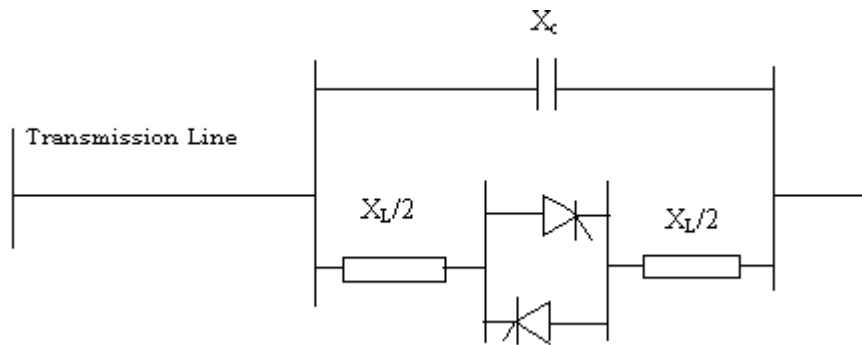


Figure 2.2: Thyristor Controlled Series Capacitor

### 2.3.1.3 Thyristor Controlled Series Reactor (TCSR)

IEEE FACTS Working Group defines Thyristor Controlled Series Reactor as “An inductive reactance compensator which consists of a series reactor shunted by a thyristor controlled reactor in order to provide a smoothly variable series inductive reactance” [18].

Generally, a TCSR as shown in Figure 2.3 consists of a series reactor bank shunted by a thyristor-controlled reactor.

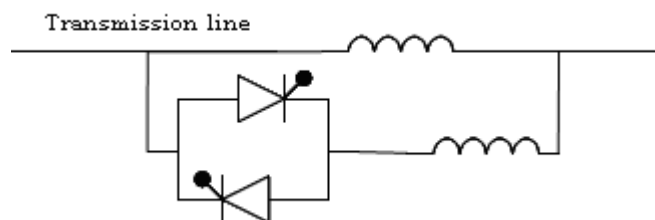


Figure 2.3: A TCSR schematic



#### 2.3.1.4 Thyristor Switched Series Capacitor (TSSC)

IEEE FACTS Working Group defines a TSSC as “A capacitive reactance compensator which consists of a series capacitor bank shunted by a thyristor switched reactor to provide a stepwise control of series capacitive reactance” [18].

As shown in Figure 2.4, a TSSC consists of a lumped capacitor,  $C$ , an inductor,  $L$ , and thyristor switches.

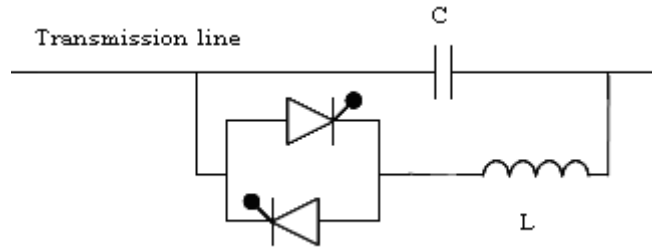


Figure 2.4: A schematic of TSSC

By switching the anti-parallel thyristors, the capacitor can be placed in and out of the transmission line. Owing to its simple configuration, such a basic model for TSSC has been developed and implemented in real system. TSSC and TCSC are the same in terms of physical connections but different in operation and control [26].

#### 2.3.2 Voltage Source Converter-Based FACTS Controllers

As mentioned previously, FACTS technologies have been successfully implemented in a large area of power system to increase the capability of the power transfer and to improve utilization of existing transmission facilities. In recent years, several VSCs have been connected together to provide multiple configurations with multi-functional FACTS controllers. The latest generation is called Convertible Static Compensator (CSC). A CSC, composed of two 100 MVA converters, has been successfully installed at the Marcy 345 kV substation of the New York Power Author (NYPA) expand transmission system [27]. The arrangement of the converters allows configuring Static Synchronous Series Compensator (SSSC), Static Synchronous Compensator (STATCOM), Unified Power Flow Controller (UPFC) and the Interline Power Flow Controller (IPFC).

Nowadays, VSC technology has become very important with development of semiconductor devices of high power self-turn off type. The rating for a converter of this type in practical application has already reached a high value [28]. Various types of Pulse Width Modulation (PWM) techniques have been used to operate the VSC which in turn provides a sinusoidal output to the AC system in inverter mode. VSC has so many advantages [29] such as:

- It is used to control the active and reactive power rapidly,
- It is used to provide a high level of power quality,
- It has less environmental impact, and
- It has capability to connect to weak AC networks, or even dead networks.

Various applications of the voltage source converter have been developed. The following are some of these applications.

- Static Synchronous Compensator (SSC) or STATCOM
- Static Synchronous Series Compensator (SSSC)
- Interphase Power Controller (IPC)
- Unified Power Flow Controller (UPFC)
- Interline Power Flow Controller (IPFC)

#### **2.3.2.1 Mathematical Model of Voltage Source Converter (VSC)**

VSC is used to generate a three phase voltage by using a DC voltage source. The on-off sequence applied to the static switches of VSC generates a three phase voltage with a fundamental frequency of 60 Hz [30]. Figure 2.5 represents a basic VSC formed using six asymmetric turn-off devices arranged in a three phase full wave converter configuration. These power semiconductor devices based on switching operation can be classified as Insulated Gate Bipolar Transistor (IGBT), Gate Turn-off Thyristor (GTO), Insulated Gate Commutated Turn-off (IGCT), MOS Turn-off (MTO) and MOS Controlled Thyristor (MCT). The frequency generated by the VSC is determined by the gate pulse pattern of the commutating devices. The amplitude of the AC voltages is determined by the magnitude of the DC voltage source. Using the common inverter configuration as shown in Figure 2.5 and applying the gate pulse pattern as shown in Figure 2.6, the phase and line voltages obtained are called 6-pulse voltages. In Figure 2.6, signals GS1, GS2, GS3, GS4, GS5, and GS6 are the gate

signals of IGBTs,  $Q_1$ ,  $Q_2$ ,  $Q_3$ ,  $Q_4$ ,  $Q_5$  and  $Q_6$ , respectively. They can only take values of 0 and 1 for the switching devices to be off and on respectively. Signals GS4, GS6 and GS2 are the logical inverses of GS1, GS3 and GS3, respectively. In real circuits, these signals are not exactly logical inverses; some dead time between the commutations of the switches in one branch has to be taken into account to prevent short circuiting the branch.

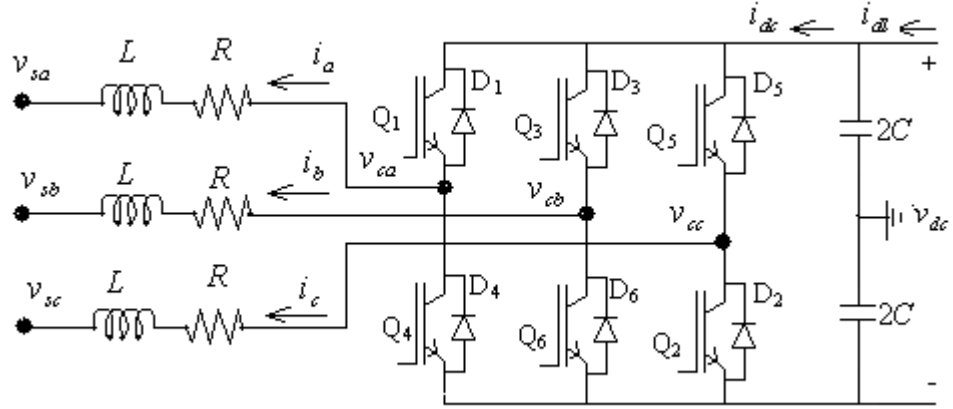


Figure 2.5: Circuit set up of a 6-pulse VSC

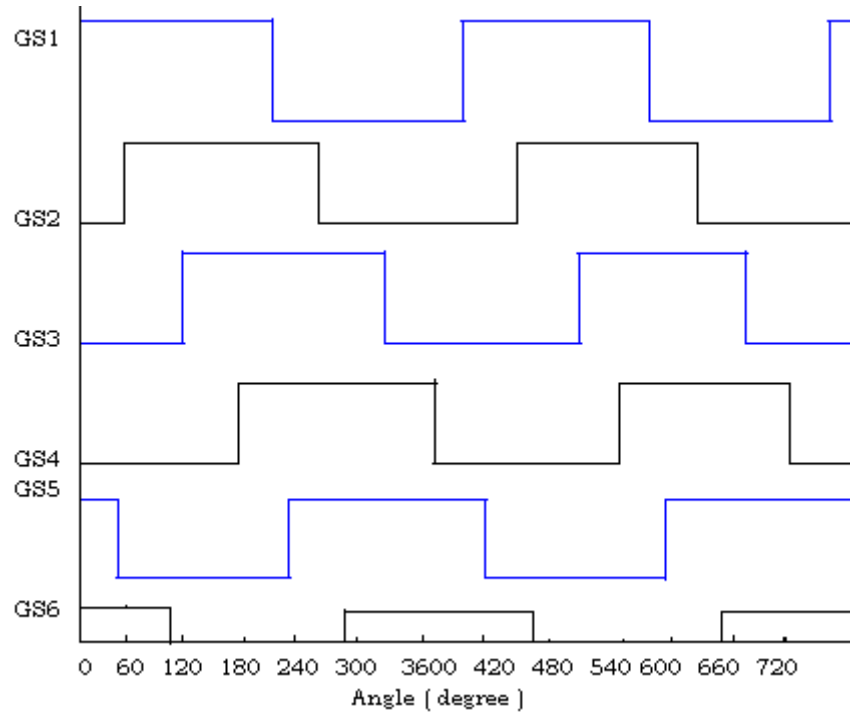


Figure 2.6: Gate pulse signal for 6-pulse VSC

A reactor is used on the input side of the VSC to smoothen the sinusoidal current on the AC network, and is also useful for providing the reference point for measurement of parameters. The capacitors on the DC side are used for the DC voltage source and for harmonic attenuation [31].

By using KVL, the voltage across the AC reactor in  $abc$ -reference frame is given by:

$$\begin{aligned} v_{ca} - v_{sa} &= L \frac{di_a}{dt} + Ri_a \\ v_{cb} - v_{sb} &= L \frac{di_b}{dt} + Ri_b \\ v_{cc} - v_{sc} &= L \frac{di_c}{dt} + Ri_c \end{aligned} \quad (2.1a)$$

or

$$v_{cab} - v_{sab} = L \frac{di_{abc}}{dt} + Ri_{abc} \quad (2.1b)$$

where  $v_{sa}$ ,  $v_{sb}$ , and  $v_{sc}$  are the instantaneous phase voltages of AC power system,  $v_{ca}$ ,  $v_{cb}$  and  $v_{cc}$  are the instantaneous phase voltages of the AC side of the converter,  $L$  is the inductance value of the reactor, and  $R$  is the equivalent resistance value of the resistance of the converter loss and the transformer loss. In order to decouple the active and reactive power controls, the synchronous  $d$ - $q$  reference frame has been used. For developing the controllers, all the phase quantities are transferred into the  $\alpha$ - $\beta$  reference by using the Clark transformation as in Equation (2.2) [32].

$$\begin{bmatrix} \alpha \\ \beta \\ 0 \end{bmatrix} = \frac{2}{3} \begin{bmatrix} 1 & -\frac{1}{2} & -\frac{1}{2} \\ 0 & \frac{\sqrt{3}}{2} & \frac{\sqrt{3}}{2} \\ \frac{1}{2} & \frac{1}{2} & \frac{1}{2} \end{bmatrix} \begin{bmatrix} a \\ b \\ c \end{bmatrix} \quad (2.2)$$

Transforming Equation (2.1) into  $\alpha$ - $\beta$  representation,

$$v_{c\alpha\beta} - v_{s\alpha\beta} = L \frac{di_{\alpha\beta}}{dt} + Ri_{\alpha\beta} \quad (2.3)$$

The relation linking  $\alpha$ - $\beta$  and  $d$ - $q$  reference frames is specified by Park's transformation as in Equation (2.4),

$$X_{dq} = X_{\alpha\beta} e^{-j\omega t} \quad (2.4)$$

where  $\omega$  is the angular speed of rotating  $d$ - $q$  reference frame, and is equal to the radial frequency of the fundamental AC voltage component.

From Equations (2.2) and (2.4),

$$\begin{aligned} v_{c\alpha\beta} &= v_{cdq} e^{j\omega t} \\ v_{s\alpha\beta} &= v_{sdq} e^{j\omega t} \\ i_{\alpha\beta} &= i_{dq} e^{j\omega t} \end{aligned} \quad (2.5)$$

Substituting Equation (2.5) in to Equation (2.3) gives:

$$\frac{di_{dq}}{dt} = \frac{v_{cdq}}{L} - \frac{v_{sdq}}{L} - \frac{R}{L} i_{dq} - j\omega R i_{dq} \quad (2.6)$$

The DC capacitor can sustain the DC voltage and filter the harmonics. The dynamic equation is represented as in Equation (2.7),

$$i_{dl} = C \frac{dv_{dc}}{dt} + i_{dc} \text{ or} \quad (2.7a)$$

$$\frac{dv_{dc}}{dt} = \frac{1}{C} (i_{dl} - i_{dc}) \quad (2.7b)$$

where  $v_{dc}$  is the instantaneous voltage of the DC side of the converter,  $i_{dc}$  is the instantaneous current injected into the converter;  $i_{dl}$  is the instantaneous current from the DC net work into the converter and the DC capacitor.

Therefore, Equations (2.6) and (2.7) define the dynamic mathematical model of the VSC.

### 2.3.2.2 Static Synchronous Compensator (SSC) or STATCOM

IEEE FACTS Working Group defines the Static Synchronous Compensator (SSC) or STATCOM as “A static synchronous generator operated as a shunt connected static var compensator whose capacitive or inductive output current can be controlled independent of the ac system voltage” [18].

From the schematic configuration of STATCOM as shown in Figure 2.7, the Static Synchronous Compensator (SSC) is essentially a voltage source converter with an energy storage unit, usually a DC capacitor. It is connected to the line through a coupling transformer which operates as a controlled Synchronous Voltage Source (SVS).

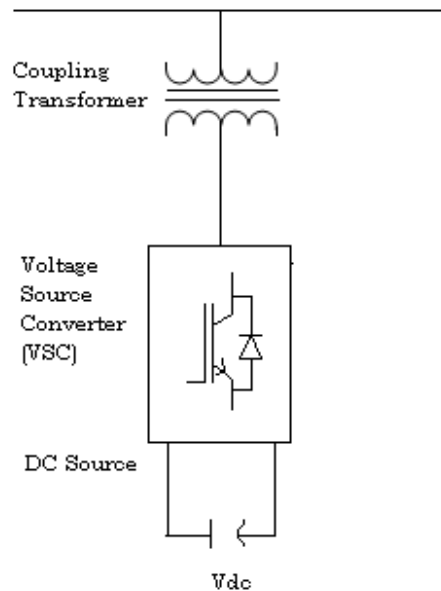


Figure 2.7: A Schematic of STATCOM

The controlled output voltage is maintained in phase with the line voltage, and can be controlled to draw either capacitive or inductive current from the line in a similar manner as in a synchronous condenser [33].

### 2.3.2.3 Static Synchronous Series Compensator (SSSC) or S<sup>3</sup>C

IEEE FACTS Working Group defined SSSC as “A static, synchronous generator operated without an external electric energy source as a series compensator whose output voltage is in quadrature with, and controllable independently of the line current for the purpose of increasing or decreasing the overall reactive voltage drop across the line and thereby controlling the transmitted electric power. The S<sup>3</sup>C may (SSSC or S<sup>3</sup>C) include transiently rated energy storage or energy absorbing devices to enhance the dynamic behavior of the power system by additional temporary real power compensation, to increase or decrease momentarily, the overall real (resistive) voltage drop across the line” [18].

As shown in Figure 2.8, the SSSC is connected in series with a transmission line through the coupling transformer. Generally an SSSC is composed of a coupling transformer, an inverter and a capacitor. The injected series voltage is regulated to change the impedance of the transmission line or more specifically the reactance of the transmission line. Hence the power flow in the transmission line system can be controlled.

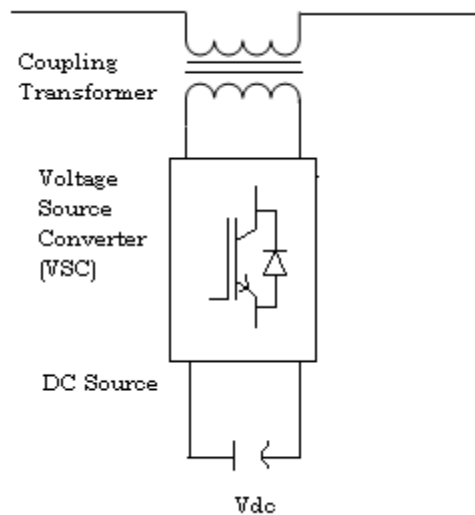


Figure 2.8: A Schematic of SSSC

### 2.3.2.4 Interphase Power Controller (IPC)

IEEE FACTS Working Group defined Interphase Power Controller (IPC) as “A series-connected controller of active and reactive power consisting, in each phase, of

inductive and capacitive branches subjected to separately phase-shifted voltages. The active and reactive powers can be set separately by adjusting the phase shifts and the branch impedances, using mechanical or electronic switches. In the case where the inductive and capacitive impedances form a conjugate couple, each terminal of the IPC is a passive current source dependent on the voltage at the other terminal” [18].

Generally, IPC as shown in Figure 2.9 is a series linked controller of active and reactive powers. It consists of inductive and capacitive branches subjected to separately phase-shifted voltages (phase-shifter 1 and phase-shifter 2). By adjusting the phase shifters and the branch impedances, the active and reactive powers can be set independently using mechanical or electronic switches.

The IPC is used to regulate both the quantity and the direction of active power transmitted through a transmission line. The IPC as shown in Figure 2.9 is a two-port circuit which is connected in series with a transmission line and in parallel with a busbar. It uses natural commutation, and has low switching frequency. The device has no important energy storage and DC port [34].

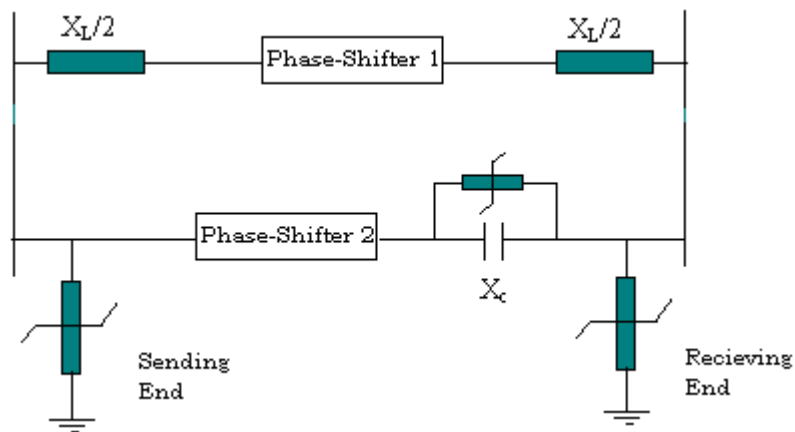


Figure 2.9: A Schematic of IPC

### 2.3.2.5 Unified Power Flow Controller (UPFC)

IEEE FACTS Working Group defined UPFC as a combination of STATCOM and SSSC which are coupled via a common dc link, to allow bi-directional flow of real power between the series output terminals of the SSSC and the shunt output terminals of the STATCOM, and are controlled to provide concurrent real and reactive series



line compensation without an external electric energy source. The UPFC, by way of angularly unconstrained series voltage injection, is able to control, concurrently or selectively, the transmission line voltage, impedance, and angle or, alternatively, the real and reactive power flow in the line. The UPFC may also provide independently controllable shunt reactive compensation [18].

Generally, as shown in Figure 2.10 a UPFC consists of two VSCs connected one in series and the other in shunt to the transmission lines, respectively. The series converter is series connected to a three-phase transmission line through three single-phase transformers. The shunt-converter is coupled with the ac bus through a three-phase transformer. Generally, the series converter can be used to control the active and reactive power flows of the transmission line at the same time the shunt converter used to control the voltages of the shunt bus [35].

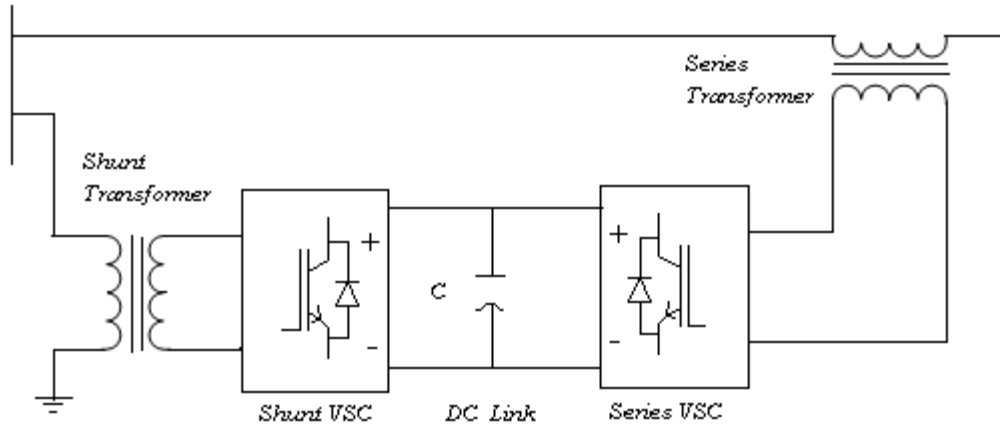


Figure 2.10: A Schematic diagram of UPFC

In other words, the series converter is used to generate a voltage source with variable amplitude and phase angle, which is added to the AC transmission line by the series connected boosting transformer. By this controllable voltage source, the branch power can be controlled. The shunt part is used to supply the active power which is injected into the branch by the series part. At the same time, it can generate or absorb some reactive power, used to control the voltage of the node where UPFC is connected [36].

### 2.3.2.6 Interline Power Flow Controller (IPFC)

The IPFC proposed by L. Gyugyi, et.al. [37] aims at resolving the problem of compensation to a number of transmission lines in a certain substation. IPFC is a new concept of FACTS controller with a unique capability of power flow management among multi-lines of a substation.

Due to the development of power electronics-based power flow controller recently, it has been made clear that many problems of power systems can be solved by combination of STATCOM and SSSC, namely UPFC which is installed in a single line. The IPFC concept provides a solution to control power flows in multiple transmission lines at a given substation [38]. Through the common DC link, any converter within the IPFC is able to transfer active power to any other converter and thereby facilitate active power transfer among the lines, together with independently controllable reactive compensation of each individual line. In this case, the power flow among the multiple series converters plays a key role in optimizing the required capacity at the minimum cost for overload management.

Generally, the IPFC consists of two or more VSCs connected together with DC links and each converter can provide series compensation for the selected line of the transmission system. In this way, the power optimization of the overall system can be realized in the form of appropriate power transfer through the common DC link from overloaded lines to underloaded lines [21]. The main objective of the IPFC is to optimize both active and reactive power flows among multi-lines, power transfer from overloaded to under loaded lines. However, it can also be utilized to compensate against reactive voltage drops and the corresponding reactive line power, and to increase the effectiveness of the compensating system against dynamic disturbances [14, 38].

The IPFC as shown in Figure 2.11 is represented by combining two voltage source converters,  $VSC_1$  and  $VSC_2$  connected together in series with transmission line 1 and transmission line 2. Both  $VSC_1$  and  $VSC_2$  are connected to transmission lines through a series transformer which extends the concept of power flow control beyond what is achievable with the known one-converter connected in series or SSSC.

The IPFC can control the three power system quantities independent of the power flows of the two lines [11]. As shown in Figure 2.11, transmission lines 1 and 2 are

connected to the same sending-end bus  $l$ , designated as provided with FACTS devices through series transformers. The receiving end buses are independent and named as bus  $m$  and bus  $n$ , respectively.

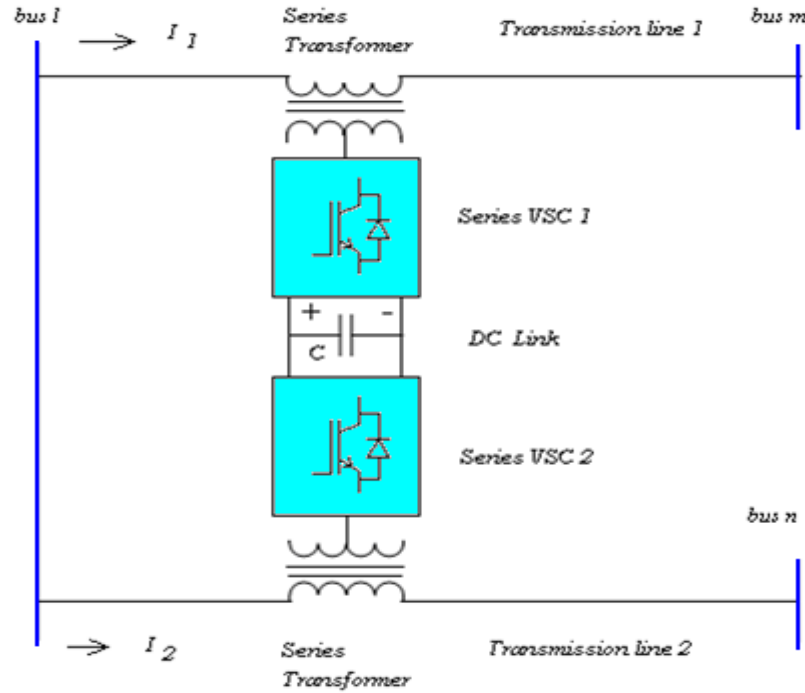


Figure 2.11: A schematic diagram of IPFC with two VSC converters

## 2.4 FACTS Controllers and Their Potential

As mentioned previously, FACTS devices are defined by IEEE as “alternating current transmission systems incorporating power electronic based and other static controller to enhance controllability and increase power transfer capability”. These devices dynamically control line impedance, line voltage, active power flow and reactive power and when storage becomes economically feasible; they can supply and absorb active power as well. All these activities are performed at high speed. There are also numerous controllers for FACTS devices and Table 2.1 shows a list of these controllers with their particular control attributes [39]. Their main control functions are mentioned at the beginning, and then followed by other functions. Generally, these functions are derived simultaneously with appropriate design specifications. Therefore, potentially, there can be more than one additional service from a FACTS controller [40].

Table 2.1: FACTS Devices and their Controller

| No | FACTS controller  | Control attributes  |
|----|---|---|
| 1  | Static VAR Compensator (SVC)                                    | Voltage control, VAR compensation, damping oscillation, transient and dynamic stability, voltage stability.   |
| 2  | Static Synchronous Compensator (STATCOM without storage)        | Voltage control, VAR compensation, damping Oscillation, voltage stability.  |
| 3  | Static Synchronous Compensator (STATCOM with storage)           | Voltage control, VAR compensation, damping oscillation, transient and dynamic stability, voltage stability, AGC.  |
| 4  | Thyristor Controlled Braking Resistor (TCBR)                    | Damping oscillation, transient and dynamic stability.   |
| 5  | Static Synchronous Series Compensator (SSSC without storage)    | Current control, damping oscillations, transient and dynamic stability, voltage stability, fault current limiting.  |
| 6  | Static Synchronous Series Compensator (SSSC with storage)       | Current control, damping oscillations, transient and dynamic stability, voltage stability.  |
| 7  | Thyristor Controlled Series Capacitor (TCSC)                    | Current control, damping oscillations, transient and dynamic stability, voltage stability, fault current limiting.  |
| 8  | Thyristor Controlled Series Reactor (TCSR)                      | Current control, damping oscillations, transient and dynamic stability, voltage stability, fault current limiting.  |
| 9  | Thyristor Controlled Voltage Regulator (TCVR)                   | Reactive power control, voltage control, damping oscillations, transient and dynamic stability, voltage stability.  |
| 10 | Thyristor Controlled Phase Shifting Transformer (TCPST or TCPR) | Active power control, damping oscillations, transient and dynamic stability, voltage stability.   |
| 11 | Unified Power Flow controller (UPFC)                            | Active and reactive power control, voltage control, VAR compensation, damping oscillations, transient and dynamic stability, voltage stability, fault current limiting. |
| 12 | Interline Power Flow Controller (IPFC)                          | Control active and reactive power flow.   |

## 2.5 Power Flow Representation in a Power System

In any power flow problem, it is required to have four variables at each bus  $l$  of the system; e.g.  $P_l$  is the net active bus power,  $Q_l$  is the net reactive bus power,  $V_l$  is the voltage magnitude at bus  $l$ , and  $\theta_l$  is the voltage phase angle. Only two of these four variables are known a priori and the load flow solution provides the solution of the remaining two variables at any bus [41]. The complex power injected by the source in the  $l^{\text{th}}$  bus of power system is

$$S_l = P_l + jQ_l = V_l I_l^* \quad ; l = 1, 2, \dots, N \quad (2.8)$$

The power flow is handled more conveniently by use of  $I_l$  rather than  $I_l^*$  [42], and the complex conjugate of Equation (2.8), is expressed as

$$S_l^* = P_l - jQ_l = I_l V_l^* \quad ; l = 1, 2, \dots, N \quad (2.9)$$

As  $I_{bus} = Y_{bus} V_{bus}$ , the relation between the injected node currents and the voltages, for the  $l^{\text{th}}$  bus is in the form,

$$\begin{bmatrix} I_1 \\ I_2 \\ \vdots \\ I_n \end{bmatrix} = \begin{bmatrix} Y_{11} & Y_{12} & \cdots & Y_{1n} \\ Y_{21} & Y_{22} & \cdots & Y_{2n} \\ \vdots & \vdots & & \vdots \\ Y_{n1} & Y_{n2} & \cdots & Y_{nn} \end{bmatrix} \begin{bmatrix} V_1 \\ V_2 \\ \vdots \\ V_n \end{bmatrix} \quad (2.10a)$$

$$I_l = \sum_{\substack{k=1 \\ k \neq l}}^N Y_{lk} V_k \quad (2.10b)$$

where  $I_l$  is the net current injected into the network at bus  $l$ .

Representing the complex voltage in a polar form and complex admittance in rectangular form,.

$$V_l = [V_l] e^{j\theta_l}$$

$$V_k = [V_k] e^{j\theta_k}$$

$$Y_{lk} = [Y_{lk}] e^{j\theta_{lk}} = [Y_{lk}] (\cos \theta_{lk} + j \sin \theta_{lk}) = G_{lk} + jB_{lk}$$

where  $Y_{lk}$ ,  $G_{lk}$  and  $B_{lk}$  are called admittance, conductance and susceptance of the branch  $l-k$  respectively. Substituting the above values in equation (2.9).

$$\begin{aligned}
P_l - Q_l &= V_l^* I_l = [V_l] e^{-j\theta_l} \sum_{k=1}^N [V_k] e^{-j\theta_k} (G_{lk} + jB_{lk}) \\
&= \sum_{k=1}^N [V_l][V_k] e^{-j(\theta_k - \theta_l)} (G_{lk} + jB_{lk}) \\
&= \sum_{k=1}^N [V_l][V_k] [\cos(\theta_l - \theta_k) - j \sin(\theta_l - \theta_k)] (G_{lk} + jB_{lk}) \\
&= \sum_{k=1}^N [V_l][V_k] [G_{lk} \cos(\theta_l - \theta_k) + jB_{lk} \sin(\theta_l - \theta_k) \\
&\quad - jG_{lk} \sin(\theta_l - \theta_k) - B_{lk} \cos(\theta_l - \theta_k)] \\
&= \sum_{k=1}^N [V_l][V_k] [(G_{lk} \cos(\theta_l - \theta_k) + B_{lk} \sin(\theta_l - \theta_k)) \\
&\quad + j(-G_{lk} \sin(\theta_l - \theta_k) + B_{lk} \cos(\theta_l - \theta_k))]
\end{aligned} \tag{2.11}$$

Hence, by separating the real and imaginary parts of equation (2.11),

$$P_l = \sum_{k=1}^N [V_l][V_k] [G_{lk} \cos(\theta_l - \theta_k) + B_{lk} \sin(\theta_l - \theta_k)] \tag{2.12}$$

$$Q_l = \sum_{k=1}^N [V_l][V_k] [G_{lk} \sin(\theta_l - \theta_k) - B_{lk} \cos(\theta_l - \theta_k)] \tag{2.13}$$

Thus Equations (2.12) and (2.13) represent the general formula for the active and reactive power injections in a power system.

### 2.5.1 Power Flow Representation with IPFC

The equivalent circuit of the IPFC with two converters is shown in Figure 2.12.

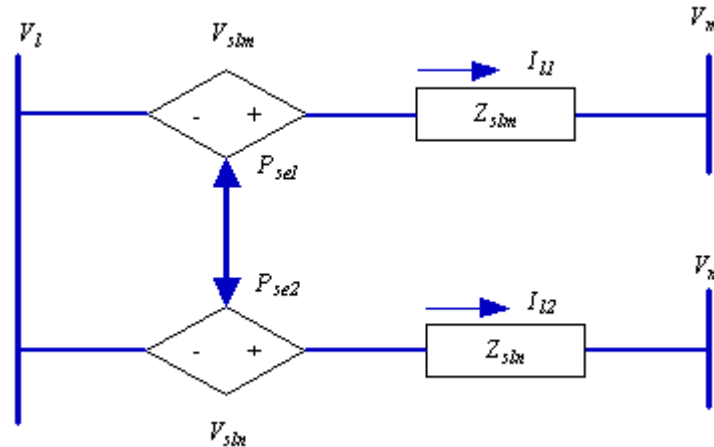


Figure 2.12: Equivalent circuit of the IPFC with two converters

where  $V_l, V_m$  and  $V_n$  represent the voltages at buses  $l, m$  and  $n$ .  $V_{slm}$  and  $V_{sln}$  represent

the injected voltage sources at branches  $l-m$  and  $l-n$  respectively.  $Z_{slm}$  and  $Z_{sln}$  are the series transformer impedances; whereas,  $P_{se1}$  and  $P_{se2}$  are the active powers exchanged through the DC link.

From the equivalent circuit of IPFC and from equations (2.12) and (2.13), assuming  $k=m, n$ , the power flow equations of IPFC are obtained as follows:

The active power injected into bus  $l$  is

$$\begin{aligned}
P_l &= [V_l][V_l][G_{ll} \cos(\theta_l - \theta_l) + B_{ll} \sin(\theta_l - \theta_l)] \\
&\quad - [V_l][V_m][G_{lm} \cos(\theta_l - \theta_m) + B_{lm} \sin(\theta_l - \theta_m)] \\
&\quad - [V_l][V_{slm}][G_{lslm} \cos(\theta_l - \theta_{slm}) + B_{lslm} \sin(\theta_l - \theta_{slm})] \\
&= [V_l]^2 G_{ll} - [V_l][V_m][G_{lm} \cos(\theta_l - \theta_m) + B_{lm} \sin(\theta_l - \theta_m)] \\
&\quad - [V_l][V_{slm}][G_{lslm} \cos(\theta_l - \theta_{slm}) + B_{lslm} \sin(\theta_l - \theta_{slm})] \\
&= [V_l]^2 G_{ll} - [V_l][V_m][G_{lm} \cos(\theta_l - \theta_m) + B_{lm} \sin(\theta_l - \theta_m)] \\
&\quad - [V_l][V_{slm}][G_{lm} \cos(\theta_l - \theta_{slm}) + B_{lm} \sin(\theta_l - \theta_{slm})]
\end{aligned} \tag{2.14}$$

The reactive power injected into the bus  $l$ ,

$$\begin{aligned}
Q_l &= [V_l][V_l][G_{ll} \sin(\theta_l - \theta_l) - B_{ll} \cos(\theta_l - \theta_l)] \\
&\quad - [V_l][V_m][G_{lm} \sin(\theta_l - \theta_m) - B_{lm} \cos(\theta_l - \theta_m)] \\
&\quad - [V_l][V_{slm}][G_{lslm} \sin(\theta_l - \theta_{slm}) - B_{lslm} \cos(\theta_l - \theta_{slm})] \\
&= -[V_l]^2 B_{ll} - [V_l][V_m][G_{lm} \sin(\theta_l - \theta_m) - B_{lm} \cos(\theta_l - \theta_m)] \\
&\quad - [V_l][V_{slm}][G_{lslm} \sin(\theta_l - \theta_{slm}) - B_{lslm} \cos(\theta_l - \theta_{slm})] \\
&= -[V_l]^2 B_{ll} - [V_l][V_m][G_{lm} \sin(\theta_l - \theta_m) - B_{lm} \cos(\theta_l - \theta_m)] \\
&\quad - [V_l][V_{slm}][G_{lm} \sin(\theta_l - \theta_{slm}) - B_{lm} \cos(\theta_l - \theta_{slm})]
\end{aligned} \tag{2.15}$$

where  $G_{lm} = G_{lslm}$  and  $B_{lm} = B_{lslm}$

The active power injected into bus  $m$ ,

$$\begin{aligned}
P_m &= [V_m][V_m][G_{mm} \cos(\theta_m - \theta_m) + B_{mm} \sin(\theta_m - \theta_m)] \\
&\quad - [V_m][V_l][G_{ml} \cos(\theta_m - \theta_l) + B_{ml} \sin(\theta_m - \theta_l)] \\
&\quad + [V_m][V_{slm}][G_{mslm} \cos(\theta_m - \theta_{slm}) + B_{mslm} \cos(\theta_m - \theta_{slm})] \\
&= [V_m]^2 G_{mm} - [V_m][V_l][G_{ml} \cos(\theta_m - \theta_l) + B_{ml} \sin(\theta_m - \theta_l)] \\
&\quad + [V_m][V_{slm}][G_{mslm} \cos(\theta_m - \theta_{slm}) + B_{mslm} \cos(\theta_m - \theta_{slm})]
\end{aligned} \tag{2.16}$$

and the reactive power injected into bus  $m$ ,

$$\begin{aligned}
Q_m &= [V_m][V_m][G_{mm} \sin(\theta_m - \theta_m) - B_{mm} \cos(\theta_m - \theta_m)] \\
&\quad - [V_m][V_l][G_{ml} \sin(\theta_m - \theta_l) - B_{ml} \cos(\theta_m - \theta_l)] \\
&\quad + [V_m][V_{slm}][G_{mslm} \sin(\theta_m - \theta_{slm}) - B_{mslm} \cos(\theta_m - \theta_{slm})] \\
&= -[V_m]^2 B_{mm} - [V_m][V_l][G_{ml} \sin(\theta_m - \theta_l) - B_{ml} \cos(\theta_m - \theta_l)] \\
&\quad + [V_m][V_{slm}][G_{ml} \sin(\theta_m - \theta_{slm}) - B_{ml} \cos(\theta_m - \theta_{slm})]
\end{aligned} \tag{2.17}$$

where  $G_{mslm} = G_{ml}$  and  $B_{mslm} = B_{ml}$

The active power injected into bus  $n$ ,

$$\begin{aligned}
P_n &= [V_n][V_n][G_{nn} \cos(\theta_n - \theta_n) + B_{nn} \sin(\theta_n - \theta_n)] \\
&\quad - [V_n][V_l][G_{nl} \cos(\theta_n - \theta_l) + B_{nl} \sin(\theta_n - \theta_l)] \\
&\quad + [V_n][V_{sln}][G_{nsln} \cos(\theta_n - \theta_{sln}) + B_{nsln} \cos(\theta_n - \theta_{sln})] \\
&= [V_n]^2 G_{nn} - [V_n][V_l][G_{nl} \cos(\theta_n - \theta_l) + B_{nl} \sin(\theta_n - \theta_l)] \\
&\quad + [V_n][V_{sln}][G_{nsln} \cos(\theta_n - \theta_{sln}) + B_{nsln} \cos(\theta_n - \theta_{sln})]
\end{aligned} \tag{2.18}$$

and the reactive power injected into bus  $n$ ,

$$\begin{aligned}
Q_n &= [V_n][V_n][G_{nn} \sin(\theta_n - \theta_n) - B_{nn} \cos(\theta_n - \theta_n)] \\
&\quad - [V_n][V_l][G_{nl} \sin(\theta_n - \theta_l) - B_{nl} \cos(\theta_n - \theta_l)] \\
&\quad + [V_n][V_{sln}][G_{nsln} \sin(\theta_n - \theta_{sln}) - B_{nsln} \cos(\theta_n - \theta_{sln})] \\
&= -[V_n]^2 B_{nn} - [V_n][V_l][G_{nl} \sin(\theta_n - \theta_l) - B_{nl} \cos(\theta_n - \theta_l)] \\
&\quad + [V_n][V_{sln}][G_{nl} \sin(\theta_n - \theta_{sln}) - B_{nl} \cos(\theta_n - \theta_{sln})]
\end{aligned} \tag{2.19}$$

where  $G_{nsln} = G_{nl}$  and  $B_{nsln} = B_{nl}$

Assuming loss less converter, the active power supplied to one converter is equal to the active power demanded by the other converter [14].

The active power injected by VSC<sub>1</sub>,



$$\begin{aligned}
P_{slm} &= [V_{slm}] [V_{slm}] [G_{slmslm} \cos(\theta_{slm} - \theta_{slm}) + B_{slmslm} \sin(\theta_{slm} - \theta_{slm})] \\
&\quad - [V_{slm}] [V_l] [G_{slml} \cos(\theta_{slm} - \theta_l) + B_{slml} \sin(\theta_{slm} - \theta_l)] \\
&\quad + [V_{slm}] [V_m] [G_{slmm} \cos(\theta_{slm} - \theta_m) + B_{slmm} \cos(\theta_{slm} - \theta_m)] \\
&= [V_{slm}]^2 G_{slmslm} - [V_{slm}] [V_l] [G_{slml} \cos(\theta_{slm} - \theta_l) + B_{slml} \sin(\theta_{slm} - \theta_l)] \\
&\quad + [V_{slm}] [V_m] [G_{slmm} \cos(\theta_{slm} - \theta_m) + B_{slmm} \cos(\theta_{slm} - \theta_m)] \\
&= [V_{slm}]^2 G_{ml} - [V_{slm}] [V_l] [G_{ml} \cos(\theta_{slm} - \theta_l) + B_{ml} \sin(\theta_{slm} - \theta_l)] \\
&\quad + [V_{slm}] [V_m] [G_{ml} \cos(\theta_{slm} - \theta_m) + B_{ml} \cos(\theta_{slm} - \theta_m)]
\end{aligned} \tag{2.20}$$

The reactive power injected by VSC<sub>1</sub>,

$$\begin{aligned}
Q_{slm} &= [V_{slm}] [V_{slm}] [G_{slmslm} \sin(\theta_{slm} - \theta_{slm}) - B_{slmslm} \cos(\theta_{slm} - \theta_{slm})] \\
&\quad - [V_{slm}] [V_l] [G_{slml} \sin(\theta_{slm} - \theta_l) - B_{slml} \cos(\theta_{slm} - \theta_l)] \\
&\quad + [V_{slm}] [V_m] [G_{slmm} \sin(\theta_{slm} - \theta_m) - B_{slmm} \cos(\theta_{slm} - \theta_m)] \\
&= -[V_{slm}]^2 B_{slmslm} - [V_{slm}] [V_l] [G_{slml} \sin(\theta_{slm} - \theta_l) - B_{slml} \cos(\theta_{slm} - \theta_l)] \\
&\quad + [V_{slm}] [V_m] [G_{slmm} \sin(\theta_{slm} - \theta_m) - B_{slmm} \cos(\theta_{slm} - \theta_m)] \\
&= -[V_{slm}]^2 B_{ml} - [V_{slm}] [V_l] [G_{ml} \sin(\theta_{slm} - \theta_l) - B_{ml} \cos(\theta_{slm} - \theta_l)] \\
&\quad + [V_{slm}] [V_m] [G_{ml} \sin(\theta_{slm} - \theta_m) - B_{ml} \cos(\theta_{slm} - \theta_m)]
\end{aligned} \tag{2.21}$$

where  $G_{slmslm} = G_{ml}$  and  $B_{slmslm} = B_{ml}$ . The active power injected by VSC<sub>2</sub>,

$$\begin{aligned}
P_{sln} &= [V_{sln}] [V_{sln}] [G_{slnsln} \cos(\theta_{sln} - \theta_{sln}) + B_{slnsln} \sin(\theta_{sln} - \theta_{sln})] \\
&\quad - [V_{sln}] [V_l] [G_{slnl} \cos(\theta_{sln} - \theta_l) + B_{slnl} \sin(\theta_{sln} - \theta_l)] \\
&\quad + [V_{sln}] [V_n] [G_{slnn} \cos(\theta_{sln} - \theta_n) + B_{slnn} \cos(\theta_{sln} - \theta_n)] \\
&= [V_{sln}]^2 G_{slnsln} - [V_{sln}] [V_l] [G_{slnl} \cos(\theta_{sln} - \theta_l) + B_{slnl} \sin(\theta_{sln} - \theta_l)] \\
&\quad + [V_{sln}] [V_n] [G_{slnn} \cos(\theta_{sln} - \theta_n) + B_{slnn} \cos(\theta_{sln} - \theta_n)] \\
&= [V_{sln}]^2 G_{nl} - [V_{sln}] [V_l] [G_{nl} \cos(\theta_{sln} - \theta_l) + B_{nl} \sin(\theta_{sln} - \theta_l)] \\
&\quad + [V_{sln}] [V_n] [G_{nl} \cos(\theta_{sln} - \theta_n) + B_{nl} \cos(\theta_{sln} - \theta_n)]
\end{aligned} \tag{2.22}$$

The reactive power injected by VSC<sub>2</sub>,

$$\begin{aligned}
Q_{sln} &= [V_{sln}] [V_{sln}] [G_{slnsln} \sin(\theta_{sln} - \theta_{sln}) - B_{slnsln} \cos(\theta_{sln} - \theta_{sln})] \\
&\quad - [V_{sln}] [V_l] [G_{slnl} \sin(\theta_{sln} - \theta_l) - B_{slnl} \cos(\theta_{sln} - \theta_l)] \\
&\quad + [V_{sln}] [V_n] [G_{slnn} \sin(\theta_{sln} - \theta_n) - B_{slnn} \cos(\theta_{sln} - \theta_n)] \\
&= -[V_{sln}]^2 B_{slnsln} - [V_{sln}] [V_l] [G_{slnl} \sin(\theta_{sln} - \theta_l) - B_{slnl} \cos(\theta_{sln} - \theta_l)] \\
&\quad + [V_{sln}] [V_n] [G_{slnn} \sin(\theta_{sln} - \theta_n) - B_{slnn} \cos(\theta_{sln} - \theta_n)] \\
&= -[V_{sln}]^2 B_{nl} - [V_{sln}] [V_l] [G_{nl} \sin(\theta_{sln} - \theta_l) - B_{nl} \cos(\theta_{sln} - \theta_l)] \\
&\quad + [V_{sln}] [V_n] [G_{nl} \sin(\theta_{sln} - \theta_n) - B_{nl} \cos(\theta_{sln} - \theta_n)]
\end{aligned} \tag{2.23}$$

where  $G_{slnsln} = G_{nl}$  and  $B_{slnsln} = B_{nl}$ .

### 2.5.2 General Power Flow Expressions with IPFC

From the equations (2.14) to (2.23) derived in section 2.5.1, the general form of active and reactive power flow expressions of IPFC branches leaving buses  $l$ ,  $m$ , and  $n$  are expressed as follows.

The active and reactive powers at the sending end,

$$P_{lk} = [V_l]^2 G_{lk} - [V_l][V_k][G_{lk} \cos(\theta_l - \theta_k) + B_{lk} \sin(\theta_l - \theta_k)] - [V_l][V_{slk}][G_{lk} \cos(\theta_l - \theta_{slk}) + B_{lk} \cos(\theta_l - \theta_{slk})] \quad (2.24)$$

$$Q_{lk} = -[V_l]^2 B_{lk} - [V_l][V_k][G_{lk} \sin(\theta_l - \theta_k) - B_{lk} \cos(\theta_l - \theta_k)] - [V_l][V_{slk}][G_{lk} \sin(\theta_l - \theta_{slk}) - B_{lk} \cos(\theta_l - \theta_{slk})] \quad (2.25)$$

The active and reactive powers at the receiving end,

$$P_{kl} = [V_{kl}]^2 G_{lk} - [V_k][V_l][G_{lk} \cos(\theta_k - \theta_l) + B_{lk} \sin(\theta_k - \theta_l)] + [V_k][V_{slk}][G_{lk} \cos(\theta_k - \theta_{slk}) + B_{lk} \cos(\theta_k - \theta_{slk})] \quad (2.26)$$

$$Q_{kl} = -[V_k]^2 B_{lk} - [V_k][V_l][G_{lk} \sin(\theta_k - \theta_l) - B_{lk} \cos(\theta_k - \theta_l)] + [V_k][V_{slk}][G_{lk} \sin(\theta_k - \theta_{slk}) - B_{lk} \cos(\theta_k - \theta_{slk})] \quad (2.27)$$

where  $P_{lk}$  ( $k = m, n$ ) is the active power flow injection at node  $l$ .

$Q_{lk}$  ( $k = m, n$ ) is the reactive power flow injection at node  $l$ .

$P_{kl}$  ( $k = m, n$ ) is the active power flow injection at node  $k$ .

$Q_{kl}$  ( $k = m, n$ ) is the reactive power flow injection at node  $k$ .

$Y_{lk} = G_{lk} + jB_{lk}$  ( $k = m, n$ ).  $Y_{lk}$ ,  $G_{lk}$  and  $B_{lk}$  are the admittance, conductance, and susceptance of branches  $l-m$  and  $l-k$ , respectively.

$$Y_{slk} = G_{lk} + jB_{lk} , G_{ll} = G_{lk} , B_{ll} = B_{lk} , G_{mm} = G_{lk} , B_{mm} = B_{lm} , G_{nn} = G_{ln} \text{ and } B_{nn} = B_{ln} .$$

The two VSCs are series connected in branches  $l-m$  and  $l-n$  of the two transmission lines. The real and reactive power mismatches at buses  $l$ ,  $m$  and  $n$  of the IPFC must be satisfied by the following condition.

$$\Delta P_i = P_{gi} - P_{di} - P_i = 0 \quad (2.28)$$

$$\Delta Q_i = Q_{gi} - Q_{di} - Q_i = 0 \quad (2.29)$$

where,  $P_{gi}$  and  $Q_{gi}$  ( $i = l, m, n$ ) are the real and the reactive power generation entering the bus  $i$ .  $P_{di}$  and  $Q_{di}$  ( $i = l, m, n$ ) are the real and the reactive power load leaving the bus  $i$ .  $P_i$  and  $Q_i$  ( $i = l, m, n$ ) are the sum of real and reactive power flow of the circuit connected to bus  $i$ , which include the power flow.

### 2.5.3 Operating Modes of IPFC

For the series injected voltage,  $V_{slk}$  of the VSC of IPFC, the operating constraint limits are [12, 44].

$$V_{slk}^{\min} \leq V_{slk} \leq V_{slk}^{\max} (k = m, n) \quad (2.30)$$

and for the phase angle,  $\theta_{slk}$

$$\theta_{slk}^{\min} \leq \theta_{slk} \leq \theta_{slk}^{\max} (k = m, n) \quad (2.31)$$

The range of operation for line current magnitude through the series VSC,

$$I_{lk}^{\min} \leq I_{lk} \leq I_{lk}^{\max} (k = m, n) \quad (2.32)$$

The MVA rating of the VSC,

$$[S_{slk}] \leq S_{slk}^{\max} (k = m, n) \quad (2.33)$$

where  $S_{slk}$  is the complex power injected in to the line by the series VSC

The circulated real power  $P_{slk}$  is limited to its maximum value as

$$[P_{slk}] \leq P_{slk}^{\max} (k = m, n) \quad (2.34)$$

#### 2.5.4 Transmission Line Loss

In order to find the transmission line losses, consider a line connecting between two buses  $l$  and  $k$  [45], the line current at bus  $l$  which is positive and measured in the direction of  $l$  to  $k$  is

$$I_{lk} = Y_{lk} (V_l - V_k) \quad (2.35)$$

The line current at bus  $k$ , measured in the direction of  $k$  to  $l$  is,

$$I_{kl} = Y_{lk} (V_k - V_l) \quad (2.36)$$

The complex powers  $S_{lk}$  from bus  $l$  to  $k$  and  $S_{kl}$  from bus  $k$  to  $l$  are

$$S_{lk} = V_l I_{lk} \quad (2.37)$$

$$S_{kl} = V_k I_{kl} \quad (2.38)$$

The power loss in line  $l$ - $k$  is the algebraic sum of the power flows in (2.37) and (2.38)

$$S_{Losslk} = S_{lk} + S_{kl} \quad (2.39)$$

From equation (2.39) the active power and reactive power loss can be expressed as follows:

$$P_{Losslk} = \text{real}(S_{losslk}) \quad (2.40)$$

$$Q_{Losslk} = \text{imag}(S_{losslk}) \quad (2.41)$$

## 2.6 Modified Newton Raphson Power Flow Algorithm

Figure 2.13 show the modified Newton Raphson algorithm used in this study.

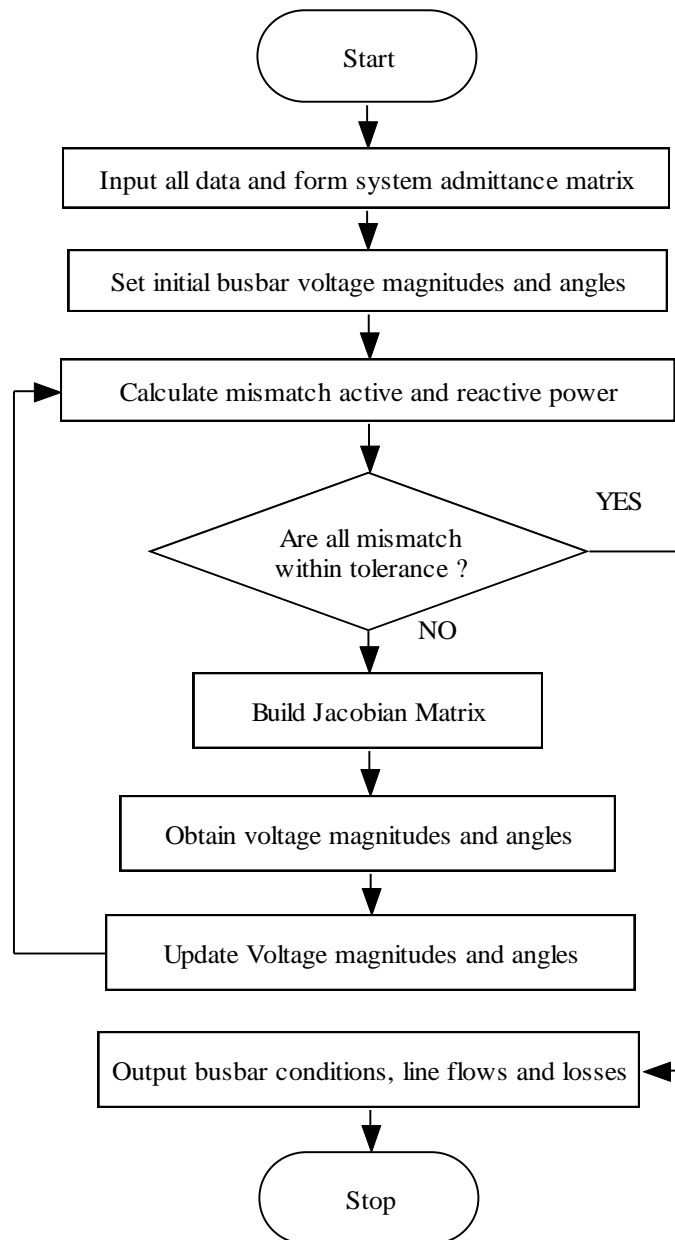


Figure 2.13: Modified Newton Raphson method

## **2.7 Summary**

This chapter has introduced flexible AC transmission system (FACTS), its objectives, benefits and types, respectively. Classification of FACTS controllers according to Thyristor-based FACTS controllers and VSC-based FACTS controllers have been discussed too. Intensive literature survey on one of the latest VSC-based FACTS controllers or well known as Interline Power Flow Controller (IPFC) has been reported. Also a brief explanation on general power flow analysis and representation of IPFC in power flow equations in a power system are discussed. The mathematical model governing IPFC operation and the operation modes were considered. Finally, a flowchart of modified Newton-Raphson method power flow and outline of the transmission line losses were also discussed as well.

## CHAPTER 3

### RESEARCH METHODOLOGY

#### 3.1 Introduction

Optimization methods have been extensively used in electrical power system operation, planning and analysis. Table 3.1 shows some papers recently published in the literature related with the main scope of three optimization techniques used in this thesis. The application of IPFC in power systems generating optimal power flow is becoming more important because of its capabilities to deal with various situations. The problem of optimal power flow involves the optimization of objective functions that can take various forms while satisfying a set of operational and physical constraints. This chapter provides an overview of three optimization techniques used, which is the main scope of the study. The second section covers the basics and an extensive literature on Particle Swarm Optimization (PSO) technique, and its algorithm. Section 3.3 covers an overview of Genetic Algorithm (GA), its control parameters and algorithm. Section 3.4 gives a brief review on Simulated Annealing (SA) and its algorithm. The last section concludes the chapter.

Table 3.1: Some papers related with PSO, GA and SA optimization techniques

| Years | Paper title related with   |   |  | Authors   |  |   |
|-------|--|---|--|---|--|---|
|       | PSO  | GA  | SA   | PSO   | GA   | SA  |
| 2005  | Application of PSO technique for optimal location of FACTS devices considering system loadability and cost of installation [46]. | Genetic algorithm based control for VSC HVDC [47].  | Power losses on distribution network: estimation using simulated annealing [48].                                   | M. Saravanan, S. Mary Raja Slochanal, P. Venkatesh, Prince Stephen Abraham. J | Hu Zhaoqing, Mao Chengxiong, Lu Jiming, Chen Man | B. A. deSouza, A. A. Sousa, J. M. C. de Albuquerque |
| 2006  | Power Flow Control in FACTS Using Particle Swarm Optimization [49].  | Optimal Location of UPFC in Power Systems for Increasing Loadability by Genetic Algorithm [50]. | Combined genetic algorithm and simulated annealing for preventive unit maintenance scheduling in power system[51]. | S.Jeyadevi S.Baskar   | A. Kazemi, D. Arabkhabori, M.Yari, J. Aghaei     | K. Suresh, N. Kumarappan                            |

### 3.1: Some papers related with PSO, GA and SA optimization techniques

| Years | Paper title related with   |  |   | Authors                                   |   |   |
|-------|--|--|---|---|---|---|
|       | PSO  | GA   | SA  | PSO                                       | GA  | SA  |
| 2007  | Optimal Location and Parameters Setting of Unified Power Flow Controller Based on Evolutionary Optimization Techniques [52]. | Optimal Location and Parameter Setting of TCSC by Both Genetic Algorithm and Particle Swarm Optimization[53]                     | Unit Commitment Using Particle Swarm-Based-Simulated Annealing Optimization Approach [54].                                      | H. I. Shaheen, G. I. Rashed, S. J. Cheng, | G.I.Rashed, H.I. Shaheen, S.J. Cheng                            | Nasser Sadati, Mahdi Hajian Majid Zamani        |
| 2008  | Evolutionary Optimization Techniques for Optimal Location and Parameter Settings of TCSC Under Single Line Contingency [55]. | Improvement of Voltage Stability and Reduce Power System Losses by Optimal GA-based Allocation of Multi-type FACTS Devices [56]. | Optimal Reactive Power Planning Based on Simulated Annealing Particle Swarm Algorithm Considering Static Voltage Stability[57]. | G. I. Rashed, H. I. Shaheen, S. J. Cheng  | H.R.Baghaee, M. Jannati, B. Vahidi, S.H.Hosseinian, H. Rastegar | Mao Yingni, Li Maojun                           |
| 2009  | Optimal Placement of FACTS devices for Multi-Objective Voltage Stability Problem[58].  | Application of HSA and GA in Optimal Placement of FACTS Devices Considering Voltage Stability and Losses [59].                   | Active power loss minimization with FACTS devices using SA/PSO technique [60].  | R. Benabid, M. Boudour M. A. Abido        | A.Parizad, A.Khazali, M. Kalantar,                              | S. Majumdar, A K Chakraborty, P.K.Chattopadhyay |

### 3.2 Particle Swarm Optimization (PSO) Technique

PSO is a population based optimization technique proposed in 1995 by James Kennedy and Russell Eberhart [61]. Generally, PSO is based on the simulation of simplified social model, and artificial life such as fish schooling and bird flocking specially [62]. Also PSO is an evolutionary programming method similar to GA which is used for global optimal design [61]. The PSO technique has a simple concept which can be implemented with a simple computer code. The PSO begins with random initial number of particles or agents in a multidimensional space.

The modification concept of current position by the particle is shown in Figure 3.1. Each particle tried to modify its velocity and position based on its own previous experience and the other neighboring particles of the swarm. For instance; the particle  $i$ , is randomly placed in two dimensional search space at the point  $X_i^k$ , this particle flies through the problem search space with a random velocity  $V_i^k$ . The particle remembers the best position achieved so far and stores it as  $Pbest_i^k$ . Then, each



particle shares the information with the neighboring particles. In other words, each particle compares its best position with those attained by other particles. Finally, each particle stores the best position achieved in the whole swarm which is called  $Gbest_i^k$  [63].

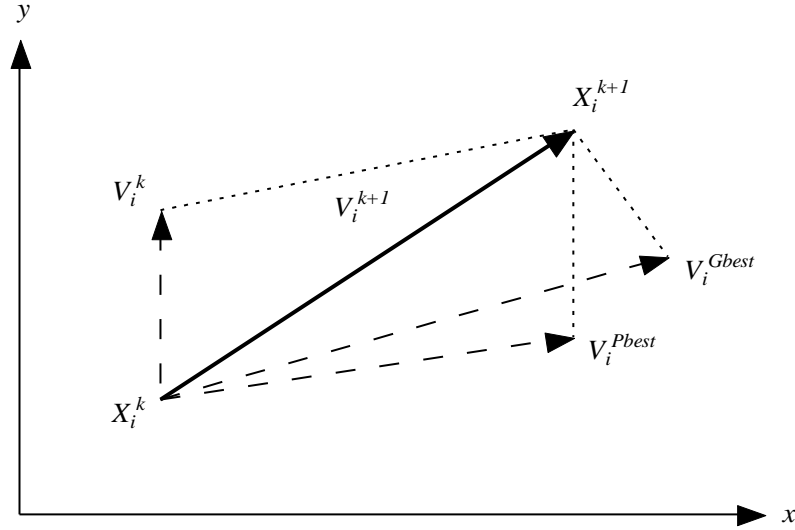


Figure 3.1: Modification of current position by PSO

In PSO algorithm each particle  $i$  is represented in a N-dimension space by its current position  $X_i = (X_{i1}, X_{i2}, \dots, X_{iN})$  and its corresponding velocity,  $V_i = (V_{i1}, V_{i2}, \dots, V_{iN})$ . In each iteration the particle,  $i$  modify its position depending on the history of the previous position and velocity information. Also the value of the fitness for particle and personal best position is represented by,  $P_i = (P_{i1}, P_{i2}, \dots, P_{iN})$  called Pbest, the subscript  $i$  range from 1 to S, where S indicates the size of the swarm, which contains the information on position and velocities. This information is the analogy of personal experience of each particle  $i$ . Moreover, each particle  $i$  knows its best value so far in the group called Gbest among the set of values Pbest. This information is the analogy of knowledge, how the other neighboring particles have performed. Pbest and Gbest denote the individual intelligence and the group intelligence [64, 65].

PSO is used to search a point, and the searching points gradually get close to the global optimal point using its Pbest and Gbest. The searching concept with particles in a solution space is shown in Figure 3.2.

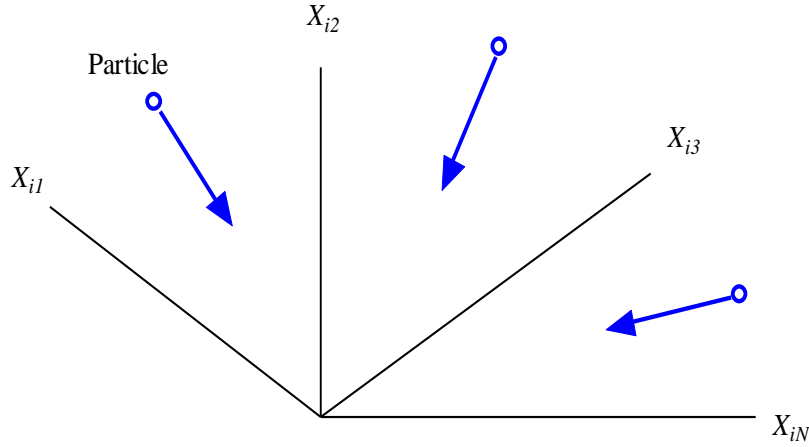


Figure 3.2: Particles in a solution space

After finding the best values the particles update its velocity and position as in equations (3.1) and (3.2).

$$V_i^{k+1} = W * V_i^k + C_1 * rand_1 * (Pbest_i^k - X_i^k) + C_2 * rand_2 * (Gbest_i^k - X_i^k) \quad (3.1)$$

$$X_i^{k+1} = X_i^k + V_i^{k+1} \quad (3.2)$$

where  $V_i^k$  is the current velocity of particle  $i$  at  $k^{th}$  iteration,  $V_i^{k+1}$  is the modified velocity of particle  $i$  at  $(k+1)^{th}$  iteration,  $W$  is the inertia weight factor,  $rand_1$  and  $rand_2$  are the random numbers between 0 and 1,  $Pbest_i^k$  is the best value found by particle  $i$  until iteration  $k$ ,  $Gbest_i^k$  is the best particle found in the group until iteration  $k$ ,  $X_i^k$  is the current position of the particle  $i$  at  $k^{th}$  iteration and  $X_i^{k+1}$  is the current position of the particle  $i$  at  $(k+1)^{th}$  iteration.

In equation (3.1) the first term  $W * V_i^k$  on the right hand side represent the previous velocity of the particle. The second and third terms,  $(C_1 * rand_1 * (Pbest_i - S_i^k))$  and  $(C_2 * rand_2 * (Gbest_i - S_i^k))$  are utilized to change the velocity of the particle. Without these terms the particle will keep searching in the same direction until it hits the

boundary. i.e., the particle tried to explore new area and, therefore, the first term corresponds with diversification in the search procedure. Generally, without the first term the velocity of the particle is only determined by using its current and best position in the history. i.e., the particle will try to converge to their Pbest and Gbest, therefore this term correspond with intensification in search procedure, [66]. Generally the individual movement of the particle is represented by the second term, and the social behavior to find the best global solution is represented by the third term [67].

### 3.2.1 Element of the Particle Swarm Optimization

When implementing the particle swarm optimization algorithm, a number of considerations should be taken into account to facilitate the convergence and prevent an “explosion” of the swarm. These considerations include swarm size, the Velocity of the particle  $V_i$ , Particle's position  $X_i$ , Inertia Weight  $W$ , selecting acceleration constants or Weighting Factors  $C_1$  and  $C_2$ .

#### 3.2.1.1 Swarm Size

It is the set of particles initialized randomly that tends to group together as they move towards the global best position [63].

#### 3.2.1.2 Velocity of the Particle

The velocity at which the  $i^{\text{th}}$  particle flies in a N-dimensional search space  $V_i = (V_{i1}, V_{i2} \dots V_{iN})$  [63]. The particle velocity should be fixed between  $V_i^{\min} \leq V_i \leq V_i^{\max}$ , where the parameter  $V_i^{\max}$  is used to determine the resolution with which the design space is to be searched between the present position and the target position. If  $V_i^{\max}$  is too high, the particles might fly past good solutions. And if  $V_i^{\max}$  is too small, particles may not explore sufficiently beyond local solutions. Typically, a range between -0.5 and 0.5 is normally adopted [68].

#### 3.2.1.3 Particle's Position

In PSO algorithm, the  $i^{\text{th}}$  particles is represented in an N-dimension vector by its current position  $X_i = (X_{i1}, X_{i2}, \dots, X_{iN})$  which represents a candidate solution, where N

is the number of optimized parameters,  $X_s$  are optimized parameters,  $X_{iN}$  is the position of the  $i^{th}$  particle with respect to  $N^{th}$  dimension [69].

### 3.2.1.4 Inertia Weight Approach PSO (IWAPSO)

An inertia weight  $W$ , in the PSO algorithm was introduced in 1998, in order to provide better control exploration [70]. The inertia weight is used to control the impact of the previous history of velocity, and thus to influence the tradeoff between global and local exploration abilities of the moving agent.

In other words, the inertia weight of PSO is a mechanism used to control the exploration and exploitation abilities of the swarm and as a mechanism to reduce the need for velocity clamping.

It has been shown that from experiments, PSO with increasing inertia weight gives better performance with quick convergence capability and aggressive movement narrowing towards the solution region [71]. In the BPSO the inertia weight is taken as a constant 1.2, where as in the IWAPSO the inertia weight is suggested to increase linearly from 0.4 to 0.9 during the simulation [64, 68]. The inertia weight is formulated as in equations (3.3):

$$W = W_{\max} - \left[ \frac{W_{\max} - W_{\min}}{iter_{\max}} \right] * iter \quad (3.3)$$

where  $W$  is the inertia weight factor,  $W_{\max}$  is the initial value of the inertia weight,  $W_{\min}$  is the final value of the inertia weight,  $iter_{\max}$  is the maximum iteration number and  $iter$  is the current iteration number.

As mentioned previously, for instance if  $W_{\max} = 0.9$  and  $W_{\min} = 0.4$ , the diversification is heavily weighted at the beginning of search procedure, while the intensification is heavily weighted at the end of the search procedure. A certain velocity, which gradually gets close to Pbests and Gbests, can be calculated. PSO using equations (3.1) and (3.3) is called inertia weight approach (IWAPSO) [66].

### 3.2.1.5 Weighting Factors $C_1$ and $C_2$

The two constants,  $C_1$  and  $C_2$ , representing the weighting factors of the acceleration terms that pull each particle  $i$  toward the  $Pbest_i$  and  $Gbest_i$  positions. The constants  $C_1$  and  $C_2$  should be within the range between 0 and 4 [65] are tuned in the process. It is observed that low values allow particles to move far from the target regions before being tugged back [68].

### 3.2.1.6 Best Particle's Position

The particle's best position is related with the best fitness value that was ever visited during the search. In other words as a particle moves all the way through the search space, it compares its fitness value at the current position to the best fitness value it has ever attained at any time up to the present time [69]. The best position that is connected with the best fitness encountered so far is called the personal best value  $Pbest$ . Therefore, the personal best position of the  $i^{th}$  particle is represented by,  $P_i = (P_{i1}, P_{i2}, \dots, P_{iN})$  where  $P_i$  can be determined and modified during the search for each particle in the swarm.

### 3.2.1.7 Global Best Position

It is the best position that is ever encountered by all particles so far and is called the  $Gbest$ .

### 3.2.1.8 Stopping Criteria

It is the condition under which the search procedures for the optimal solution stop. In other words the stopping criteria in this thesis are, good fitness value, reaching maximum number of iterations, or no further improvement in fitness.

## 3.2.2 Parameter Selection for Particle Swarm Optimization

To ensure the convergence of PSO, adjustments on various control parameters need to be carefully made in order to achieve a better a performance of the algorithm. The

simulations are tested with different combinations of control parameters. By properly adjusting the swarm size, number of iterations, inertia weight and weighting factors the objective function is made to converge to the minimum value, satisfying the constraints. It is observed that the control parameters as listed in Table 3-2 returned optimal objective functions for the IPFC power flow problem.

Table 3.2: PSO parameters

| Parameters                              | Rate                              |
|---|-----------------------------------|
| maximum iterations                      | 100                               |
| Swarm size, $S$                         | 35                                |
| Problem dimension                       | 4                                 |
| Inertia weight factors $W$              | Increase linearly from 0.4 to 0.9 |
| Weighting factor $C_1$ and $C_2$        | Between 0 and 4                   |
| The random number $rand_1$ and $rand_2$ | Between 0 and 1                   |

### 3.2.3 Variants of PSO

Different variants of the PSO algorithm have been described in the literature. A number of these variants have been proposed to incorporate either the capabilities of other evolutionary computation techniques, for instance hybrid versions of PSO or the adaptation of PSO parameters for an improved performance (adaptive PSO). In other cases, the nature of the problem to be solved requires the PSO to work under complex environments as in the case of the multi-objective or constrained optimization problems or tracking dynamic systems. This next section presents one of the variations to the original formulation that can be included to improve its performance, such as constriction factor approach particle swarm optimization.

### 3.2.3.1 Constriction Factor Approach Particle Swarm Optimization (CFAPSO)

In both basic PSO and CFAPSO, the maximum and minimum velocities are set to a priori values to keep away from the infeasible combinations. In basic PSO, these values are kept constant. However, in CFAPSO, the velocity,  $V^{i+1}$  is modified by a factor known as constriction factor,  $K$  such that  $(V^{i+1} = K V^i)$ , [72]. This modification increases the performance of modified PSO. The constriction factor,  $K$  is selected between (0, 1). By properly selecting the constriction factor,  $K$  the velocities can be maintained in a constant interval without exceeding the set velocities. The constriction factor value can be either fixed or varied randomly. In fixed CFA, a fixed value (say 0.78, as mentioned previously,  $K$  should be between 0 and 1 by proper selection to maintain the velocities in constant interval without exceeding the set velocities) is chosen. To improve the effectiveness of the approach, the value of  $K$  may be selected inversely proportional to the inertia weight,  $W$ . In order to ensure convergence of the PSO algorithm, the velocity of the CFA is expressed as in (3.4) and (3.5).

$$V_i^{k+1} = K[V_i^k + C_1 * rand_1 * (Pbest_i^k - X_i^k) + C_2 * rand_2 * (Gbest_i^k - X_i^k)] \quad (3.4)$$

$$K = \frac{2}{2 - \varphi - \sqrt{\varphi^2 - 4\varphi}} \quad (3.5)$$

where  $\varphi = C_1 + C_2$ ,  $\varphi > 0$ .

Typically, if  $\varphi = 4.1$ , then the constriction factor  $K = 0.729$  and  $C_1 = C_2 = 2.05$ . As  $\varphi$  increases above 4.0,  $K$  gets smaller [66]. For instance, if  $\varphi = 5.0$ , then the constriction factor  $K = 0.382$ , and the damping effect is even more pronounced. Therefore the constant  $\varphi$  is used to control the convergence characteristic of the system [73, 74].

### 3.2.4 The Proposed PSO for Optimal Parameters of the VSCs of IPFC

The proposed algorithm procedure steps to find optimal parameters of IPFC and to minimize the transmission line losses are described as follows:

- 1- Set the initial parameters of the PSO and the power system parameters together with the IPFC.
- 2- Initialize  $i^{th}$  particles of random solution with initial positions  $X_i$  and velocities  $V_i$ .
- 3- Power flow is computed using modified Newton-Raphson method to compute the optimal parameters of the VSCs of IPFC.
- 4- Calculate the objective function,  $F$  for all particles ( $F$  is the total active power loss).

$$\text{Minimize } F = \sum_{k=(m,n)}^N P_{loss} \quad (3.6)$$

- 5- Calculate the personal best position of the  $i^{th}$  particle, such that  $F_{Ni} < F_{Ni}$ ,  $i > 1$ , then set  $Pbest = X_{Ni}$  and keep track of the overall best value  $Gbest$ , and its location.
- 6- Calculate the global best position  $Gbest$ , such that the best of  $Pbests$  is set as  $Gbest$
- 7- Update the inertia weight as in equation (3.3)
- 8- Estimate the new particle velocity and position as in equations (3.1) and (3.2)
- 9- If stopping criterion is satisfied then go to the next step else go to step 2. (The stopping criteria are, good fitness value, reaching maximum number of iterations, or no further improvement in fitness).
- 10- Print the optimal parameters of IPFC controller and the transmission line losses.
- 11- Stop

The control parameters that are to be determined optimally are the magnitudes and phase angles of the injected voltage of VSCs of IPFC. Figure 3 illustrates the flowchart for searching an optimal solution using the PSO.



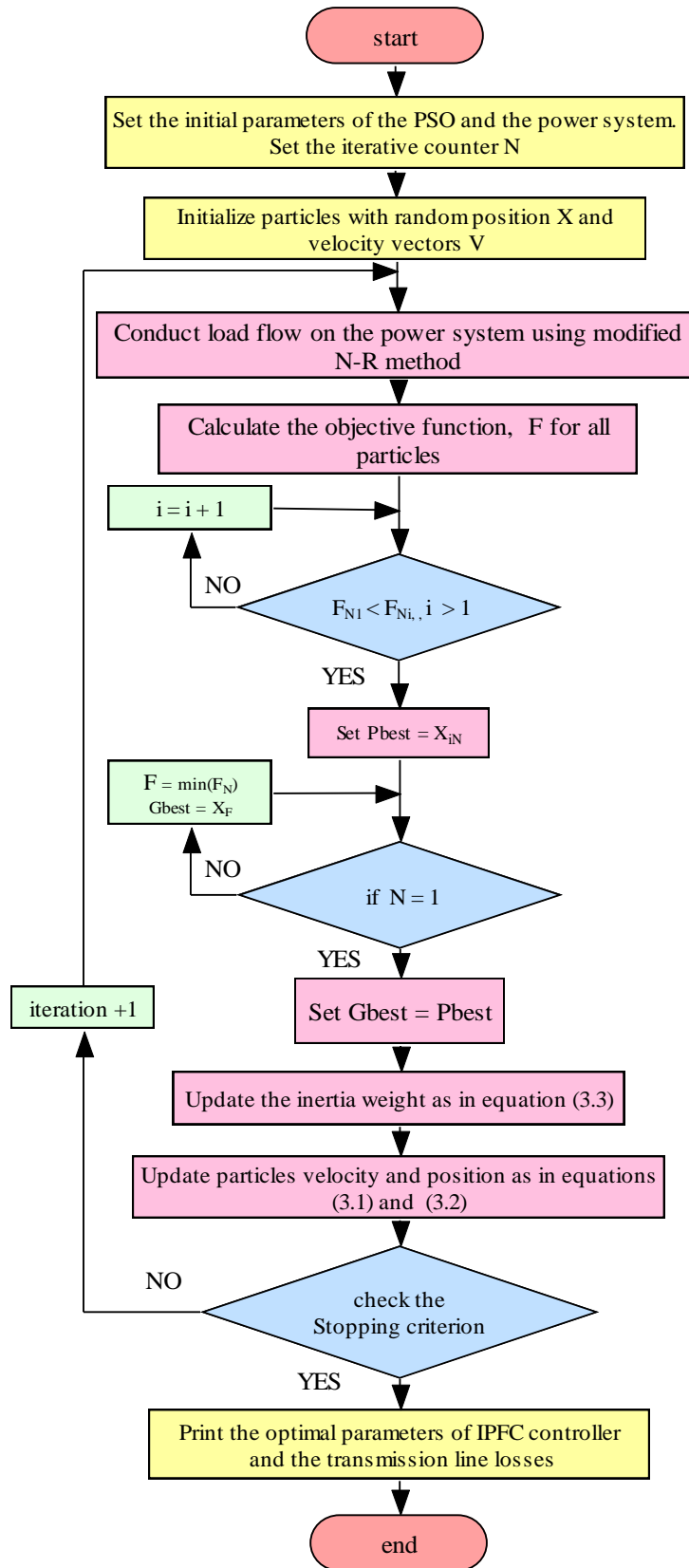


Figure 3.3: Proposed algorithm flowchart of PSO

### **3.2.5 Advantages of Particle Swarm Optimization**

Particle swarm optimization algorithm has the following advantages [63, 75] over other evolutionary algorithms:

- It is a derivative-free optimization technique different than many conventional techniques.
- It can handle objective functions of any type (e.g. non-convex, non-differentiable, and discontinuous).
- It has a few parameters to adjust.
- It is easy to implement and program with basic mathematical and logic operations.
- PSO does not require a good initial population to look for the optimal solution.
- It has the capability to escape local minima.
- It has the flexibility to be integrated with other optimization techniques to form hybrid tools.

### **3.2.6 Applications of PSO to Power System**

PSO is the new evolutionary computational technique, and there are a few applications. In the general filed, the PSO was applied to neural network learning algorithm, human tremor analysis, rule extraction in fuzzy neural network, battery pack state of charge estimation, computer numerical controlled milling optimization, [66]. And also it is applied to design of a periodic antenna arrays, chip design and project crashing analysis [75]. In this section different fields of applications of PSO technique to power systems problems as discussed in [76] are shown in Table 3.3 by technical areas.

Table 3.3: Application of PSO

| No | Application field                             | Type of PSO used   |
|----|---|--|
| 1  | Economic dispatch                             | Conventional PSO, Evolutionary Programming PSO (EPSO)  |
| 2  | Reactive power and voltage control            | Conventional PSO, integer PSO and Adaptive PSO   |
| 3  | Power system reliability and security         | Conventional PSO, Binary PSO   |
| 4  | Generation expansion problem                  | Conventional PSO, stretching PSO (SPSO), composite PSO (C-PSO)   |
| 5  | State estimation                              | Conventional PSO, Hybrid PSO (GA-PSO)  |
| 6  | Load flow and optimal power flow              | Conventional PSO, Hybrid PSO (GA-PSO), vector evaluated PSO (VEPSO), PSO with passive congregation (PSOPC), dissipative PSO (DPSO) |
| 7  | Control tuning                                | Conventional PSO   |
| 8  | System identification and intelligent control | Conventional PSO, Hybrid PSO (GA-PSO)  |
| 9  | Electric machinery                            | Conventional PSO   |
| 10 | Capacitor placement                           | Conventional PSO, integer PSO  |
| 11 | Generator maintenance scheduling              | Conventional PSO, Evolutionary Programming PSO (EPSO)  |
| 12 | Short term load forecasting                   | Conventional PSO   |
| 13 | Generator contribution to transmission system | Vector evaluated PSO (VEPSO)   |

### 3.3 Genetic Algorithm (GA) Technique

The GA technique was invented by John Holland in the early 1970's [77]. GA technique can be defined as a search technique used in computing to find exact or approximate solutions to optimization and search problems. GA is a particular group of evolutionary algorithms that use techniques inspired by evolutionary biology such as inheritance, selection, crossover and mutation. The procedure of a GA starts with a randomly selected population of chromosomes. As shown in Figure 3.4 each chromosome consists of genes or individual variables of the problem to be solved

[78]. Based on the attributes of the problem, different positions of each chromosome are encoded as characters, bits or numbers. The position is sometimes referred to as genes and is changed randomly within a range during process. The set of chromosomes during a stage of computations are called a population. An objective function is used to compute the best of each chromosome. Through the evaluation two basic operators such as crossover and mutation, are used to simulate the natural reproduction and mutation of species.

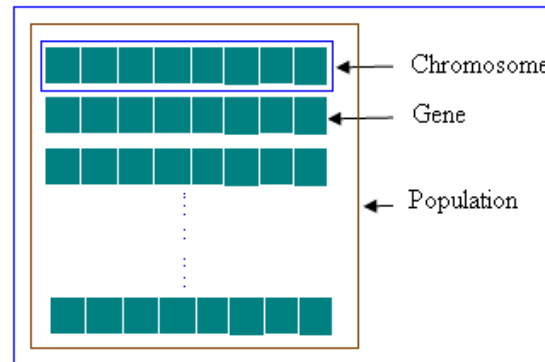


Figure 3.4: Gene string and chromosome

The GA is based on the mechanism of natural selection. The optimal solution can be sought after from a population of solutions by using random process [79]. During the optimization procedure, the operator's selection, crossover and mutation are applied to the current population to produce a new generation form.

The main parts of the simple GA i.e. the solution encoding the generation of the initial solution, the objective function, and the stop criterion are first described [80].

1. Encoding, parameters of the search space can be coded as binary strings of fixed length.
2. Initialization generates randomly initial population strings which develop to the next generation by genetic operators.
3. A fitness function is used to evaluate the quality of solutions coded by strings.
4. Selection process, allows strings with higher fitness to appear with higher probability in the next generation.
5. Crossover and mutation process – the crossover is used to combine two parents by exchanging parts of their strings, by starting from a randomly selected crossover points. By this way new solutions inheriting desirable

qualities from both parents are derived. Mutation flips single bits in a string, which prevents the GA from premature convergence, by exploiting new regions in search space.

6. Termination, in this case the new strings replace the existing string. The run continues until the stopping criterion is reached.

### **3.3.1 Genetic Algorithm Operators**

The GA optimization algorithm, implemented in the simulation tool developed for the power system network presented in this thesis, uses only three operators, selection, crossover and mutation to produce a new population for the next generation while minimizing the objective function.

### **3.3.2 Selection Process**

Selection is the process of determining the number of times, or trials, a particular individual are chosen for reproduction and, thus, the number of offspring that an individual will produce. A probabilistic selection is performed based upon the individuals. The individuals that have the better fitness value, have a better chance of being selected [81].

#### **3.3.2.1 Mate Selection**

The large number of fit members of the population is assigned the utmost probability of being selected for mating [78]. There are two general ways of choosing mates; the first one is roulette wheel and the second one is tournament selection.

#### **3.3.2.2 Roulette Wheel Selection**

In roulette wheel selection the population must first be sorted. Every chromosome is assigned a probability of selection on the basis of either its rank in the sorted population or its objective function. Rank order selection is the easiest execution of roulette wheel selection. In order to create the roulette wheel selection the following MATLAB code is used.

{

```
Parents=1:natsel; prob=parents/sum (parents); Odds= [0 cumsum (prob)];
}
```

Assuming natsel = 4, and then by applying the above MATLAB commands

```
Parents = [1 2 3 4]; Prob = [0.1 0.2 0.3 0.4]; Odds = [0 0.1 0.3 0.6 1];
```

Thus, Figure 3.5 shows the roulette wheel for a selection pool of four parents. The chromosomes with higher objective function have a low percent chance of being selected than chromosomes with low objective function. In this case, the best chromosome has a 40% probability of being selected. As more parents are added, the percent chance of a chromosome being selected changes.

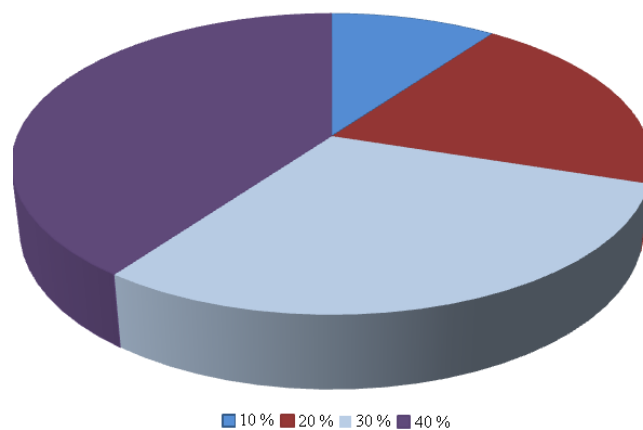


Figure 3.5: Roulette wheel probabilities for four parents in the mating pool.

### 3.3.2.3 Tournament Selection

Tournament selection is the second approach used to finding parents randomly, by selecting two small groups of chromosomes from the mating pool. In each group, the chromosome with the lowest objective function becomes a parent. Enough of these tournaments are held to generate the required number of parents. The tournament repeats for every parent needed. Tournament selection works well with thresholding, because the population never needs sorting. Sort speed becomes an issue only with large population sizes. Figure 3.6 shows the tournament selection process when three chromosomes are chosen for each tournament.

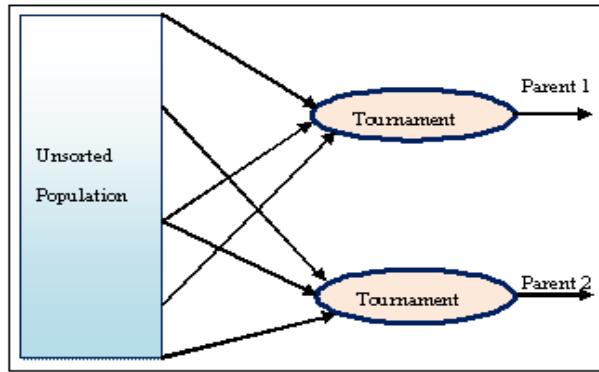


Figure 3.6: Tournament selection.

Tournament selections result in nearly the same probability of selection for the chromosomes as Rank order roulette wheel.

### 3.3.3 Crossover

Crossover is an essential operator of producing new chromosomes in the GA. similar to its counterpart in nature. Crossover produces new individuals that have some parts of both parent's genetic material [82]. In other words once the population for reproduction is selected, the individuals are paired off and “mated” using a crossover procedure. By selecting a cross point randomly for each pairing, two new individuals are created by joining the first part of the first string with the second part of the second string, and vice versa [83]. Figure 3.7 illustrate crossover operation which is called single-point crossover, two point crossover and uniform crossover.

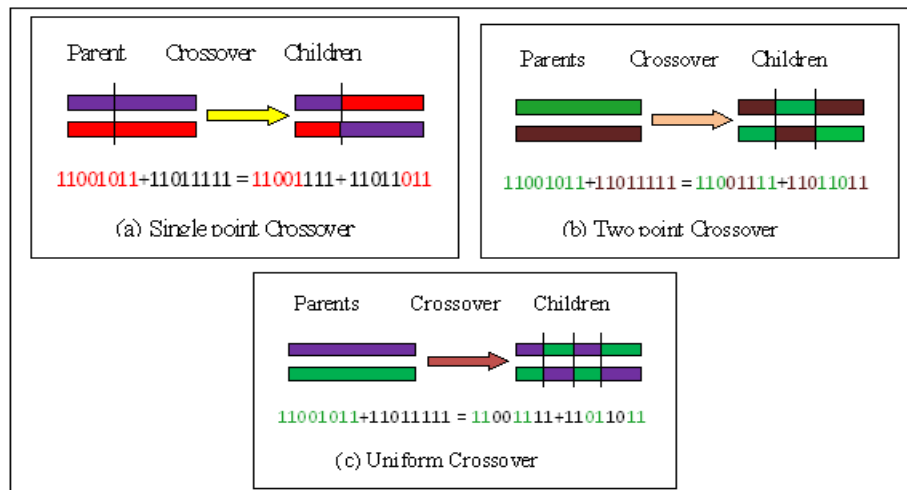


Figure 3.7: Crossover operation

When a single point crossover is selected, a binary string from beginning of chromosome to the crossover point is copied from one parent, and the rest is copied from the second parent. While when two crossover points are selected, binary string from beginning of chromosome to the first crossover point is copied from one parent, the part from the first to the second crossover point is copied from the second parent and the rest is copied from the first parent. In a uniform crossover a number of bits are randomly copied from the first parent or from the second parent.

### 3.3.4 Mutation

Mutation is used for a random process where one allele of a gene is replaced by another to produce a new genetic structure [82]. The mutation is used at the final generations when the majority of the individuals present are of similar quality. A variable mutation rate is very important for the search efficiency. Its setting is much more critical than that of crossover rate. In the case of binary encoding, mutation is carried out by flipping bits at random, with some small probability between 0.001 and 0.05. For real-valued encoding, the mutation operator is implemented by random replacement. A different possibility is to add or subtract or multiply by a random amount (e.g., uniformly or Gaussian distributed) [83]. Figure 3.8 shows the mutation process in genetic algorithms.

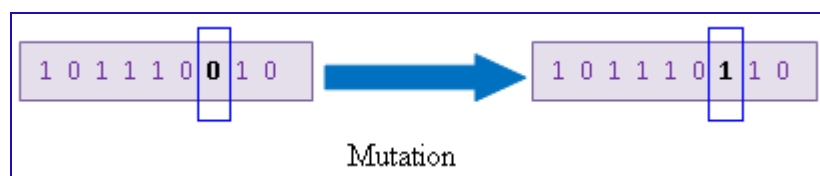


Figure 3.8: Mutation operation

### 3.3.5 Termination Criteria

Termination of the algorithm is followed by one of the stopping criteria:

1. Generations specifies the maximum number of iterations the GA performs.
2. Time limit specifies the maximum time in seconds the GA runs before stopping.
3. Stall generations — if the weighted average change in the fitness function value over stall generations is less than function tolerance, the algorithm stops.



4. Stall time limit — if there is no improvement in the best fitness value for an interval of time in seconds specified by stall time limit, the algorithm stops.

### **3.3.6 Implementation of GA Technique for Optimal Parameters of IPFC**

The GA starts similar to any other optimization algorithm, by defining the optimization parameters. It also stops similar to any other optimization algorithm too, by testing for convergence characteristic of the objective function. The procedure of the proposed GA algorithm is as follows:

1. Define the initial parameters of the system and control parameters of GA.
2. Randomly generate initial population of chromosomes of size N:  $X_1, X_2, \dots, X_N$ .
3. Conduct load flow using modified Newton Raphson method.
4. Evaluate the fitness of each chromosome  $f(X_1), f(X_2), \dots, f(X_N)$ .
5. Is the stopping criterion satisfied? Yes stop, else go to step 7.
6. Select pair of chromosomes for mating.
7. By using the crossover probability, create two offspring by exchanging part of the two selected chromosome.
8. By using the mutation probability, change the gene values in the two offspring chromosomes randomly.
9. Replace the resulting chromosomes in the new population.
10. Check the size of the new population equal to N? No, go to step 7 else go to step 12
11. Change the current chromosome population with new population
12. Check the stopping criteria if satisfied to stop else repeat from step 4 up to 12 until the stopping criterion is satisfied.

The control parameters that are to be determined optimally are the magnitudes and phase angles of the injected voltage of VSCs of IPFC.

Figure 3.9 shows a flowchart of proposed GA technique.

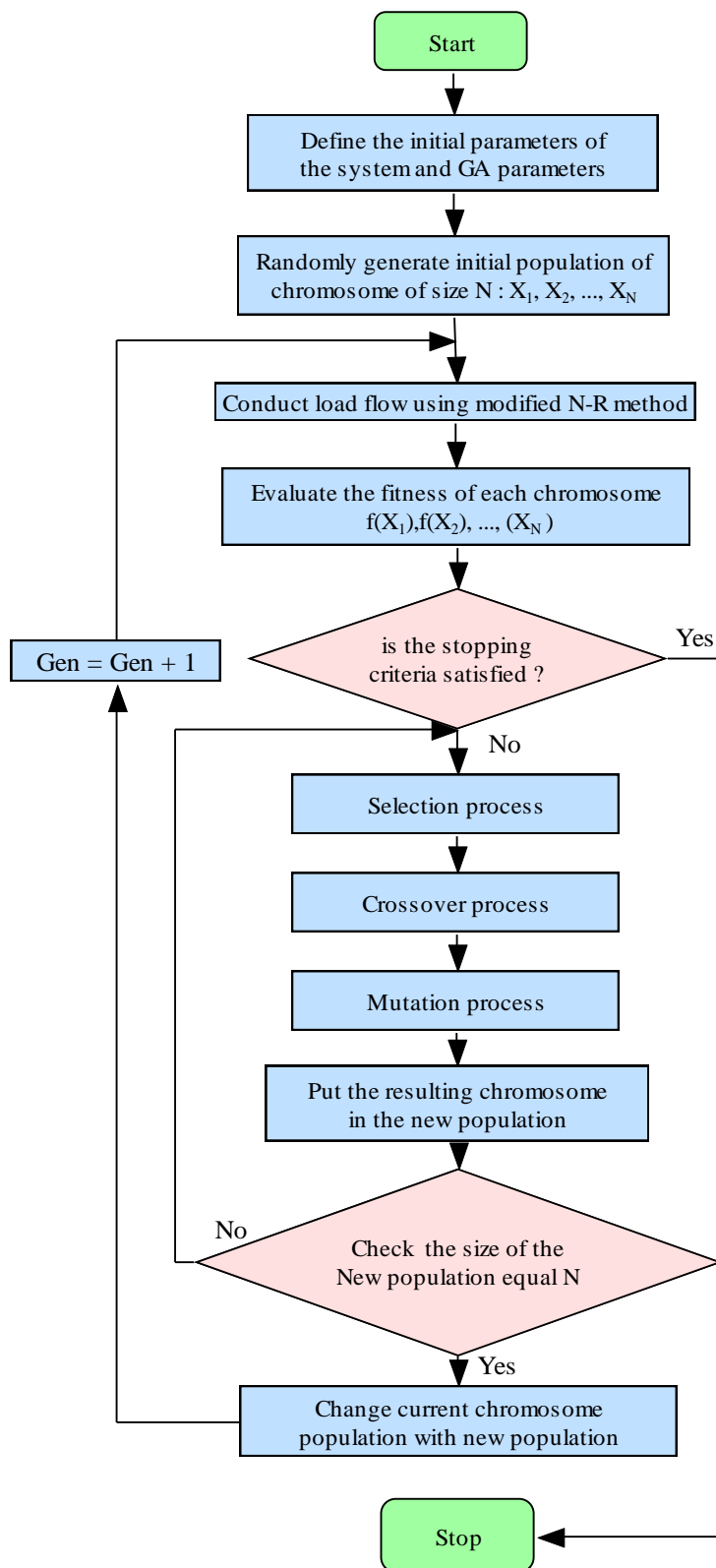


Figure 3.9: Flowchart of GA technique

### 3.3.7 Comparison Between GA and Traditional Search Algorithms

GA differs from the traditional searching algorithms [84]. They could be summarized as follows:

- As opposed to a single point, the GAs work with a population of binary strings, searching many peak values in parallel.
- Instead of using the parameters themselves, the GAs work directly with strings of characters representing the parameters set.
- Instead of deterministic rules, the GAs use probabilistic transition rules.
- Instead of derivatives or other auxiliary knowledge, the GAs use objective function information.
- GA has the potential to get the solutions in many different areas of the search space simultaneously.

### 3.4 Simulated Annealing (SA) Technique

The SA is an optimization technique proposed in 1983 by Kirkpatrick, Gelatt and Vecchi [85] to find the global minimum of an objective function that may possess a number of local minima [86]. The SA takes the analogy of the physical annealing of molten particles of a solid. Starting with high temperature the molten particles are allowed to cool slowly until they are solidified at a low temperature. This physical annealing process is used to find near-global or global optimum solutions for combinatorial optimization problems [87]. In order to solve any optimization problem by SA method three main parameters are required [88]. Such as:

- Firstly, the annealing temperature,  $T$ . This parameter permits the SA technique not to be entrapped in local minima through the use of the Boltzmann's function.
- Secondly the number of iterations at constant temperature,  $M_0$ . A low number of  $M_0$  will result in being trapped in local minimum.
- Thirdly the cooling strategy,  $\rho_0$ . If the annealing temperature is decreased fast the algorithm will be trapped in local minimum regardless of proper  $T$  and  $M_0$  tuning.

The above three parameters should be set at the beginning of the simulation and the effect on the others parameters through sensitivity analysis of the simulation for every optimization problem, is to be studied.

### 3.4.1 Simulated Annealing Physical Concepts

The procedure of heating up a solid to a high temperature followed by slow cooling achieved by decreasing the temperature of the environment in steps is called annealing. At every step the temperature is maintained constant for a period of time which is sufficient for the solid to reach thermal equilibrium [89]. The solid has a lot of configurations at equilibrium point, each corresponding to different spins of the electrons and to specific energy levels. And the probability of a specified configuration,  $P_{con}$ , is specified by Boltzmann distribution as in (3.4)

$$P_{con} = K * \exp^{(-E_{con}/T)} \quad (3.4)$$

where  $K$  is a constant and  $E_{con}$  is the energy of the given configuration.

Monte Carlo method was proposed by Metropolis et.al 1953 [90] to simulate the procedure of reaching thermal equilibrium at a constant temperature,  $T$ . Based on this method; a randomly generated perturbation of the current configuration of the solid is applied so that a trial configuration is obtained. Let  $E_c$  and  $E_t$  represent the energy level of current and trial configurations. Therefore:

Assume  $E_c < E_t$ , till a lower energy level has been reached and the trial solution has to be altered.

If  $E_c > E_t$ , after that the trial configuration is accepted as the current configuration with probability as follows:

$$\exp^{(E_c - E_t)} \quad (3.5)$$

where  $T$  is the control parameter of the cooling schedule.

The procedure continues where a change to a configuration of higher energy level is not necessarily rejected. Finally thermal equilibrium is reached after a great number of perturbations, where the probability of a configuration approaches Boltzmann Distribution. By gradually decreasing  $T$  and repeating Metropolis simulation, new lower energy levels become reachable. As  $T$  approaches zero, the least amount of energy configurations will have a positive probability of happening.

### **3.4.2 SA Techniques Factors**

When designing the SA techniques some factors are needed to be considered [91] as follows:

#### **3.4.2.1 Initialization**

The initial temperature should be high enough to permit all candidate solutions to be acceptable. Also an initial solution should be generated randomly from the feasible region.

#### **3.4.2.2 Markov Length**

To reach Boltzmann distribution, the iteration number,  $M$  used in each temperature should be set appropriately high for the objective function values.

#### **3.4.2.3 Step Size**

At each movement the step size should be decreased with the decrease of temperature. The reasonable solutions at lower temperature are near to optimal solution. The stochastic search tends to be deterministic search when temperature is low. So that if the step size is too big, at low temperature, a number of feasible solutions will be discarded, therefore computation time will be wasted.

#### **3.4.2.4 Termination Criterion**

The SA algorithm is stopped when one of the following stopping criteria are met.

1. When the maximum iterations bound the number of iterations is reached.

2. When the time limit bounds the number of seconds the algorithm runs is reached.
3. When the neighbor solution was not improved after a period.
4. When the objective function goes below the objective limit.

### 3.4.3 An implementation of SA Technique for Optimal Parameters of IPFC

For the solution of an optimization problem with SA, the following steps are required.

1. Randomly select an initial solution vector  $x_1$  in the bounded parameter space, and calculate the objective function  $f(x_1)$ .
2. Estimate an initial temperature  $T_{(0)} = T_{init}$ .
3. Conduct the load flow using modified Newton –Raphson method.
4. Select a new solution vector,  $x_2$  and evaluate the corresponding objective function value  $f(x_2)$ .
5. Calculate the difference of the objective functions,  $\Delta f = f(x_2) - f(x_1)$ .
6. If the difference of the objective functions,  $\Delta f < 0$ , then the solution vector  $x_2$  is accepted, otherwise if  $\Delta f > 0$  accept the solution vector according to the probability of acceptance  $p_{(k)} = e^{-\Delta f/T(k)}$  or else go to step 7.
7. Update store or set  $x_1 = x_2$  and  $f(x_1) = f(x_2)$  and weight the current simulated temperature with the coefficient  $\lambda$ , where  $0 < \lambda < 1$ , decreasing the simulated temperature successively at every iteration, so that at the  $(k+1)^{st}$  iteration:  
 $T(k+1) = \lambda T(k)$ , where  $k$  is the iteration index,
8. Check the stopping criteria, if the current simulated temperature is lower or equal to the final temperature, i.e.,  $T(k) \leq T_{final}$ , then accept the current solution vector as being optimum, otherwise return to Step 3 and repeat the process.
9. Stop

The control parameters that are to be determined optimally are the magnitudes and phase angles of the injected voltage of VSCs of IPFC.

The flow chart of SA algorithm is presented in Figure 3.10

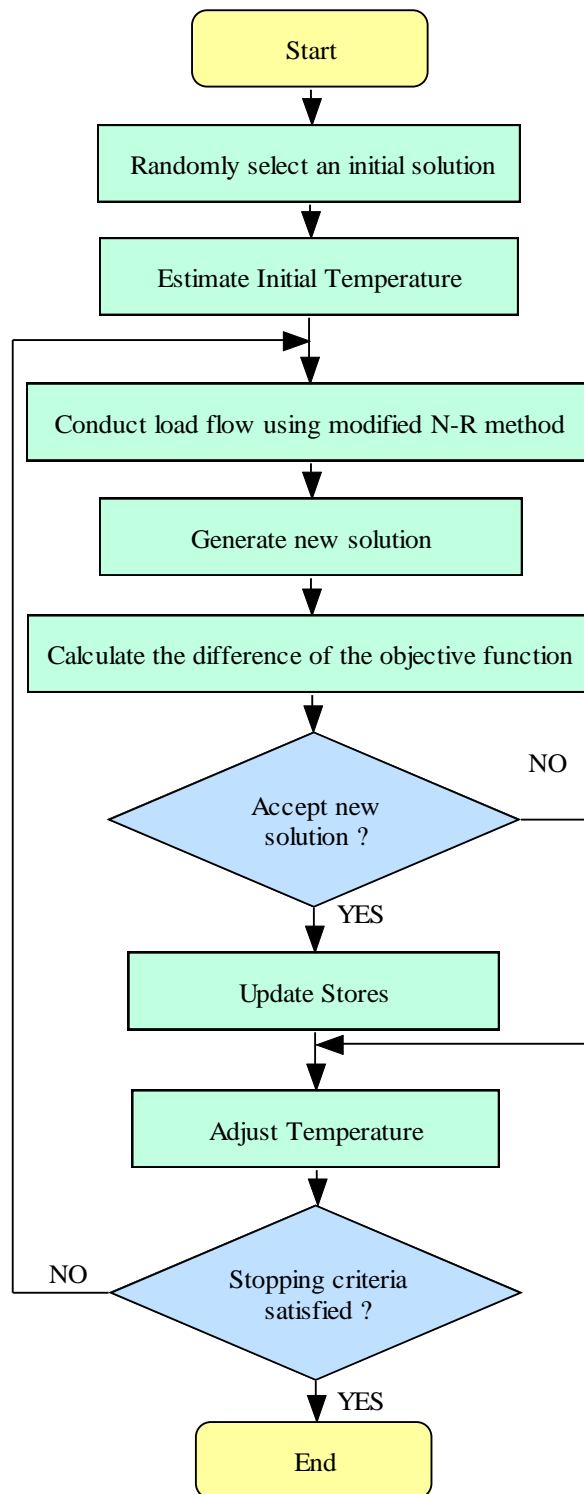


Figure 3.10: Flow chart of a SA

### 3.5 Global Optimization Toolbox in MATLAB

Global optimization toolbox provides methods that search for global solutions to problems that include multiple maxima or minima [92]. It includes global search, GA, and SA solvers. The solvers can be used to solve optimization problems where the objective or constraint function is continuous, discontinuous, and stochastic, does not possess derivatives, or includes simulations or black-box functions with undefined values for some parameter settings.

#### 3.5.1 GA Solver

GA solvers support algorithmic customization. GA variant can be created by modifying initial population and fitness scaling options or by defining parent selection, crossover, and mutation functions. Figure 3.11 show the GA solver windows

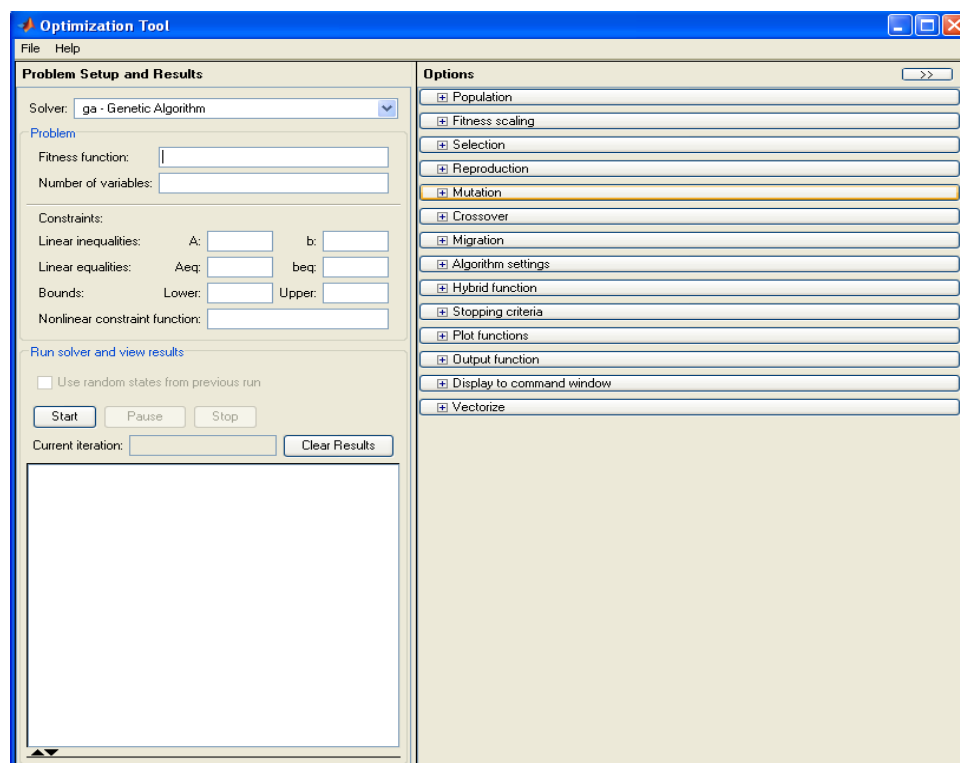


Figure 3.11: GA solver

The following steps should be defined when the GA solver is used:



- **Fitness Function**

The fitness function is the objective function that needs to be minimized. This objective function can specify as a function handle of the form (`@LFunction`), where (`LFunction.m`) is an M-file that returns a scalar.

- **Number of Variables**

The numbers of variables are the number of independent variables that required for the fitness function.

- **Constraints**

The lower and upper bounds on the variables and is defined as the vector.

- **Population**

The population options are used to specify options for the population of the GA.

- **Population Type** It used to specify the type of the input given to the fitness function. Population type can be set to double vector, or Bit string.
- **Population Size** It used to specify the number of individuals in each generation. If we assume the population size as a vector of length greater than 1, then the algorithm creates multiple subpopulations. Each entry of the vector specifies the size of a subpopulation.

- **Fitness Scaling**

It is used to convert raw fitness scores returned by the fitness function to values in a range that is suitable for the selection function.

- **Selection**

It is used to choose parents for the next generation based on their scaled values from the fitness scaling function and the following

- **Roulette Simulates** a roulette wheel with the area of each segment proportional to its expectation. The algorithm then uses a random number to select one of the sections with a probability equal to its area.

- **Tournament Selects** each parent by choosing individuals at random, the number of which you can specify by Tournament size, and then choosing the best individual out of that set to be a parent.

- **Reproduction**

It is used to determine how the GA creates children at each new generation based on the following crossover fraction.

- **Crossover Fraction**

It is used to specify the fraction of the next generation that produce by crossover. The remaining individuals in the next generation can be produces by mutation. The crossover fraction can be set between 0 and 1.

- **Mutation**

It is used to make small random changes in the individuals in the population, which provide genetic diversity and enable the GA to search a broader space. The following adaptive feasible function used for mutation.

- **Adaptive Feasible**

It is used to randomly generate directions that are adaptive with respect to the last successful or unsuccessful generation. By proper chose step length along each direction to satisfied a linear constraints and bounds.

- **Crossover**

It is used to combines two individuals, or parents, to form a new individual, or child, for the next generation. The following single point is used in our algorithm:

- **Single Point**

It is used to choose a random integer n between 1 and Number of variables, and selects the vector entries numbered less than or equal to n from the first parent, selects genes numbered greater than n from the second parent, and concatenates these entries to form the child. For example:

$$p1 = [a \ b \ c \ d \ e \ f \ g \ h]$$

p2 = [1 2 3 4 5 6 7 8]

Random crossover point = 3

Child = [a b c 4 5 6 7 8]

### ○ **Stopping Criteria**

Termination of the algorithm is followed by one of the stopping criteria:

- Generations specifies the maximum number of iterations the GA technique performs.
- Time limit specifies the maximum time in seconds the GA technique runs before stopping.
- Stall generations, if the weighted average change in the fitness function value over stall generations is less than function tolerance, the algorithm stops.
- Stall time limit, if there is no improvement in the best fitness value for an interval of time in seconds specified by stall time limit, the algorithm stops.

### ○ **Plot Functions**

It is used to plot various aspects of the GA technique as it is executing. Each one draws in a separate axis on the display window. The following function.

- Best individual plots the vector entries of the individual with the best fitness function value in each generation.
- A best fitness plot is used to plot the best function value in each generation versus iteration number.
- A distance plot is used to plot the average distance between individuals at each generation.
- Fitness of each individual is used to plot the fitness of each individual
- Stopping plots is used to plot the stopping criteria levels.

### 3.5.2 SA Solver

SA solver solves optimization problems with a probabilistic search algorithm that mimics the physical process of annealing, in which a material is heated and then the temperature is slowly lowered to reduce defects, hence minimizing the system energy [93]. By analogy, every iterations of a SA technique seeks to improve the current minimum by slowly reducing the scope of the search.

The SA algorithm accepts all newest points that lower the objective, but also, with a certain probability, points that move up the objective. Therefore, with accepting points that move up the objective, the algorithm avoids being trapped in local minima in early iterations and is capable to explore globally for better solutions. SA algorithm allows solving bound-constrained or unconstrained optimization problems and does not require that the functions be differentiable or continuous. Figure 3.12 show window of SA Solver.

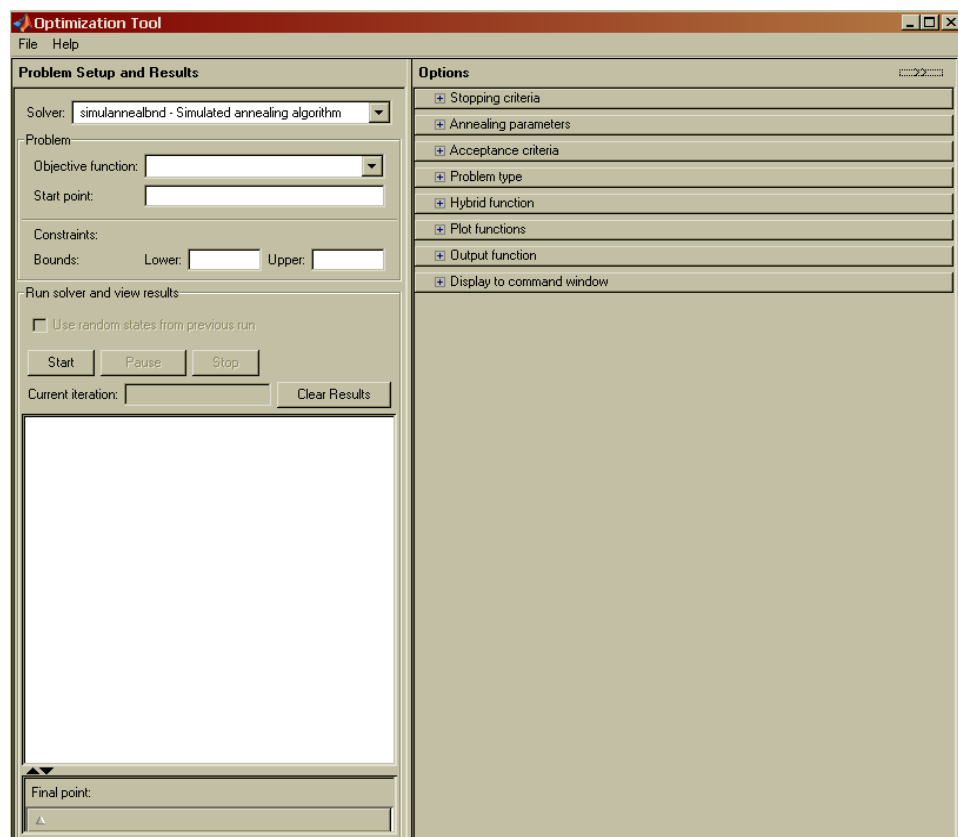


Figure 3.12: SA solver

The following steps should be defined when the SA solver is used:

- **Objective Function**

It is used to define the function required to minimize. Specify the function as an anonymous function or as a function to handle of the form (@LFanalysis.m), where (LFanalysis.m) is an M-file that returns a scalar function value.

- **Start Point**

It is used to define the initial point of the SA technique search.

- **Constraints**

It is the lower and upper bounds on the variables and is defined as the vector.

- **Stopping Criteria**

- Maximum iteration is defined as the number of iterations the algorithm takes.
- Maximum function evaluation is defined as the number of function evaluations the algorithm performs.
- Time limit is defined as the number of seconds the algorithm runs.
- Function tolerance is used to stop the algorithm if the average change in the objective function after stall iterations is below function tolerance.
- Objective limit is used to stop the algorithm if the objective function goes below Objective limit.

- **Annealing Parameters**

Annealing function specifies the function used to generate new points for the next iteration:

- Fast annealing takes random steps, with size proportional to temperature.
- Exponential temperature update temperature decreases as  $0.95^N$  where N is the number of iteration.

- **Plot Functions**

It is used to plot interval enters the number of iterations between consecutive calls to the plot function.

- A best function value plot is the lowest objective function to date.
- A best point plot is the best location to date.
- Stopping criteria plots is the stopping criteria levels.
- Temperature plot is plots the temperature at each iteration.
- Current point plots are the current location at each iteration.

- Current function value plots are the current function value at each iteration.

### **3.6 Summary**

In this chapter the basic concepts of intelligent optimization techniques have been provided. A detailed explanation on PSO technique was considered, i.e. elements of PSO, parameters selection and variants of PSO. Also the proposed PSO algorithm, PSO advantages and application to power systems including IPFC have been discussed too. Similarly, an overview of GA technique, GA operators, selection process, termination criteria and implementation of GA for obtaining optimal parameters of IPFC were discussed. A comparison between GA and traditional search algorithms was briefly explained. Also in a similar way, a brief introduction to SA technique, SA control parameters and its implementation to find the optimal parameters of VSC of IPFC have been discussed. Finally, the global optimization toolboxes in MATLAB, GA solver and SA solver were considered.

## **CHAPTER 4**

### **RESULTS OF SIMULATION AND DISCUSSION**

#### **4.1 Introduction**

In order to demonstrate the application of FACTS controller, IPFC together with proposed optimization techniques, simulation studies are carried out on the standard IEEE-14 and 30-bus power systems. The equivalent circuit of each VSC of an IPFC is a voltage source represented by voltage magnitude and angle, and series impedance. The simulation is performed using MATLAB 7.6 and computer PC with the following specifications: (i) Microsoft Window XP; Professional; Version 2002; Service Pack 3 and (ii) Manufactured and supported by : Dell Optiplex 330; Intel® Core™ 2Duo CPU; E7300@ 2.66GHz; 2.66 GHz, 0.98 GB of RAM; Physical Address Extension.

#### **4.2 Case 1 Standard IEEE 14-bus power system**

To verify the effectiveness of the proposed algorithms, MATLAB m-file is developed for power flow for all simulations and is applied to the standard IEEE 14-bus test power system. The IPFC devices installed in lines 1-2 and 1-5, are represented as voltage sources as shown in Appendix B, Figure B1. First the results obtained with the algorithms by using three types of PSO, named basic particle swarm optimization (BPSO), inertia weight approach particle swarm optimization (IWAPSO) and constriction factor approach particle swarm optimization (CFAPSO), have been compared to those calculated by power flow solution without IPFC and with IPFC. The system transmission line losses for the three operating conditions without IPFC, with IPFC, and with IPFC, and PSO have been calculated too. Next using GA technique, the optimal parameters of the IPFC and the transmission line losses of IEEE 14-bus power system are investigated. In a similar way, SA technique is used to derive the optimal parameters of the IPFC, minimizing the transmission line losses of the system.

#### 4.2.1 Power Flow Analysis of IEEE 14-bus Power System without IPFC

Power flow simulations were performed using the Newton–Raphson method shown in Appendix A1. The bus voltages data and the lines data of the system are as in Appendix B [94]. Under these operating conditions, the voltages of generator buses are chosen as reported in Table 4.1.

Table 4.1: Voltages of generator buses of the IEEE 14-bus power system

| Bus Number | Voltage magnitude (pu) |
|------------|------------------------|
| 1          | 1.060                  |
| 2          | 1.045                  |
| 3          | 1.010                  |
| 6          | 1.070                  |
| 8          | 1.090                  |

The results obtained for line flows, line losses and the Newton-Raphson load flow analysis of the IEEE 14-bus power system without IPFC are presented in Appendixes C1 and C2. The transmission line losses during the operating conditions without IPFC for line 1-2 and 1-5 and total line loss are reported in Table 4.2 and the voltage profile of all the buses is as shown in Figure 4.1.

Table 4.2: Transmission line losses of the IEEE 14-bus power system without IPFC

| From Bus To Bus | Line Losses in MW |
|-----------------|-------------------|
| 1 - 2           | 4.309             |
| 1 - 5           | 2.773             |
| Total Losses MW | 13.593            |

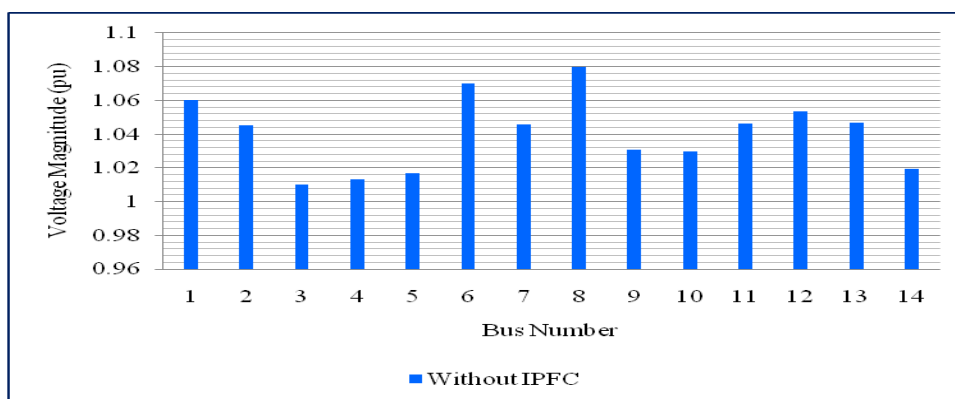


Figure 4.1: The voltage profile of IEEE 14-bus power system without IPFC



#### 4.2.2 Power Flow Analysis of IEEE 14-bus Power System with IPFC

As shown in Appendix A2 some modifications are made to model the IPFC device as voltage source with voltage magnitude and phase angle in series with the transmission line. By changing the line impedance  $Z_{lk}$  between buses  $l-k$  ( $k=m,n$ ) so that the admittance matrix of the system can be modified to consider the insertion of the series sources impedances as

$$Z_{lk} = (R_{lk} + R_{slk}) + j(X_{lk} + X_{slk}) \quad (4.1)$$

where  $R_{lk}$  and  $R_{slk}$  are the transmission line and series voltage source resistances respectively.  $X_{lk}$  and  $X_{slk}$  are the transmission line and series voltage source reactances respectively. Therefore, the transmission lines admittance  $Y_{lk}$  will be

$$Y_{lk} = \frac{1}{Z_{lk}} = G_{lk} + jB_{lk} \quad (4.2)$$

where  $G_{lk}$  and  $B_{lk}$  are the conductance and susceptance of the transmission line. The modified Jacobian and the linearized power flow equations are presented in Appendix A2. The power flow analysis mathematical model is simulated when the IPFC is connected between lines 1-2 and 1-5. After adding the source impedances ( $Z_{s12} = 0.001938 + j0.005917$  and  $Z_{s15} = 0.005403 + j0.022304$ ) to lines 1-2 and 1-5 respectively ( $Z_{s12}$  and  $Z_{s15}$  are the impedances of VSC<sub>1</sub> and VSC<sub>2</sub> connected to the lines 1-2 and 1-5), the results obtained for line flows, line losses and the Newton-Raphson load flow analysis of IEEE 14-bus power system with IPFC are presented in Appendixes C3 and C4. The optimal injected voltage magnitudes ( $V_{inj}$  (pu)) and the angles ( $\theta_{inj}$  (rad)) for the first and for the second transmission lines (i.e. 1-2 and 1-5) and the minimized line losses are reported in Table 4.3. The total line loss of the IEEE 14-bus power system is also presented.

Table 4.3: The control parameters of the IPFC and the system losses of IEEE 14-bus power system

| Optimization parameter | Lines |       |
|------------------------|-------|-------|
|                        | 1-2   | 1-5   |
| $V_{inj}$ (pu)         | 0.040 | 0.040 |
| $\theta_{inj}$ (rad)   | 1.040 | 1.040 |
| Lines losses (MW)      | 0.125 | 0.064 |
| Total losses (MW)      | 4.936 |       |

It is observed from Tables 4.2 and 4.3, that the reduction of the line losses are from 4.309 MW to 0.125MW for the line 1-2, and from 2.273 MW to 0.064 MW for the line 1-5 and the total losses are reduced from 13.593 MW to 4.936 MW. In other words, the transmission line losses are reduced by 97.10 % and 97.20 % for the first and second transmission lines 1-2 and 1-5 respectively, and 63.69 % for the total loss of the IEEE 14-bus power system when the IPFC is installed between the lines 1-2 and 1-5. Figure 4.2 show the voltage profile of the IEEE 14-bus power system for the power flow when the IPFC is installed between lines 1-2 and 1-5.

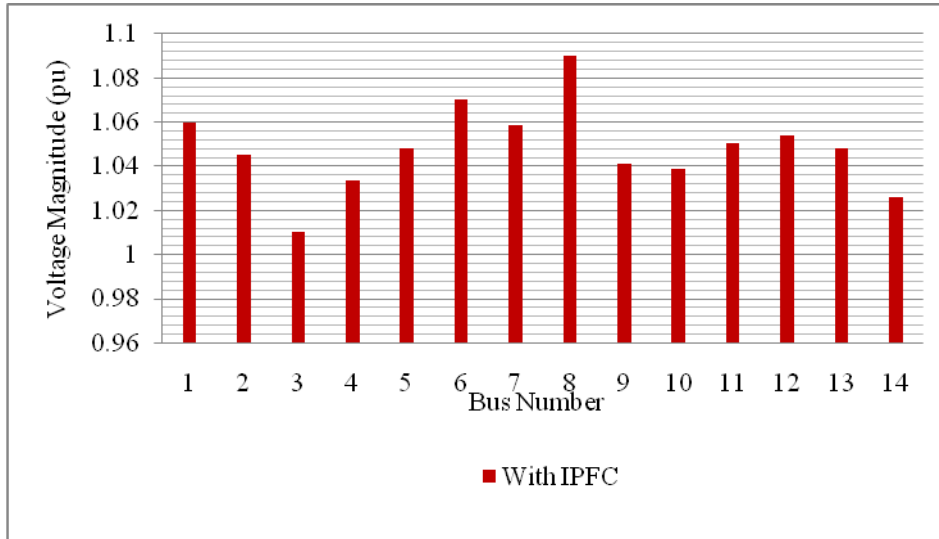


Figure 4.2: The voltage profile of IEEE 14-bus power system with IPFC

As shown in Tables 4.2 and 4.3, the total power losses of the system are decreased to 4.936 MW, i.e. by approximately 63.69 %. The voltage profile of the system with and without IPFC devices are shown in Figure 4.3. It is observed that the reactive

power introduced by the IPFC devices caused an improvement in the voltage of buses number 4, 5, 7, 8, 9, 10, 11, 12, 13 and 14. This improvement resulted in lower reactive power flow in the lines and hence reduction in the real power loss.

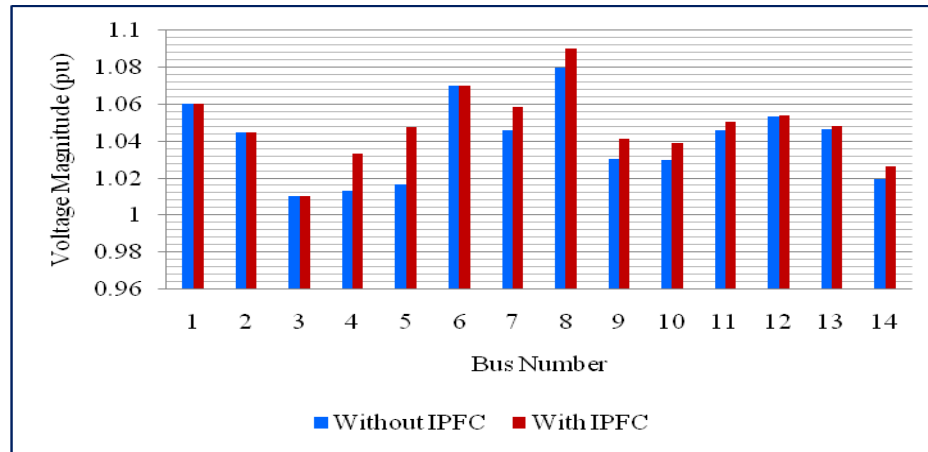


Figure 4.3: The voltage profile of IEEE 14-bus power system without and with IPFC

#### 4.2.3 Power Flow Analysis of IEEE 14-bus Power System with IPFC and using PSO

In this case the IPFC device installed on the transmission lines of IEEE 14-bus power system is considered by connecting the IPFC between lines 1-2 and 1-5. Proper control parameters for different types of PSO variants i.e. for BPSO, IWAPSO and CFAPSO are selected as in Table 4.4, as explained in Section 3.2.2, Table 3-2.

Table 4.4: PSO control Parameters

| Control parameters                      | PSO Type        |                 |                 |
|---|-----------------|-----------------|-----------------|
|   | BPSO            | IWAPSO          | CFAPSO          |
| Number of Iterations                    | 100             | 100             | 100             |
| Swarm size $S$                          | 35              | 35              | 35              |
| Problem dimension                       | 4               | 4               | 4               |
| Inertia weight factor $W$               | 1.2             | 0.4 – 0.9       | -               |
| Weighting factor $C_1$ and $C_2$        | $C_1 = C_2 = 2$ | $C_1 = C_2 = 2$ | $C_1 = C_2 = 2$ |
| The random number $rand_1$ and $rand_2$ | Between 0 and 1 | Between 0 and 1 | Between 0 and 1 |
| q coefficient                           | -               | -               | 4.9             |

The voltages of generator buses in the system are used as in Table 4.1, such that the generators supply as much reactive power to the system as they can before inserting any extra reactive power source. The boundary constraints for the injected voltage magnitudes are between ( $0 < V_{inj} < 0.15$ ) and angles between ( $-\pi/2 < \theta_{inj} < \pi/2$ ).

The three types of PSO are applied to minimize the transmission line losses and to find the optimal parameters of the injected voltage source magnitude and angle of VSCs of the IPFC. After setting the limits for the injected voltage magnitudes and angles of VSC of IPFC, the power flow simulation is performed. The results obtained for line flows, line losses and the Newton Raphson load flow analysis of the IEEE 14-bus power system with IPFC and BPSO, IWAPSO and CFAPSO are presented in Appendixes C5 to C10. The injected voltage magnitudes and angles of VSC of IPFC and the system line losses for the three variants of PSO are presented as in Table 4.5.

Table 4.5: The control parameters of IPFC and the system losses of IEEE 14-bus power system

| Optimization parameter | PSO types |        |        |        |        |        |
|------------------------|-----------|--------|--------|--------|--------|--------|
|                        | BPSO      |        | IWAPSO |        | CFAPSO |        |
| Line                   | 1-2       | 1-5    | 1-2    | 1-5    | 1-2    | 1-5    |
| $V_{inj}$ (pu)         | 0.0457    | 0.0552 | 0.0457 | 0.0573 | 0.0457 | 0.0558 |
| $\theta_{inj}$ (rad)   | 1.0253    | 0.6439 | 1.0253 | 0.5962 | 1.0253 | 0.6296 |
| Line losses (MW)       | 0.0120    | 0.0030 | 0.0120 | 0.0030 | 0.0120 | 0.0030 |
| Total line losses (MW) | 4.6300    |        | 4.6300 |        | 4.6300 |        |

As observed from Tables 4.2 and 4.5, the total power loss of the system is reduced to 4.630 MW when the PSO is used i.e. reduced by approximately 65.94 %.

The variation of objective function i.e the total line losses with the change in number of iterations in BPSO, IWAPSO and CFAPSO are shown in Figures 4.4, 4.5 and 4.6 respectively. It is observed that the objective function reached a global minimum after nearly 50 iterations out of 100 and the simulation running time is 24.107 seconds for the BPSO. When the IWAPSO is used the objective function reached a global

minimum after nearly 22 iterations out of 100 and the simulation running time is 25.413 seconds similarly in case of CFAPSO it is observed that the objective function reached a global minimum after nearly 12 iterations out of 100 and the simulation running time is 24.107 seconds. As the swarm function in PSO code requires an initial value of the objective function, different initial values are for each version of PSO are tried in the simulations until a minimum value of active power losses are obtained, satisfying the constraints.

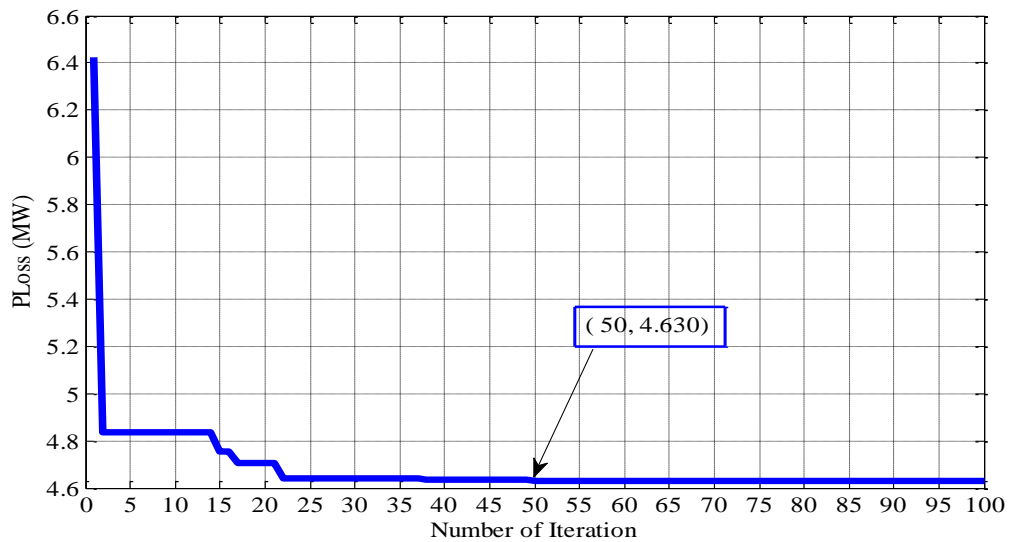


Figure 4.4: Variation of total line losses with the change in iterations by BPSO

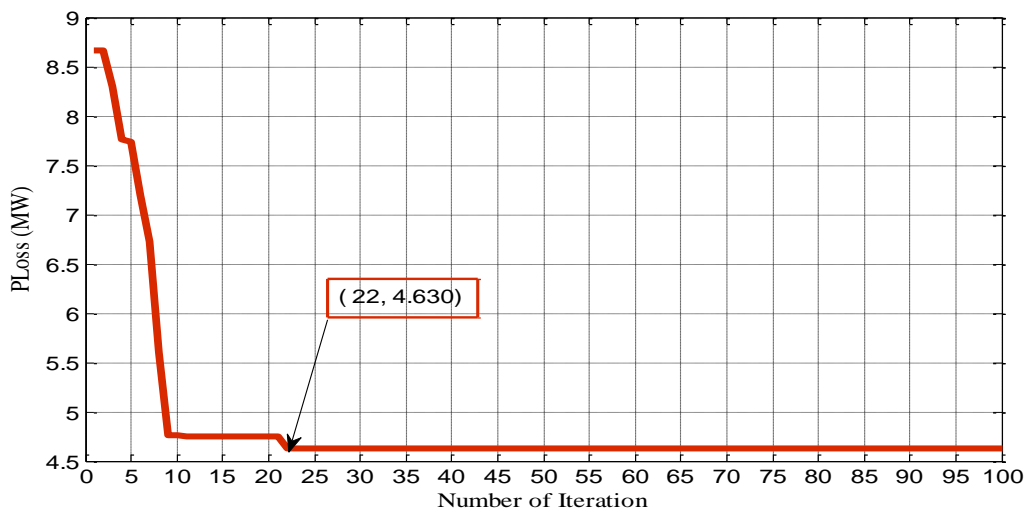


Figure 4.5: Variation of total line losses with the change in iterations by IWAPSO

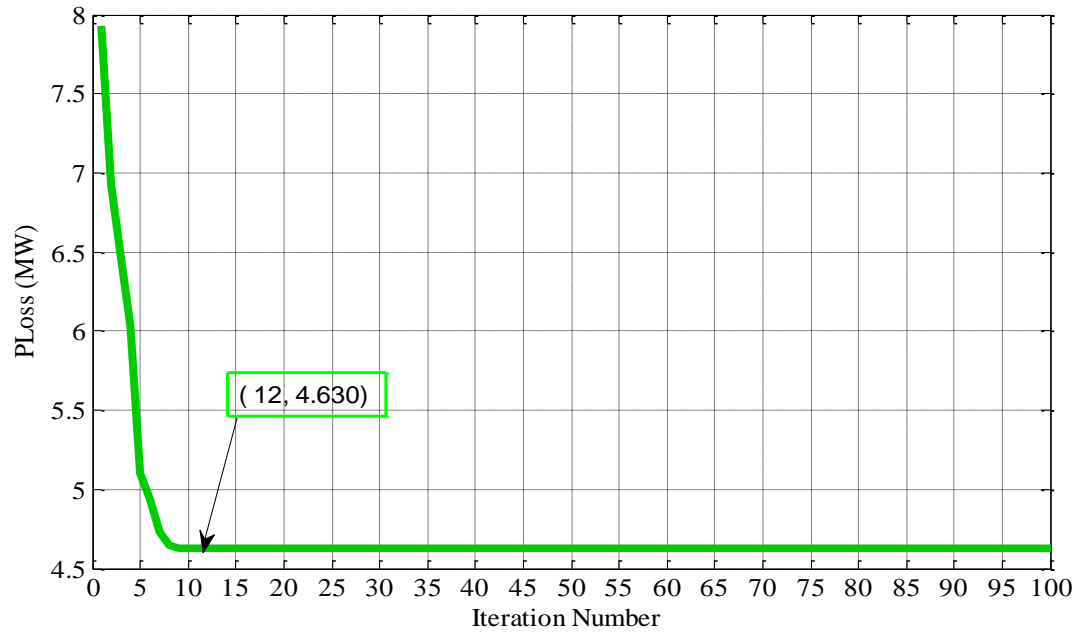


Figure 4.6: Variation of total line losses with the change in iterations by CFAPSO

Figures 4.7, 4.8 and 4.9 shows the voltage profile of IEEE 14-bus power system for the power flow with IPFC and using BPSO, IWAPSO or CFAPSO techniques.

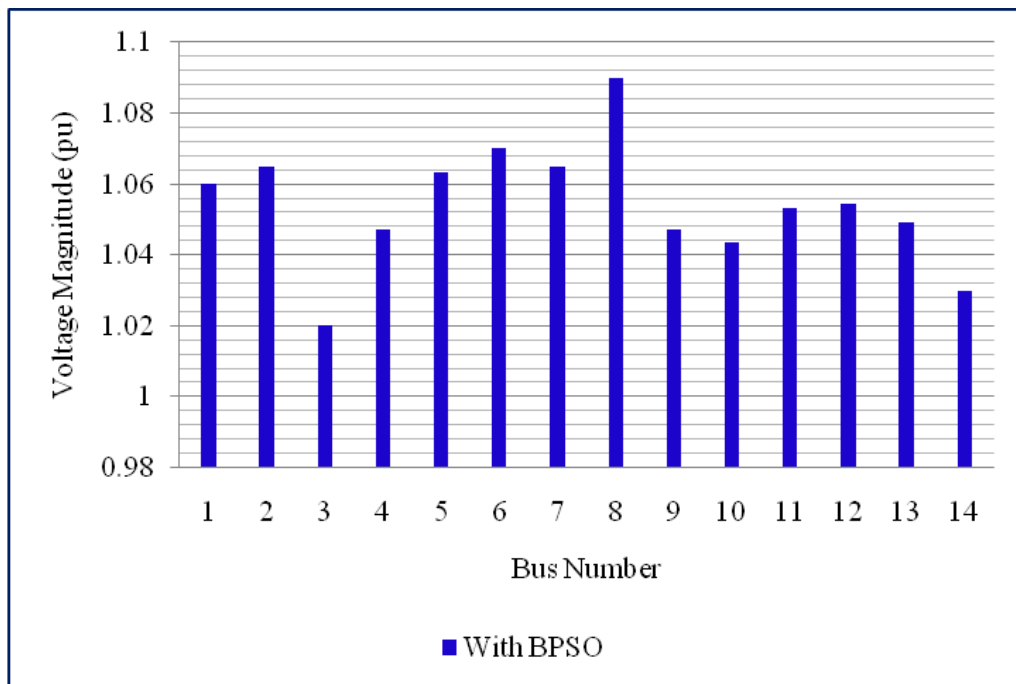


Figure 4.7: The voltage profile of IEEE 14-bus power system with IPFC and BPSO

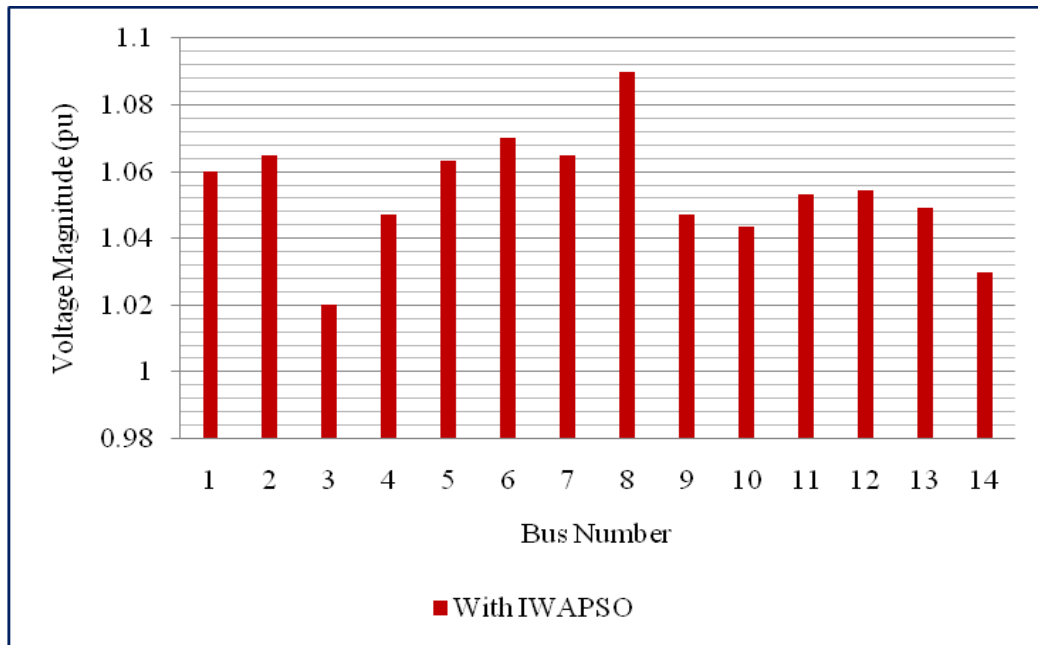


Figure 4.8: The voltage profile of IEEE 14-bus power system with IPFC and IWAPSO

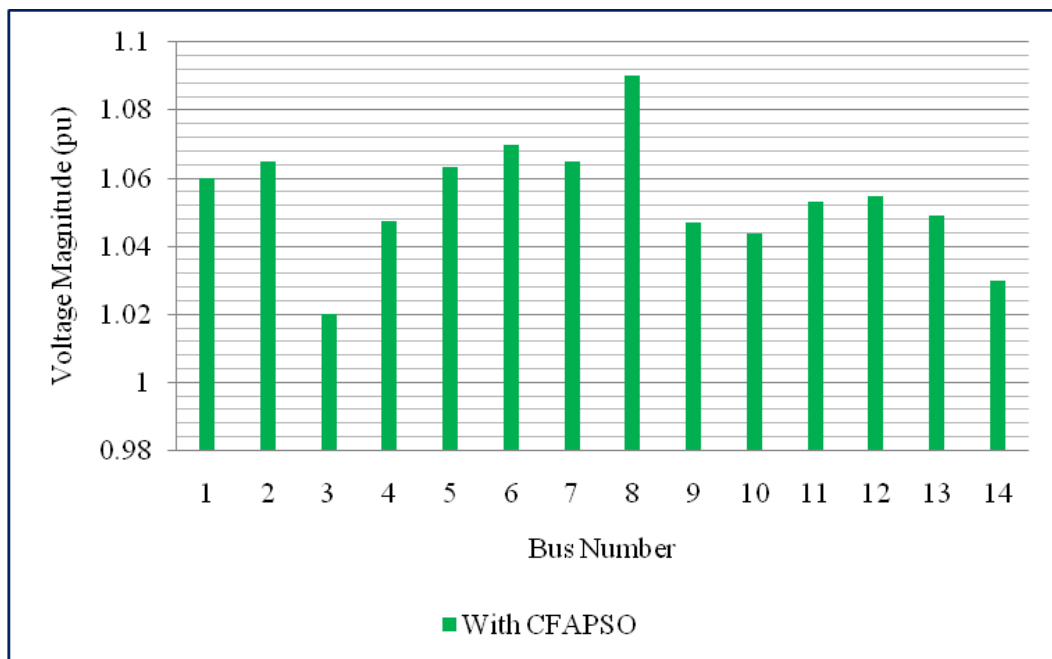


Figure 4.9: The voltage profile of IEEE 14-bus power system with IPFC and CFAPSO

Figure 4.10 shows the voltage profile of IEEE 14- bus system for the power flow with IPFC and together with BPSO, IWAPSO and CFAPSO, respectively

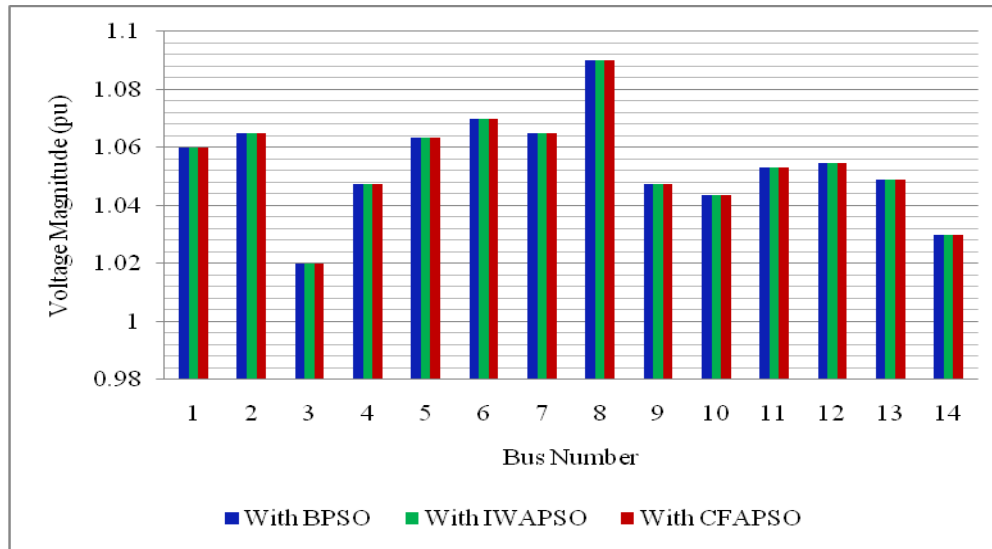


Figure 4.10: The voltage profile of IEEE 14-bus power system with IPFC and BPSO, IWAPSO and CFAPSO techniques

Figure 4.11 shows the voltage profile of the IEEE 14-bus power system with IPFC and with IPFC and PSO

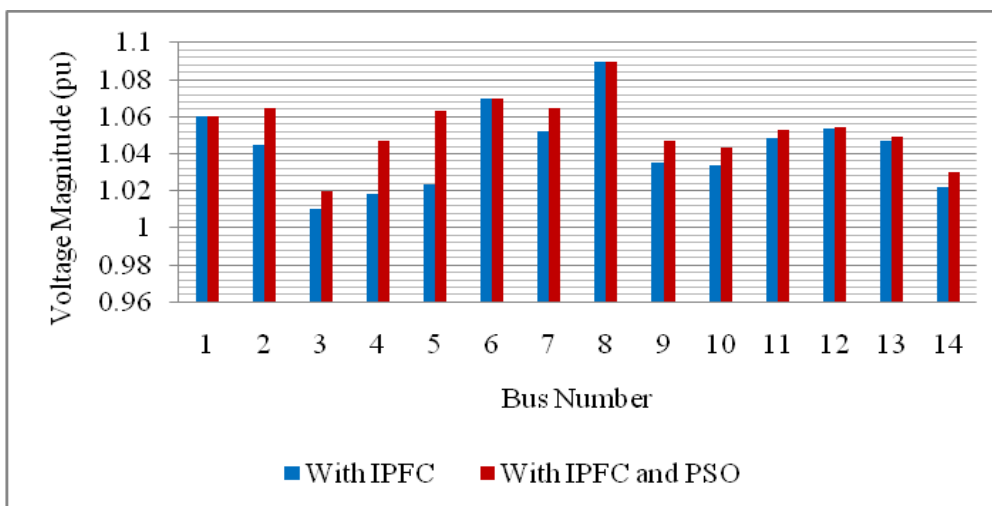


Figure 4.11: The voltage profile of IEEE 14-bus power system with IPFC and with IPFC using PSO

Figures 4.12 show the voltage profile of the IEEE 14-bus power system without IPFC, with IPFC and with IPFC using PSO. As observed in Figure 4.12, the reactive



power introduced by the IPFC devices caused an improvement in the voltage of buses 2, 3, 4, 5, 7, 9, 10, 11, 12, 13 and 14. This improvement resulted in lower reactive power flows in the lines and hence reduction in the real power loss. Also more improvement in the voltage profile has been observed in buses 2, 3, 4, 5, 7, 8, 9, 10, 11, 12, 13 and 14 when PSO algorithm is applied to the system.

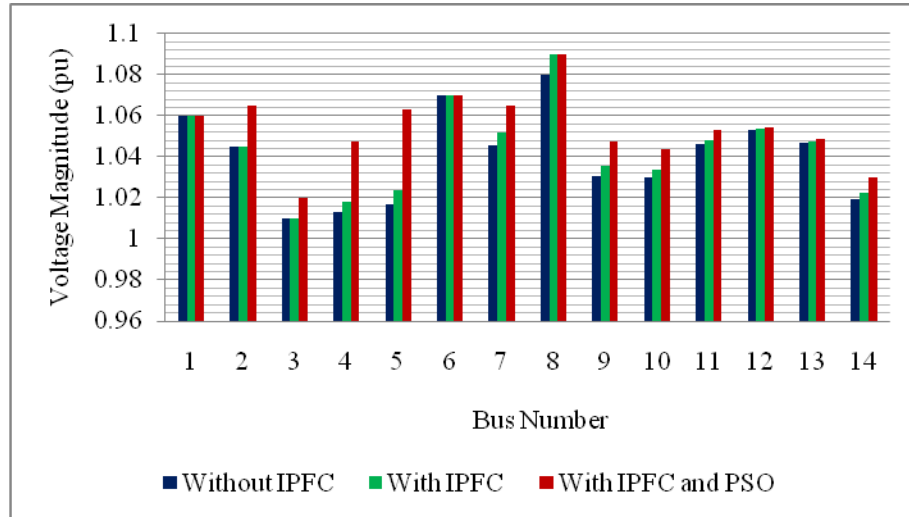


Figure 4.12: The voltage profile of IEEE 14-bus power system without IPFC, with IPFC and with IPFC using PSO

#### 4.2.4 Power Flow Analysis of IEEE 14-bus Power System with IPFC using GA

In this case the IPFC device parameters are obtained using GA technique, minimizing the transmission line losses. The IPFC is connected between lines 1-2 and 1-5 of the IEEE 14-bus power system. The GA control parameters are selected as in Table 4.6.

Table 4.6: GA control parameters

| Control parameter      | Description            |
|------------------------|------------------------|
| Population size        | 35                     |
| Crossover fraction     | 0.8                    |
| Generations            | 100                    |
| Time limit             | 100                    |
| Stall generation limit | 100                    |
| Stall time limit       | 100                    |
| Selection fuction      | @selectionroulette     |
| Crossover fuction      | @crossoversinglepoint  |
| Mutation function      | @mutationadaptfeasible |

The GA technique is applied to minimize the transmission line losses and to find the optimal parameters of VSCs of the IPFC. The voltages of generator buses in the system were selected as in Table 4.1, such that the generators supply as much reactive power to the system as they can before inserting any extra reactive power source. After setting the limits for the injected voltage magnitudes between  $0 < V_{inj} < 0.15$  and angles between  $-\pi/2 < \theta_{inj} < \pi/2$ , the results obtained for line flows, line losses and the Newton Raphson load flow analysis of the IEEE 14-bus power system with IPFC and GA are presented in Appendixes C11 and C12. The optimal values of the injected voltage magnitudes and angles of the IPFC found by the GA technique are as reported in Table 4.7.

Table 4.7: Optimal parameters of IPFC and the system line losses with GA

| Optimization parameter | lines  |        |
|------------------------|--------|--------|
|                        | 1-2    | 1-5    |
| $V_{inj}$ (pu)         | 0.0447 | 0.0457 |
| $\theta_{inj}$ (rad)   | 0.8912 | 1.0646 |
| Lines losses (MW)      | 0.012  | 0.003  |
| Total line losses (MW) | 4.720  |        |

As observed from Tables 4.2 and 4.7, the power loss of the system is reduced to 0.012 MW, 0.003 MW and 4.720 MW, when the GA is used i.e. reduced by approximately 99.7 %, 99.8 % and 65.3 % for the transmission lines 1-2, 1-5 and the total active power losses respectively. The fitness of each individual and the current best individual of the optimal parameters of the injected voltage and angle are shown in Figure 4.13, and 4.14, respectively. From Figure 4.13, it is observed that the optimal parameters of the injected voltages and angles are 0.0447, 0.0457 pu and 0.8912, 1.0646 rad for transmission lines 1-2 and 1-5, respectively.

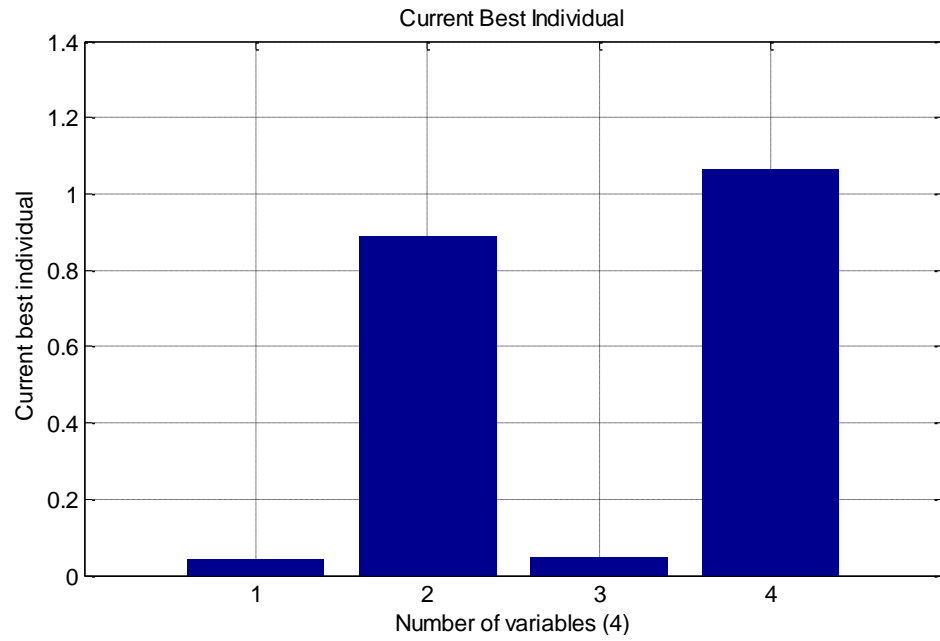


Figure 4.13: Current best individual of the optimal parameters

Figure 4.14 shows the fitness of each individual variable when the optimal parameters reached a best value. It is observed that the fitness of each individual are almost equal when the optimal parameters are found.

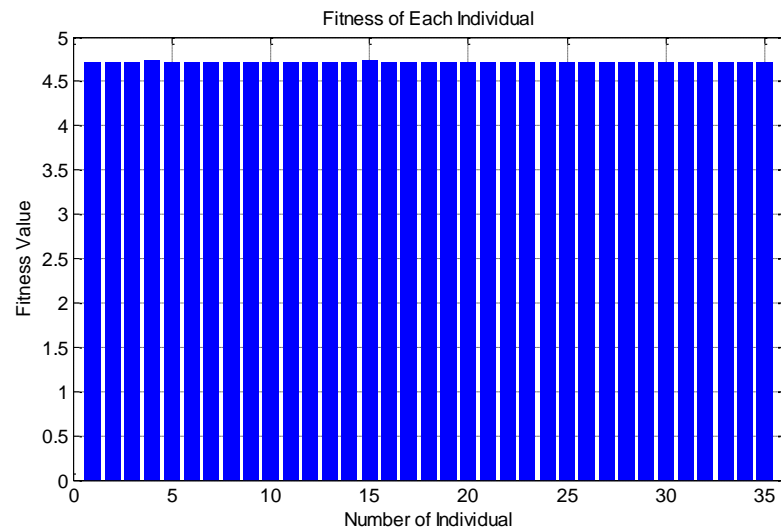


Figure 4.14: Fitness of each individual

The average distance between individual and the variation of the fitness value of best function value with the change in number of generation in GA are shown in Figures 4.15, and 4.16, respectively. It is observed that the objective function reached

a global minimum after nearly 40 iterations out of 100 and the simulation running time is 29.595 seconds for the GA.

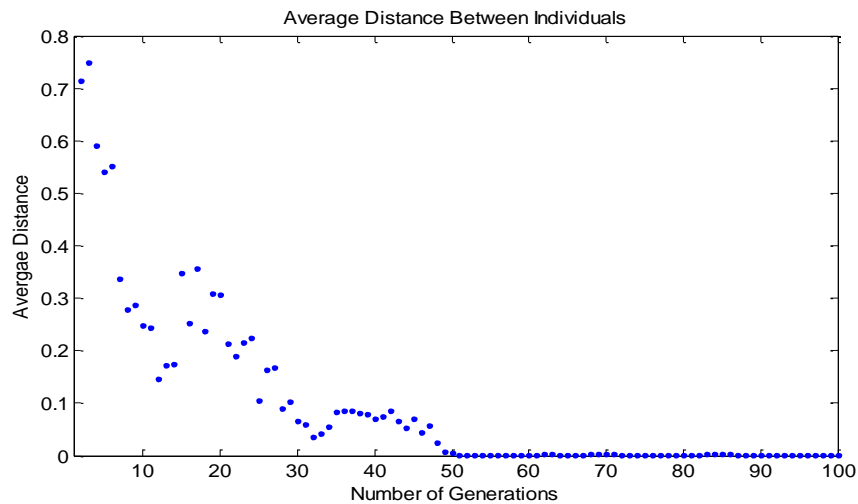


Figure 4.15: Average distance value with the change in number of generation of GA

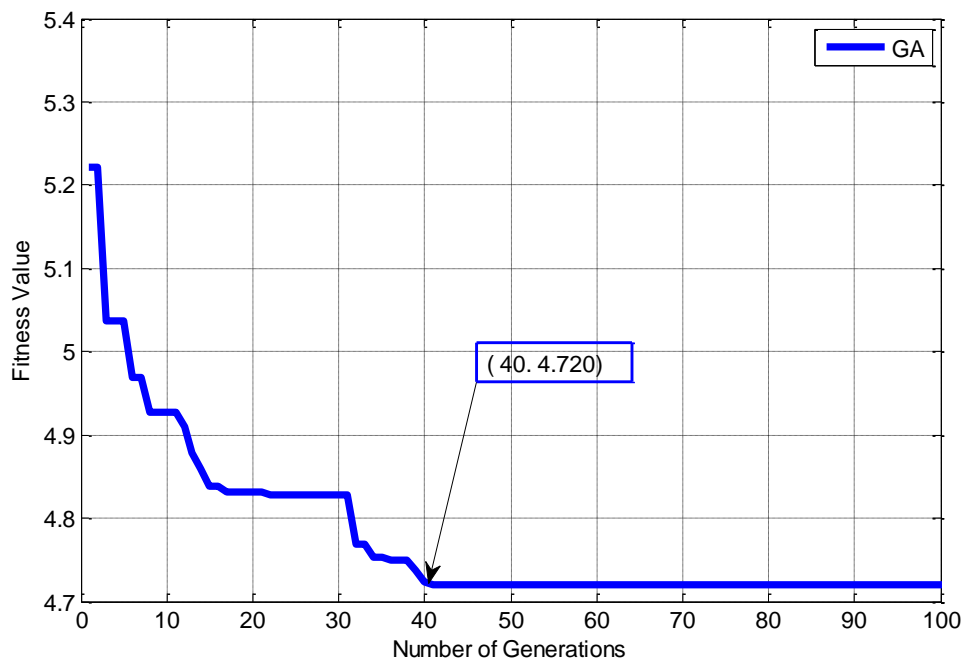


Figure 4.16: Variation of best function value with the change in number of generation of GA

As shown in Figure 4.17, the stopping criteria are met after nearly 1 % of stall time limit and that means there is no improvement in the best fitness, 3 % of Stall generations, 27 % of the total time limit and 100 % of generations specifies the maximum number of iterations.

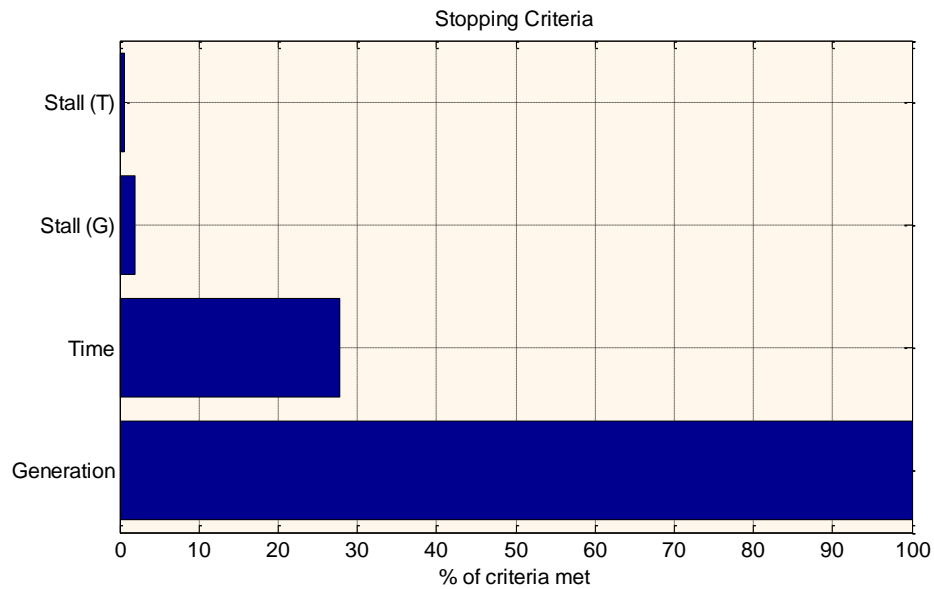


Figure 4.17: stopping criteria percentages

Figure 4.18 shows the voltage profile of IEEE 14-bus power system for the power flow with IPFC and using GA.

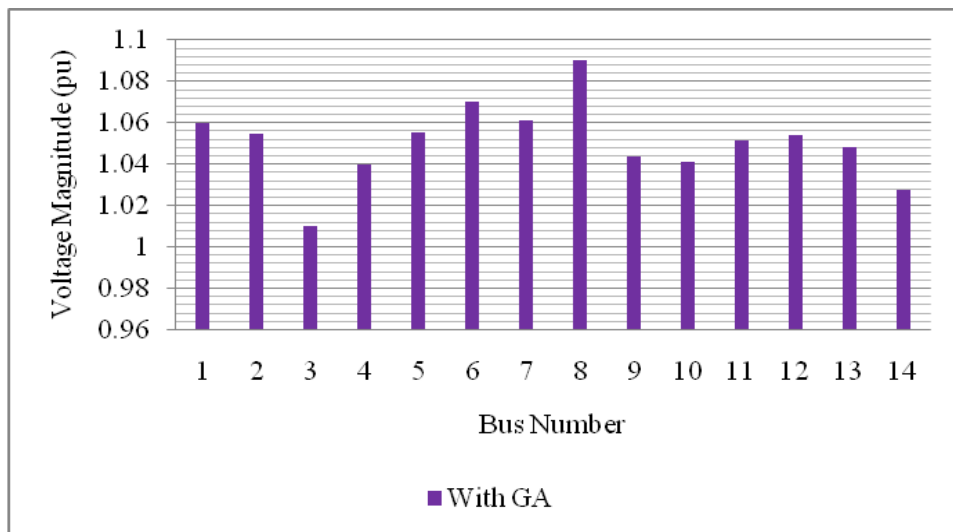


Figure 4.18: The voltage profile of IEEE 14-bus power system with IPFC using GA

Figures 4.19 show the voltage profile of the IEEE 14-bus power system with IPFC, and with IPFC using GA. It is observed that there is an improvement of the voltages profile of some buses such as 2, 4, 5, 7, 9, 10, 11 and 14 when GA technique is used.

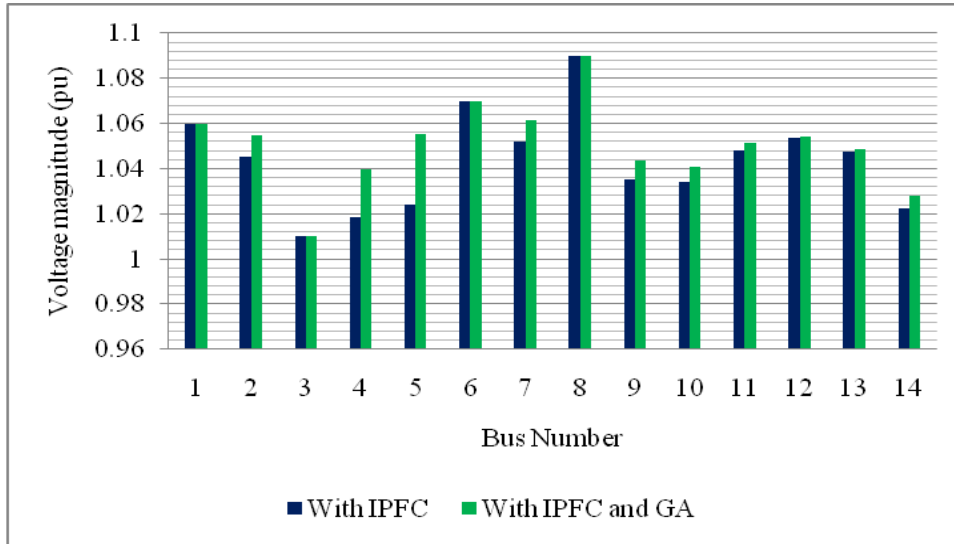


Figure 4.19: The voltage profile of IEEE 14-bus power system with IPFC and with IPFC using GA

Figures 4.20 show the voltage profile of the IEEE 14-bus power system without IPFC, with IPFC and with IPFC using GA.

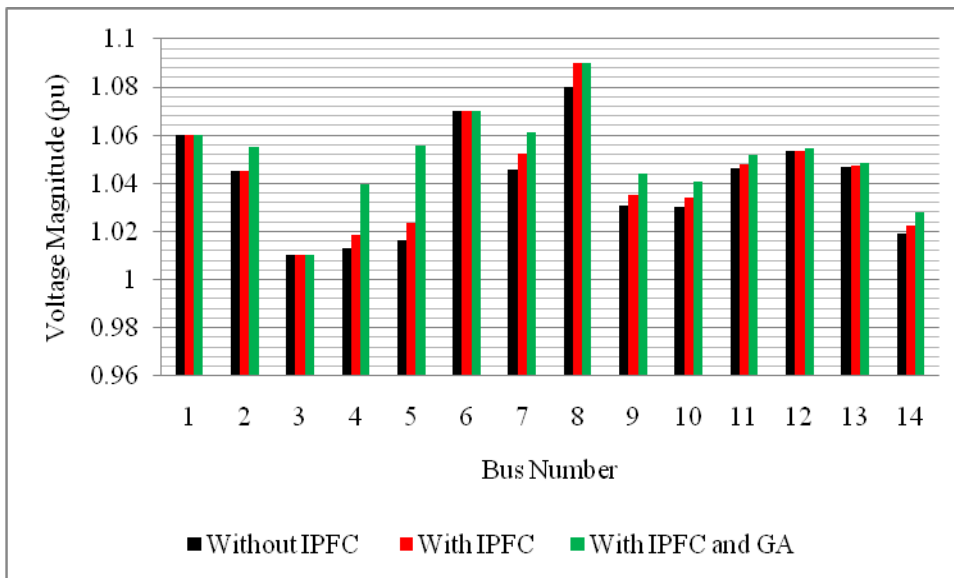


Figure 4.20: The voltage profile of IEEE 14-bus power system without IPFC, with IPFC and with IPFC using GA

As observed in Figure 4.20, the reactive power introduced by the IPFC devices caused an improvement in the voltage of buses 4, 5, 7, 8, 9, 10, 11 and 14. This

improvement resulted in lower reactive power flows in the lines and hence reduction in the real power loss. Also more improvement in the voltage profile has been observed in buses 2, 4, 5, 7, 9, 10, 11, 12, 13 and 14 when GA algorithm is applied to the system.

#### 4.2.5 Power Flow Analysis of IEEE 14-bus Power System with IPFC using SA

In this case the IPFC device was installed on the transmission lines which are connected between lines 1-2 and 1-5. The control parameters of SA are selected based on simulation with different combinations which return minimum objective function. Finally the parameters listed in Table 4.8 are selected to test the power flow analysis of IEEE 14-bus power system.

Table 4.8: SA control parameters

| Control parameters                      | Description     |
|---|-----------------|
| Initial temperature                     | 100             |
| Maximum number of iterations            | 300             |
| Annealing function                      | @annealing fast |
| Temperature function                    | @temperatureexp |
| Termination tolerance on function value | 1e-6            |
| Stall iteration limit                   | 2000            |
| Time limit                              | 100 sec         |

The SA is applied to minimize the transmission line losses and to find the optimal parameters of the injected voltage source magnitude and angle of VSCs of the IPFC. The voltages of generator buses in the system were considered as in Table 4.1, such that the generators supply as much reactive power to the system as they can before inserting any extra reactive power source. After setting the boundary conditions for the injected voltage magnitudes between  $0 < V_{inj} < 0.15$  and angles between  $-\pi/2 < \theta_{inj} < \pi/2$ , the results obtained for line flows, line losses and the Newton Raphson load flow analysis of IEEE 14-bus power system with IPFC and SA are presented in Appendices C13 and C14. The optimal values of the injected voltage magnitudes and angles found by the SA technique are reported in Table 4.9.

Table 4.9: The control parameter and the system losses

| Optimization parameter | lines  |        |
|------------------------|--------|--------|
|                        | 1-2    | 1-5    |
| $V_{inj}$ (pu)         | 0.0568 | 0.0449 |
| $\Theta_{inj}$ (rad)   | 0.8355 | 0.9864 |
| Lines Losses (MW)      | 0.025  | 0.003  |
| Total Losses (MW)      | 4.648  |        |

As observed from Table 4.2 and 4.9, the power loss of the system is reduced to 0.025, 0.003 and 4.648 MW, when the SA is used i.e. reduced by approximately 99.4 %, 99.8 % and 65.8 % for the transmission lines 1-2, 1-5 and the total active power losses respectively. The current point and the best point of the optimal parameters of the injected voltage and angle are shown in Figure 4.21, and 4.22 respectively. It is observed that the optimal parameters of the injected voltages and angles are 0.0568, 0.0449 pu and 0.8355, 0.9864 rad for transmission lines 1-2 and 1-5 respectively.

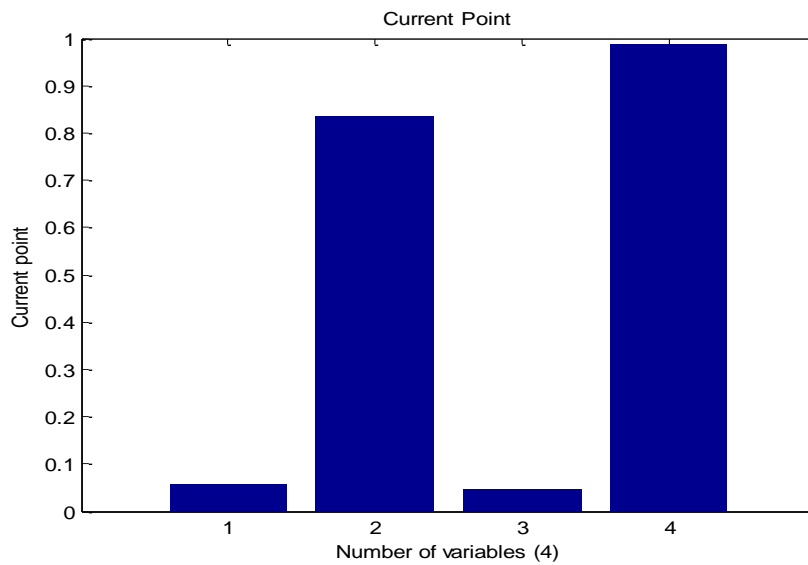


Figure 4.21: current points of the optimal parameters



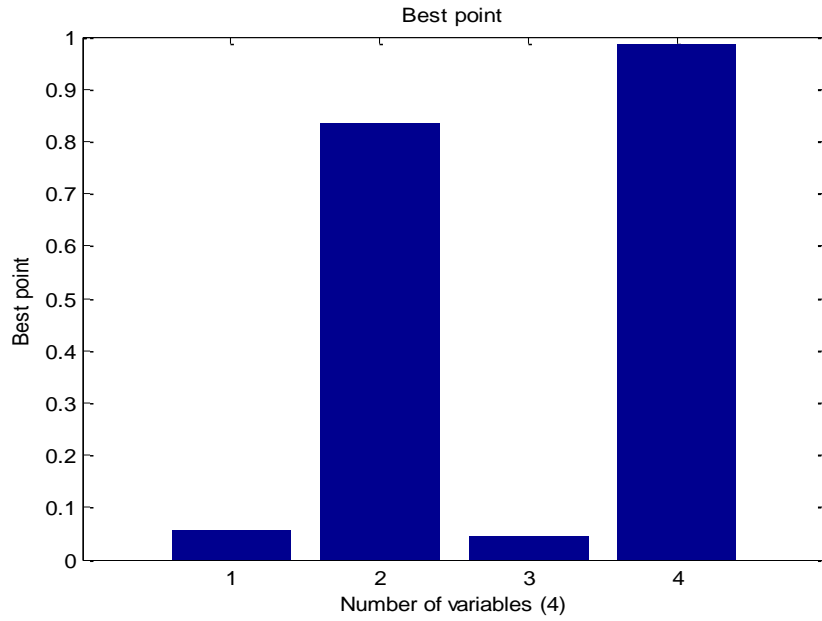


Figure 4.22: best point of the optimal parameters

Figure 4.23 shows the current temperature of each variable when the optimal parameters are reached a best value. It is observed that the temperature is the control parameter in SA technique which is decreased gradually from 100 C° as initial temperature to nearly  $1.9 \times 10^{-5}$  C° when the objective function reached a global minimum.

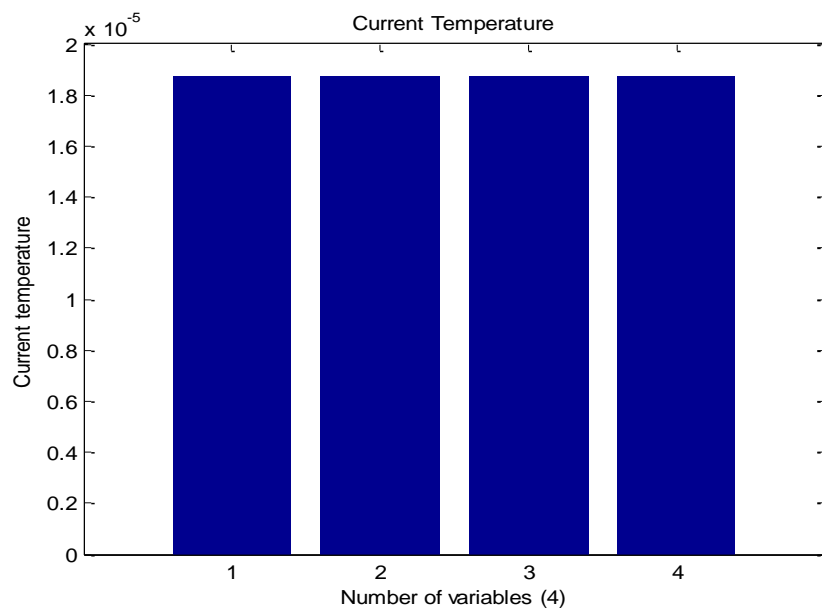


Figure 4.23: Temperatures of the optimal parameters

The variation of the current function value and best function value with the change in number of iterations in SA are shown in Figure 4.24, and 4.25 respectively. It is observed that the objective function reached a global minimum after nearly 185 iterations out of 300 and the simulation running time is 14.52 seconds.

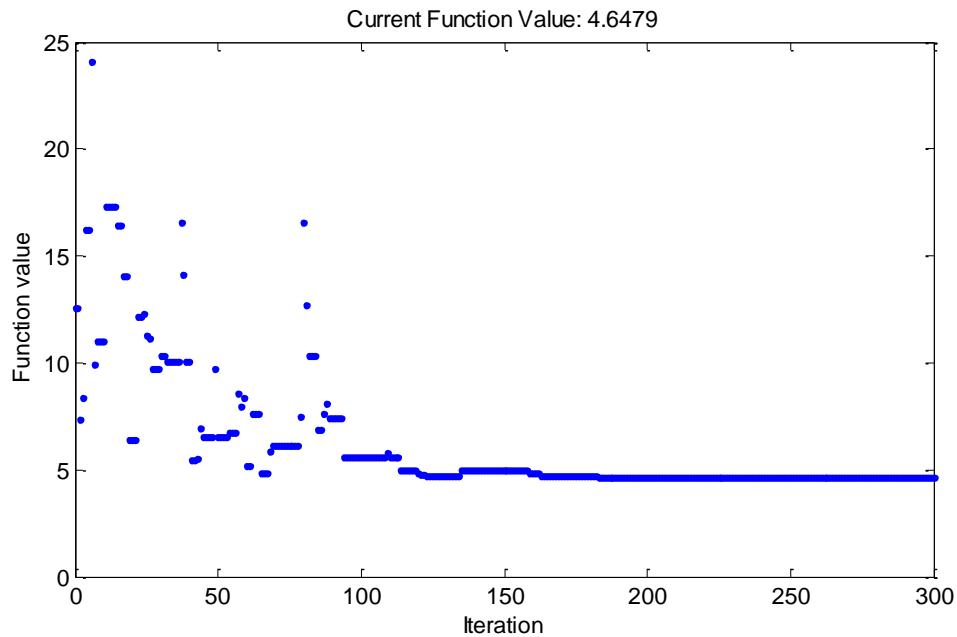


Figure 4.24: The variation of the current objective function value with the change in iterations by SA

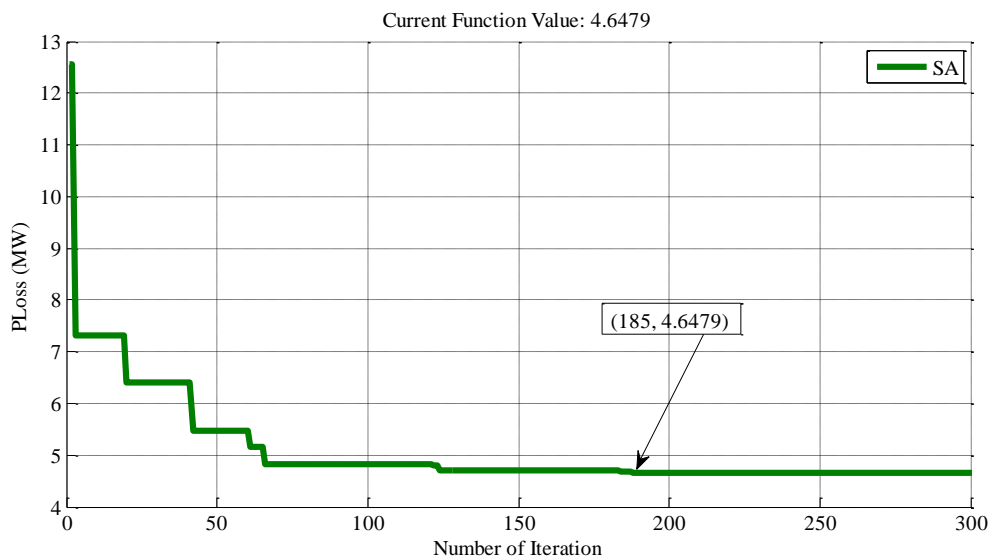


Figure 4.25: Variation of best objective function value with the change in iterations by SA

As shown in Figure 4.26 the stopping criteria is met after nearly 13 % of the total time limit of 100 seconds set in the algorithm, 100 % of the maximum iterations and 3 % of the function tolerance.

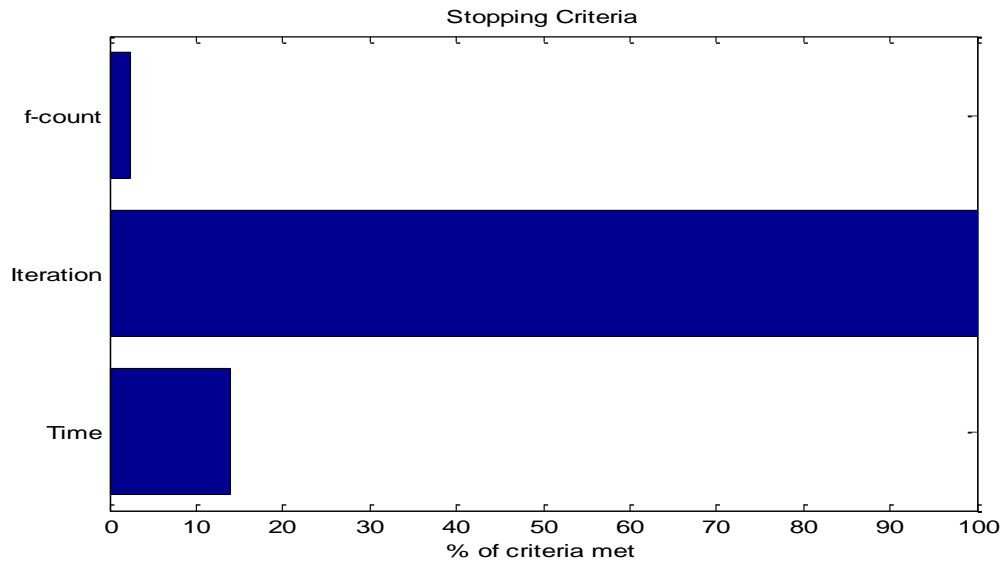


Figure 4.26: The stopping criteria

Figure 4.27 shows the voltage profile of IEEE 14-bus power system for the power flow with IPFC and using SA.

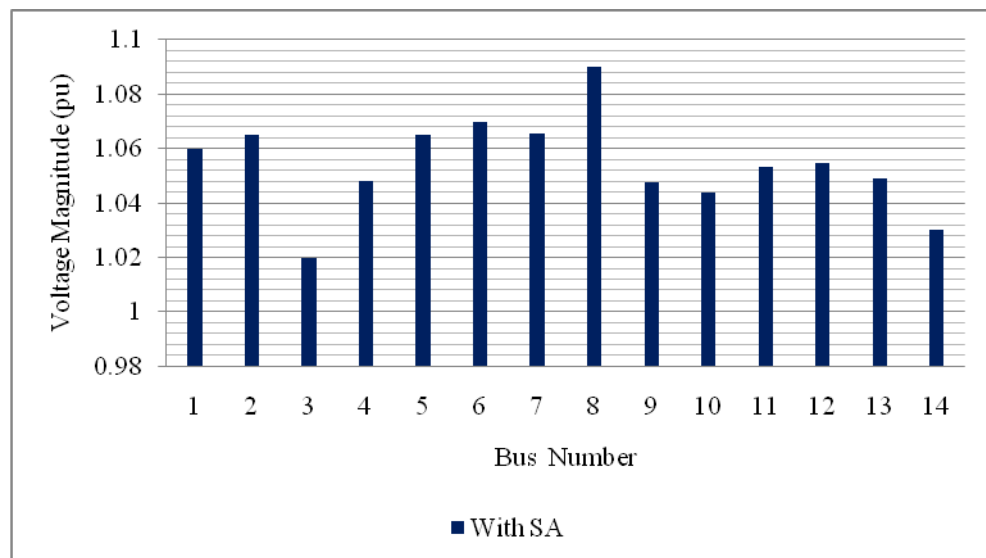


Figure 4.27: The voltage profile of IEEE 14-bus power system with IPFC using SA

The voltage profile of the IEEE 14-bus power system with IPFC and with IPFC using SA is shown in Figures 4.28.

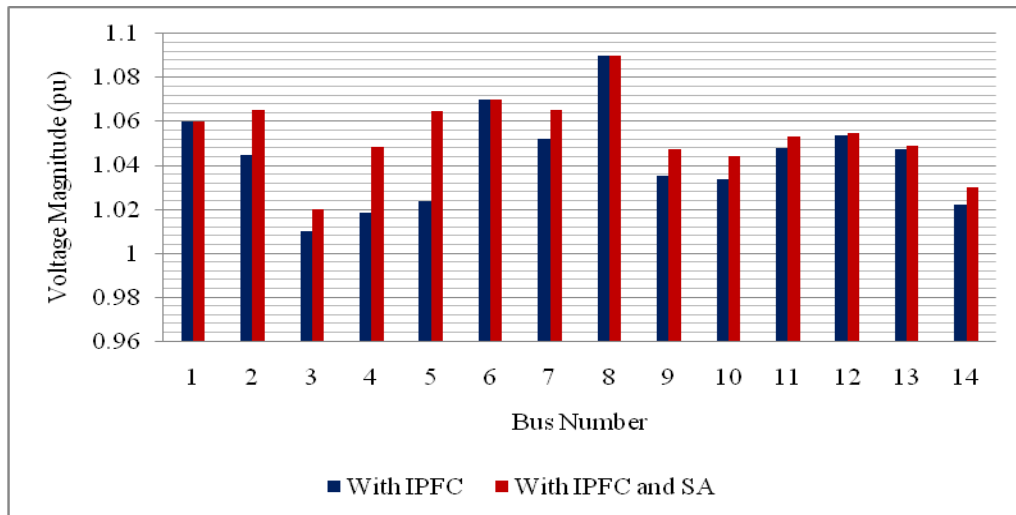


Figure 4.28: The voltage profile of IEEE 14-bus power system with IPFC and with IPFC using SA

Figure 4.29 shows the voltage profile of the IEEE 14-bus power system without IPFC, with IPFC and with IPFC using SA. As observed in Figure 4.29, the reactive power introduced by the IPFC devices caused an improvement in the voltage of buses 4, 5, 7, 8, 9, 10, 11, 12, 13 and 14. This improvement resulted in lower reactive power flows in the lines and hence reduction in the real power loss. Also more improvement in the voltage profile has been observed in buses 2, 3, 4, 5, 7, 8, 9, 10, 11, 12, 13 and 14 when SA algorithm is applied to the system.

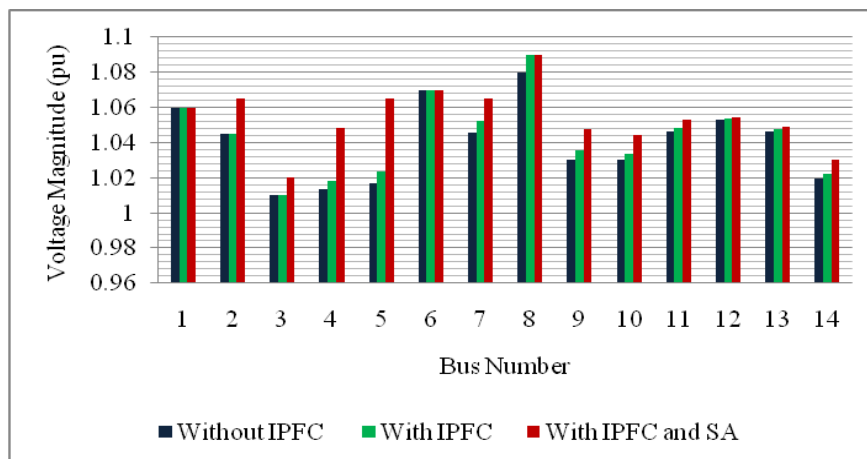


Figure 4.29: The voltage profile of IEEE 14-bus power system without IPFC, with IPFC, and with IPFC using SA

#### 4.2.6 Comparison of Simulation Results with PSO, GA and SA Techniques of IEEE 14-bus Power System

The PSO, GA and SA techniques are applied to minimize the transmission line active power losses and to find the optimal parameters of the injected voltage magnitude and angle of VSCs of the IPFC. The voltages of generator buses are same as in Table 4.1, such that the generators supply as much reactive power to the system as they can before inserting any extra reactive power source. After setting the limits for the injected voltage magnitudes of VSC between  $0.0 < V_{inj} < 0.15$  and the angles between  $-\pi/2 < \theta_{inj} < \pi/2$ , and setting each optimization method control parameters, the simulation on power flow analysis program is performed. The active power line losses are minimized using each optimization technique subjected to the constraints on the voltage magnitudes and angles of VSCs of IPFC. The simulation results of injected voltages magnitude and angles and the system line active power losses of the specified lines are obtained with each optimization technique. Also the total active power losses of the IEEE 14-bus power of the system obtained from the power flow analysis are presented in Table 4.10.

Table 4.10: The IPFC parameters and the transmission line active power losses

| Optimization parameter | Optimization Methods |        |        |        |        |        |
|------------------------|----------------------|--------|--------|--------|--------|--------|
|                        | CFAPSO               |        | GA     |        | SA     |        |
| Lines                  | 1-2                  | 1-5    | 1-2    | 1-5    | 1-2    | 1-5    |
| $V_{inj}$ (pu)         | 0.0457               | 0.0558 | 0.0639 | 0.0452 | 0.0568 | 0.0449 |
| $\theta_{inj}$ (rad)   | 1.0253               | 0.6296 | 0.9269 | 0.9963 | 0.8355 | 0.9864 |
| Lines losses (MW)      | 0.0120               | 0.0030 | 0.099  | 0.003  | 0.025  | 0.003  |
| Total losses (MW)      | 4.6300               |        | 4.720  |        | 4.648  |        |

As observed from Tables 4.2 and 4.10, the total active power loss of the system is reduced to 4.63 MW, 4.720 MW and 4.648 MW, i.e. reduced by approximately 65.94 %, 65.23 % and 65.81% when the PSO, GA and SA methods are used respectively. Table 4.11 reports a comparison of number of iterations and simulation running time required by PSO, GA and SA optimization methods respectively.

Table 4.11: Comparison between optimization methods

| Item                         | Optimization method |        |        |
|------------------------------|---------------------|--------|--------|
|                              | PSO                 | GA     | SA     |
| Number of iterations         | 12                  | 40     | 185    |
| Simulation running time, sec | 24.107              | 29.595 | 14.520 |

It is observed that the time taken for minimizing the objective function by SA technique is only 14.52 sec whereas the other two techniques required more time.

The variations of objective functions with the change in number of iterations are shown in Figure 4.30. It is observed that the objective functions reached a global minimum after nearly 12, 40 and 185 iterations with PSO, GA and SA methods respectively.

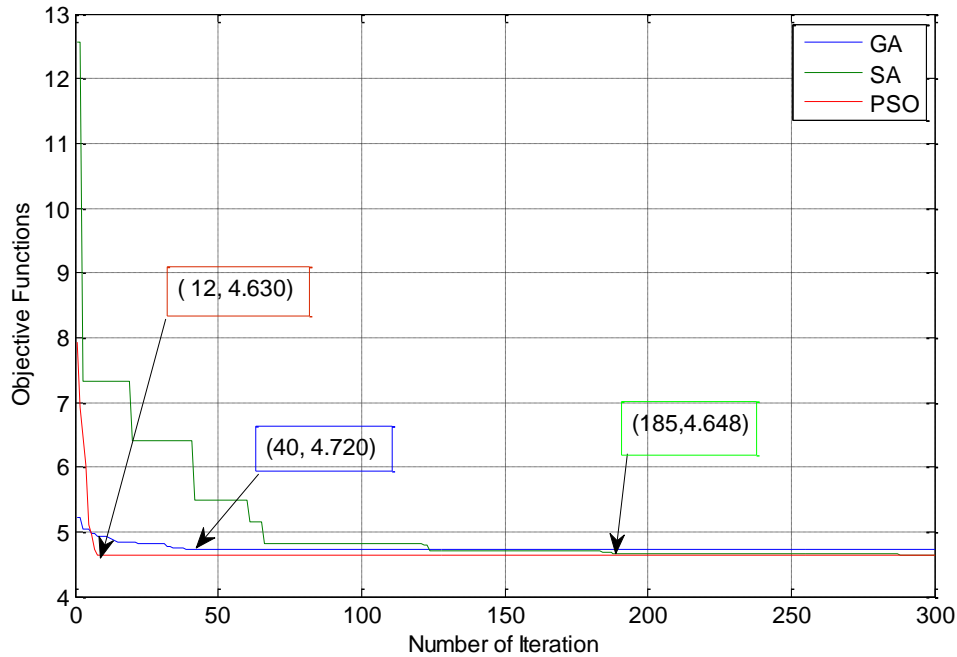


Figure 4.30: Variation of objective function with the change in iterations

The voltage profile of IEEE 14-bus power system for the power flow with IPFC and using PSO, GA and SA methods is presented in Figure 4.31. The voltage profiles of the system without IPFC, with IPFC, and with IPFC and PSO or GA or SA together, are compared as shown in Figure 4.32. Therefore, it is clearly observed that from the above results PSO is the best method in terms of loss minimization.

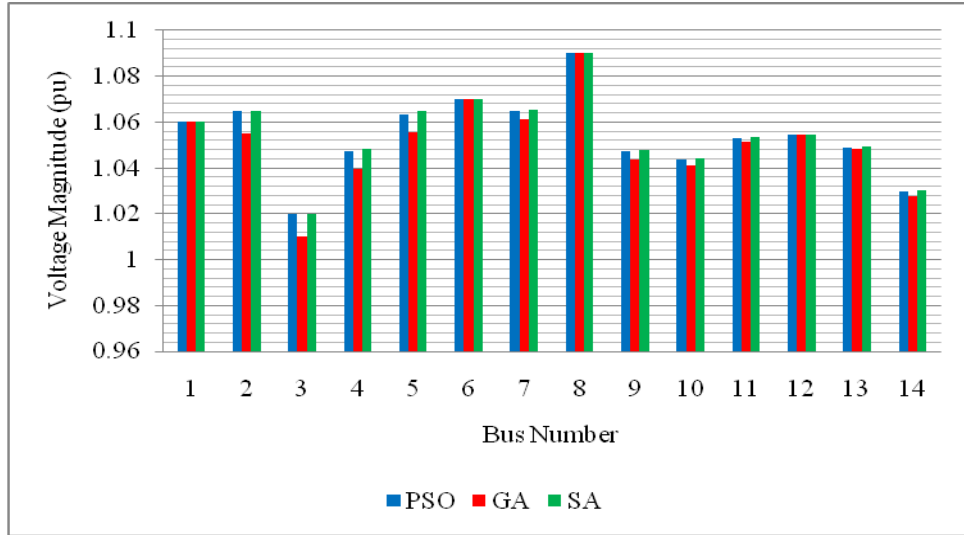


Figure 4.31: The voltage profile of IEEE 14-bus power system with IPFC together with PSO or GA or SA technique

As observed in Figure 4.32, the reactive power introduced by the IPFC devices caused an improvement in the voltage of buses 4, 5, 7, 8, 9, 10, 11 and 14. This improvement resulted in lower reactive power flows in the lines and hence reduction in the real power loss. Also more improvement in the voltage profile has been observed in buses 2, 3, 4, 5, 7, 8, 9, 10, 11, 12, 13 and 14 when PSO, GA and SA techniques are applied to the system. Also it is observed that, GA has less improvement in the voltage profile compare to the PSO, and SA techniques.

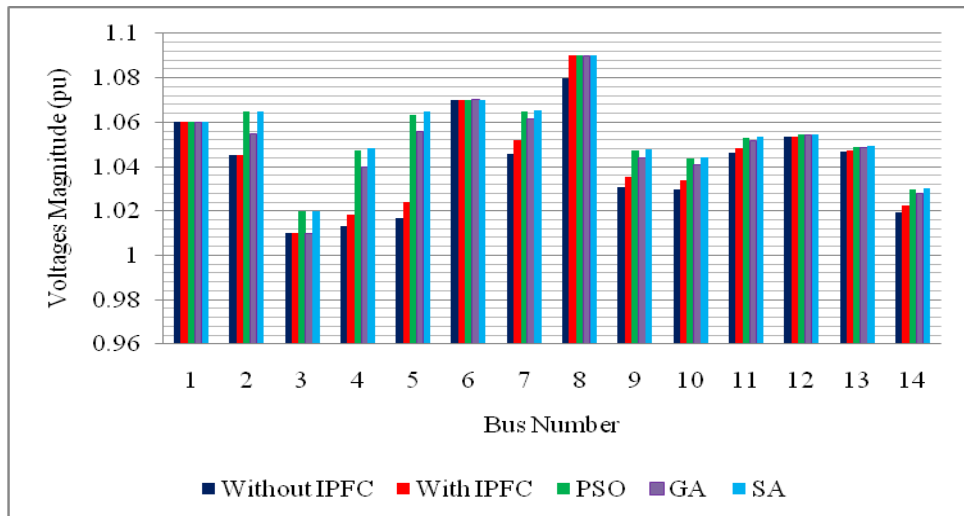


Figure 4.32: The voltage profile of IEEE 14-bus power system without IPFC, with IPFC and with IPFC together with PSO or GA or SA technique

### 4.3 Case 2 Standard IEEE 30-bus Power System

To verify the effectiveness of the proposed algorithm MATLAB m-file is developed for power flow for all simulations and are applied to the standard IEEE 30-bus power test system. The IPFC devices installed in lines 1-2 and 1-3, are represented as voltage sources as shown in Appendix B, Figure B.2. First the results obtained with the algorithms by using PSO, have been compared to those calculated by power flow solution without IPFC and with IPFC. The system transmission line losses for the three operating conditions without IPFC, with IPFC, and with IPFC, and PSO have been calculated too. Next using GA technique, the optimal parameters of the IPFC and the transmission line losses of IEEE 30-bus power system are investigated. In similar way, SA technique is used to derive the optimal parameters of the IPFC, minimizing the transmission line losses of the system.

#### 4.3.1 Power Flow Analysis of IEEE 30-bus Power System without IPFC

Simulation is performed on power flow analysis mathematical model using Newton Raphson method as shown in Appendix A1, setting the bus voltages data and the lines data as reported in Appendix B2 [94]. Therefore under these operating conditions, the generators bus voltages of IEEE 30-bus power system are used as reported in Table 4.12, such that the generators supply as much reactive power to the system as they can before inserting any extra reactive power source.

Table 4.12: The voltages of generator buses

| Bus Number | Voltage magnitude (pu) |
|------------|------------------------|
| 1          | 1.060                  |
| 2          | 1.043                  |
| 5          | 1.010                  |
| 8          | 1.010                  |
| 11         | 1.082                  |
| 13         | 1.071                  |

The results obtained of line flows; line losses and the Newton-Raphson load flow analysis of IEEE 30-bus power system without IPFC are presented in Appendixes D1 and D2. The transmission lines losses during the operating conditions without IPFC for line 1-2 and 1-3 and total line losses are reported in Table 4.13.



Table 4.13: Transmission line losses of IEEE 30-bus power system without IPFC

| From Bus To Bus | Line losses in MW |
|-----------------|-------------------|
| 1 - 2           | 5.179             |
| 1 - 3           | 3.116             |
| Total Losses MW | 17.528            |

And the voltage profile of all the buses are as shown in Figure 4.33.

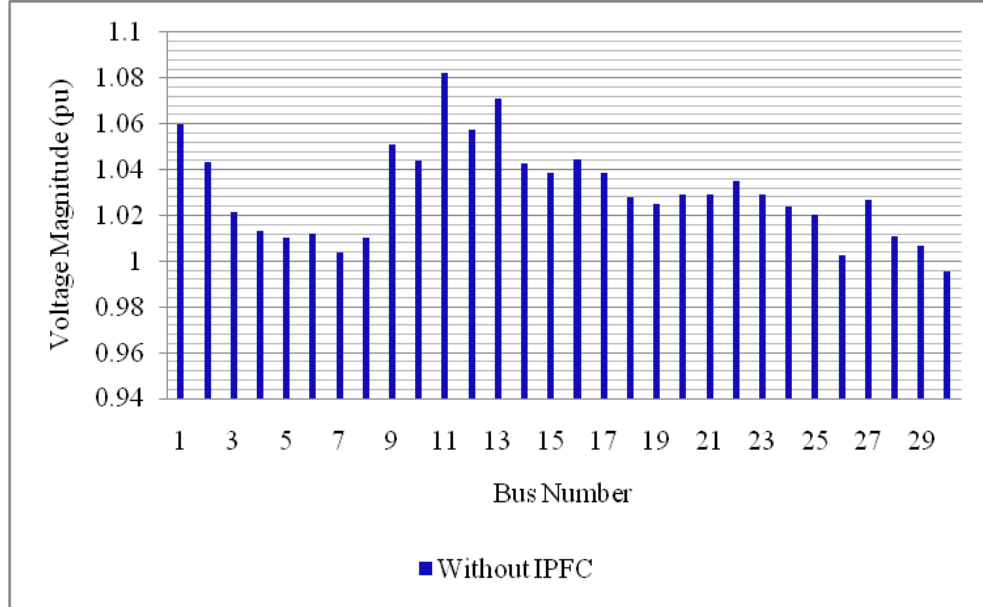


Figure 4.33: The voltage profile of IEEE 30-bus power system without IPFC

#### 4.3.2 Power Flow Analysis of IEEE 30-bus Power System with IPFC

In this case, power flow analysis is simulated with the IPFC connected between lines 1-2 and 1-3. After adding the sources impedances such as ( $Z_{l2} = 0.00192 + j0.00575$  and  $Z_{l3} = 0.00452 + j0.01652$ ) to lines 1-2 and 1-3 respectively, ( $Z_{s12}$  and  $Z_{s13}$  are the impedances of VSC<sub>1</sub> and VSC<sub>2</sub> connected to the lines 1-2 and 1-3), the results obtained of line flows, line losses and the Newton-Raphson load flow analysis of IEEE 30-bus power system with IPFC are presented in Appendixes D3 and D4. The optimal injected voltage magnitudes ( $V_{inj}$  (pu)) and the angles ( $\theta_{inj}$  (rad)) for the first and for the second transmission lines (i.e. 1-2 and 1-3) and the minimized line losses are reported in Table 4.14. The total line loss of the IEEE 30-bus power system is also presented.

Table 4.14: The control parameter and the system losses of IEEE 30-bus power system with IPFC

| Line                 | 1-2   | 1-3   |
|----------------------|-------|-------|
| $V_{inj}$ (pu)       | 0.046 | 0.046 |
| $\theta_{inj}$ (rad) | 1.400 | 1.400 |
| Lines Losses (MW)    | 0.510 | 0.158 |
| Total Losses (MW)    | 9.648 |       |

It is observed from Tables 4.13 and 4.14, the reduction of the line losses are from 5.179 to 0.510 for the line 1-2, and from 3.116 to 0.158 for the line 1-3 and the total losses are reduced from 17.528 to 9.648. In other word the transmission line losses are reduced by 90.15 % and 94.93 % for the first and second transmission lines 1-2 and 1-3 respectively and 44.96 % for the total loss of the IEEE 30-bus power system when the IPFC is installed between the lines 1-2 and 1-3.

Figure 4.34 shows the voltage profile of IEEE 30-bus power system for the power flow when the IPFC is installed between lines 1-2 and 1-3.

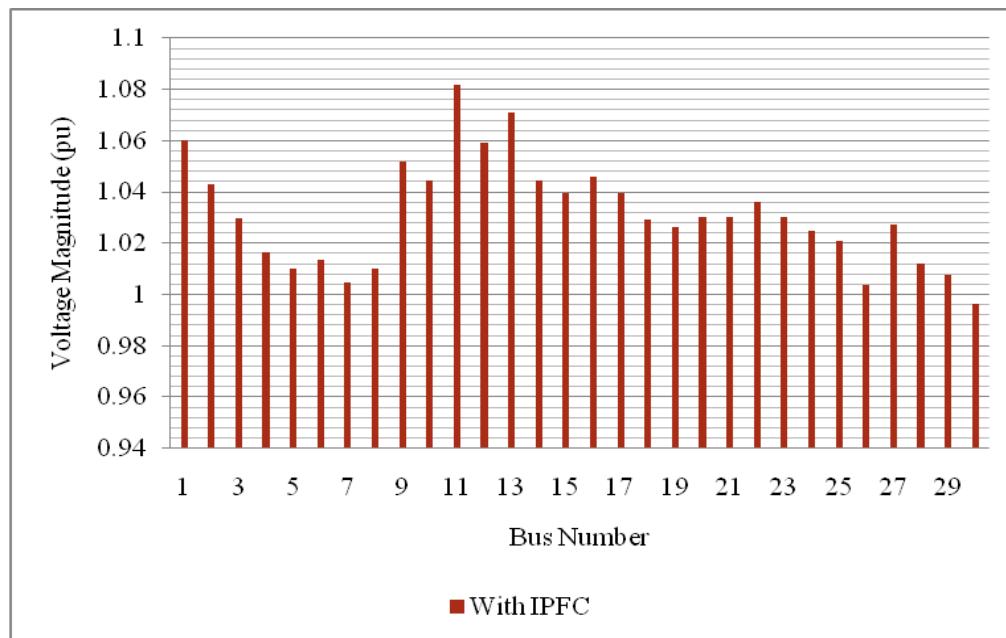


Figure 4.34: The voltage profile of IEEE 30-bus power system with IPFC

As shown in Tables 4.13 and 4.14, the total power losses of the system are decreased from 17.528 MW to 9.648 MW, i.e. by approximately 44.96 %. The

voltage profile of the system with and without IPFC devices are shown in Figure. 4.35. As compared to the voltage profile in the Figure 4.35, the reactive power introduced by the IPFC devices caused an improvement in the voltage of some buses. This improvement resulted in lower reactive power flow in the lines and hence reduction in the real power loss.

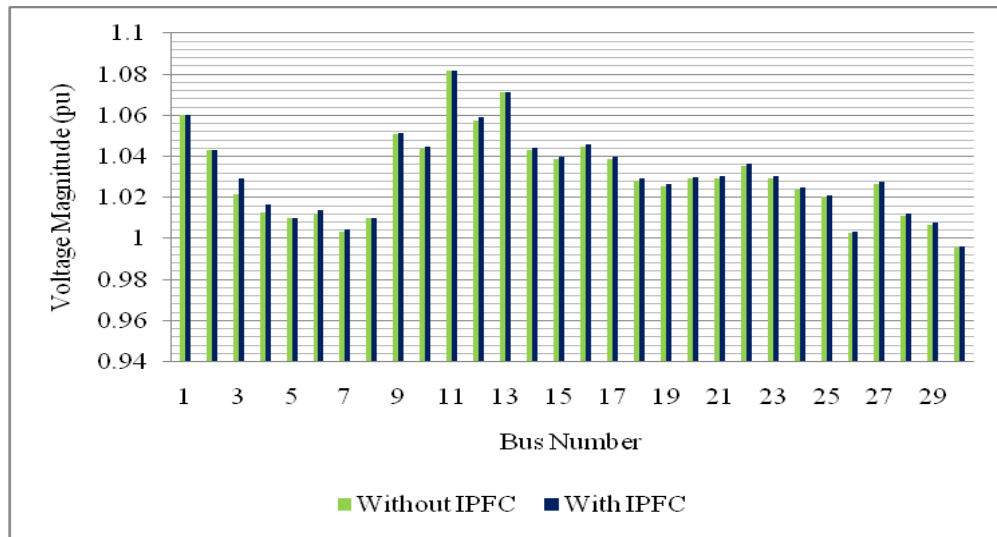


Figure 4.35: The voltage profile of IEEE 30-bus power system without and with IPFC

### 4.3.3 Power Flow Analysis of IEEE 30-bus Power System with IPFC and using PSO

In this case the IPFC device installed on the transmission line of the IEEE 30-bus power system is considered connected between line 1-2 and 1-3. Proper control parameters of PSO are selected as in Table 4.15

Table 4.15: PSO control parameters

| Control parameters  | Value           |
|---|-----------------|
| Number of Iterations                                      | 100             |
| Swarm size S  | 35              |
| Problem dimension   | 4               |
| Inertia weight factor W                                   | 0.9 to 0.4      |
| Weighting factor C1 and C2                                | C1 = C2 = 2     |
| The random number rand <sub>1</sub> and rand <sub>2</sub> | Between 0 and 1 |

The voltages of generator buses in the system are used as in Table 4.12, such that the generators supply as much reactive power to the system as they can before inserting any extra reactive power source. The boundary conditions for the injected voltage magnitudes are between  $0.0 < V_{inj} < 0.15$  and the angles between  $-\pi/2 < \theta_{inj} < \pi/2$ . The PSO is applied to minimize the transmission line losses and to find the optimal parameters of the injected voltage source magnitude and angle of VSC of IPFC. After setting the limits for the injected voltages and angles of VSC, the simulation on power flow analysis program is performed. The results obtained for line flows, line losses and the Newton-Raphson load flow analysis of IEEE 30-bus power system with IPFC and PSO are presented in Appendixes D5 and D6. The injected voltage magnitudes and angles of VSC of IPFC and the system line losses for the PSO are presented as in Table 4.16.

Table 4.16: The control parameter of IPFC and the system losses of IEEE 30-bus power system

| Optimization parameter | Lines |       |
|------------------------|-------|-------|
|                        | 1-2   | 1-3   |
| $V_{inj}$ (pu)         | 0.044 | 0.082 |
| $\theta_{inj}$ (rad)   | 1.088 | 1.062 |
| Lines losses (MW)      | 0.026 | 0.012 |
| Total losses (MW)      | 8.789 |       |

As observed from Tables 4.13 and 4.16, lines 1-2 and 1-3 losses and the total power loss of the system is reduced to 0.026 MW, 0.012 MW and 8.789 MW when the PSO is used i.e. reduced by approximately 99.49 %, 99.61 % and 49.86 % respectively.

The variation of objective function i.e. total line losses with the change in number of iterations in PSO is shown in Figure 4.36. It is observed that the objective function reached a global minimum after nearly 20 iterations.

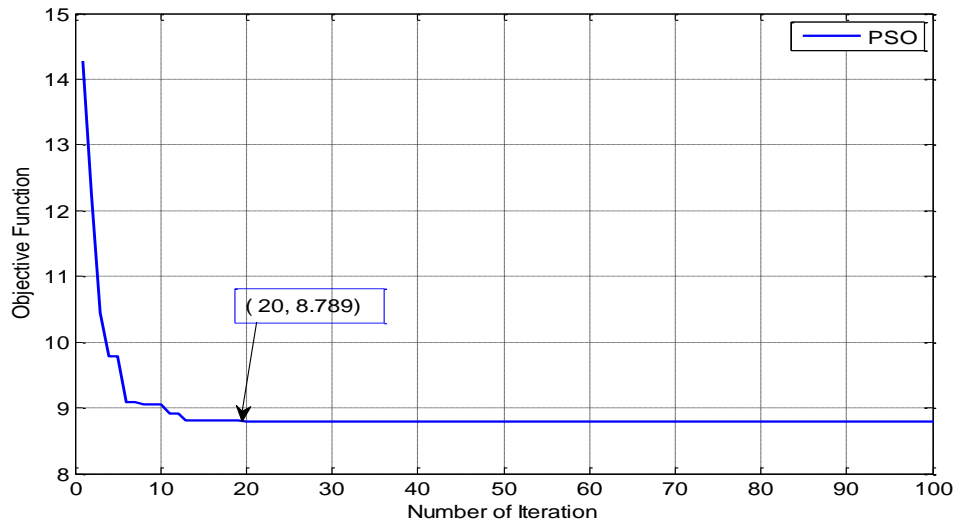


Figure 4.36: Variation of total line losses with the change in iterations by PSO

Figure 4.37, shows the voltage profile of IEEE 30-bus power system for the power flow with IPFC and PSO technique.

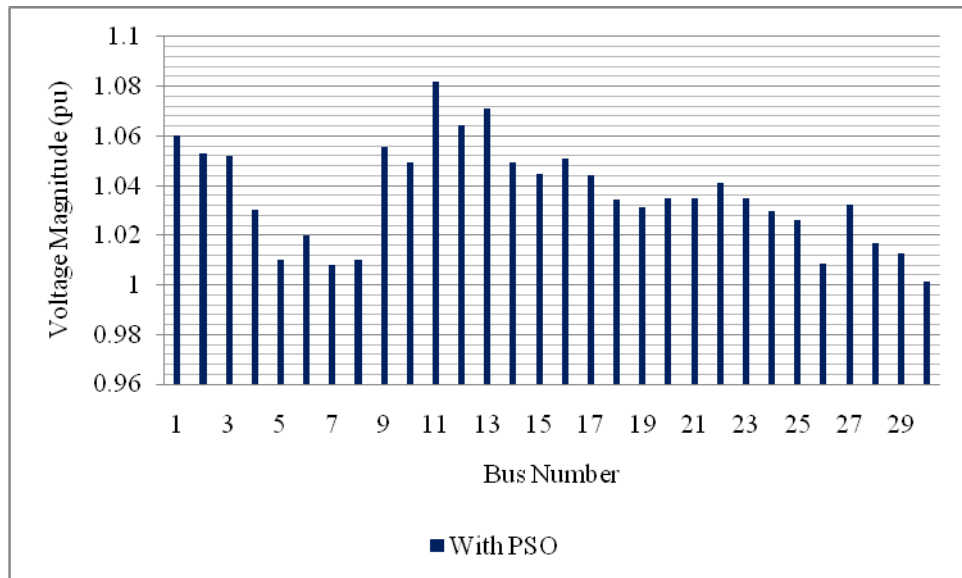


Figure 4.37: The voltage profile of IEEE 30-bus power system with IPFC and PSO

The voltage profiles of the system without IPFC, with IPFC, and with IPFC and PSO together, are compared as shown in Figure 4.38. As observed in Figure 4.38, the reactive power introduced by the IPFC devices caused an improvement in the voltage of buses 3, 4, 9, 12, and also in the buses 14 to 30. This improvement resulted in lower reactive power flows in the lines and hence reduction in the real power loss.

Also more improvement in the voltage profile has been observed in buses 2, 3, 4, 6, 7, 9, 10, 12, and also in the buses 14 to 30 when PSO algorithm is applied to the system.

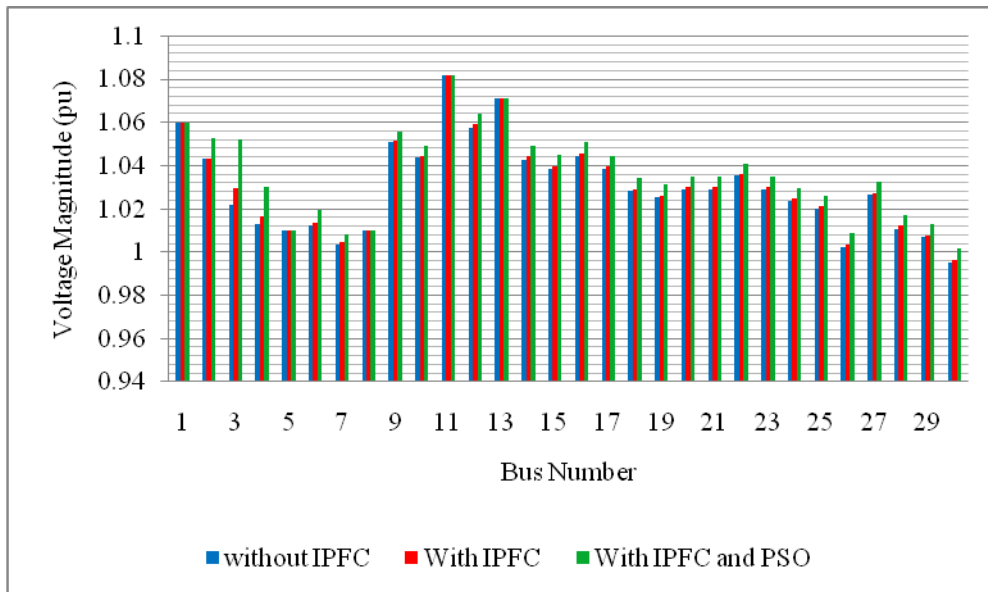


Figure 4.38: The voltage profile of IEEE 30-bus power system without IPFC, with IPFC and with IPFC using PSO

#### 4.3.4 Power Flow Analysis of IEEE 30-bus Power System with IPFC using GA

In this case the IPFC device parameters are obtained using GA minimizing the transmission line losses. The IPFC is connected between lines 1-2 and 1-3 of IEEE 30-bus power system. The GA control parameters are selected as in Table 4.17.

Table 4.17: GA control parameters

| Control parameters     | Description            |
|------------------------|------------------------|
| Population Size        | 35                     |
| Crossover fraction     | 0.85                   |
| Generations            | 100                    |
| Time limit             | 200                    |
| Stall generation limit | 100                    |
| Stall time limit       | 100                    |
| Selection function     | @selectionroulette     |
| Crossover function     | @crossoveringlepoint   |
| Mutation function      | @mutationadaptfeasible |

The GA technique is applied to minimize the transmission line losses and to find the optimal parameters of VSCs of the IPFC. The voltages of generators buses in the system were selected as in Table 4.12, such that the generators supply as much reactive power to the system as they can before inserting any extra reactive power source. After setting the limits for the injected voltage magnitudes between ( $0 < V_{inj} < 0.15$ ) and angles between ( $-\pi/2 < \theta_{inj} < \pi/2$ ), the results obtained for line flows, line losses and the Newton-Raphson load flow analysis of IEEE 30-bus power system with IPFC and GA are presented in Appendixes D7 and D8. The optimal values of the injected voltage magnitudes and angles of the IPFC found by the GA technique are reported in Table 4.18.

Table 4.18: Optimal parameters of IPFC and the system losses

| Optimization parameter | lines  |        |
|------------------------|--------|--------|
|                        | 1-2    | 1-3    |
| $V_{inj}$ (pu)         | 0.0812 | 0.0439 |
| $\theta_{inj}$ (rad)   | 1.1455 | 1.0879 |
| lines losses (MW)      | 0.026  | 0.012  |
| Total line losses (MW) | 8.789  |        |

As observed from Tables 4.13 and 4.18, lines 1-2 and 1-3 losses and the total power loss of the system is reduced to 0.026 MW, 0.012 MW and 8.789 MW when the PSO is used i.e. reduced by approximately 99.49 %, 99.61 % and 49.86 % respectively.

The fitness of each individual and the current best individual of the optimal parameters of the injected voltage and angle are shown in Figure 4.39, and 4.40 respectively. From Figure 4.39 it is observed that the optimal parameters of the injected voltages and angles are 0.0812, 0.0439 pu and 1.1455, 1.0879 rad for transmission lines 1-2 and 1-3 respectively.

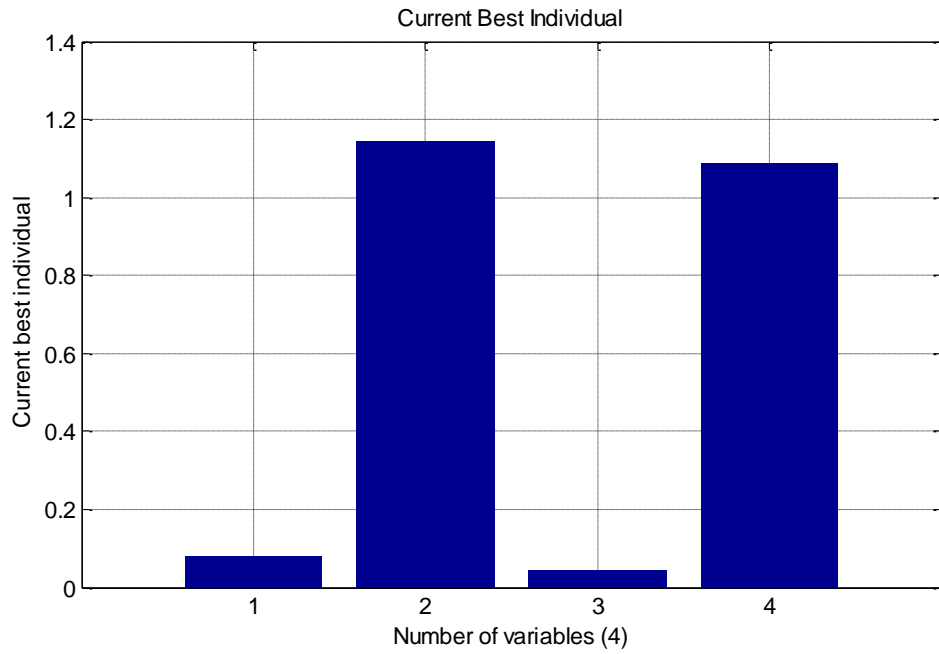


Figure 4.39: current points of the optimal parameters

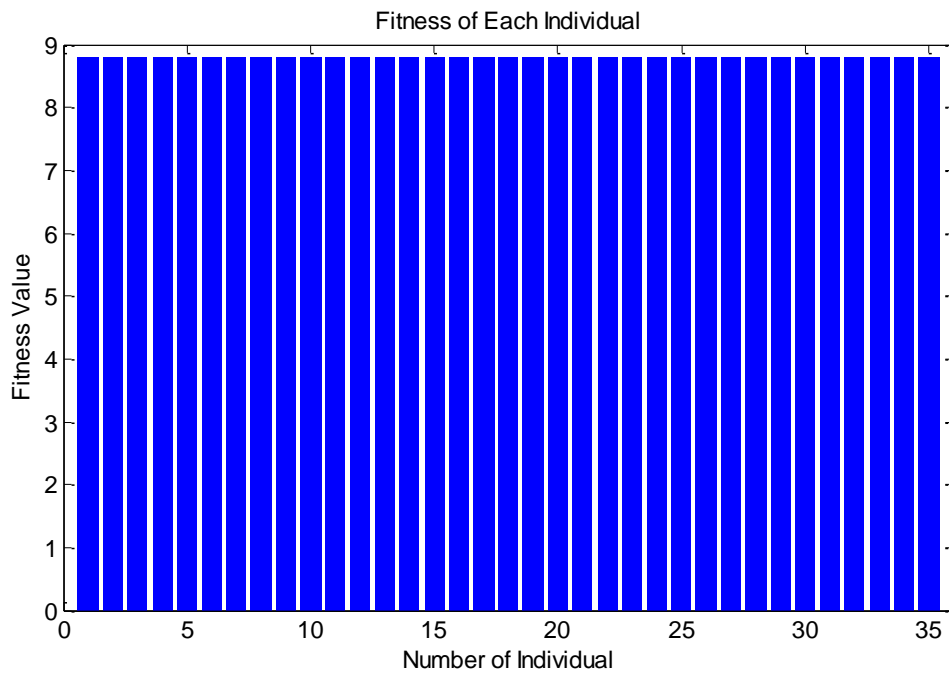


Figure 4.40: Fitness of each individual

Figure 4.40: show the fitness of each individual variable when the optimal parameters are reached a best value. It is observed that the fitness of each individual is almost equal when the optimal parameters are found.



The average distance between individual and the variation of the fitness value of best function value with the change in number of generations in GA are shown in Figure 4.41, and 4.42 respectively. It is observed that the objective function reached a global minimum after nearly 45 iterations out of 100 and the simulation running time is 131.2356 seconds for the GA.

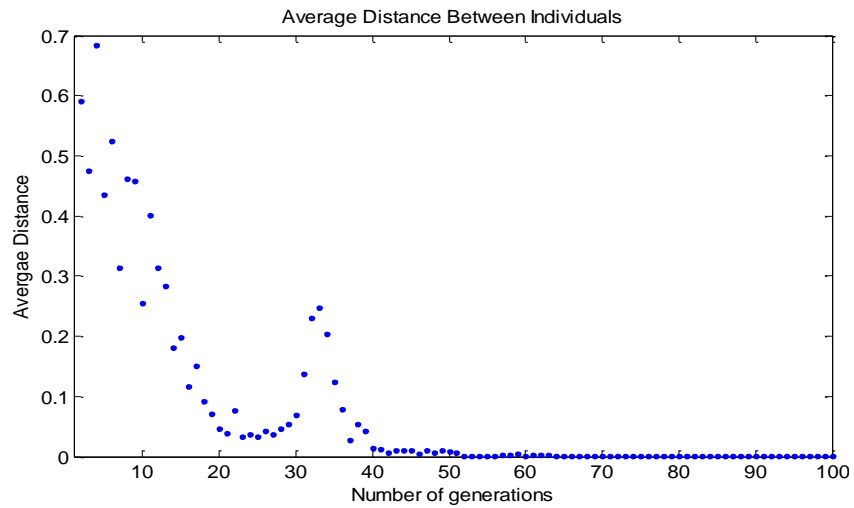


Figure 4.41: Average distance value with the change in number of generation of GA

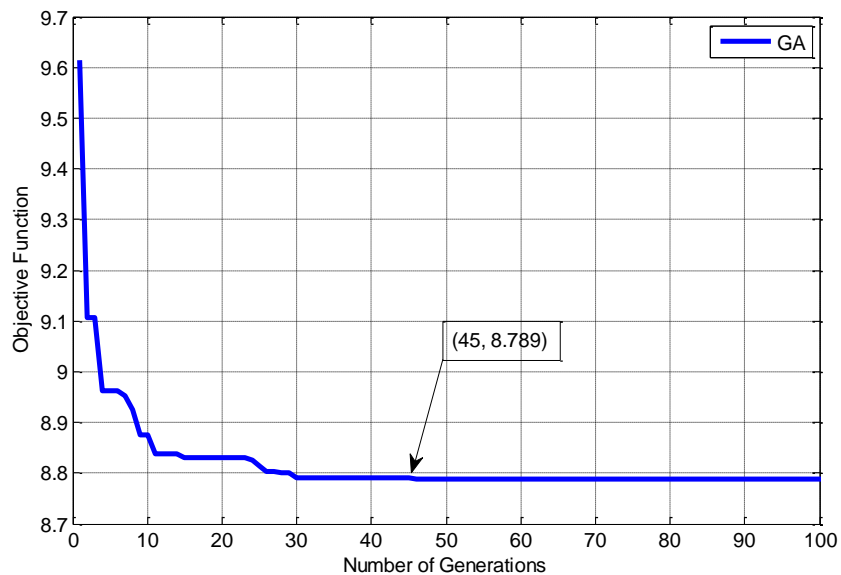


Figure 4.42: Variation of best function value with the change in number of generations of GA

As shown in Figure 4.43 the stopping criteria are met after nearly 5 % of stall time limit and that means there is no further improvement in the best fitness, 4 % of Stall generations, 65 % of the total time limit and 100 % of generations specifies the maximum number of iterations.

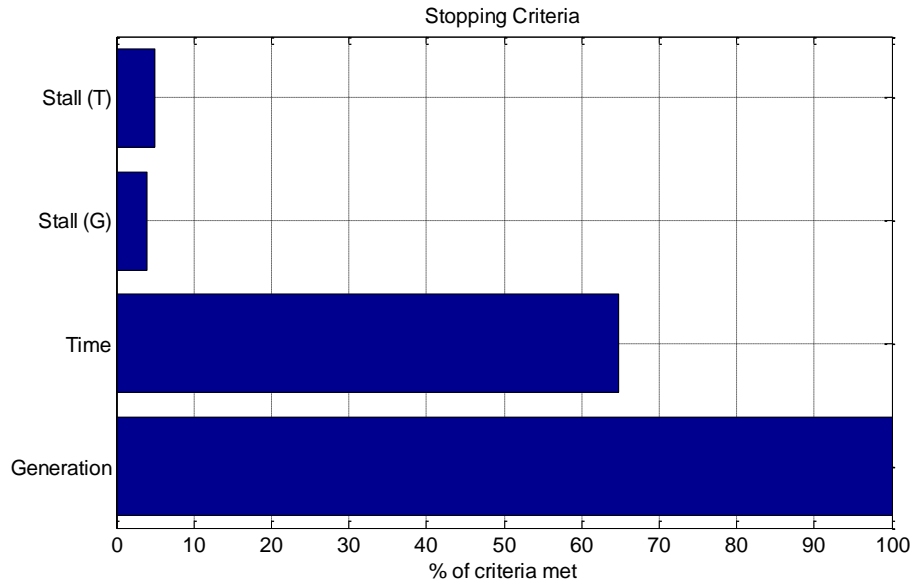


Figure 4.43: stopping criteria percentages

Figure 4.44 shows the voltage profile of IEEE 30-bus power system for the power flow with IPFC and using GA.

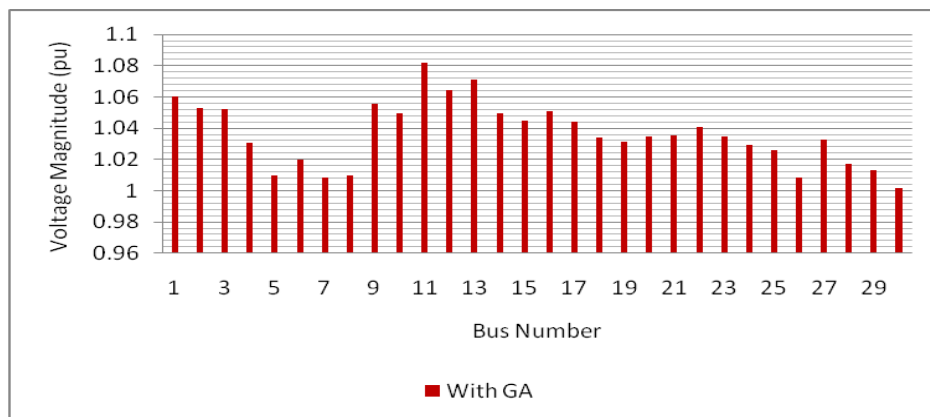


Figure 4.44: The voltage profile of IEEE 30-bus power system with IPFC using GA

Figures 4.45 shows the voltage profile of the IEEE 30-bus power system with IPFC and with IPFC using GA

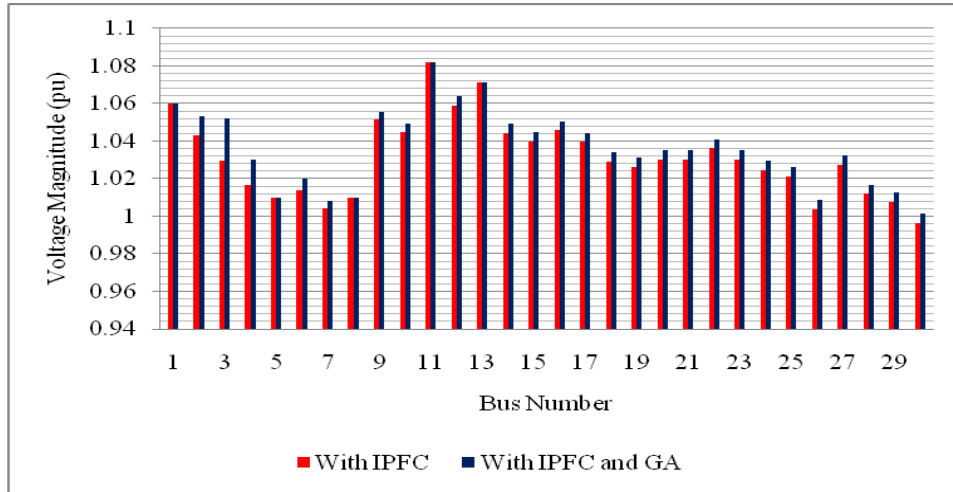


Figure 4.45: The voltage profile of IEEE 30-bus power system with IPFC and with IPFC using GA

Figures 4.46 shows the voltage profile of the IEEE 30-bus power system without IPFC, with IPFC and with IPFC using GA

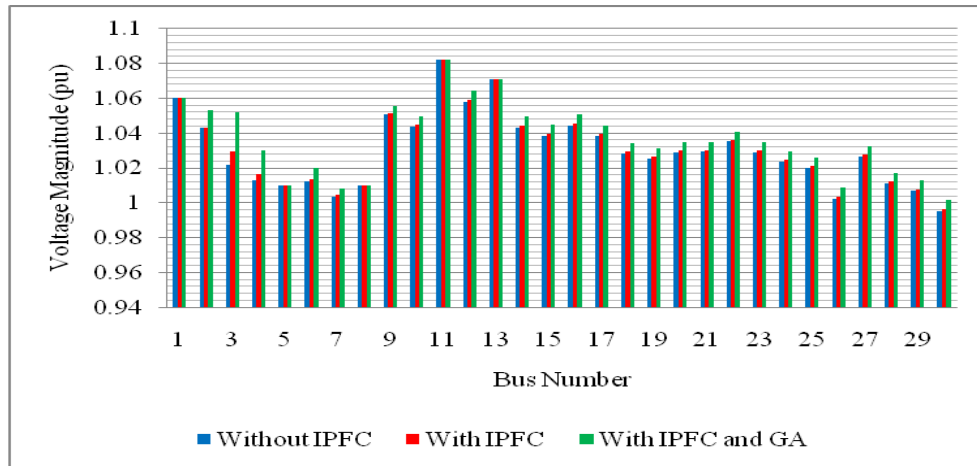


Figure 4.46: The voltage profile of IEEE 30-bus power system without IPFC, with IPFC and with IPFC using GA

As observed in Figure 4.46, the reactive power introduced by the IPFC devices caused an improvement in the voltage of buses 3, 4, 9, 10, 12 and also in the buses 14 to 30. This improvement resulted in lower reactive power flows in the lines and hence reduction in the real power loss. Also more improvement in the voltage profile has

been observed in buses 2, 3, 4, 6, 7, 9, 10, 12, and also in the buses 14 to 30 when GA algorithm is applied to the system.

#### 4.3.5 Power Flow Analysis of IEEE 30-bus Power System with IPFC using SA

In this case the IPFC device was installed on the transmission lines which are connected between lines 1-2 and 1-3. The control parameters of SA are selected based on simulation with different combinations which return minimum objective function. Finally the parameters listed in Table 4.19 are selected to test the power flow analysis of IEEE 30-bus system.

Table 4.19: SA control parameters

| Control parameters                      | Description     |
|---|-----------------|
| Initial temperature                     | 100             |
| Maximum number of iterations            | 250             |
| Annealing function                      | @annealing fast |
| Temperature function                    | @temperatureexp |
| Termination tolerance on function value | $1e^{-6}$       |
| Stall iteration limit                   | 2000            |
| Time limit in sec                       | 100             |

The SA is applied to minimize the transmission line losses and to find the optimal parameters of the injected voltage source magnitude and angle of VSCs of the IPFC. The voltages of generator buses in the system were considered as in Table 4.12, such that the generators supply as much reactive power to the system as they can before inserting any extra reactive power source. After setting the boundary conditions for the injected voltage magnitudes between  $0 < V_{inj} < 0.15$  and angles between  $-\pi/2 < \theta_{inj} < \pi/2$ , the results obtained for line flows, line losses and the Newton Raphson load flow analysis of IEEE 30-bus power system with IPFC and SA are presented in Appendices D9 and D10. The optimal values of the injected voltage magnitudes and angles found by the SA technique are reported in Table 4.20.

Table 4.20: The control parameter and the system losses

| Optimization<br>parameter      | lines  |        |
|--------------------------------|--------|--------|
|                                | 1-2    | 1-3    |
| $V_{inj}$ (pu)                 | 0.0830 | 0.0439 |
| $\theta_{inj}$ (rad)           | 1.0154 | 1.1249 |
| Active power Lines losses (MW) | 0.026  | 0.017  |
| Total active power losses (MW) | 8.792  |        |

As observed from Tables 4.13 and 4.20, the active power losses of the system is reduced to 0.026, 0.017 and 8.792 MW, when the SA is used i.e. reduced by approximately 99.50 %, 99.45 % and 49.84 % for the transmission lines 1-2, 1-3 and the total active power losses respectively. The current point and the best point of the optimal parameters of the injected voltage and angle are shown in Figure 4.47, and 4.48 respectively. It is observed that the optimal parameters of the injected voltages and angles are 0.0830, 0.0439 pu and 1.0154, 1.1249 rad for transmission lines 1-2 and 1-3 respectively.

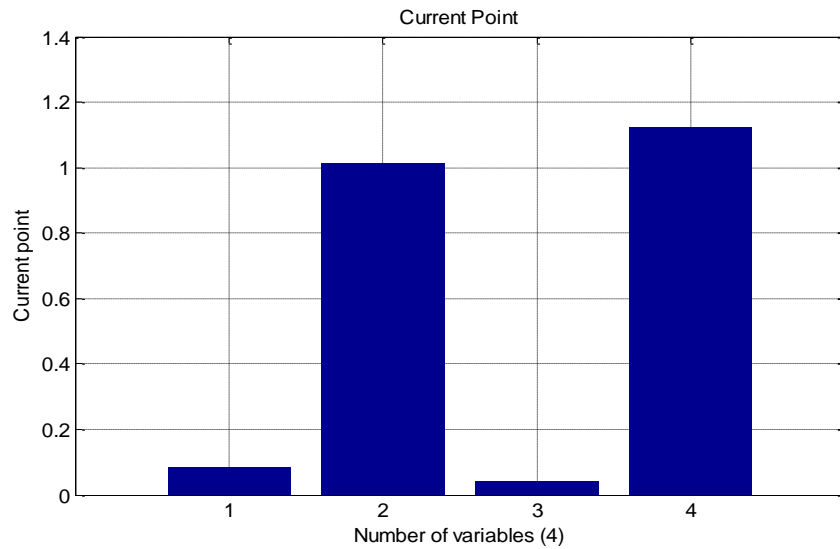


Figure 4.47: Current points of the optimal parameters

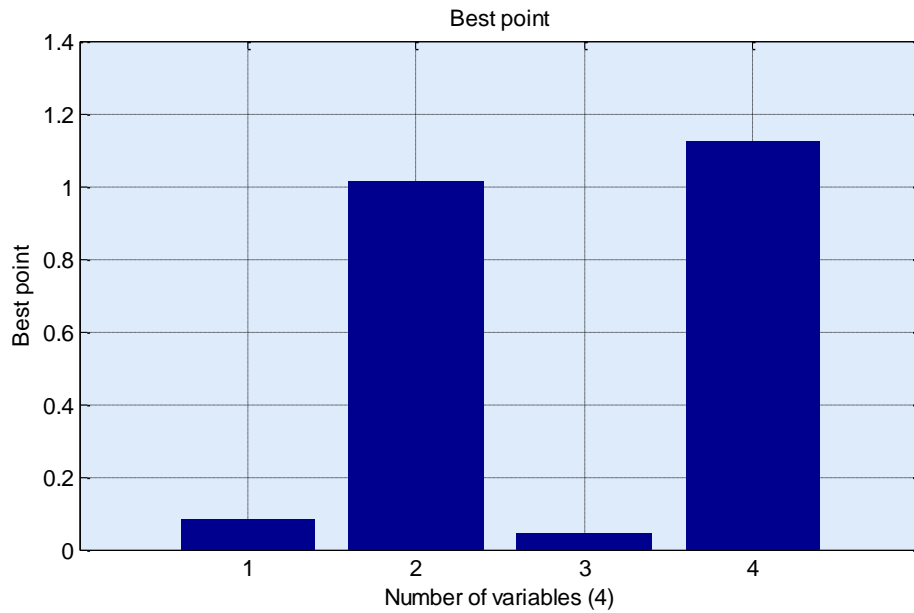


Figure 4.48: Best point of the optimal parameters

Figure 4.49 shows the current temperature of each variable when the optimal parameters are reached a best value. It is observed that the temperature is the control parameter in SA technique which is decreased gradually from 100 C° as initial temperature to nearly  $2.5 \times 10^{-4}$  C° when the objective function reached a global minimum.

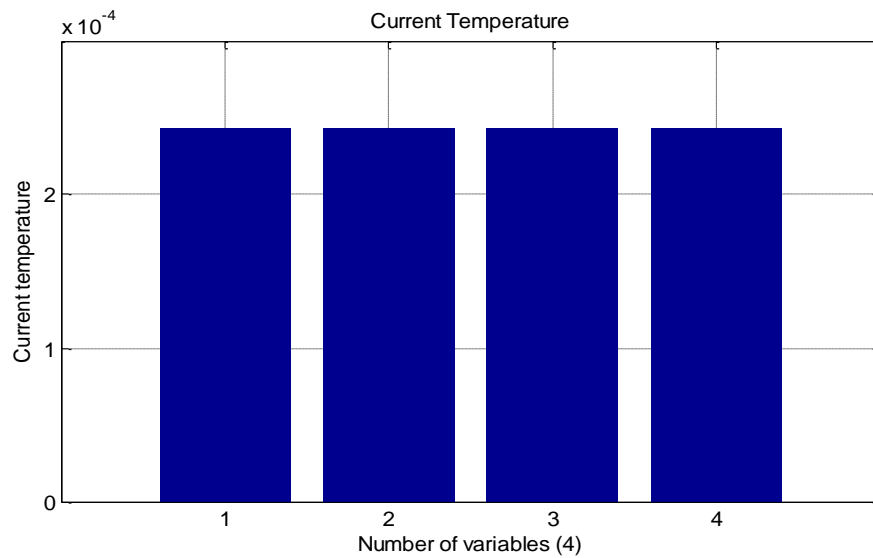


Figure 4.49: Current temperatures of the optimal parameters

The variation of the current function value and best function value with the change in number of iterations in SA are shown in Figure 4.50, and 4.51 respectively. It is observed that the objective function reached a global minimum after nearly 170 iterations out of 250 and the simulation running time is 23.957 seconds for the SA.

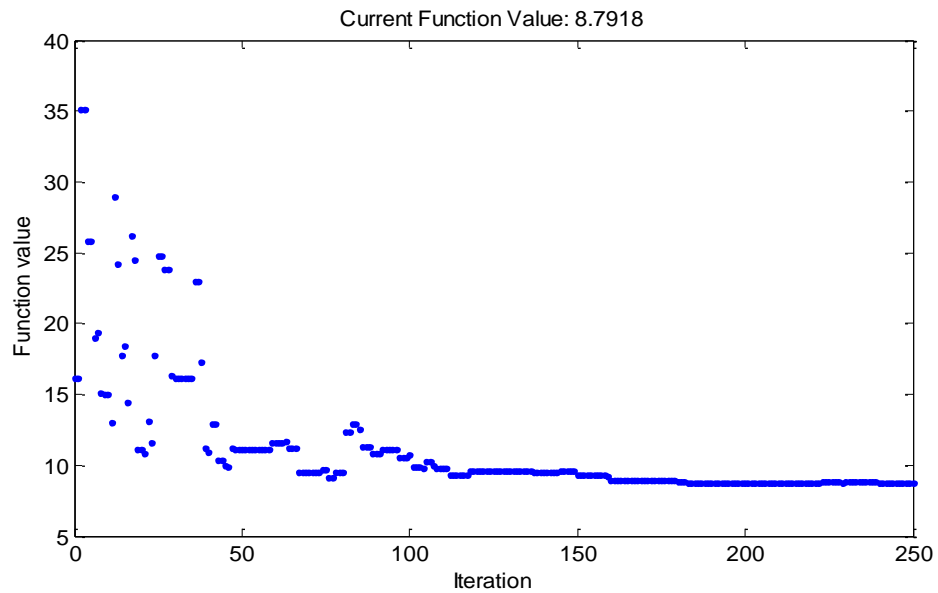


Figure 4.50: The variation of the current objective function value with the change in iterations by SA

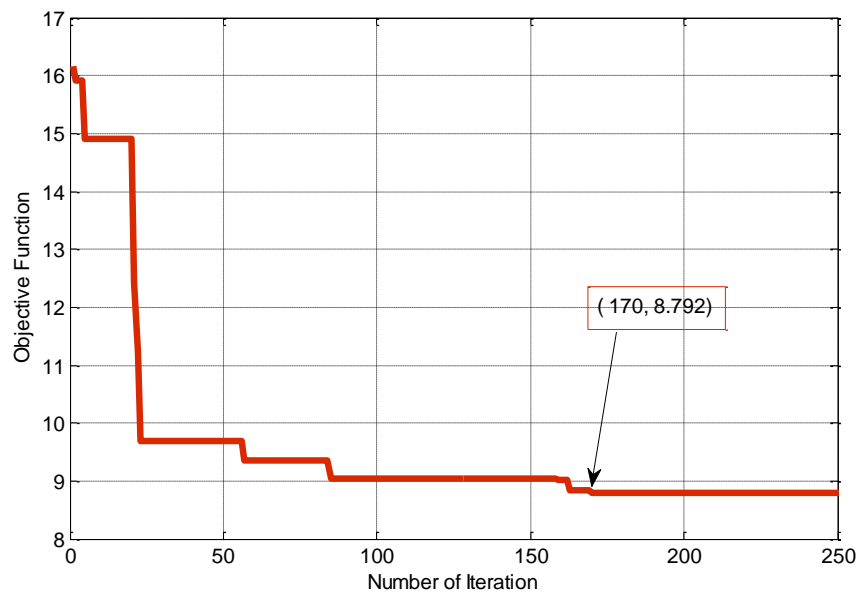


Figure 4.51: Variation of best objective function value with the change in iterations by SA

As shown in Figure 4.52 the stopping criteria is met after nearly 23 % of the total time limit of 200 seconds set in the algorithm, 100 % of the maximum iterations and 2 % of the function tolerance.

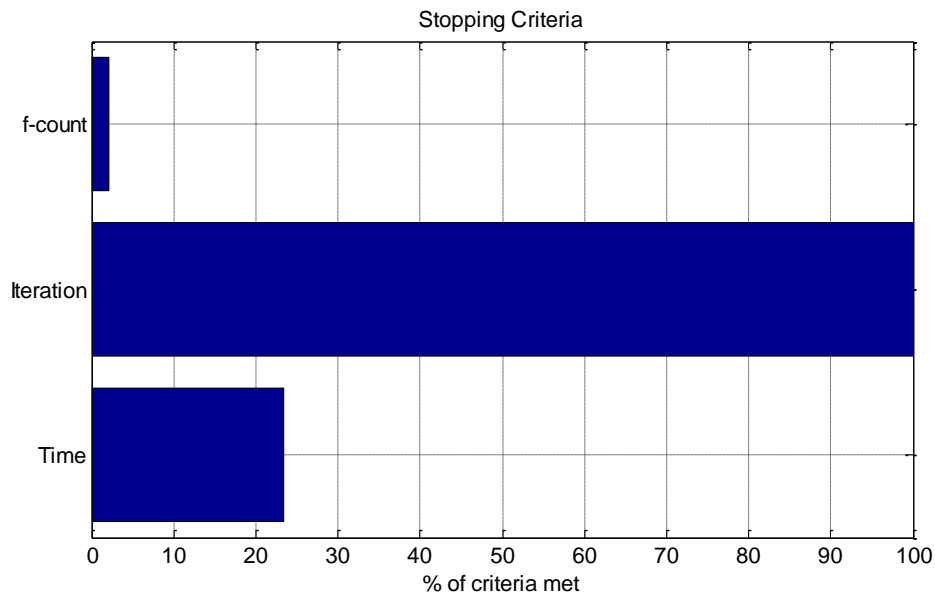


Figure 4.52: The stopping criteria

Figure 4.53 shows the voltage profile of IEEE 30-bus power system for the power flow with IPFC and using SA.

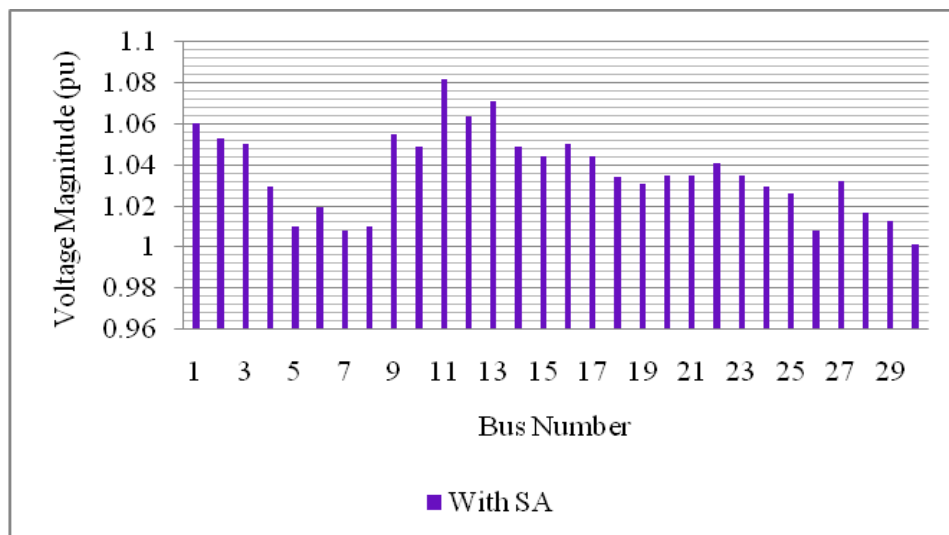


Figure 4.53: The voltage profile of IEEE 30-bus power system with IPFC using SA

The voltage profile of the IEEE 30-bus system with IPFC and with IPFC using SA is shown in Figures 4.54.



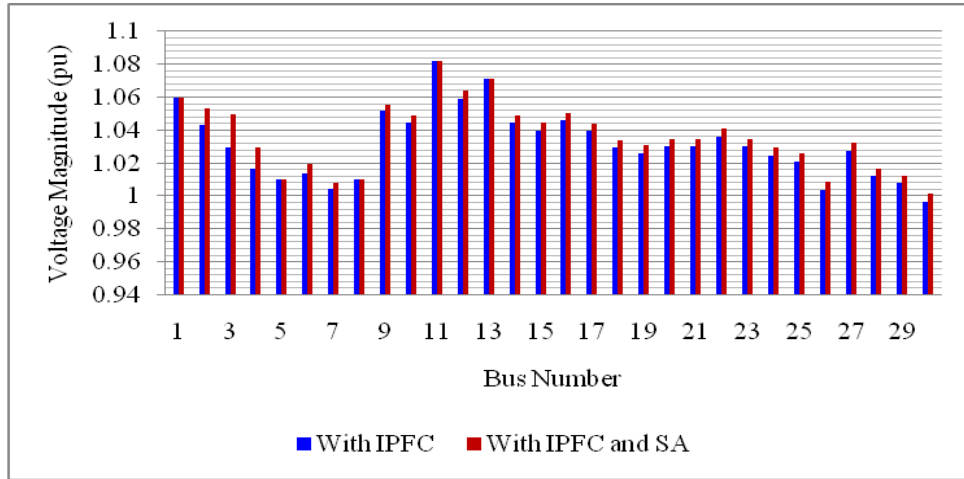


Figure 4.54: The voltage profile of IEEE 30-bus power system with IPFC and with IPFC using SA

Figure 4.55 shows the voltage profile of the IEEE 30-bus power system without IPFC, with IPFC and with IPFC using SA. As observed in Figure 4.55, the reactive power introduced by the IPFC devices caused an improvement in the voltage of buses 3, 4, 6, 9, 12 and also in the buses 14 to 30. This improvement resulted in lower reactive power flows in the lines and hence reduction in the real power loss. Also more improvement in the voltage profile has been observed in buses 2, 3, 4, 6, 7, 9, 10, 12, and also in the buses 14 to 30 when SA algorithm is applied to the system.

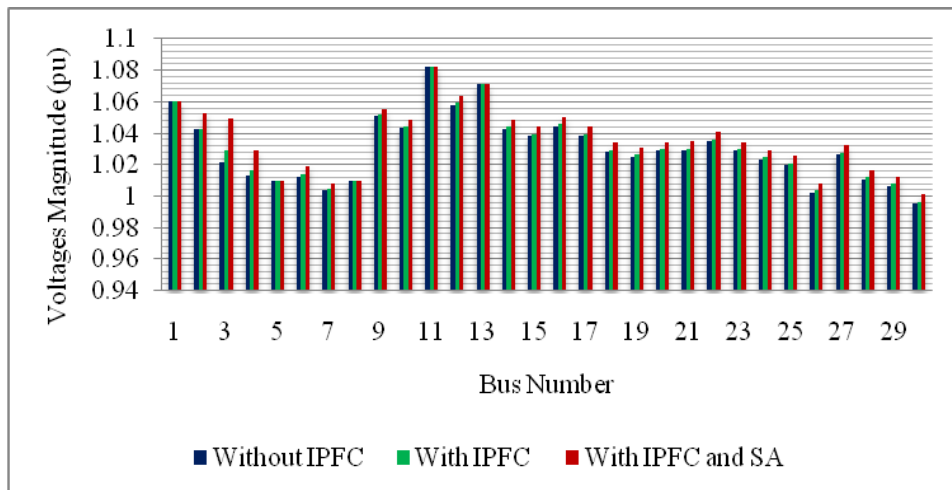


Figure 4.55: The voltage profile of IEEE 30- bus system without IPFC, with IPFC, and with IPFC using SA

#### 4.3.6 Comparison of Simulation Results with PSO, GA and SA Techniques of IEEE 30-bus Power System

The PSO, GA and SA techniques are applied to minimize the transmission line active power losses and to find the optimal parameters of the injected voltage magnitude and angle of VSCs of the IPFC. The voltages of generator buses are same as in Table 4.12, such that the generators supply as much reactive power to the system as they can before inserting any extra reactive power source. After setting the limits for the injected voltage magnitudes of VSC between  $0.0 < V_{inj} < 0.15$  and the angles between  $-\pi/2 < \theta_{inj} < \pi/2$ , and setting each optimization method control parameters, the simulation on power flow analysis program is performed. The active power line losses are minimized using each optimization technique subjected to the constraints on the voltage magnitudes and angles of VSCs of IPFC. The simulation results of injected voltage magnitudes and angles and the system line active power losses of the specified lines are obtained with each optimization technique. Also the total active power losses of the IEEE 30-bus power of the system obtained from the power flow analysis are presented in Table 4.21.

Table 4.21: The IPFC parameters and the transmission line active power losses

| Optimization Parameter | Optimization Methods |        |        |        |        |        |
|------------------------|----------------------|--------|--------|--------|--------|--------|
|                        | PSO                  |        | GA     |        | SA     |        |
| Line                   | 1-2                  | 1-3    | 1-2    | 1-3    | 1-2    | 1-3    |
| $V_{inj}$ (pu)         | 0.0439               | 0.0842 | 0.0812 | 0.0439 | 0.0830 | 0.0439 |
| $\theta_{inj}$ (rad)   | 1.0878               | 0.9820 | 1.1455 | 1.0879 | 1.0154 | 1.1249 |
| Lines losses (MW)      | 0.026                | 0.012  | 0.026  | 0.012  | 0.026  | 0.017  |
| Total line losses (MW) | 8.789                |        | 8.789  |        | 8.792  |        |

As observed from Tables 4.13 and 4.21, the total active power loss of the system is reduced to 8.789 MW, 8.789 MW and 8.792 MW, i.e. reduced by approximately 49.86 %, 49.86 % and 49.84% when the PSO, GA and SA methods are used respectively.

Table 4.22 reports a comparison of number of iterations and simulation running time required by PSO, GA and SA optimization methods respectively.

Table 4.22: Comparison between optimization methods

| Item                         | Optimization method |     |     |
|------------------------------|---------------------|-----|-----|
|                              | PSO                 | GA  | SA  |
| Number of iterations         | 20                  | 45  | 170 |
| Simulation running time, sec | 121                 | 131 | 24  |

It is observed that the time taken for minimizing the objective function by SA technique is only 24 sec where as the other two techniques required more time.

The variations of objective functions with the change in number of iterations are shown in Figure 4.56. It is observed that the objective functions reached a global minimum after nearly 20, 45 and 170 iterations with PSO, GA and SA methods respectively.

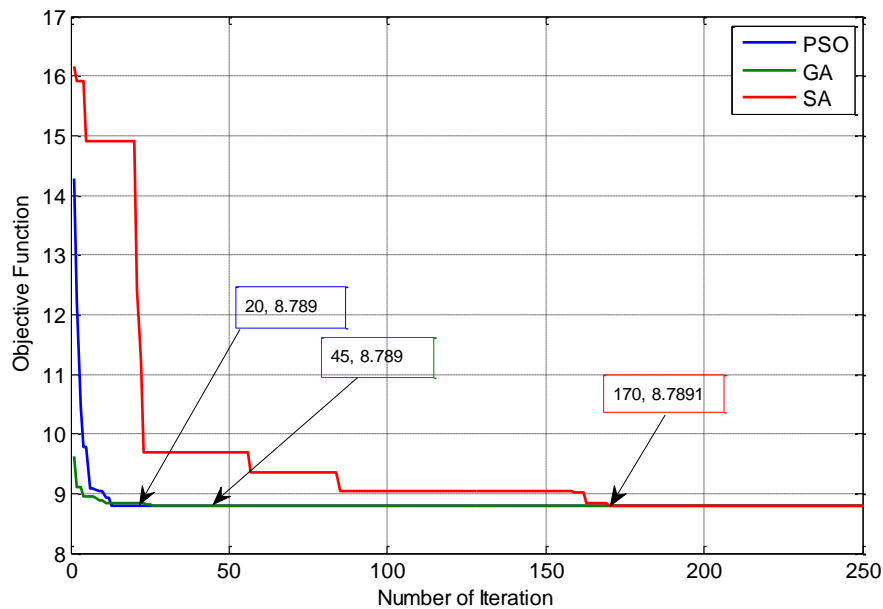


Figure 4.56: Variation of objective function with the change in iterations

The voltage profile of IEEE 30-bus power system for the power flow with IPFC and using PSO, GA and SA methods is presented in Figure 4.57. The voltage profiles of the system without IPFC, with IPFC, and with IPFC and PSO or GA or SA together, are compared as shown in Figure 4.58.

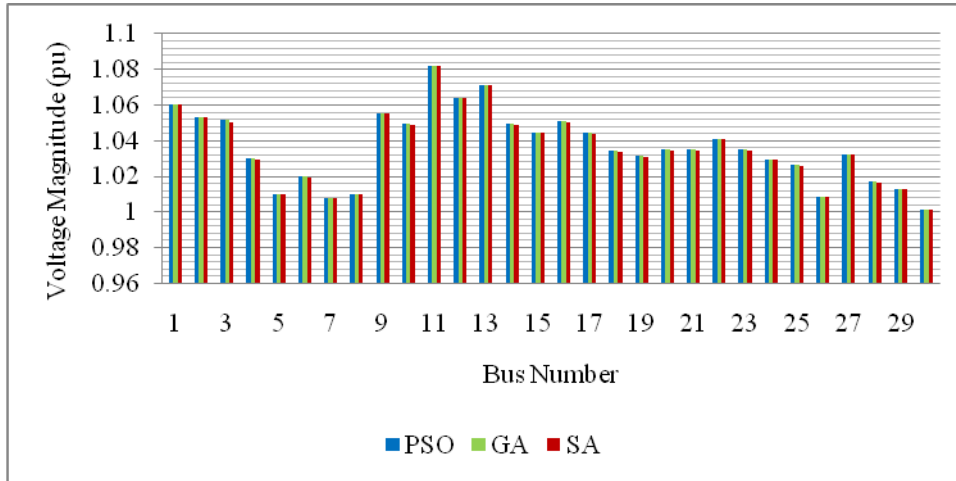


Figure 4.57: The voltage profile of IEEE 30-bus power system with IPFC together with and PSO or GA or SA technique

As observed in Figure 4.58, the reactive power introduced by the IPFC devices caused an improvement in the voltage of buses 3, 4, 6, 9, 12 and also in the buses 14 to 30. This improvement resulted in lower reactive power flows in the lines and hence reduction in the real power loss. Also more improvement in the voltage profile is observed in buses 2, 3, 4, 6, 7, 9, 10, 12 and also in the buses 14 to 30 when PSO, GA and SA techniques are applied to the system.

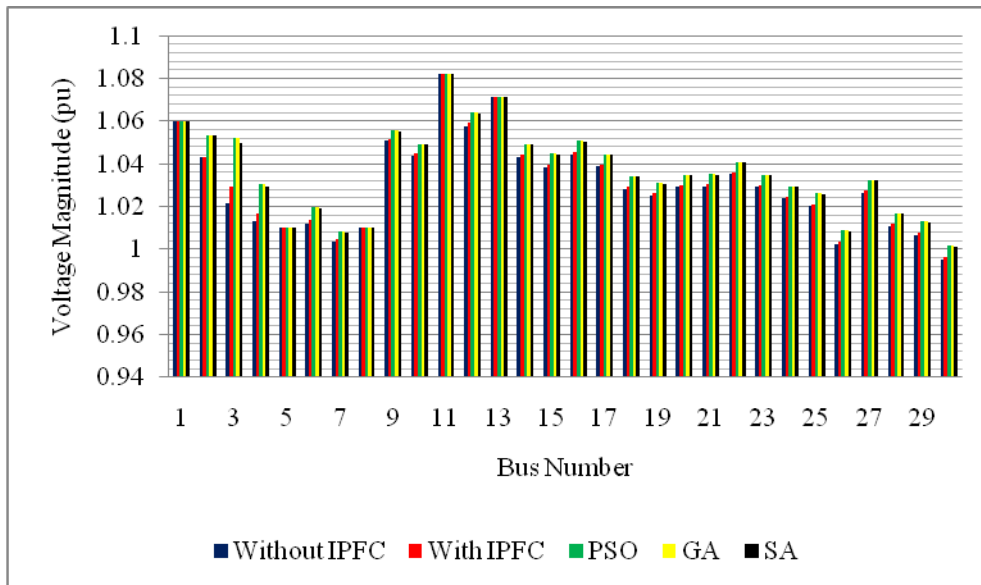


Figure 4.58: The voltage profile of IEEE 30-bus power system without IPFC, with IPFC and with IPFC together with PSO or GA or SA technique.

#### **4.4 Summary**

In this chapter, simulation results and discussions on standard IEEE 14-bus and 30-bus power systems are presented. The PSO, GA and SA techniques are applied to minimize the transmission line active power losses and to find the optimal parameters of the injected voltage magnitudes and angles of VSCs of the IPFC. From the simulations, it is observed that, the minimum value of active power loss obtained by PSO technique is less compared to the GA and SA techniques for both the benchmark power systems. The reactive power introduced by the IPFC devices caused an improvement in the voltage of some buses. Also, it is observed that the time taken for minimizing the active power loss by SA technique is small compared to PSO and GA techniques.

## **CHAPTER 5**

### **CONCLUSIONS AND RECOMMENDATIONS**

#### **5.1 Conclusions**

In this thesis, “Intelligent Optimization of Interline Power Flow Controller in Transmission System”, the mathematical model of an IPFC system with two VSCs has been developed and tested in MATLAB software environment using modified Newton-Raphson method and three intelligent optimization techniques viz., PSO, GA and SA.

The voltage profiles of standard IEEE 14-bus and 30-bus power systems have been compared and it's observed that the reactive power introduced by the IPFC devices caused an improvement in the voltage of some buses. This improvement resulted in lower reactive power flows in the lines and hence reduction in the real power loss, which is the objective function in the optimization techniques.

The MATLAB codes using the intelligent optimization techniques have been proposed to obtain the optimal parameters of the injected voltage source magnitudes and angles of VSCs of IPFC and to minimize the transmission line losses of standard benchmark IEEE 14-bus and 30-bus power systems.

The active power line losses have been minimized using PSO, GA and SA techniques subjected to the constraints on the voltage magnitudes and angles of VSCs of IPFC. It is proved and validated from the simulation results that the minimum value of total active power loss obtained by PSO technique is less compared to GA and SA techniques.

It is also observed from the simulation results that the SA technique required less execution time for minimizing the objective function whereas, the other two techniques i.e. PSO and GA required more time.

Generally, simulation results have demonstrated the effectiveness and accuracy of the optimal parameters of the IPFC and minimization of transmission line losses of IEEE 14-bus and IEEE 30-bus benchmark power systems by the proposed three intelligent optimization techniques.

## **5.2 Significant Contributions**

The main contributions of the work are as follows:

- The mathematical model of the power flow equations of IPFC using modified Newton-Raphson method has been developed and tested in MATLAB 7.6 software environment together with the general power flow equations of the standard IEEE 14-bus and 30-bus power systems.
- Three intelligent optimization technique codes, i.e. PSO, GA and SA codes have been proposed and tested using MATLAB software to obtain the optimal parameters of VSCs of IPFC and to minimize the transmission line losses.

## **5.3 Recommendations for Future Work**

This thesis “Intelligent Optimization of Interline Power Flow Controller in Transmission System” outlines OPF problem incorporating IPFC which coordinate to minimize the total active power losses in a power system network. Further studies are needed for OPF with multiple objective functions to minimize both the active power losses and IPFC capacity as well.

In this thesis, only three intelligent optimization techniques namely, PSO, GA and SA are used. The work can also be further extended using different intelligent optimization techniques to find the optimal parameters of VSCs of IPFC and to minimize the transmission line losses.

## REFERENCES

- [1] Y. Zhang and C. Chen, "A Novel Power Injection Model of IPFC for Power Flow Analysis Inclusive of Practical Constraints," *IEEE Transactions on Power Systems*, vol. 21, 2006, pp. 1550-1556.
- [2] J. Zhang and A. Yokoyama, "A Comparison between the UPFC and the IPFC in Optimal Power Flow Control and Power Flow Regulation," *38th North American Power Symposium*, 2006, pp. 339-345.
- [3] S. Bhowmick, B. Das, and N. Kumar, "An Advanced IPFC Model to Reuse Newton Power Flow Codes," *IEEE Transactions on Power Systems*, vol. 24, 2009, pp. 525-532.
- [4] S. Teerathana, A. Yokoyama, Y. Nakachi, and M. Yasumatsu, "An Optimal Power Flow Control Method of Power System by Interline Power Flow Controller (IPFC)," *7th International Power Engineering Conference*, Singapore: 2005, pp. 1-6.
- [5] S. Salem and V.K. Fellow, "Simulation and Controller Design of an Interline Power Flow Controller in EMTP RV," *International conference on power system transients*, Lyon: 2007, pp. 1-8.
- [6] M. Basu, "Optimal Power Flow with FACTS Devices using Differential Evolution," *International Journal of Electrical Power & Energy Systems*, vol. 30, 2008, pp. 150-156.
- [7] V. H. Quintana and M. Santos- Nieto " Reactive Power dispatch by successive Quadratic Programming", *IEEE Transaction, Power System*, Vol 4, pp 425 - 435, September 1989.
- [8] S. Granville, " Optimal reactive Dispatch through Interior Point Methods" *IEEE Transaction on Power system*, Vol 9, No. 1, pp 136 - 146, February 1994.
- [9] A. Elzonkoly, "Optimal Sizing of SSSC Controllers to Minimize Transmission Loss and Anovel Model of SSSC to Study Transient Response," *Electric Power Systems Research*, vol. 78, 2008, pp. 1856-1864.
- [10] S. Teerathana and A. Yokoyama, "An Optimal Power Flow Control Method of Power System using Interline Power Flow Controller (IPFC)," *2004 IEEE Region 10 Conference TENCON*, Ieee, 2004, pp. 343-346.
- [11] X. Zhang, C. Rehtanz, and B. Pa, *Flexible AC Transmission Systems Modelling and Control*, Berlin Heidelberg: Springer, 2006.



- [12] X. Wei, J. H. Chow, B. Fardanesh, and A. Edris, "A Dispatch Strategy for An Interline Power Flow Controller Operating at Rated Capacity," *IEEE Transactions on Power Systems*, vol. 19, 2004, pp. 934 - 941.
- [13] A. M. Elzonkoly, "Optimal Sizing of SSSC Controllers to Minimize Transmission Loss and a Novel Model of SSSC to Study Transient Response," *Engineering and Technology*, vol. 18, 2006, pp. 255-261.
- [14] J. Zhang and A. Yokoyama, "Optimal Power Flow Control for Congestion Management by Interline Power Flow Controller (IPFC)," *International Conference on Power System Technology*, 2006, pp. 1-6.
- [15] N. G. Hingorani, "Power Electronics in Electric Utilities: Role of Power Electronics in Future Power Systems," *Proceedings of the IEEE*, vol. 76, 1988, pp. 481 - 482.
- [16] N. Hingorani, "FACTS-Flexible AC Transmission System," *International Conference on AC and DC Power Transmission*, 1991, pp. 1-7.
- [17] K. R. Padiyar and A. M. Kulkarni, "Flexible AC Transmission Systems: A status Review," *Control*, vol. 22, 1997, pp. 781-796.
- [18] A. Edris, M. H. Baker, J. Lemay, and J. Reeve, "Proposed Terms and Definitions for Flexible AC Tsansmission System (FACTS)," *IEEE Transactions on Power Delivery*, vol. 12, 1997, pp. 1848-1853.
- [19] R. K. Varma, "Introduction to FACTS Controllers," *Power Systems Conference and Exposition*, 2009, pp. 1-6.
- [20] K. R. Padyar, *FACTS Controllers in Power Transmission and Distribution*, New age international publishers, 2007.
- [21] J. Chen, T. T. Lie, and D. M. Vilathgamuwa, "Basic Control of Interline Power Flow Controller," *Power Engineering Society Winter Meeting*, 2002, pp. 521-525.
- [22] B. Mumyakmaz, X. Jin, C. Wang, and T. C. Cheng, "Static VAR Compensator with Neural Network Control," *Transmission and Distribution Conference*, vol. 2, 1999, pp. 542-549.
- [23] M. Noroozian, N. Petersson, B. Thorvaldson, A. Nilsson, and C. Taylor, "Benefits of SVC and STATCOM for Electric Utility Application," *Transmission and Distribution Conference and Exposition*, 2003, pp. 1143 - 1150.
- [24] V. Rajderkar and V. Chandrakar, "Comparison of Series FACTS Devices Via Optimal Location in a Power System for Congestion Management," *Power and Energy Engineering Conference*, 2009, pp. 1-5.

- [25] B. Zhang and Q. Ding, "The Development of FACTS and Its Control," *Advances in Power System Control, Operation and Management*, 1997, pp. 48-53.
- [26] M. O. Faruque, V. Dinavahi, S. Santoso, and R. Adapa, "Review of Electromagnetic Transient Models for Non-VSC FACTS," *IEEE Transactions on Power Delivery*, vol. 20, 2005, pp. 1065-1079.
- [27] A. Edris and L. Gyugyi, "Power Electronics-based T and D Controllers Technology Developments," *Transmission and Distribution Conference and Exposition*, Ieee, 2003, pp. 1180-1186.
- [28] S. Douangsyla, P. Indarack, A. Kanthee, M. Kando, S. Kittiratsatcha, and V. Kinnares, "Modeling for PWM Voltage Source Converter Controlled Power Transfer," *IEEE International Symposium on Communications and Information Technology, 2004. ISCIT 2004. Communications and Information Technology*, vol. 2004, 2004, pp. 875-878.
- [29] V. K. Sood, *HVDC and FACTS Controllers Application of Static Converter in Power System*, New York: Kluwer Academic Publishers, 2004.
- [30] P. Zuniga Haro and J. Ramirez, "Static Synchronous Series Compensator Operation Based on 48-pulse VSC," *Power Symposium, 2005. Proceedings of the 37th Annual North American*, 2005, pp. 102-109.
- [31] T. M. Haileselassie, M. Molinas, and T. Undeland, "Multi-Terminal VSC-HVDC System for Integration of Offshore Wind Farms and Green Electrification of Platforms in the North Sea," *Converter*, 2008, pp. 1-8.
- [32] W. Liu and Z. Cai, "Model Analysis and Robust Control Design of VSC-HVDC Converter with dq0 Axis," *Third International Conference on Electric Utility Deregulation and Restructuring and Power Technologies*, 2008, pp. 1792-1796.
- [33] Q. Yu, P. Li, W. Liu, and X. Xie, "Overview of STATCOM Technologies," *IEEE International Conference on Electric Utility Deregulation, Restructuring and Power Technologies*, 2004, pp. 647 - 652.
- [34] M. T. Bina and D. C. Hamill, "A Classification Scheme for FACTS Controllers," *European Power Electronics Conference*, Lausanne: 1999.
- [35] H. K. Karegar and S. Golmohamadzaheh, "A New Method for Small Signal Modeling of UPFC," *IEEE 2nd International on Power and Energy Conference*, Johor Baharu: 2008, pp. 844-848.
- [36] P. Ye, Y. Ye, and J. Song, "A Reliable UPFC Control Method for Optimal Power Flow Calculation," *Power Engineering Society General Meeting*, 2004, pp. 1178 - 1183.

- [37] L. Gyugyi, K. Sen, and C. Schauder, "The Interline Power Flow Controller Concept: A new Approach to :Power Flow Management in Transmission Systems," *IEEE Transactions on Power Delivery*, vol. 14, 1999, pp. 1115-1123.
- [38] S. Teerathana, A. Yokoyama, Y. Nakachi, and M. Yasumatsu, "An Optimal Power Flow Control Method of Power System by Interline Power Flow Controller (IPFC)," *The 7th International on Power Engineering Conference*, 2005, pp. 1075 - 1080.
- [39] N. Hingorani, "Role of FACTS in a Deregulated Market," *Power Engineering Society Summer Meeting*, 2000, pp. 1463-1467.
- [40] A. Kazemi and H. Andami, "FACTS Devices in Deregulated Electric Power Systems: A Review," *IEEE International Conference on Electric Utility Deregulation, Restructuring and Power Technologies*, 2004, pp. 337 - 342.
- [41] A. Chakrabarti and S. Halder, *Power System Analysis, Operation and Control*, New Delhi: Prentic Hall of India, 2006.
- [42] D. Kothari and I. Nagrath, *Modern PowerSystem Analysis*, Tata McGraw Hill, 2003.
- [43] J. Zhang and A. Yokoyama, "Optimal Power Flow Control for Congestion Management by Interline Power Flow Controller (IPFC)," *International Conference on Power System Technology*, 2006, pp. 1-6.
- [44] S. Teerathana and A. Yokoyama, "An Optimal Power Flow Control Method of Power System using Interline Power Flow Controller (IPFC)," *IEEE Region 10 Conference TENCON 2004.*, vol. 3, 2004, pp. 343-346.
- [45] H. Saadat, *PowerSystem Analysis*, McGraw-Hill Primis Custom Publishing, 2002.
- [46] M. Saravanan, S.M. Slochanal, P. Venkatesh, and P.S. J, "Application of PSO technique for optimal location of FACTS devices considering system loadability and cost of installation," *Power Engineering Conference*, vol. 2, 2005, pp. 716 - 721.
- [47] H. Zhaoqing, M. Chengxiong, L. Jiming, and C. Man, "Genetic algorithm based control for VSC HVDC," *2005 IEEE/PES Transmission & Distribution Conference & Exposition: Asia and Pacific*, 2005, pp. 1-5.
- [48] B. A. Albuquerque, D. S. Aj, and S. J. De, "Power losses on distribution network: estimation using simulated annealing," *Power*, 2005, pp. 1041-1044.
- [49] S. Jeyadevi and S. Baskar, "Power flow control in FACTS using Particle Swarm Optimization," *International Conference on Power Electronics*, 2006, pp. 226-231.

- [50] A. Kazemi, D. Arabkhabori, M. Yari, and J. Aghaei, "Optimal Location of UPFC in Power Systems for Increasing Loadability by Genetic Algorithm," *Proceedings of the 41st International Universities Power Engineering Conference*, 2006, pp. 774-779.
- [51] K. Suresh and N. Kumarappan, "Combined genetic algorithm and simulated annealing for preventive unit maintenance scheduling in power system," *IEEE Power Engineering Society General Meeting*, 2006, pp. 1-5.
- [52] H. I. Shaheen, G. I. Rashed, and S. J. Cheng, "Optimal Location and Parameters Setting of Unified Power Flow Controller Based on Evolutionary Optimization Techniques," *Power Engineering Society General Meeting*, 2007, pp. 1-8.
- [53] K. V. Phpehu, J. K. Dkrr, F. R. Bk, P. V. Frp, V. Kxvw, H. G. Fq, D. Q. Ru, O. Lpshgdqfhv, and R. I. Wudqvplvvlrq, "Optimal Location and Parameter Setting of TCSC by Both Genetic Algorithm and Particle Swarm Optimization," *Industrial Electronics*, 2007, pp. 1141-1147.
- [54] N. Sadati, M. Hajian, M. Zamani, and E. Ui, "Unit Commitment Using Particle Swarm-Based-Simulated Annealing Optimization Approach," *Swarm Intelligence Symposium*, 2007, pp. 297-302.
- [55] G. I. Rashed, H. I. Shaheen, and S. J. Cheng, "Evolutionary optimization techniques for optimal location and parameter settings of TCSC under single line contingency," *IEEE Power and Energy Society General Meeting - Conversion and Delivery of Electrical Energy in the 21st Century*, 2008, pp. 1-9.
- [56] H. Baghaee, M. Jannati, B. Vahidi, S. Hosseinian, and H. Rastegar, "Improvement of voltage stability and reduce power system losses by optimal GA-based allocation of multi-type FACTS devices," *2008 11th International Conference on Optimization of Electrical and Electronic Equipment*, 2008, pp. 209-214.
- [57] Y. Mao and M. Li, "Optimal Reactive Power Planning Based on Simulated Annealing Particle Swarm Algorithm Considering Static Voltage Stability," *International Conference on Intelligent Computation Technology and Automation (ICICTA)*, 2008, pp. 106-110.
- [58] R. Benabid, M. Boudour, and M.a. Abido, "Optimal placement of FACTS devices for multi-objective voltage stability problem," *2009 IEEE/PES Power Systems Conference and Exposition*, 2009, pp. 1-11.
- [59] A. Parizad, A. Khazali, and M. Kalantar, "Application of HSA and GA in Optimal Placement of FACTS Devices Considering Voltage Stability and Losses," *Electric Power and Energy Conversion Systems*, 2009, pp. 1-7.

- [60] S. Majumdar, "Active Power Loss Minimization With FACTS Devices Using SA / PSO Techniques .," *Third International Conference on Power Systems*, 2009, pp. 25-29.
- [61] J. Kennedy and R. Eberhart, "Particle Swarm Optimization," *Proc. of IEEE International Conference on Neural Networks*, 1995, pp. 1942-1948.
- [62] R. Benabid, M. Boudour, and A. Hellal, "Non-dominated Sorting Particle Swarm Optimization ( NSPSO ) for Static Voltage Stability using TCSC and SVC," *4th international conference on computer integrated manufacturing*, 2007.
- [63] E. Abdelsalam, "Optimal Capacitor Placement and Sizing in Unbalanced Distribution Systems with Harmonics Consideration using PSO," 2008, pp. 8-12.
- [64] M. Saravanan, S. M. Slochanal, P. Venkatesh, and J. P. Abraham, "Application of Particle Swarm Optimization Technique for Optimal Location of FACTS Devices Considering Cost of Installation and System Loadability," *Electric Power Systems Research*, vol. 77, 2007, pp. 276-283.
- [65] K. Chandrasekaran, K. A. Jeyaraj, I. Sahayasenthamil, and D. M. Saravanan, "A new Method to Incorporate FACTS Devices in Optimal Power Flow using Particle Swarm Optimization," *Journal of Theoretical and Applied Information Technology*, 2009.
- [66] K.Y. Lee and M. A. El-Sharkawi, *Modern Heuristic Optimization Techniques: Theory and Applications to Power Systems*, Hoboken, New Jersey.: 2008.
- [67] V. Rashtchi, H. Shayeghi, M. Mahdavi, A. Kimiyaghalam, and E. Rahimpour, "Using an Improved PSO Algorithm for Parameter Identification of Transformer Detailed Model," *International Journal of Electrical Power and Energy Systems Engineering*, 2008.
- [68] P. A. Raj, T. G. Palanivelu, and R. Gnanadass, "Optimal Power Flow Solution for Combined Economic Emission dispatch Problem using Particle Swarm Optimization Technique," *J. Electrical Systems*, vol. 1, 2007, pp. 13-25.
- [69] M. Mahdi, "Optimal Power Flow with FACTS Devices," 2004, pp. 46-60.
- [70] Y. Shi and R. Eberhart, "A Modified Particle Swarm Optimizer," *Evolutionary Computation Proceedings*, 1998, pp. 69-73.
- [71] T. A. Rahman, S. Zaiton, and M. Hashim, "New Particle Swarm Optimizer with Sigmoid Increasing Inertia Weight," *International Journal of Computer Science and Security (IJCSS)*, vol. 1, 2007, pp. 43-52.
- [72] S. Kannan, S. M. Slochanal, P. Subbaraj, and N. P. Padhy, "Application of Particle Swarm Optimization Technique and its Variants to Generation

- Expansion Planning Problem," *Electric Power Systems Research*, vol. 70, 2004, pp. 203-210.
- [73] S. Naka, T. Genji, K. Miyazato, and Y. Fukuyama, "Hybrid Particle Swarm Optimization based Distribution State Estimation using Constriction Factor Approach," *Proceeding of International Conference of SCIS & ISIS*, Tsukuba: 2002, pp. 1-6.
  - [74] G. Baskar and M. R. Mohan, "Security Constrained Economic Load Dispatch using Improved Particle Swarm Optimization Suitable for Utility System," *Electrical Power and Energy Systems*, vol. 30, 2008, pp. 609-613.
  - [75] M. R. AlRashidi and M. E. El-Hawary, "A Survey of Particle Swarm Optimization Applications in Electric Power Systems," *IEEE Transactions on Evolutionary Computation*, 2009, pp. 913-918.
  - [76] Y. del Valle, G. Venayagamoorthy, S. Mohagheghi, J. Hernandez, and R. Harley, "Particle Swarm Optimization: Basic Concepts, Variants and Applications in Power Systems," *IEEE Transactions on Evolutionary Computation*, 2008, pp. 171-195.
  - [77] F. Hayes-Roth, "Review of "Adaptation in Natural and Artificial Systems by John H. Holland,"" *Portal*, 1975, pp. 15 - 15.
  - [78] R. L. Haupt and D. H. Werner, *Genetic Algorithms in Electromagnetics*, Hoboken, New Jersey.: John Wiley & Sons, Inc., Publication, 2007.
  - [79] S. Gerbex, R. Cherkaoui, and A. Germond, "Optimal Location of FACTS Devices to Enhance Power System Security," *Power Tech Conference Proceedings, 2003 IEEE Bologna*, Bologna, Italy: 2003.
  - [80] H. C. Leung, "Genetic Algorithm for Optimal Capacitor Selection and Optimal Power Flow with FACTS Devices.," 2004, p. 130.
  - [81] E. G. Shopova and N. G. Vaklieva-bancheva, "BASIC—A genetic Algorithm for Engineering Problems Solution," *Computer and Chemical Engineering*, vol. 30, 2006, pp. 1293-1309.
  - [82] S. Najafi, M. Abedi, and S. Hosseini, "A Novel Approach to Optimal Allocation of SVC using Genetic Algorithms and Continuation Power Flow," *IEEE International Power and Energy Conference*, Putrajaya, Malaysia: 2006, pp. 202-206.
  - [83] D. T. Dubrow and M. Krarti, "Genetic-Algorithm Based Approach to Optimize Building Envelope Design for Residential Buildings," *Building and Environment*, vol. 45, 2010, pp. 1574-1581.

- [84] T. Bouktir, L. Slimani, and M. Belkacemi, "A Genetic Algorithm for Solving the Optimal Power Flow Problem," *Leonardo Journal of Sciences*, 2004, pp. 44-58.
- [85] S. Kirkpatrick, C. D. Gelatt, and M. P. Vecchi, "Optimization by Simulated Annealing," *American Association for the Advancement of Science*, vol. 220, 1983, pp. 671-680.
- [86] D. Bertsimas and J. Tsitsiklis, "Simulated Annealing," vol. 8, 1993, pp. 10-15.
- [87] K. P. Wong, "Solving Power System Optimization Problems Using Simulated Annealing," *Engineering Applications of Artificial Intelligence*, vol. 8, 1995, pp. 665-670.
- [88] C. A. Roa-sepulveda and B. J. Pavez-lazo, "A solution to the Optimal Power Flow using Simulated Annealing," *Electrical Power and Energy Systems*, vol. 25, 2003, pp. 47-57.
- [89] C. C. Rajan and M. R. Mohan, "An Evolutionary Programming Based Simulated Annealing Method for Solving The Unit Commitment Problem," *International Journal of Electrical Power & Energy Systems*, vol. 29, 2007, pp. 540-550.
- [90] N. Metropolis, A. W. Rosenbluth, M. N. Rosenbluth, A. H. Teller, and E. Teller, "Equation of State Calculations by Fast Computing Machines," *Chem. Phys*, vol. 21, 1953, pp. 1087-1092.
- [91] T. Xu, H. Wei, and Z. Wang, "Study on Continuous Network Design Problem using Simulated Annealing and Genetic Algorithm," *Expert Systems with Applications*, vol. 36, 2009, pp. 2735-2741.
- [92] MathWork, "Global Optimization Toolbox 3.0," *Parallel Computing*, 1984, pp. 1-13.
- [93] MathWork, "Simulated Annealing Solver," *MathWork*, 1984.
- [94] R. Christie, "Power Systems Test Case Archive," *World Journal Of The International Linguistic Association*, 1993, pp. 1962-1962.

## LIST OF PUBLICATIONS

1. Khalid.H.Mohamed, K. S. Rama Rao, Khairul Nisak Bt Md. Hasan” Optimal Power Flow and Interline Power Flow Controllers using Particle Swarm Optimization Technique,” TENCON 2009 - 2009 IEEE Region 10 Conference, Suntec Singapore International Convention & Exhibition Centre 1Raffles Boulevard, Suntec City, Singapore,pp. 1 – 6, November 2009.
2. Khalid. H. Mohamed, K.S.Rama Rao, Khairul Nisak Bt Md. Hasan,” Interline Power Flow Controllers and Optimal Power Flow using Particle Swarm Optimization Technique,” International Conference: Electrical Energy and Industrial Electronic Systems EEIES2009, Parkroyal Penang, Pulau Pinang, Malaysia ,7-8 December 2009.
3. Khalid. H. Mohamed, K.S.Rama Rao, Khairul Nisak Bt Md. Hasan,” Application of Particle Swarm Optimization and its Variants to Interline Power Flow Controllers and Optimal Power Flow,” The 3rd International Conference on Intelligent and Advanced Systems ICIAS, Kuala Lumpur Convention Centre, Kuala Lumpur, Malaysia ,15-17 June 2010.
4. Khalid. H. Mohamed, K.S.Rama Rao, Khairul Nisak Bt Md. Hasan,” Optimal Parameters of Interline Power Flow Controller using Particle Swarm Optimization,” International Symposium On Information Technology ITsim 2010, Kuala Lumpur Convention Centre, Kuala Lumpur, Malaysia ,15-17 June 2010.
5. <Submitted> Khalid. H. Mohamed, K.S.Rama Rao, Khairul Nisak Bt Md. Hasan” Intelligent Optimization Techniques for Optimal Power Flow using Interline Power Flow Controller,’ The 2010 IEEE International Conference on Power and Energy (PECon 2010), Kuala Lumpur, Malaysia, November 29, 2010.



## APPENDICES

### *Appendix A: power flow equations and Newton-Raphson Method*

#### *A.1 General power flow equations and Newton-Raphson Method*

As mentioned in section 2.5 the admittance matrix in a power system is related to the current injections at a bus to the bus voltages. The equation describing the performance of the network in the bus admittance form is given by (A1).

$$I_{bus} = Y_{bus} V_{bus} \quad (A1)$$

From equations (2.12) and (2.13), the real and reactive powers, respectively constitute a set of nonlinear algebraic equations in terms of independent variables, voltage magnitude in per unit, and phase angle in radians.

$$P_l = \sum_{k=1}^N [V_l][V_k][G_{lk} \cos(\theta_l - \theta_k) + B_{lk} \sin(\theta_l - \theta_k)] \quad (A2)$$

$$Q_l = \sum_{k=1}^N [V_l][V_k][G_{lk} \sin(\theta_l - \theta_k) - B_{lk} \cos(\theta_l - \theta_k)] \quad (A3)$$

Thus, Equations (A2) and (A3) represent the general formula for the active and reactive power flows of a given power system. Both of the equations are linearized on compact form by Taylor's first order approximation as in (A4)

$$\begin{bmatrix} \Delta P \\ \Delta Q \end{bmatrix} = \begin{bmatrix} \frac{\partial P}{\partial \delta} & \frac{\partial P}{\partial |V|} \\ \frac{\partial Q}{\partial \delta} & \frac{\partial Q}{\partial |V|} \end{bmatrix} \begin{bmatrix} \Delta \delta \\ \Delta |V| \end{bmatrix} \quad (A4)$$

In Newton-Raphson method, the mismatch equation can be related to the voltage  $\Delta|V|$  and power angle change  $\Delta\delta$  with power mismatch  $[\Delta P, \Delta Q]$ . To bring symmetry in the elements of the coefficient matrix,  $\Delta|V|/|V|$  is taken as problem variable in place of  $\Delta|V|$ . Then, equation (A4) is modified as in (A5)

$$\begin{bmatrix} \Delta P \\ \Delta Q \end{bmatrix} = \begin{bmatrix} \frac{\partial P}{\partial \delta} & \frac{\partial P}{\partial |V|} |V| \\ \frac{\partial Q}{\partial \delta} & \frac{\partial Q}{\partial |V|} |V| \end{bmatrix} \begin{bmatrix} \Delta \delta \\ \frac{\Delta |V|}{|V|} \end{bmatrix} \quad (A5)$$

In symbolic form, the equation (A5) is written as in (A6).

$$\begin{bmatrix} \Delta P \\ \Delta Q \end{bmatrix} = \begin{bmatrix} J_1 & J_2 \\ J_3 & J_4 \end{bmatrix} \begin{bmatrix} \Delta \delta \\ \frac{\Delta |V|}{|V|} \end{bmatrix} \quad (\text{A6})$$

The matrix  $\begin{bmatrix} J_1 & J_2 \\ J_3 & J_4 \end{bmatrix}$  is known as Jacobian matrix. The elements of the Jacobian matrix are then obtained as follows:

For quadrant-1 [ $J_1$ ], derivative of real power injection with  $\delta$ , the diagonal element of  $J_1$  is given by Equation (A7).

$$\frac{dP_l}{d\delta_l} = V_l V_k (-G_{lk} \sin(\delta_l - \delta_k) + B_{lk} \cos(\delta_l - \delta_k)), k = 1:N, k \neq l \quad (\text{A7})$$

And, the off diagonal element of  $J_1$  is expressed by (A8).

$$\frac{dP_l}{d\delta_k} = V_l V_k (G_{lk} \sin(\delta_l - \delta_k) - B_{lk} \cos(\delta_l - \delta_k)), k \neq l \quad (\text{A8})$$

For quadrant-2 [ $J_2$ ], derivative of real power injection with  $V$ , the diagonal element of  $J_2$  is given by (A9).

$$\frac{dP_l}{d|V_l|} = V_k (G_{lk} \cos(\delta_l - \delta_k) + B_{lk} \sin(\delta_l - \delta_k)), k = 1:N, k \neq l \quad (\text{A9})$$

And, the off diagonal element of  $J_2$  is given by (A10).

$$\frac{dP_l}{d|V_k|} = V_l (G_{lk} \cos(\delta_l - \delta_k) + B_{lk} \sin(\delta_l - \delta_k)), k \neq l \quad (\text{A10})$$

For quadrant-3 [ $J_3$ ], derivative of reactive power with  $\delta$ , the diagonal element of  $J_3$  is given by (A11).

$$\frac{dQ_l}{d\delta_l} = V_l V_k (G_{lk} \cos(\delta_l - \delta_k) + B_{lk} \sin(\delta_l - \delta_k)), k = 1:N, k \neq l \quad (\text{A11})$$

And, the off diagonal element of  $J_3$  is as shown in (A12).

$$\frac{dQ_l}{d\delta_k} = V_l V_k (-G_{lk} \cos(\delta_l - \delta_k) - B_{lk} \sin(\delta_l - \delta_k)), k \neq l \quad (\text{A12})$$

For quadrant-4 [ $J_4$ ], derivative of reactive power with  $V$ , the diagonal element of  $J_4$  is as shown in (A13).

$$\frac{dQ_l}{d|V_l|} = V_k (G_{lk} \sin(\delta_l - \delta_k) - B_{lk} \cos(\delta_l - \delta_k)), k = 1:N, k \neq l \quad (\text{A13})$$

And, the off diagonal element of  $J_4$  is given by (A14).

$$\frac{dQ_l}{d|V_k|} = V_l (G_{lk} \sin(\delta_l - \delta_k) - B_{lk} \cos(\delta_l - \delta_k)), k \neq l \quad (A14)$$

The solution procedures for Newton-Raphson method of power flow analysis are as follows:

1. Read the line data and bus data of the power network; construct the bus admittance matrix.
2. Set  $k = 0$ . Assume a starting solution. Usually a flat start is assumed in which all the unknown phase angles are taken as zero and the unknown voltage magnitudes are taken as 1.0 p.u.
3. Compute the mismatch powers i.e. the error vector. If the elements of error vector are less than the specified tolerance, the problem is solved and hence go to Step 7; otherwise proceed to Step 4.
4. Compute the elements of sub-matrices  $J_1, J_2, J_3$  and  $J_4$ . Solve

$$\begin{bmatrix} \Delta P \\ \Delta Q \end{bmatrix}_K = \begin{bmatrix} J_1 & J_2 \\ J_2 & J_3 \end{bmatrix}_K \begin{bmatrix} \Delta \delta \\ \frac{\Delta |V|}{|V|} \end{bmatrix} \quad \text{for} \quad \begin{bmatrix} \Delta \delta \\ \frac{\Delta |V|}{|V|} \end{bmatrix} \quad (A15)$$

5. Update the solution as

$$\begin{bmatrix} \delta \\ V \end{bmatrix}_{k+1} = \begin{bmatrix} \delta \\ V \end{bmatrix}_k + \begin{bmatrix} \Delta \delta \\ \frac{\Delta V}{V} \end{bmatrix} \quad (A16)$$

6. Set  $k = k + 1$  and go to Step 3.
7. Calculate line flows and the transmission line loss.

## A.2 Newton – Raphson power flow method for IPFC

From the general power flow equation of IPFC, equations (2.24)-(2.27) are considered as:

$$P_l = V_l^2 G_{lk} - V_l V_k [G_{lk} \cos(\delta_l - \delta_k) + B_{lk} \sin(\delta_l - \delta_k)] - V_l V_{sik} [G_{lk} \cos(\delta_l - \delta_{sik}) + B_{lk} \sin(\delta_l - \delta_{sik})] \quad (A17)$$

$$Q_l = -V_l^2 B_{lk} - V_l V_k [G_{lk} \sin(\delta_l - \delta_k) - B_{lk} \cos(\delta_l - \delta_k)] - V_l V_{sik} [G_{lk} \sin(\delta_l - \delta_{sik}) - B_{lk} \cos(\delta_l - \delta_{sik})] \quad (A18)$$

$$P_m = V_m^2 G_{ml} - V_m V_l [G_{ml} \cos(\delta_m - \delta_l) + B_{ml} \sin(\delta_m - \delta_l)] \\ + V_m V_{slm} [G_{ml} \cos(\delta_m - \delta_{slm}) + B_{ml} \sin(\delta_m - \delta_{slm})] \quad (A19)$$

$$Q_m = -V_m^2 B_{ml} - V_m V_l [G_{ml} \sin(\delta_m - \delta_l) - B_{ml} \cos(\delta_m - \delta_l)] \\ - V_m V_{slm} [G_{ml} \sin(\delta_m - \delta_{slm}) - B_{ml} \cos(\delta_m - \delta_{slm})] \quad (A20)$$

$$P_n = V_n^2 G_{nl} - V_n V_l [G_{nl} \cos(\delta_n - \delta_l) + B_{nl} \sin(\delta_n - \delta_l)] \\ + V_n V_{sln} [G_{nl} \cos(\delta_n - \delta_{sln}) + B_{nl} \sin(\delta_n - \delta_{sln})] \quad (A21)$$

$$Q_n = -V_n^2 B_{nl} - V_n V_l [G_{nl} \sin(\delta_n - \delta_l) - B_{nl} \cos(\delta_n - \delta_l)] \\ - V_n V_{sln} [G_{nl} \sin(\delta_n - \delta_{sln}) - B_{nl} \cos(\delta_n - \delta_{sln})] \quad (A22)$$

From operating principle of the IPFC, the active power supplied to one converter is equal to the active power demanded by the other.

$$\text{Real} (V_{slm} I_{lm}^* + V_{slm} I_{ln}^*) = 0 \quad (A23)$$

or in other words,

$$P_{slm} = V_{slm}^2 G_{lm} - V_l V_{slm} [G_{lm} \cos(\delta_l - \delta_{slm}) - B_{lm} \sin(\delta_l - \delta_{slm})] \\ + V_m V_{slm} [G_{lm} \cos(\delta_m - \delta_{slm}) - B_{lm} \sin(\delta_m - \delta_{slm})] \quad (A24)$$

$$P_{sln} = V_{sln}^2 G_{ln} - V_l V_{sln} [G_{ln} \cos(\delta_l - \delta_{sln}) - B_{ln} \sin(\delta_l - \delta_{sln})] \\ + V_n V_{sln} [G_{ln} \cos(\delta_n - \delta_{sln}) - B_{ln} \sin(\delta_n - \delta_{sln})] \quad (A25)$$

And therefore,

$$P_{ex} = P_{slm} + P_{sln} = 0 \quad (A26)$$

where  $V_l$ ,  $V_m$  and  $V_n$  are the nodal voltage magnitudes at node  $l$ ,  $m$  and  $n$  and,  $\delta_l$ ,  $\delta_m$  and  $\delta_n$  are the nodal voltage phase angles at node  $l$ ,  $m$  and  $n$ .

$V_{slm} < \delta_{slm}$  and  $V_{sln} < \delta_{sln}$  are the injected voltage at transmission lines  $l - m$  and  $l - n$ , equations (A17 – A22) can be solved efficiently using Newton Raphson method. It requires a set of linearized equations for expressing the relationship between changes in active and reactive powers and nodal voltage magnitude and phase angles. The linearized relationship takes the following form for an n-node network as in (A27).

$$\begin{bmatrix} P_{ml}^{spec} - P_{ml} \\ Q_{ml}^{spec} - Q_{ml} \\ P_{nl}^{spec} - P_{nl} \\ -P_{ex} \\ \Delta P_l \\ \Delta Q_l \\ \Delta P_m \\ \Delta Q_m \\ \Delta P_n \\ \Delta Q_n \end{bmatrix} \begin{bmatrix} \frac{dP_{ml}}{d\delta_{slm}} & \frac{dP_{ml}}{dV_{slm}} & \frac{dP_{ml}}{d\delta_{sin}} & \frac{dP_{ml}}{dV_{sin}} & \frac{dP_{ml}}{d\delta_l} & \frac{dP_{ml}}{dV_l} & \frac{dP_{ml}}{d\delta_m} & \frac{dP_{ml}}{dV_m} & \frac{dP_{ml}}{d\delta_n} & \frac{dP_{ml}}{dV_n} \\ \frac{dQ_{ml}}{d\delta_{slm}} & \frac{dQ_{ml}}{dV_{slm}} & \frac{dQ_{ml}}{d\delta_{sin}} & \frac{dQ_{ml}}{dV_{sin}} & \frac{dQ_{ml}}{d\delta_l} & \frac{dQ_{ml}}{dV_l} & \frac{dQ_{ml}}{d\delta_m} & \frac{dQ_{ml}}{dV_m} & \frac{dQ_{ml}}{d\delta_n} & \frac{dQ_{ml}}{dV_n} \\ \frac{d\delta_{slm}}{dP_{nl}} & \frac{dV_{slm}}{dP_{nl}} & \frac{d\delta_{sin}}{dP_{nl}} & \frac{dV_{sin}}{dP_{nl}} & \frac{d\delta_l}{dP_{nl}} & \frac{dV_l}{dP_{nl}} & \frac{d\delta_m}{dP_{nl}} & \frac{dV_m}{dP_{nl}} & \frac{d\delta_n}{dP_{nl}} & \frac{dV_n}{dP_{nl}} \\ \frac{d\delta_{slm}}{dP_{ex}} & \frac{dV_{slm}}{dP_{ex}} & \frac{d\delta_{sin}}{dP_{ex}} & \frac{dV_{sin}}{dP_{ex}} & \frac{d\delta_l}{dP_{ex}} & \frac{dV_l}{dP_{ex}} & \frac{d\delta_m}{dP_{ex}} & \frac{dV_m}{dP_{ex}} & \frac{d\delta_n}{dP_{ex}} & \frac{dV_n}{dP_{ex}} \\ \frac{d\delta_{slm}}{dP_l} & \frac{dV_{slm}}{dP_l} & \frac{d\delta_{sin}}{dP_l} & \frac{dV_{sin}}{dP_l} & \frac{d\delta_l}{dP_l} & \frac{dV_l}{dP_l} & \frac{d\delta_m}{dP_l} & \frac{dV_m}{dP_l} & \frac{d\delta_n}{dP_l} & \frac{dV_n}{dP_l} \\ \frac{d\delta_{slm}}{dQ_l} & \frac{dV_{slm}}{dQ_l} & \frac{d\delta_{sin}}{dQ_l} & \frac{dV_{sin}}{dQ_l} & \frac{d\delta_l}{dQ_l} & \frac{dV_l}{dQ_l} & \frac{d\delta_m}{dQ_l} & \frac{dV_m}{dQ_l} & \frac{d\delta_n}{dQ_l} & \frac{dV_n}{dQ_l} \\ \frac{d\delta_{slm}}{dP_m} & \frac{dV_{slm}}{dP_m} & \frac{d\delta_{sin}}{dP_m} & \frac{dV_{sin}}{dP_m} & \frac{d\delta_l}{dP_m} & \frac{dV_l}{dP_m} & \frac{d\delta_m}{dP_m} & \frac{dV_m}{dP_m} & \frac{d\delta_n}{dP_m} & \frac{dV_n}{dP_m} \\ \frac{d\delta_{slm}}{dQ_m} & \frac{dV_{slm}}{dQ_m} & \frac{d\delta_{sin}}{dQ_m} & \frac{dV_{sin}}{dQ_m} & \frac{d\delta_l}{dQ_m} & \frac{dV_l}{dQ_m} & \frac{d\delta_m}{dQ_m} & \frac{dV_m}{dQ_m} & \frac{d\delta_n}{dQ_m} & \frac{dV_n}{dQ_m} \\ \frac{d\delta_{slm}}{dP_n} & \frac{dV_{slm}}{dP_n} & \frac{d\delta_{sin}}{dP_n} & \frac{dV_{sin}}{dP_n} & \frac{d\delta_l}{dP_n} & \frac{dV_l}{dP_n} & \frac{d\delta_m}{dP_n} & \frac{dV_m}{dP_n} & \frac{d\delta_n}{dP_n} & \frac{dV_n}{dP_n} \\ \frac{d\delta_{slm}}{dQ_n} & \frac{dV_{slm}}{dQ_n} & \frac{d\delta_{sin}}{dQ_n} & \frac{dV_{sin}}{dQ_n} & \frac{d\delta_l}{dQ_n} & \frac{dV_l}{dQ_n} & \frac{d\delta_m}{dQ_n} & \frac{dV_m}{dQ_n} & \frac{d\delta_n}{dQ_n} & \frac{dV_n}{dQ_n} \end{bmatrix} \begin{bmatrix} \Delta\delta_{slm} \\ \Delta V_{slm} \\ \Delta\delta_{sin} \\ \Delta V_{sin} \\ \Delta\delta_l \\ \Delta V_l \\ \Delta\delta_m \\ \Delta V_m \\ \Delta\delta_n \\ \Delta V_n \end{bmatrix} \quad (A27)$$

where  $\Delta P_l$ ,  $\Delta Q_l$ ,  $\Delta P_m$ ,  $\Delta Q_m$ ,  $\Delta P_n$  and  $\Delta Q_n$  are the active and reactive power mismatches at buses  $l$ ,  $m$  and  $n$ .

$P_l$ ,  $Q_l$ ,  $P_m$ ,  $Q_m$ ,  $P_n$  and  $Q_n$  are the sum of the active and reactive power leaving the buses  $l$ ,  $m$  and  $n$ .

In Jacobian matrix, the first four rows represent the IPFC power flow control and active power exchange balance constraints as in equation (A27).

where

$$P_{kl} - P_{kl}^{spec} = 0 \quad (A28)$$

$$Q_{kl} - Q_{kl}^{spec} = 0, k = m, n \quad (A29)$$

$P_{kl}^{spec}$ ,  $Q_{kl}^{spec}$  are specified active and reactive power flow control references

$$\left. \begin{aligned} P_{kl} &= \text{Real}(V_k I_{kl}^*) \\ Q_{kl} &= \text{imag}(V_k I_{kl}^*), k = m, n \end{aligned} \right\} \quad (A30)$$

$\Delta P_l = P_l^{net} - P_l^{calc}$  is the active power mismatch at node  $l$ .

$\Delta Q_l = Q_l^{net} - Q_l^{calc}$  is the reactive power mismatch at node  $l$ .

$P_l^{calc}$  and  $Q_l^{calc}$  are the calculated active and reactive powers at node  $l$ .

$P_l^{net} = P_l^{gen} - P_l^{load}$  is the net scheduled active power at node  $l$ .

$Q_l^{net} = Q_l^{gen} - Q_l^{load}$  is the net scheduled reactive power at node  $l$ .

$P_l^{gen}$  and  $Q_l^{gen}$  are the active and reactive power generated at node  $l$ .

$P_l^{load}$  and  $Q_l^{load}$  are the active and reactive power consumed by the load at node  $l$ .

$\Delta\delta_l$  and  $\Delta|V_l|$  are the incremental changes in nodal voltage magnitude and phase angle at node  $l$ . and for node  $m$  and  $n$  also same as node  $l$ .

$\Delta|V_{slm}|$  and  $\Delta\delta_{slm}$  are the injected voltage magnitude and angle at transmission line connected between node  $l - m$ .

$\Delta|V_{sln}|$  and  $\Delta\delta_{sln}$  are the injected voltage magnitude and angle at transmission line connected between node  $l - n$ .

$r$  represents the  $r^{th}$  iterative step

The elements of Jacobian can be found by differentiating equations (A17 – A26) with respect to  $\delta_{slm}, V_{slm}, \delta_{sln}, V_{sln}, \delta_b, V_l, \delta_m, V_m, \delta_n, V_n$

To simplify the calculation, divide Jacobian into four quadrants as in (A31).

$$J = \begin{bmatrix} J_1 & J_2 \\ J_3 & J_4 \end{bmatrix} \quad (A31)$$

Therefore, the sub matrix of Jacobian  $J_1$  is given as in (A32).

$$J_1 = \begin{bmatrix} \frac{dP_{ml}}{d\delta_{slm}} & \frac{dP_{ml}}{dV_{slm}} & \frac{dP_{ml}}{d\delta_{sln}} & \frac{dP_{ml}}{dV_{sln}} \\ \frac{dQ_{ml}}{d\delta_{slm}} & \frac{dQ_{ml}}{dV_{slm}} & \frac{dQ_{ml}}{d\delta_{sln}} & \frac{dQ_{ml}}{dV_{sln}} \\ \frac{dP_{nl}}{d\delta_{slm}} & \frac{dP_{nl}}{dV_{slm}} & \frac{dP_{nl}}{d\delta_{sln}} & \frac{dP_{nl}}{dV_{sln}} \\ \frac{dP_{ex}}{d\delta_{slm}} & \frac{dP_{ex}}{dV_{slm}} & \frac{dP_{ex}}{d\delta_{sln}} & \frac{dP_{ex}}{dV_{sln}} \end{bmatrix} \quad (A32)$$

From equation (A19),

$$J_1(1,1) = \frac{dP_m}{d\delta_{slm}} = V_m V_{slm} [G_{ml} \sin(\delta_m - \delta_{slm}) - B_{ml} \cos(\delta_m - \delta_{slm})] \quad (A33)$$

$$J_1(1,2) = \frac{dP_m}{dV_{slm}} = V_m [G_{ml} \cos(\delta_m - \delta_{slm}) + B_{ml} \sin(\delta_m - \delta_{slm})] \quad (A34)$$

$$J_1(1,3) = \frac{dP_m}{d\delta_{slm}} = 0 \quad (A35)$$

$$J_1(1,4) = \frac{dP_m}{dV_{slm}} = 0 \quad (A36)$$

From equation (A20),

$$J_1(2,1) = \frac{dQ_{ml}}{d\delta_{slm}} = -V_m V_{slm} [-G_{ml} \cos(\delta_m - \delta_{slm}) - B_{ml} \sin(\delta_m - \delta_{slm})] \quad (A37)$$

$$J_1(2,2) = \frac{dQ_{ml}}{dV_{slm}} = -V_m [G_{ml} \sin(\delta_m - \delta_{slm}) - B_{ml} \cos(\delta_m - \delta_{slm})] \quad (A38)$$

$$J_1(2,3) = \frac{dQ_{ml}}{d\delta_{slm}} = 0 \quad (A39)$$

$$J_1(2,4) = \frac{dQ_{ml}}{dV_{slm}} = 0 \quad (A40)$$

From equation (A21),

$$J_1(3,1) = \frac{dP_{nl}}{d\delta_{slm}} = 0 \quad (A41)$$

$$J_1(3,2) = \frac{dP_{nl}}{dV_{slm}} = 0 \quad (A42)$$

$$J_1(3,3) = \frac{dP_{nl}}{d\delta_{sln}} = V_n V_{sln} [G_{nl} \sin(\delta_n - \delta_{sln}) - B_{nl} \cos(\delta_n - \delta_{sln})] \quad (A43)$$

$$J_1(3,4) = \frac{dP_{nl}}{dV_{sln}} = V_n [G_{nl} \cos(\delta_n - \delta_{sln}) + B_{nl} \sin(\delta_n - \delta_{sln})] \quad (A44)$$

From equation (A26),

$$J_1(4,1) = \frac{dP_{sx}}{d\delta_{slm}} = -V_l V_{slm} [G_{lm} \sin(\delta_l - \delta_{slm}) + B_{lm} \cos(\delta_l - \delta_{slm})] \\ + V_m V_{slm} [G_{lm} \sin(\delta_m - \delta_{slm}) + B_{lm} \cos(\delta_m - \delta_{slm})] \quad (A45)$$

$$J_1(4,2) = \frac{dP_{sx}}{dV_{slm}} = 2V_{slm} G_{lm} - V_l [G_{lm} \cos(\delta_l - \delta_{slm}) - B_{lm} \sin(\delta_l - \delta_{slm})] \\ + V_m [G_{lm} \cos(\delta_m - \delta_{slm}) - B_{lm} \sin(\delta_m - \delta_{slm})] \quad (A46)$$

$$J_1(4,3) = \frac{dP_{sx}}{d\delta_{sln}} = -V_l V_{sln} [G_{ln} \sin(\delta_l - \delta_{sln}) + B_{ln} \cos(\delta_l - \delta_{sln})] \\ + V_n V_{sln} [G_{ln} \sin(\delta_n - \delta_{sln}) + B_{ln} \cos(\delta_n - \delta_{sln})] \quad (A47)$$

$$J_1(4,4) = \frac{dP_{sx}}{dV_{sln}} = 2V_{sln}G_{ln} - V_l[G_{ln}\cos(\delta_l - \delta_{sln}) - B_{ln}\sin(\delta_l - \delta_{sln})] \\ + V_n[G_{ln}\cos(\delta_n - \delta_{sln}) - B_{ln}\sin(\delta_n - \delta_{sln})] \quad (A48)$$

Therefore, the sub matrix of jacobian  $J_2$  is given as in (A49).

$$J_2 = \begin{bmatrix} \frac{dP_{ml}}{d\delta_l} & \frac{dP_{ml}}{dV_l} & \frac{dP_{ml}}{d\delta_m} & \frac{dP_{ml}}{dV_m} & \frac{dP_{ml}}{d\delta_n} & \frac{dP_{ml}}{dV_n} \\ \frac{dQ_{ml}}{d\delta_l} & \frac{dQ_{ml}}{dV_l} & \frac{dQ_{ml}}{d\delta_m} & \frac{dQ_{ml}}{dV_m} & \frac{dQ_{ml}}{d\delta_n} & \frac{dQ_{ml}}{dV_n} \\ \frac{dP_{nl}}{d\delta_l} & \frac{dP_{nl}}{dV_l} & \frac{dP_{nl}}{d\delta_m} & \frac{dP_{nl}}{dV_m} & \frac{dP_{nl}}{d\delta_n} & \frac{dP_{nl}}{dV_n} \\ \frac{dP_{sx}}{d\delta_l} & \frac{dP_{sx}}{dV_l} & \frac{dP_{sx}}{d\delta_m} & \frac{dP_{sx}}{dV_m} & \frac{dP_{sx}}{d\delta_n} & \frac{dP_{sx}}{dV_n} \end{bmatrix} \quad (A49)$$

Therefore, from equation (A19),

$$J_2(1,1) = \frac{dP_{ml}}{d\delta_l} = -V_m V_l [G_{ml}\sin(\delta_m - \delta_l) - B_{ml}\cos(\delta_m - \delta_l)] \quad (A50)$$

$$J_2(1,2) = \frac{dP_{ml}}{dV_l} = -V_m [G_{ml}\cos(\delta_m - \delta_l) + B_{ml}\sin(\delta_m - \delta_l)] \quad (A51)$$

$$J_2(1,3) = \frac{dP_{ml}}{d\delta_m} = -V_m V_l [-G_{ml}\sin(\delta_m - \delta_l) + B_{ml}\cos(\delta_m - \delta_l)] \\ + V_m V_{slm} [G_{ml}\sin(\delta_m - \delta_{slm}) + B_{ml}\cos(\delta_m - \delta_{slm})] \quad (A52)$$

$$J_2(1,4) = \frac{dP_{ml}}{dV_m} = 2V_m G_{ml} - V_l [G_{ml}\cos(\delta_m - \delta_l) + B_{ml}\sin(\delta_m - \delta_l)] \\ + V_m V_{slm} [G_{ml}\cos(\delta_m - \delta_{slm}) + B_{ml}\sin(\delta_m - \delta_{slm})] \quad (A53)$$

$$J_2(1,5) = \frac{dP_{ml}}{d\delta_n} = 0 \quad (A54)$$

$$J_2(1,6) = \frac{dP_{ml}}{dV_n} = 0 \quad (A55)$$

From equation (A20),

$$J_2(2,1) = \frac{dQ_{ml}}{d\delta_l} = -V_m V_l [-G_{ml}\cos(\delta_m - \delta_l) - B_{ml}\sin(\delta_m - \delta_l)] \quad (A56)$$

$$J_2(2,2) = \frac{dQ_{ml}}{dV_l} = -V_m [G_{ml}\sin(\delta_m - \delta_l) - B_{ml}\cos(\delta_m - \delta_l)] \quad (A57)$$

$$J_2(2,3) = \frac{dQ_{ml}}{d\delta_m} = -V_m V_l [G_{ml}\cos(\delta_m - \delta_l) + B_{ml}\sin(\delta_m - \delta_l)] \\ - V_m V_{slm} [G_{ml}\cos(\delta_m - \delta_{slm}) + B_{ml}\sin(\delta_m - \delta_{slm})] \quad (A58)$$



$$J_2(2,4) = \frac{dQ_{ml}}{dV_m} = -V_l[G_{ml} \sin(\delta_m - \delta_l) - B_{ml} \cos(\delta_m - \delta_l)] \\ -V_{slm}[G_{ml} \sin(\delta_m - \delta_{slm}) - B_{ml} \cos(\delta_m - \delta_{slm})] \quad (A59)$$

$$J_2(2,5) = \frac{dQ_{ml}}{d\delta_n} = 0 \quad (A60)$$

$$J_2(2,6) = \frac{dQ_{ml}}{dV_n} = 0 \quad (A61)$$

From equation (A21),

$$J_2(3,1) = \frac{dP_{nl}}{d\delta_l} = -V_n V_l[G_{nl} \sin(\delta_n - \delta_l) - B_{nl} \cos(\delta_n - \delta_l)] \quad (A62)$$

$$J_2(3,2) = \frac{dP_{nl}}{dV_l} = -V_n[G_{nl} \cos(\delta_n - \delta_l) + B_{nl} \sin(\delta_n - \delta_l)] \quad (A63)$$

$$J_2(3,3) = \frac{dP_{nl}}{d\delta_m} = 0 \quad (A64)$$

$$J_2(3,4) = \frac{dP_{nl}}{dV_m} = 0 \quad (A65)$$

$$J_2(3,5) = \frac{dP_{nl}}{d\delta_n} = -V_n V_l[-G_{nl} \sin(\delta_n - \delta_l) + B_{nl} \cos(\delta_n - \delta_l)] \\ +V_n V_{sln}[-G_{nl} \sin(\delta_n - \delta_{sln}) + B_{nl} \cos(\delta_n - \delta_{sln})] \quad (A66)$$

$$J_2(3,6) = \frac{dP_{nl}}{dV_n} = -V_l[G_{nl} \cos(\delta_n - \delta_l) + B_{nl} \sin(\delta_n - \delta_l)] \\ +V_{sln}[G_{nl} \sin(\delta_n - \delta_{sln}) + B_{nl} \sin(\delta_n - \delta_{sln})] \quad (A67)$$

From equation (A26),

$$J_2(4,1) = \frac{dP_{sx}}{d\delta_l} = -V_l V_{slm}[-G_{lm} \sin(\delta_l - \delta_{slm}) - B_{lm} \cos(\delta_l - \delta_{slm})] \\ -V_l V_{sln}[-G_{ln} \sin(\delta_l - \delta_{sln}) - B_{ln} \cos(\delta_l - \delta_{sln})] \quad (A68)$$

$$J_2(4,2) = \frac{dP_{sx}}{dV_l} = -V_{slm}[G_{lm} \cos(\delta_l - \delta_{slm}) - B_{lm} \sin(\delta_l - \delta_{slm})] \\ -V_{sln}[G_{ln} \cos(\delta_l - \delta_{sln}) - B_{ln} \sin(\delta_l - \delta_{sln})] \quad (A69)$$

$$J_2(4,3) = \frac{dP_{sx}}{d\delta_m} = V_m V_{slm}[-G_{lm} \sin(\delta_m - \delta_{slm}) - B_{lm} \cos(\delta_m - \delta_{slm})] \quad (A70)$$

$$J_2(4,4) = \frac{dP_{sx}}{dV_m} = V_{slm}[G_{lm} \cos(\delta_m - \delta_{slm}) - B_{lm} \sin(\delta_m - \delta_{slm})] \quad (A71)$$

$$J_2(4,5) = \frac{dP_{sx}}{d\delta_n} = V_n V_{sin} [-G_{ln} \sin(\delta_n - \delta_{sin}) - B_{ln} \cos(\delta_n - \delta_{sin})] \quad (A72)$$

$$J_2(4,6) = \frac{dP_{sx}}{dV_n} = V_{sin} [G_{ln} \cos(\delta_n - \delta_{sin}) - B_{ln} \sin(\delta_n - \delta_{sin})] \quad (A73)$$

Therefore, the sub matrix of Jacobian  $J_3$  is shown as in (A72).

$$J_3 = \begin{bmatrix} \frac{dP_l}{d\delta_{sim}} & \frac{dP_l}{dV_{sim}} & \frac{dP_l}{d\delta_{sin}} & \frac{dP_l}{dV_{sin}} \\ \frac{dQ_l}{d\delta_{sim}} & \frac{dQ_l}{dV_{sim}} & \frac{dQ_l}{d\delta_{sin}} & \frac{dQ_l}{dV_{sin}} \\ \frac{dP_m}{d\delta_{sim}} & \frac{dP_m}{dV_{sim}} & \frac{dP_m}{d\delta_{sin}} & \frac{dP_m}{dV_{sin}} \\ \frac{dQ_m}{d\delta_{sim}} & \frac{dQ_m}{dV_{sim}} & \frac{dQ_m}{d\delta_{sin}} & \frac{dQ_m}{dV_{sin}} \\ \frac{dP_n}{d\delta_{sim}} & \frac{dP_n}{dV_{sim}} & \frac{dP_n}{d\delta_{sin}} & \frac{dP_n}{dV_{sin}} \\ \frac{dQ_n}{d\delta_{sim}} & \frac{dQ_n}{dV_{sim}} & \frac{dQ_n}{d\delta_{sin}} & \frac{dQ_n}{dV_{sin}} \end{bmatrix} \quad (A72)$$

From equation (A17),

$$J_3(1,1) = \frac{dP_l}{d\delta_{sim}} = -V_l V_{sim} [G_{lm} \sin(\delta_l - \delta_{sim}) - B_{lm} \cos(\delta_l - \delta_{sim})] \quad (A73)$$

$$J_3(1,2) = \frac{dP_l}{dV_{sim}} = -V_l [G_{lm} \cos(\delta_l - \delta_{sim}) + B_{lm} \sin(\delta_l - \delta_{sim})] \quad (A74)$$

$$J_3(1,3) = \frac{dP_l}{d\delta_{sin}} = -V_l V_{sin} [G_{ln} \sin(\delta_l - \delta_{sin}) - B_{ln} \cos(\delta_l - \delta_{sin})] \quad (A75)$$

$$J_3(1,4) = \frac{dP_l}{dV_{sin}} = -V_l [G_{ln} \cos(\delta_l - \delta_{sin}) + B_{ln} \sin(\delta_l - \delta_{sin})] \quad (A76)$$

From equation (A18),

$$J_3(2,1) = \frac{dQ_l}{d\delta_{sim}} = -V_l V_{sim} [-G_{lm} \cos(\delta_l - \delta_{sim}) - B_{lm} \sin(\delta_l - \delta_{sim})] \quad (A77)$$

$$J_3(2,2) = \frac{dQ_l}{dV_{sim}} = -V_l [G_{lm} \sin(\delta_l - \delta_{sim}) - B_{lm} \cos(\delta_l - \delta_{sim})] \quad (A78)$$

$$J_3(2,3) = \frac{dQ_l}{d\delta_{sin}} = -V_l V_{sin} [-G_{ln} \cos(\delta_l - \delta_{sin}) - B_{ln} \sin(\delta_l - \delta_{sin})] \quad (A79)$$

$$J_3(2,4) = \frac{dQ_l}{dV_{sin}} = -V_l [G_{ln} \sin(\delta_l - \delta_{sin}) - B_{ln} \cos(\delta_l - \delta_{sin})] \quad (A80)$$

From equation (A19)

$$J_3(3,1) = \frac{dP_m}{d\delta_{sim}} = V_m V_{sim} [G_{ml} \sin(\delta_m - \delta_{sim}) - B_{ml} \cos(\delta_m - \delta_{sim})] \quad (A81)$$

$$J_3(3,2) = \frac{dP_m}{dV_{sim}} = V_m [G_{ml} \cos(\delta_m - \delta_{sim}) + B_{ml} \sin(\delta_m - \delta_{sim})] \quad (A82)$$

$$J_3(3,3) = \frac{dP_m}{d\delta_{sin}} = 0 \quad (A83)$$

$$J_3(3,4) = \frac{dP_m}{dV_{sin}} = 0 \quad (A84)$$

From equation (A20),

$$J_3(4,1) = \frac{dQ_m}{d\delta_{sim}} = -V_m V_{sim} [-G_{lm} \cos(\delta_m - \delta_{sim}) - B_{lm} \sin(\delta_m - \delta_{sim})] \quad (A85)$$

$$J_3(4,2) = \frac{dQ_m}{dV_{sim}} = -V_m [G_{lm} \sin(\delta_m - \delta_{sim}) - B_{lm} \cos(\delta_m - \delta_{sim})] \quad (A86)$$

$$J_3(4,3) = \frac{dQ_m}{d\delta_{sin}} = 0 \quad (A87)$$

$$J_3(4,4) = \frac{dQ_m}{dV_{sin}} = 0 \quad (A88)$$

From equation (A21),

$$J_3(5,1) = \frac{dP_n}{d\delta_{sim}} = 0 \quad (A89)$$

$$J_3(5,2) = \frac{dP_n}{dV_{sim}} = 0 \quad (A90)$$

$$J_3(5,3) = \frac{dP_n}{d\delta_{sin}} = V_n V_{sin} [G_{ln} \sin(\delta_n - \delta_{sin}) - B_{ln} \cos(\delta_n - \delta_{sin})] \quad (A91)$$

$$J_3(5,4) = \frac{dP_n}{dV_{sin}} = V_n [G_{ln} \cos(\delta_n - \delta_{sin}) + B_{ln} \sin(\delta_n - \delta_{sin})] \quad (A92)$$

From equation (A22),

$$J_3(6,1) = \frac{dQ_n}{d\delta_{sim}} = 0 \quad (A93)$$

$$J_3(6,2) = \frac{dQ_n}{dV_{sim}} = 0 \quad (A94)$$

$$J_3(6,3) = \frac{dQ_n}{d\delta_{sin}} = -V_n V_{sin} [-G_{ln} \cos(\delta_n - \delta_{sin}) - B_{ln} \sin(\delta_n - \delta_{sin})] \quad (A95)$$

$$J_3(6,4) = \frac{dQ_n}{dV_{sin}} = -V_n [G_{ln} \sin(\delta_n - \delta_{sin}) - B_{ln} \cos(\delta_n - \delta_{sin})] \quad (A96)$$

Therefore, the sub matrix of Jacobian  $J_4$  is shown as in (A97).

$$J_4 = \begin{bmatrix} \frac{dP_l}{d\delta_l} & \frac{dP_l}{dV_l} & \frac{dP_l}{d\delta_m} & \frac{dP_l}{dV_m} & \frac{dP_l}{d\delta_n} & \frac{dP_l}{dV_n} \\ \frac{dQ_l}{d\delta_l} & \frac{dQ_l}{dV_l} & \frac{dQ_l}{d\delta_m} & \frac{dQ_l}{dV_m} & \frac{dQ_l}{d\delta_n} & \frac{dQ_l}{dV_n} \\ \frac{dP_m}{d\delta_l} & \frac{dP_m}{dV_l} & \frac{dP_m}{d\delta_m} & \frac{dP_m}{dV_m} & \frac{dP_m}{d\delta_n} & \frac{dP_m}{dV_n} \\ \frac{dQ_m}{d\delta_l} & \frac{dQ_m}{dV_l} & \frac{dQ_m}{d\delta_m} & \frac{dQ_m}{dV_m} & \frac{dQ_m}{d\delta_n} & \frac{dQ_m}{dV_n} \\ \frac{dP_n}{d\delta_l} & \frac{dP_n}{dV_l} & \frac{dP_n}{d\delta_m} & \frac{dP_n}{dV_m} & \frac{dP_n}{d\delta_n} & \frac{dP_n}{dV_n} \\ \frac{dQ_n}{d\delta_l} & \frac{dQ_n}{dV_l} & \frac{dQ_n}{d\delta_m} & \frac{dQ_n}{dV_m} & \frac{dQ_n}{d\delta_n} & \frac{dQ_n}{dV_n} \end{bmatrix} \quad (A97)$$

From equation (A17),

$$J_4(1,1) = \frac{dP_l}{d\delta_l} = -V_l V_m [-G_{lm} \sin(\delta_l - \delta_m) + B_{lm} \cos(\delta_l - \delta_m)] \\ - V_l V_{slm} [-G_{lm} \sin(\delta_l - \delta_{slm}) + B_{lm} \cos(\delta_l - \delta_{slm})] \quad (A98)$$

$$J_4(1,2) = \frac{dP_l}{dV_l} = 2V_l G_{lm} - V_m [G_{lm} \cos(\delta_l - \delta_m) + B_{lm} \sin(\delta_l - \delta_m)] \\ - V_{slm} [G_{lm} \cos(\delta_l - \delta_{slm}) + B_{lm} \sin(\delta_l - \delta_{slm})] \quad (A99)$$

$$J_4(1,3) = \frac{dP_l}{d\delta_m} = -V_l V_m [G_{lm} \sin(\delta_l - \delta_m) - B_{lm} \cos(\delta_l - \delta_m)] \quad (A100)$$

$$J_4(1,4) = \frac{dP_l}{dV_l} = -V_l [G_{lm} \cos(\delta_l - \delta_m) + B_{lm} \sin(\delta_l - \delta_m)] \quad (A101)$$

$$J_4(1,5) = \frac{dP_l}{d\delta_n} = -V_l V_n [G_{ln} \sin(\delta_l - \delta_n) - B_{ln} \cos(\delta_l - \delta_n)] \quad (A102)$$

$$J_4(1,6) = \frac{dP_l}{dV_n} = -V_l [G_{ln} \cos(\delta_l - \delta_n) - B_{ln} \sin(\delta_l - \delta_n)] \quad (A103)$$

From equation (A18),

$$J_4(2,1) = \frac{dQ_l}{d\delta_l} = -V_l V_m [-G_{lm} \cos(\delta_l - \delta_m) + B_{lm} \sin(\delta_l - \delta_m)] \\ - V_l V_{slm} [-G_{lm} \cos(\delta_l - \delta_{slm}) + B_{lm} \sin(\delta_l - \delta_{slm})] \quad (A104)$$

$$J_4(2,2) = \frac{dQ_l}{dV_l} = -2V_l B_{lm} - V_m [-G_{lm} \sin(\delta_l - \delta_m) - B_{lm} \cos(\delta_l - \delta_m)]$$

$$-V_{slm}[-G_{lm}\sin(\delta_l - \delta_{slm}) - B_{lm}\cos(\delta_l - \delta_{slm})] \quad (A105)$$

$$J_4(2,3) = \frac{dQ_l}{d\delta_m} = -V_l V_m[-G_{lm}\cos(\delta_l - \delta_m) - B_{lm}\sin(\delta_l - \delta_m)] \quad (A106)$$

$$J_4(2,4) = \frac{dQ_l}{dV_m} = V_l[G_{lm}\sin(\delta_l - \delta_m) - B_{lm}\cos(\delta_l - \delta_m)] \quad (A107)$$

$$J_4(2,5) = \frac{dQ_l}{d\delta_n} = -V_l V_n[-G_{ln}\cos(\delta_l - \delta_n) - B_{ln}\sin(\delta_l - \delta_n)] \quad (A108)$$

$$J_4(2,6) = \frac{dQ_l}{dV_n} = V_l[G_{ln}\sin(\delta_l - \delta_n) - B_{ln}\cos(\delta_l - \delta_n)] \quad (A109)$$

From equation (A19),

$$J_4(3,1) = \frac{dP_m}{d\delta_l} = -V_m V_l[G_{ml}\sin(\delta_m - \delta_l) - B_{ml}\cos(\delta_m - \delta_l)] \quad (A110)$$

$$J_4(3,2) = \frac{dP_m}{dV_l} = -V_m[G_{ml}\cos(\delta_m - \delta_l) + B_{ml}\sin(\delta_m - \delta_l)] \quad (A111)$$

$$J_4(3,3) = \frac{dP_m}{d\delta_m} = -V_m V_l[-G_{ml}\sin(\delta_m - \delta_l) + B_{ml}\cos(\delta_m - \delta_l)] \\ + V_m V_{slm}[-G_{ml}\sin(\delta_m - \delta_{slm}) + B_{ml}\cos(\delta_m - \delta_{slm})] \quad (A112)$$

$$J_4(3,4) = \frac{dP_m}{dV_m} = 2V_m G_{lm} - V_l[G_{ml}\cos(\delta_m - \delta_l) + B_{ml}\sin(\delta_m - \delta_l)] \\ + V_{slm}[G_{ml}\cos(\delta_m - \delta_{slm}) + B_{ml}\sin(\delta_m - \delta_{slm})] \quad (A113)$$

$$J_4(3,5) = \frac{dP_m}{d\delta_n} = 0 \quad (A114)$$

$$J_4(3,6) = \frac{dP_m}{dV_n} = 0 \quad (A115)$$

From equation (A20),

$$J_4(4,1) = \frac{dQ_m}{d\delta_l} = -V_m V_l[-G_{ml}\cos(\delta_m - \delta_l) - B_{ml}\sin(\delta_m - \delta_l)] \quad (A116)$$

$$J_4(4,2) = \frac{dQ_m}{dV_l} = -V_m[G_{ml}\sin(\delta_m - \delta_l) - B_{ml}\cos(\delta_m - \delta_l)] \quad (A117)$$

$$J_4(4,3) = \frac{dQ_m}{d\delta_m} = -V_m V_l[-G_{ml}\cos(\delta_m - \delta_l) + B_{ml}\sin(\delta_m - \delta_l)] \\ - V_{slm}[G_{ml}\cos(\delta_m - \delta_{slm}) + B_{ml}\sin(\delta_m - \delta_{slm})] \quad (A118)$$

$$J_4(4,4) = \frac{dQ_m}{dV_m} = -2V_m B_{lm} - V_l [G_{ml} \sin(\delta_m - \delta_l) - B_{ml} \cos(\delta_m - \delta_l)] \\ - V_{slm} [G_{ml} \sin(\delta_m - \delta_{slm}) - B_{ml} \cos(\delta_m - \delta_{slm})] \quad (A119)$$

$$J_4(4,5) = \frac{dQ_m}{d\delta_n} = 0 \quad (A120)$$

$$J_4(4,6) = \frac{dQ_m}{dV_n} = 0 \quad (A121)$$

From equation (A21),

$$J_4(5,1) = \frac{dP_n}{d\delta_l} = -V_n V_l [G_{nl} \sin(\delta_n - \delta_l) - B_{nl} \cos(\delta_n - \delta_l)] \quad (A122)$$

$$J_4(5,2) = \frac{dP_n}{dV_l} = -V_n [G_{nl} \cos(\delta_n - \delta_l) + B_{nl} \sin(\delta_n - \delta_l)] \quad (A123)$$

$$J_4(5,3) = \frac{dP_n}{d\delta_m} = 0 \quad (A124)$$

$$J_4(5,4) = \frac{dP_n}{dV_m} = 0 \quad (A125)$$

$$J_4(5,5) = \frac{dP_n}{d\delta_n} = -V_n V_l [-G_{nl} \sin(\delta_n - \delta_l) + B_{nl} \cos(\delta_n - \delta_l)] \\ + V_n V_{sln} [-G_{nl} \sin(\delta_n - \delta_{sln}) + B_{nl} \cos(\delta_n - \delta_{sln})] \quad (A126)$$

$$J_4(5,6) = \frac{dP_n}{dV_n} = 2V_n G_{nl} - V_l [G_{nl} \cos(\delta_n - \delta_l) + B_{nl} \sin(\delta_n - \delta_l)] \\ + V_{sln} [G_{nl} \cos(\delta_n - \delta_{sln}) + B_{nl} \sin(\delta_n - \delta_{sln})] \quad (A127)$$

From equation (A22),

$$J_4(6,1) = \frac{dQ_n}{d\delta_l} = -V_n V_l [-G_{nl} \cos(\delta_n - \delta_l) - B_{nl} \sin(\delta_n - \delta_l)] \quad (A128)$$

$$J_4(6,2) = \frac{dQ_n}{dV_l} = -V_n [G_{nl} \sin(\delta_n - \delta_l) - B_{nl} \cos(\delta_n - \delta_l)] \quad (A129)$$

$$J_4(6,3) = \frac{dQ_n}{d\delta_m} = 0 \quad (A130)$$

$$J_4(6,4) = \frac{dQ_n}{dV_m} = 0 \quad (A131)$$

$$J_4(6,5) = \frac{dQ_n}{d\delta_n} = -V_n V_l [-G_{nl} \cos(\delta_n - \delta_l) + B_{nl} \sin(\delta_n - \delta_l)] \\ - V_n V_{sln} [G_{nl} \cos(\delta_n - \delta_{sln}) + B_{nl} \sin(\delta_n - \delta_{sln})] \quad (A132)$$

$$\begin{aligned}
J_4(6,6) = \frac{dQ_n}{dV_n} = & -2V_n B_{nl} - V_l [G_{nl} \sin(\delta_n - \delta_l) - B_{nl} \cos(\delta_n - \delta_l)] \\
& - V_{sin} [G_{nl} \sin(\delta_n - \delta_{sin}) - B_{nl} \cos(\delta_n - \delta_{sin})] \quad (A133)
\end{aligned}$$

*Appendix B: IEEE standard bus Power System data*

*Appendix B1: IEEE standard 14-bus power System*

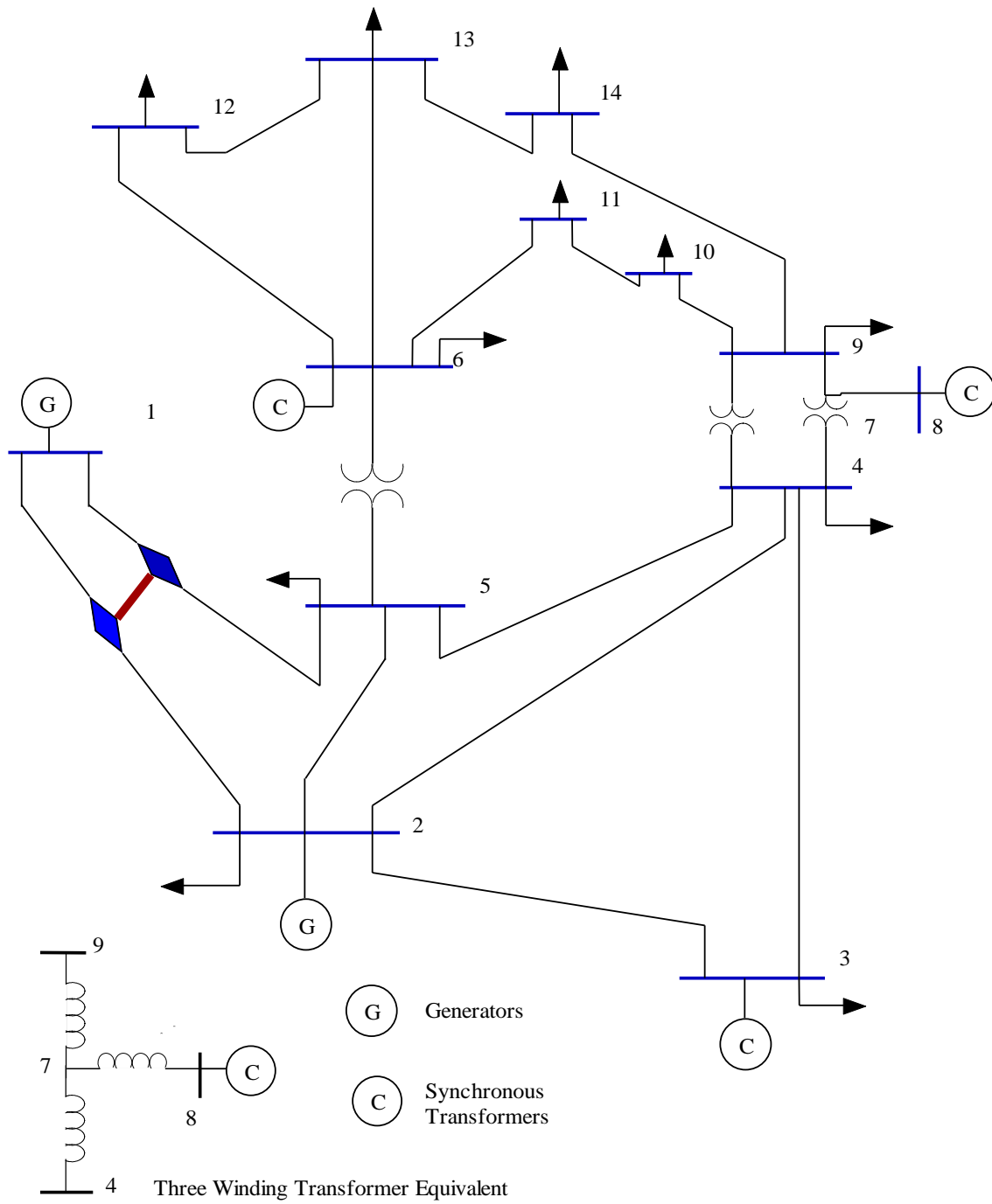


Figure B. 1: IEEE 14-bus power system diagram



Table B- 1: IEEE 14-bus system network data [94]

| Bus No. | Bus Type | Voltage        |              | Load      |               | Generation |               |
|---------|----------|----------------|--------------|-----------|---------------|------------|---------------|
|         |          | Magnitude p.u. | Angle degree | Active MW | Reactive MVAR | Active MW  | Reactive MVAR |
| 1       | 1        | 1.060          | 00.00        | 00.0      | 00.0          | 232.4      | -16.9         |
| 2       | 2        | 1.045          | -04.98       | 21.7      | 12.7          | 40.0       | 42.4          |
| 3       | 2        | 1.010          | -12.72       | 94.2      | 19.0          | 0.0        | 23.4          |
| 4       | 3        | 1.019          | -10.33       | 47.8      | -A25          | 0.0        | 00.0          |
| 5       | 3        | 1.020          | -08.78       | 07.6      | 01.6          | 0.0        | 00.0          |
| 6       | 2        | 1.070          | -14.22       | 11.2      | 07.5          | 0.0        | 12.2          |
| 7       | 3        | 1.062          | -13.37       | 00.0      | 00.0          | 0.0        | 00.0          |
| 8       | 2        | 1.090          | -13.36       | 00.0      | 00.0          | 0.0        | 17.4          |
| 9       | 3        | 1.056          | -14.94       | 29.5      | 16.6          | 0.0        | 00.0          |
| 10      | 3        | 1.051          | -15.10       | 09.0      | 05.8          | 0.0        | 00.0          |
| 11      | 3        | 1.057          | -14.79       | 03.5      | 01.8          | 0.0        | 00.0          |
| 12      | 3        | 1.055          | -15.07       | 06.1      | 01.6          | 0.0        | 00.0          |
| 13      | 3        | 1.050          | -15.16       | 13.5      | 05.8          | 0.0        | 00.0          |
| 14      | 3        | 1.036          | -16.04       | 14.9      | 05.0          | 0.0        | 00.0          |

Table B- 2: IEEE 14-bus system regulated bus data

| Bus No. | Voltage Magnitude p.u. | Maximum MVAR capability | Minimum MVAR Capability |
|---------|------------------------|-------------------------|-------------------------|
| 2       | 1.045                  | 50.0                    | -40.0                   |
| 3       | 1.010                  | 40.0                    | 0.0                     |
| 6       | 1.070                  | 24.0                    | -6.0                    |
| 8       | 1.090                  | 24.0                    | -6.0                    |

Table B- 3: IEEE 14-bus system transformer data

| Transformer Destination | Tap Setting |
|-------------------------|-------------|
| 4 - 7                   | 0.978       |
| 4 - 9                   | 0.969       |
| 5 - 6                   | 0.932       |

Table B- 4: IEEE 14-bus system line data [94]

| From Bus No. | To Bus No. | Resistance $R$ (p.u.) | Reactance $X$ (p.u.) | Line charging $B$ (p.u.) |
|--------------|------------|-----------------------|----------------------|--------------------------|
| 1            | 2          | 0.01938               | 0.05917              | 0.0528                   |
| 1            | 5          | 0.05403               | 0.22304              | 0.0492                   |
| 2            | 3          | 0.04699               | 0.19797              | 0.0438                   |
| 2            | 4          | 0.05811               | 0.17632              | 0.0340                   |
| 2            | 5          | 0.05695               | 0.17388              | 0.0346                   |
| 3            | 4          | 0.06701               | 0.17103              | 0.0128                   |
| 4            | 5          | 0.01335               | 0.04211              | 0.0                      |
| 4            | 7          | 0.0                   | 0.20912              | 0.0                      |
| 4            | 9          | 0.0                   | 0.55618              | 0.0                      |
| 5            | 6          | 0.0                   | 0.25202              | 0.0                      |
| 6            | 11         | 0.09498               | 0.19890              | 0.0                      |
| 6            | 12         | 0.12291               | 0.25581              | 0.0                      |
| 6            | 13         | 0.06615               | 0.13027              | 0.0                      |
| 7            | 8          | 0.0                   | 0.17615              | 0.0                      |
| 7            | 9          | 0.0                   | 0.11001              | 0.0                      |
| 9            | 10         | 0.03181               | 0.08450              | 0.0                      |
| 9            | 14         | 0.12711               | 0.27038              | 0.0                      |
| 10           | 11         | 0.08205               | 0.19207              | 0.0                      |
| 12           | 13         | 0.22092               | 0.19988              | 0.0                      |
| 13           | 14         | 0.17093               | 0.34802              | 0.0                      |

Appendix B2: IEEE 30-bus power System

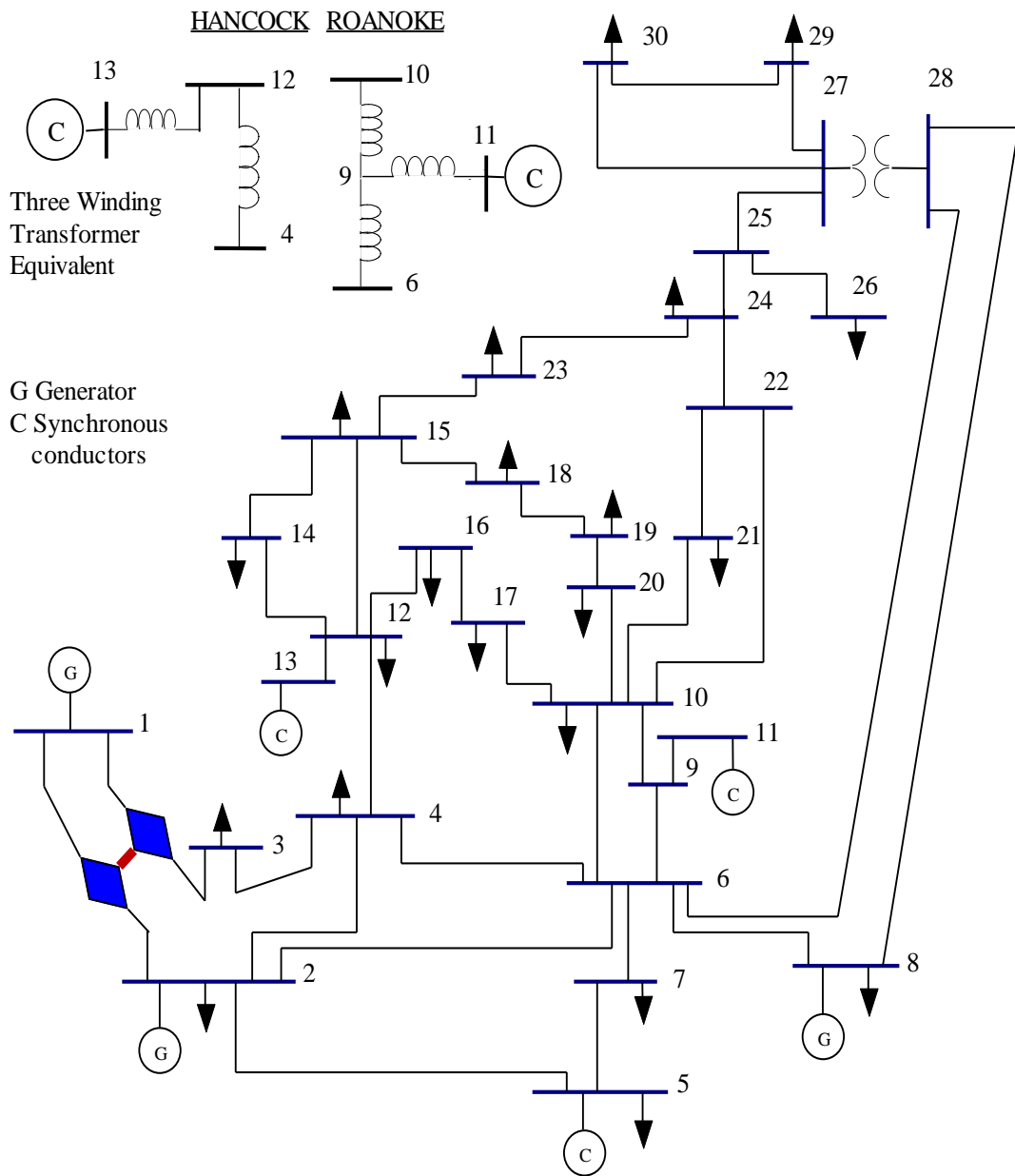


Figure B. 2: IEEE 30-bus system diagram

Table B- 5: IEEE 30-bus system network data [94]

| Bus No. | Bus Type | Voltage        |              | Load      |               | Generation |               |
|---------|----------|----------------|--------------|-----------|---------------|------------|---------------|
|         |          | Magnitude p.u. | Angle degree | Active MW | Reactive MVAR | Active MW  | Reactive MVAR |
| 1       | 1        | 1.060          | 0.0          | 0.0       | 0.0           | 260.2      | -16.1         |
| 2       | 2        | 1.043          | -5.0         | 21.7      | 12.7          | 40.0       | 50.0          |
| 3       | 3        | 1.021          | -7.0         | 2.4       | 1.2           | 0.0        | 0.0           |
| 4       | 3        | 1.012          | -9.62        | 7.6       | 1.6           | 0.0        | 0.0           |
| 5       | 2        | 1.010          | -14.37       | 94.2      | 19.0          | 0.0        | 37.0          |
| 6       | 3        | 1.010          | -11.34       | 0.0       | 0.0           | 0.0        | 0.0           |
| 7       | 3        | 1.002          | -13.12       | 22.8      | 10.9          | 0.0        | 0.0           |
| 8       | 2        | 1.010          | -12.10       | 30.0      | 30.0          | 0.0        | 37.3          |
| 9       | 3        | 1.051          | -14.38       | 0.0       | 0.0           | 0.0        | 0.0           |
| 10      | 3        | 1.045          | -15.97       | 5.8       | 2.0           | 0.0        | 0.0           |
| 11      | 2        | 1.082          | -14.39       | 0.0       | 0.0           | 0.0        | 16.2          |
| 12      | 3        | 1.057          | -15.24       | 11.2      | 7.5           | 0.0        | 0.0           |
| 13      | 2        | 1.071          | -15.24       | 0.0       | 0.0           | 0.0        | 10.6          |
| 14      | 3        | 1.042          | -16.13       | 6.2       | 1.6           | 0.0        | 0.0           |
| 15      | 3        | 1.038          | -16.22       | 8.2       | 2.5           | 0.0        | 0.0           |
| 16      | 3        | 1.045          | -15.83       | 3.5       | 1.8           | 0.0        | 0.0           |
| 17      | 3        | 1.040          | -16.14       | 9.0       | 5.8           | 0.0        | 0.0           |
| 18      | 3        | 1.028          | -16.82       | 3.2       | 0.9           | 0.0        | 0.0           |
| 19      | 3        | 1.026          | -17.00       | 9.5       | 3.4           | 0.0        | 0.0           |
| 20      | 3        | 1.030          | -16.80       | 2.2       | 0.7           | 0.0        | 0.0           |
| 21      | 3        | 1.033          | -16.42       | 17.5      | 11.2          | 0.0        | 0.0           |
| 22      | 3        | 1.033          | -16.41       | 0.0       | 0.0           | 0.0        | 0.0           |
| 23      | 3        | 1.027          | -16.61       | 3.2       | 1.6           | 0.0        | 0.0           |
| 24      | 3        | 1.021          | -16.78       | 8.7       | 6.7           | 0.0        | 0.0           |
| 25      | 3        | 1.017          | -16.35       | 0.0       | 0.0           | 0.0        | 0.0           |
| 26      | 3        | 1.000          | -16.77       | 3.5       | 2.3           | 0.0        | 0.0           |
| 27      | 3        | 1.023          | -15.82       | 0.0       | 0.0           | 0.0        | 0.0           |
| 28      | 3        | 1.007          | -11.97       | 0.0       | 0.0           | 0.0        | 0.0           |
| 29      | 3        | 1.003          | -17.06       | 2.4       | 0.9           | 0.0        | 0.0           |
| 30      | 3        | 0.992          | -17.94       | 10.6      | 1.9           | 0.0        | 0.0           |

Table B- 6: IEEE 30-bus system regulated bus data

| Bus No. | Voltage Magnitude p.u. | Maximum MVAR capability | Minimum MVAR Capability |
|---------|------------------------|-------------------------|-------------------------|
| 2       | 1.045                  | 50.0                    | -40.0                   |
| 5       | 1.010                  | 40.0                    | -40.0                   |
| 8       | 1.010                  | 40.0                    | -10.0                   |
| 11      | 1.082                  | 24.0                    | -6.0                    |
| 13      | 1.071                  | 24.0                    | -6.0                    |

Table B- 7: IEEE 30-bus system transformer data

| Transformer Destination | Tap Setting |
|-------------------------|-------------|
| 6 - 9                   | 0.978       |
| 6 - 10                  | 0.969       |
| 4 - 12                  | 0.932       |
| 28 - 27                 | 0.968       |

Table B- 8: IEEE 30-bus system line data [94]

| From Bus No. | To Bus No. | Resistance $R$ (p.u.) | Reactance $X$ (p.u.) | Line charging $B$ (p.u.) | From Bus No. | To Bus No. | Resistance $R$ (p.u.) | Reactance $X$ (p.u.) | Line charging $B$ (p.u.) |
|--------------|------------|-----------------------|----------------------|--------------------------|--------------|------------|-----------------------|----------------------|--------------------------|
| 1            | 2          | 0.0192                | 0.0575               | 0.0528                   | 18           | 19         | 0.0639                | 0.1292               | 0.0                      |
| 1            | 3          | 0.0452                | 0.1652               | 0.0408                   | 19           | 20         | 0.0340                | 0.0680               | 0.0                      |
| 2            | 4          | 0.0570                | 0.1737               | 0.0368                   | 10           | 20         | 0.0936                | 0.2090               | 0.0                      |
| 3            | 4          | 0.0132                | 0.0379               | 0.0084                   | 10           | 17         | 0.0324                | 0.0845               | 0.0                      |
| 2            | 5          | 0.0472                | 0.1983               | 0.0418                   | 10           | 21         | 0.0348                | 0.0749               | 0.0                      |
| 2            | 6          | 0.0581                | 0.1763               | 0.0374                   | 10           | 22         | 0.0727                | 0.1499               | 0.0                      |
| 4            | 6          | 0.0119                | 0.0414               | 0.0090                   | 21           | 22         | 0.0116                | 0.0236               | 0.0                      |
| 5            | 7          | 0.0460                | 0.1160               | 0.0204                   | 15           | 23         | 0.1000                | 0.2020               | 0.0                      |
| 6            | 7          | 0.0267                | 0.0820               | 0.0170                   | 22           | 24         | 0.1150                | 0.1790               | 0.0                      |
| 6            | 8          | 0.0120                | 0.0420               | 0.0090                   | 23           | 24         | 0.1320                | 0.2700               | 0.0                      |
| 6            | 9          | 0.0                   | 0.2080               | 0.0                      | 24           | 25         | 0.1885                | 0.3292               | 0.0                      |
| 6            | 10         | 0.0                   | 0.5560               | 0.0                      | 25           | 26         | 0.2544                | 0.3800               | 0.0                      |
| 9            | 11         | 0.0                   | 0.2080               | 0.0                      | 25           | 27         | 0.1093                | 0.2087               | 0.0                      |
| 9            | 10         | 0.0                   | 0.1100               | 0.0                      | 28           | 27         | 0.0                   | 0.3960               | 0.0                      |
| 4            | 12         | 0.0                   | 0.2560               | 0.0                      | 27           | 29         | 0.2198                | 0.4153               | 0.0                      |
| 12           | 13         | 0.0                   | 0.1400               | 0.0                      | 27           | 30         | 0.3202                | 0.6027               | 0.0                      |
| 12           | 14         | 0.1231                | 0.2559               | 0.0                      | 29           | 30         | 0.2399                | 0.4533               | 0.0                      |
| 12           | 15         | 0.0662                | 0.1304               | 0.0                      | 8            | 28         | 0.0636                | 0.2000               | 0.0428                   |
| 12           | 16         | 0.0945                | 0.1987               | 0.0                      | 6            | 28         | 0.0169                | 0.0599               | 0.0130                   |
| 14           | 15         | 0.2210                | 0.1997               | 0.0                      | 18           | 19         | 0.0639                | 0.1292               | 0.0                      |
| 16           | 17         | 0.0524                | 0.1923               | 0.0                      | 19           | 20         | 0.0340                | 0.0680               | 0.0                      |
| 15           | 18         | 0.1073                | 0.2185               | 0.0                      | 10           | 20         | 0.0936                | 0.2090               | 0.0                      |

### Appendix C:

#### *Line flows, line losses and Newton-Raphson load flow analysis of IEEE 14-bus power system*

Table C- 1: Line flows and line losses of IEEE 14-bus system without IPFC

| From       | To  | P       | Q       | From | To  | P        | Q       | Line Loss     |        |
|------------|-----|---------|---------|------|-----|----------|---------|---------------|--------|
| Bus        | Bus | MW      | MVar    | Bus  | Bus | MW       | MVar    | MW            | Mvar   |
| 1          | 2   | 157.080 | -17.484 | 2    | 1   | -152.772 | 30.639  | <b>4.309</b>  | 13.155 |
| 1          | 5   | 75.513  | 7.981   | 5    | 1   | -72.740  | 3.464   | <b>2.773</b>  | 11.445 |
| 2          | 3   | 73.396  | 5.936   | 3    | 2   | -71.063  | 3.894   | 2.333         | 9.830  |
| 2          | 4   | 55.943  | 2.935   | 4    | 2   | -54.273  | 2.132   | 1.670         | 5.067  |
| 2          | 5   | 41.733  | 4.738   | 5    | 2   | -40.813  | -1.929  | 0.920         | 2.809  |
| 3          | 4   | -23.137 | 7.752   | 4    | 3   | 23.528   | -6.753  | 0.391         | 0.998  |
| 4          | 5   | -59.585 | 11.574  | 5    | 4   | 60.064   | -10.063 | 0.479         | 1.511  |
| 4          | 7   | 27.066  | -15.396 | 7    | 4   | -27.066  | 17.327  | -0.000        | 1.932  |
| 4          | 9   | 15.464  | -2.640  | 9    | 4   | -15.464  | 3.932   | 0.000         | 1.292  |
| 5          | 6   | 45.889  | -20.843 | 6    | 5   | -45.889  | 26.617  | 0.000         | 5.774  |
| 6          | 11  | 8.287   | 8.898   | 11   | 6   | -8.165   | -8.641  | 0.123         | 0.257  |
| 6          | 12  | 8.064   | 3.176   | 12   | 6   | -7.984   | -3.008  | 0.081         | 0.168  |
| 6          | 13  | 18.337  | 9.981   | 13   | 6   | -18.085  | -9.485  | 0.252         | 0.496  |
| 7          | 8   | 0.000   | -20.362 | 8    | 7   | -0.000   | 21.030  | 0.000         | 0.668  |
| 7          | 9   | 27.066  | 14.798  | 9    | 7   | -27.066  | -13.840 | 0.000         | 0.957  |
| 9          | 10  | 4.393   | -0.904  | 10   | 9   | -4.387   | 0.920   | 0.006         | 0.016  |
| 9          | 14  | 8.637   | 0.321   | 14   | 9   | -8.547   | -0.131  | 0.089         | 0.190  |
| 10         | 11  | -4.613  | -6.720  | 11   | 10  | 4.665    | 6.841   | 0.051         | 0.120  |
| 12         | 13  | 1.884   | 1.408   | 13   | 12  | -1.873   | -1.398  | 0.011         | 0.010  |
| 13         | 14  | 6.458   | 5.083   | 14   | 13  | -6.353   | -4.869  | 0.105         | 0.215  |
| Total loss |     |         |         |      |     |          |         | <b>13.593</b> | 56.910 |

Table C- 2 : Newton Raphson Load flow Analysis of IEEE 14-bus system without IPFC

| Bus No | V pu   | Angle Degree | Injection |         | Generation |         | Load    |        |
|--------|--------|--------------|-----------|---------|------------|---------|---------|--------|
|        |        |              | MW        | MVar    | MW         | Mvar    | MW      | MVar   |
| 1      | 1.0600 | 0.0000       | 232.593   | -15.233 | 232.593    | -15.233 | 0.000   | 0.000  |
| 2      | 1.0450 | -4.9891      | 18.300    | 35.228  | 40.000     | 47.928  | 21.700  | 12.700 |
| 3      | 1.0100 | -12.7492     | -94.200   | 8.758   | 0.000      | 27.758  | 94.200  | 19.000 |
| 4      | 1.0132 | -10.2420     | -47.800   | 3.900   | 0.000      | 0.000   | 47.800  | -3.900 |
| 5      | 1.0166 | -8.7601      | -7.600    | -1.600  | 0.000      | 0.000   | 7.600   | 1.600  |
| 6      | 1.0700 | -14.4469     | -11.200   | 15.526  | 0.000      | 23.026  | 11.200  | 7.500  |
| 7      | 1.0457 | -13.2368     | -0.000    | 0.000   | -0.000     | 0.000   | 0.000   | 0.000  |
| 8      | 1.0800 | -13.2368     | 0.000     | 21.030  | 0.000      | 21.030  | 0.000   | 0.000  |
| 9      | 1.0305 | -14.8201     | -29.500   | -16.600 | 0.000      | 0.000   | 29.500  | 16.600 |
| 10     | 1.0299 | -15.0360     | -9.000    | -5.800  | 0.000      | 0.000   | 9.000   | 5.800  |
| 11     | 1.0461 | -14.8581     | -3.500    | -1.800  | 0.000      | 0.000   | 3.500   | 1.800  |
| 12     | 1.0533 | -15.2973     | -6.100    | -1.600  | 0.000      | 0.000   | 6.100   | 1.600  |
| 13     | 1.0466 | -15.3313     | -13.500   | -5.800  | 0.000      | 0.000   | 13.500  | 5.800  |
| 14     | 1.0193 | -16.0717     | -14.900   | -5.000  | 0.000      | 0.000   | 14.900  | 5.000  |
| Total  |        |              | 13.593    | 31.009  | 272.593    | 104.509 | 259.000 | 73.500 |

Table C- 3: Line flows and line losses of IEEE 14-bus system with IPFC

| From<br>Bus | To<br>Bus | P<br>MW | Q<br>MVar | From<br>Bus | To<br>Bus | P<br>MW | Q<br>MVar | Line Loss    |        |
|-------------|-----------|---------|-----------|-------------|-----------|---------|-----------|--------------|--------|
|             |           |         |           |             |           |         |           | MW           | Mvar   |
| 1           | 2         | 17.557  | 18.717    | 2           | 1         | -17.432 | -18.335   | <b>0.125</b> | 0.381  |
| 1           | 5         | 10.597  | 2.791     | 5           | 1         | -10.533 | -2.529    | <b>0.064</b> | 0.262  |
| 2           | 3         | 60.474  | 7.365     | 3           | 2         | -58.877 | -0.637    | 1.597        | 6.728  |
| 2           | 4         | 30.875  | -2.467    | 4           | 2         | -30.365 | 4.016     | 0.511        | 1.549  |
| 2           | 5         | 8.160   | -4.312    | 5           | 2         | -8.115  | 4.448     | 0.044        | 0.136  |
| 3           | 4         | -35.323 | 1.083     | 4           | 3         | 36.144  | 1.011     | 0.820        | 2.094  |
| 4           | 5         | -95.147 | -3.632    | 5           | 4         | 96.281  | 7.207     | 1.133        | 3.575  |
| 4           | 7         | 26.441  | -12.139   | 7           | 4         | -26.441 | 13.761    | 0.000        | 1.621  |
| 4           | 9         | 15.127  | -0.941    | 9           | 4         | -15.127 | 2.101     | 0.000        | 1.159  |
| 5           | 6         | 46.774  | -7.585    | 6           | 5         | -46.774 | 12.388    | 0.000        | 4.803  |
| 6           | 11        | 8.904   | 6.216     | 11          | 6         | -8.806  | -6.011    | 0.098        | 0.205  |
| 6           | 12        | 8.066   | 2.817     | 12          | 6         | -7.988  | -2.654    | 0.078        | 0.163  |
| 6           | 13        | 18.603  | 8.605     | 13          | 6         | -18.360 | -8.127    | 0.243        | 0.478  |
| 7           | 8         | -0.000  | -18.814   | 8           | 7         | 0.000   | 19.370    | 0.000        | 0.556  |
| 7           | 9         | 26.441  | 17.110    | 9           | 7         | -26.441 | -16.137   | 0.000        | 0.974  |
| 9           | 10        | 3.733   | 1.682     | 10          | 9         | -3.728  | -1.669    | 0.005        | 0.013  |
| 9           | 14        | 8.335   | 1.990     | 14          | 9         | -8.249  | -1.807    | 0.086        | 0.183  |
| 10          | 11        | -5.272  | -4.131    | 11          | 10        | 5.306   | 4.211     | 0.034        | 0.080  |
| 12          | 13        | 1.888   | 1.054     | 13          | 12        | -1.879  | -1.046    | 0.009        | 0.008  |
| 13          | 14        | 6.739   | 3.373     | 14          | 13        | -6.651  | -3.193    | 0.088        | 0.180  |
| Total loss  |           |         |           |             |           |         |           | <b>4.936</b> | 25.149 |



Table C- 4 : Newton-Raphson load flow analysis of IEEE 14-bus system with IPFC

| Bus No | V pu   | Angle Degree | Injection |         | Generation |         | Load    |        |
|--------|--------|--------------|-----------|---------|------------|---------|---------|--------|
|        |        |              | MW        | MVar    | MW         | Mvar    | MW      | MVar   |
| 1      | 1.0600 | 0.0000       | 28.153    | 15.778  | 28.153     | 15.778  | 0.000   | 0.000  |
| 2      | 1.0450 | -0.3847      | 82.077    | -26.769 | 103.777    | -14.069 | 21.700  | 12.700 |
| 3      | 1.0100 | -6.7087      | -94.200   | -2.441  | -0.000     | 16.559  | 94.200  | 19.000 |
| 4      | 1.0334 | -3.3505      | -47.800   | 3.900   | 0.000      | 0.000   | 47.800  | -3.900 |
| 5      | 1.0478 | -1.2556      | 124.406   | 31.047  | 132.006    | 32.647  | 7.600   | 1.600  |
| 6      | 1.0700 | -6.8789      | -11.200   | -3.120  | -0.000     | 4.380   | 11.200  | 7.500  |
| 7      | 1.0587 | -6.1837      | -0.000    | 0.000   | -0.000     | 0.000   | 0.000   | 0.000  |
| 8      | 1.0900 | -6.1837      | 0.000     | 19.370  | 0.000      | 19.370  | 0.000   | 0.000  |
| 9      | 1.0413 | -7.6956      | -29.500   | -16.600 | 0.000      | 0.000   | 29.500  | 16.600 |
| 10     | 1.0388 | -7.8344      | -9.000    | -5.800  | 0.000      | 0.000   | 9.000   | 5.800  |
| 11     | 1.0506 | -7.4807      | -3.500    | -1.800  | 0.000      | 0.000   | 3.500   | 1.800  |
| 12     | 1.0541 | -7.7512      | -6.100    | --1.600 | 0.000      | 0.000   | 6.100   | 1.600  |
| 13     | 1.0482 | -7.8262      | -13.500   | -5.800  | 0.000      | 0.000   | 13.500  | 5.800  |
| 14     | 1.0261 | -8.7686      | -14.900   | -5.000  | 0.000      | 0.000   | 14.900  | 5.000  |
| Total  |        |              | 4.936     | 1.165   | 263.936    | 74.665  | 259.000 | 73.500 |

Table C- 5: Line flows and line losses of IEEE 14-bus system with IPFC and BPSO

| From<br>Bus | To<br>Bus | P<br>MW  | Q<br>MVar | From<br>Bus | To<br>Bus | P<br>MW | Q<br>MVar | Line Loss    |        |
|-------------|-----------|----------|-----------|-------------|-----------|---------|-----------|--------------|--------|
|             |           |          |           |             |           |         |           | MW           | Mvar   |
| 1           | 2         | -3.633   | -6.953    | 2           | 1         | 3.644   | 6.988     | <b>0.012</b> | 0.036  |
| 1           | 5         | 1.331    | -1.740    | 5           | 1         | -1.328  | 1.750     | <b>0.003</b> | 0.010  |
| 2           | 3         | 58.520   | 13.122    | 3           | 2         | -57.029 | -6.845    | 1.490        | 6.278  |
| 2           | 4         | 27.293   | 2.276     | 4           | 2         | -26.909 | -1.110    | 0.384        | 1.166  |
| 2           | 5         | 3.015    | 0.067     | 5           | 2         | -3.011  | -0.054    | 0.005        | 0.014  |
| 3           | 4         | -37.171  | -0.603    | 4           | 3         | 38.061  | 2.875     | 0.890        | 2.272  |
| 4           | 5         | -100.741 | -6.071    | 5           | 4         | 101.980 | 9.981     | 1.240        | 3.911  |
| 4           | 7         | 26.557   | -8.391    | 7           | 4         | -26.557 | 9.838     | 0.000        | 1.446  |
| 4           | 9         | 15.232   | 0.590     | 9           | 4         | -15.231 | 0.552     | 0.000        | 1.142  |
| 5           | 6         | 46.518   | -0.799    | 6           | 5         | -46.518 | 5.296     | 0.000        | 4.497  |
| 6           | 11        | 8.787    | 4.940     | 11          | 6         | -8.703  | -4.763    | 0.084        | 0.177  |
| 6           | 12        | 8.014    | 2.654     | 12          | 6         | -7.937  | -2.495    | 0.077        | 0.159  |
| 6           | 13        | 18.517   | 7.945     | 13          | 6         | -18.283 | -7.483    | 0.235        | 0.462  |
| 7           | 8         | 0.000    | -15.166   | 8           | 7         | -0.000  | 15.523    | 0.000        | 0.357  |
| 7           | 9         | 26.557   | 17.527    | 9           | 7         | -26.557 | -16.545   | 0.000        | 0.982  |
| 9           | 10        | 3.830    | 2.917     | 10          | 9         | -3.824  | -2.899    | 0.007        | 0.018  |
| 9           | 14        | 8.458    | 2.784     | 14          | 9         | -8.366  | -2.588    | 0.092        | 0.196  |
| 10          | 11        | -5.176   | -2.901    | 11          | 10        | 5.203   | 2.963     | 0.027        | 0.062  |
| 12          | 13        | 1.837    | 0.895     | 13          | 12        | -1.829  | -0.888    | 0.008        | 0.008  |
| 13          | 14        | 6.612    | 2.571     | 14          | 13        | -6.534  | -2.412    | 0.078        | 0.159  |
| Total loss  |           |          |           |             |           |         |           | <b>4.630</b> | 23.351 |

Table C- 6: Newton-Raphson load flow analysis of IEEE 14-bus system with IPFC  
and BPSO

| Bus<br>No | V<br>pu | Angle<br>Degree | Injection |         | Generation |         | Load    |        |
|-----------|---------|-----------------|-----------|---------|------------|---------|---------|--------|
|           |         |                 | MW        | MVar    | MW         | Mvar    | MW      | MVar   |
| 1         | 1.0600  | 0.0000          | -2.302    | -14.423 | -2.302     | -14.423 | 0.000   | 0.000  |
| 2         | 1.0650  | 0.0448          | 92.473    | 13.085  | 114.173    | 25.785  | 21.700  | 12.700 |
| 3         | 1.0200  | -5.7503         | -94.200   | -10.392 | 0.000      | 8.608   | 94.200  | 19.000 |
| 4         | 1.0473  | -2.3601         | -47.800   | 3.900   | -0.000     | -0.000  | 47.800  | -3.900 |
| 5         | 1.0633  | -0.2186         | 144.159   | 41.261  | 151.759    | 42.861  | 7.600   | 1.600  |
| 6         | 1.0700  | -5.7296         | -11.200   | -12.310 | 0.000      | -4.810  | 11.200  | 7.500  |
| 7         | 1.0649  | -5.1516         | -0.000    | -0.000  | -0.000     | -0.000  | 0.000   | 0.000  |
| 8         | 1.0900  | -5.1516         | 0.000     | 15.523  | 0.000      | 15.523  | 0.000   | 0.000  |
| 9         | 1.0472  | -6.6529         | -29.500   | -16.600 | -0.000     | -0.000  | 29.500  | 16.600 |
| 10        | 1.0437  | -6.7740         | -9.000    | -5.800  | -0.000     | -0.000  | 9.000   | 5.800  |
| 11        | 1.0531  | -6.3797         | -3.500    | -1.800  | -0.000     | -0.000  | 3.500   | 1.800  |
| 12        | 1.0546  | -6.6049         | -6.100    | -1.600  | -0.000     | -0.000  | 6.100   | 1.600  |
| 13        | 1.0490  | -6.6927         | -13.500   | -5.800  | -0.000     | -0.000  | 13.500  | 5.800  |
| 14        | 1.0299  | -7.6800         | -14.900   | -5.000  | -0.000     | -0.000  | 14.900  | 5.000  |
| Total     |         |                 | 4.630     | 0.045   | 263.630    | 73.545  | 259.000 | 73.500 |

Table C- 7: Line flows and line losses of IEEE 14-bus system with IPFC and  
IWAPSO

| From<br>Bus | To<br>Bus | P<br>MW  | Q<br>MVar | From<br>Bus | To<br>Bus | P<br>MW | Q<br>MVar | Line Loss    |        |
|-------------|-----------|----------|-----------|-------------|-----------|---------|-----------|--------------|--------|
|             |           |          |           |             |           |         |           | MW           | MVar   |
| 1           | 2         | -3.633   | -6.952    | 2           | 1         | 3.645   | 6.988     | <b>0.012</b> | 0.036  |
| 1           | 5         | 1.331    | -1.740    | 5           | 1         | -1.328  | 1.750     | <b>0.003</b> | 0.010  |
| 2           | 3         | 58.520   | 13.122    | 3           | 2         | -57.029 | -6.845    | 1.490        | 6.278  |
| 2           | 4         | 27.293   | 2.276     | 4           | 2         | -26.909 | -1.109    | 0.384        | 1.166  |
| 2           | 5         | 3.015    | 0.067     | 5           | 2         | -3.011  | -0.053    | 0.005        | 0.014  |
| 3           | 4         | -37.171  | -0.603    | 4           | 3         | 38.061  | 2.875     | 0.890        | 2.272  |
| 4           | 5         | -100.741 | -6.071    | 5           | 4         | 101.980 | 9.982     | 1.240        | 3.911  |
| 4           | 7         | 26.557   | -8.391    | 7           | 4         | -26.557 | 9.838     | 0.000        | 1.446  |
| 4           | 9         | 15.232   | 0.590     | 9           | 4         | -15.232 | 0.552     | 0.000        | 1.142  |
| 5           | 6         | 46.518   | -0.799    | 6           | 5         | -46.518 | 5.296     | 0.000        | 4.497  |
| 6           | 11        | 8.787    | 4.940     | 11          | 6         | -8.703  | -4.763    | 0.084        | 0.177  |
| 6           | 12        | 8.014    | 2.654     | 12          | 6         | -7.937  | -2.495    | 0.077        | 0.159  |
| 6           | 13        | 18.517   | 7.945     | 13          | 6         | -18.283 | -7.483    | 0.235        | 0.462  |
| 7           | 8         | 0.000    | -15.166   | 8           | 7         | 0.000   | 15.523    | 0.000        | 0.357  |
| 7           | 9         | 26.557   | 17.527    | 9           | 7         | -26.557 | -16.545   | -0.000       | 0.982  |
| 9           | 10        | 3.830    | 2.917     | 10          | 9         | -3.824  | -2.899    | 0.007        | 0.018  |
| 9           | 14        | 8.458    | 2.784     | 14          | 9         | -8.366  | -2.588    | 0.092        | 0.196  |
| 10          | 11        | -5.176   | -2.901    | 11          | 10        | 5.203   | 2.963     | 0.027        | 0.062  |
| 12          | 13        | 1.837    | 0.895     | 13          | 12        | -1.829  | -0.888    | 0.008        | 0.008  |
| 13          | 14        | 6.612    | 2.571     | 14          | 13        | -6.534  | -2.412    | 0.078        | 0.159  |
| Total loss  |           |          |           |             |           |         |           | <b>4.630</b> | 23.351 |

Table C- 8 Newton-Raphson load flow analysis of IEEE 14-bus system with IPFC  
and IWAPSO

| Bus<br>No | V<br>pu | Angle<br>Degree | Injection |         | Generation |         | Load    |        |
|-----------|---------|-----------------|-----------|---------|------------|---------|---------|--------|
|           |         |                 | MW        | MVar    | MW         | Mvar    | MW      | MVar   |
| 1         | 1.0600  | 0.0000          | 28.153    | -14.423 | 2.302      | -14.423 | 0.000   | 0.000  |
| 2         | 1.0650  | 0.0448          | 82.077    | 13.085  | 114.172    | 25.785  | 21.700  | 12.700 |
| 3         | 1.0200  | -5.7503         | -94.200   | -10.392 | 0.000      | 8.608   | 94.200  | 19.000 |
| 4         | 1.0473  | -2.3601         | -47.800   | 3.900   | -0.000     | -0.000  | 47.800  | -3.900 |
| 5         | 1.0633  | -0.2186         | 124.406   | 41.262  | 151.759    | 42.862  | 7.600   | 1.600  |
| 6         | 1.0700  | -5.7296         | -11.200   | -12.310 | 0.000      | -4.810  | 11.200  | 7.500  |
| 7         | 1.0649  | -5.1517         | -0.000    | -0.000  | 0.000      | -0.000  | 0.000   | 0.000  |
| 8         | 1.0900  | -5.1517         | 0.000     | 15.523  | -0.000     | 15.523  | 0.000   | 0.000  |
| 9         | 1.0472  | -6.6529         | -29.500   | -16.600 | -0.000     | -0.000  | 29.500  | 16.600 |
| 10        | 1.0437  | -6.7740         | -9.000    | -5.800  | -0.000     | -0.000  | 9.000   | 5.800  |
| 11        | 1.0531  | -6.3798         | -3.500    | -1.800  | -0.000     | -0.000  | 3.500   | 1.800  |
| 12        | 1.0546  | -6.6049         | -6.100    | -1.600  | -0.000     | -0.000  | 6.100   | 1.600  |
| 13        | 1.0490  | -6.6927         | -13.500   | -5.800  | -0.000     | -0.000  | 13.500  | 5.800  |
| 14        | 1.0299  | -7.6800         | -14.900   | -5.000  | -0.000     | -0.000  | 14.900  | 5.000  |
| Total     |         |                 | 4.630     | 0.045   | 263.630    | 73.545  | 259.000 | 73.500 |

Table C- 9: Line flows and line losses of IEEE 14-bus system with IPFC and CFAPSO

| From<br>Bus | To<br>Bus | P<br>MW  | Q<br>MVar | From<br>Bus | To<br>Bus | P<br>MW | Q<br>MVar | Line Loss    |        |
|-------------|-----------|----------|-----------|-------------|-----------|---------|-----------|--------------|--------|
|             |           |          |           |             |           |         |           | MW           | Mvar   |
| 1           | 2         | -3.633   | -6.953    | 2           | 1         | 3.644   | 6.988     | <b>0.012</b> | 0.036  |
| 1           | 5         | 1.331    | -1.740    | 5           | 1         | -1.328  | 1.750     | <b>0.003</b> | 0.010  |
| 2           | 3         | 58.520   | 13.122    | 3           | 2         | -57.029 | -6.845    | 1.490        | 6.278  |
| 2           | 4         | 27.293   | 2.276     | 4           | 2         | -26.909 | -1.109    | 0.384        | 1.166  |
| 2           | 5         | 3.015    | 0.067     | 5           | 2         | -3.011  | -0.053    | 0.005        | 0.014  |
| 3           | 4         | -37.171  | -0.603    | 4           | 3         | 38.061  | 2.875     | 0.890        | 2.272  |
| 4           | 5         | -100.741 | -6.071    | 5           | 4         | 101.980 | 9.982     | 1.240        | 3.911  |
| 4           | 7         | 26.557   | -8.391    | 7           | 4         | -26.557 | 9.838     | 0.000        | 1.446  |
| 4           | 9         | 15.232   | 0.590     | 9           | 4         | -15.232 | 0.552     | 0.000        | 1.142  |
| 5           | 6         | 46.518   | -0.799    | 6           | 5         | -46.518 | 5.296     | 0.000        | 4.497  |
| 6           | 11        | 8.787    | 4.940     | 11          | 6         | -8.703  | -4.763    | 0.084        | 0.177  |
| 6           | 12        | 8.014    | 2.654     | 12          | 6         | -7.937  | -2.495    | 0.077        | 0.159  |
| 6           | 13        | 18.517   | 7.945     | 13          | 6         | -18.283 | -7.483    | 0.235        | 0.462  |
| 7           | 8         | 0.000    | -15.166   | 8           | 7         | -0.000  | 15.523    | 0.000        | 0.357  |
| 7           | 9         | 26.557   | 17.527    | 9           | 7         | -26.557 | -16.545   | 0.000        | 0.982  |
| 9           | 10        | 3.830    | 2.917     | 10          | 9         | -3.824  | -2.899    | 0.007        | 0.018  |
| 9           | 14        | 8.458    | 2.784     | 14          | 9         | -8.366  | -2.588    | 0.092        | 0.196  |
| 10          | 11        | -5.176   | -2.901    | 11          | 10        | 5.203   | 2.963     | 0.027        | 0.062  |
| 12          | 13        | 1.837    | 0.895     | 13          | 12        | -1.829  | -0.888    | 0.008        | 0.008  |
| 13          | 14        | 6.612    | 2.571     | 14          | 13        | -6.534  | -2.412    | 0.078        | 0.159  |
| Total loss  |           |          |           |             |           |         |           | <b>4.630</b> | 23.351 |

Table C- 10 : Newton-Raphson load flow analysis of IEEE 14-bus system with IPFC  
and CFAPSO

| Bus<br>No | V<br>pu | Angle<br>Degree | Injection |         | Generation |         | Load    |        |
|-----------|---------|-----------------|-----------|---------|------------|---------|---------|--------|
|           |         |                 | MW        | MVar    | MW         | Mvar    | MW      | MVar   |
| 1         | 1.0600  | 0.0000          | -2.302    | -14.423 | 2.302      | -14.423 | 0.000   | 0.000  |
| 2         | 1.0650  | 0.0448          | 92.473    | 13.085  | 114.173    | 25.785  | 21.700  | 12.700 |
| 3         | 1.0200  | -5.7503         | -94.200   | -10.392 | 0.000      | 8.608   | 94.200  | 19.000 |
| 4         | 1.0473  | -2.3601         | -47.800   | 3.900   | -0.000     | -0.000  | 47.800  | -3.900 |
| 5         | 1.0633  | -0.2186         | 144.159   | 41.261  | 151.759    | 42.861  | 7.600   | 1.600  |
| 6         | 1.0700  | -5.7296         | -11.200   | -12.310 | 0.000      | -4.810  | 11.200  | 7.500  |
| 7         | 1.0649  | -5.1516         | -0.000    | -0.000  | -0.000     | -0.000  | 0.000   | 0.000  |
| 8         | 1.0900  | -5.1516         | 0.000     | 15.523  | 0.000      | 15.523  | 0.000   | 0.000  |
| 9         | 1.0472  | -6.6529         | -29.500   | -16.600 | -0.000     | -0.000  | 29.500  | 16.600 |
| 10        | 1.0437  | -6.7740         | -9.000    | -5.800  | -0.000     | -0.000  | 9.000   | 5.800  |
| 11        | 1.0531  | -6.3797         | -3.500    | -1.800  | -0.000     | -0.000  | 3.500   | 1.800  |
| 12        | 1.0546  | -6.6049         | -6.100    | -1.600  | -0.000     | -0.000  | 6.100   | 1.600  |
| 13        | 1.0490  | -6.6927         | -13.500   | -5.800  | -0.000     | -0.000  | 13.500  | 5.800  |
| 14        | 1.0299  | -7.6800         | -14.900   | -5.000  | -0.000     | -0.000  | 14.900  | 5.000  |
| Total     |         |                 | 4.630     | 0.045   | 263.630    | 73.545  | 259.000 | 73.500 |

Table C- 11: Line flows and line losses of IEEE 14-bus system with IPFC and GA

| From<br>Bus | To<br>Bus | P<br>MW  | Q<br>MVar | From<br>Bus | To<br>Bus | P<br>MW | Q<br>MVar | Line Loss    |        |
|-------------|-----------|----------|-----------|-------------|-----------|---------|-----------|--------------|--------|
|             |           |          |           |             |           |         |           | MW           | Mvar   |
| 1           | 2         | 1.119    | 7.777     | 2           | 1         | -1.107  | -7.741    | <b>0.012</b> | 0.036  |
| 1           | 5         | 2.104    | 1.421     | 5           | 1         | -2.101  | -1.407    | <b>0.003</b> | 0.014  |
| 2           | 3         | 58.280   | 12.985    | 3           | 2         | -56.775 | -6.644    | 1.505        | 6.341  |
| 2           | 4         | 26.932   | 0.917     | 4           | 2         | -26.553 | 0.233     | 0.379        | 1.150  |
| 2           | 5         | 2.618    | -1.178    | 5           | 2         | -2.614  | 1.190     | 0.004        | 0.013  |
| 3           | 4         | -37.425  | -1.707    | 4           | 3         | 38.347  | 4.060     | 0.922        | 2.353  |
| 4           | 5         | -101.075 | -5.446    | 5           | 4         | 102.340 | 9.438     | 1.266        | 3.992  |
| 4           | 7         | 26.375   | -10.468   | 7           | 4         | -26.375 | 11.991    | 0.000        | 1.524  |
| 4           | 9         | 15.106   | -0.253    | 9           | 4         | -15.106 | 1.392     | 0.000        | 1.138  |
| 5           | 6         | 46.848   | -4.211    | 6           | 5         | -46.848 | 8.875     | 0.000        | 4.664  |
| 6           | 11        | 8.967    | 5.613     | 11          | 6         | -8.874  | -5.419    | 0.093        | 0.194  |
| 6           | 12        | 8.057    | 2.738     | 12          | 6         | -7.979  | -2.576    | 0.078        | 0.162  |
| 6           | 13        | 18.624   | 8.295     | 13          | 6         | -18.384 | -7.822    | 0.240        | 0.473  |
| 7           | 8         | 0.000    | -17.205   | 8           | 7         | -0.000  | 17.668    | -0.000       | 0.463  |
| 7           | 9         | 26.375   | 17.333    | 9           | 7         | -26.375 | -16.361   | 0.000        | 0.973  |
| 9           | 10        | 3.662    | 2.268     | 10          | 9         | -3.657  | -2.254    | 0.005        | 0.014  |
| 9           | 14        | 8.318    | 2.368     | 14          | 9         | -8.231  | -2.182    | 0.087        | 0.186  |
| 10          | 11        | -5.343   | -3.546    | 11          | 10        | 5.374   | 3.619     | 0.031        | 0.073  |
| 12          | 13        | 1.879    | 0.976     | 13          | 12        | -1.870  | -0.968    | 0.009        | 0.008  |
| 13          | 14        | 6.754    | 2.990     | 14          | 13        | -6.669  | -2.818    | 0.085        | 0.173  |
| Total loss  |           |          |           |             |           |         |           | <b>4.720</b> | 23.944 |



Table C- 12: Newton-Raphson load flow analysis of IEEE 14-bus system with IPFC  
and GA

| Bus<br>No | V<br>pu | Angle<br>Degree | Injection |         | Generation |        | Load    |        |
|-----------|---------|-----------------|-----------|---------|------------|--------|---------|--------|
|           |         |                 | MW        | MVar    | MW         | Mvar   | MW      | MVar   |
| 1         | 1.0600  | 0.0000          | 3.223     | 3.468   | 3.223      | 3.468  | 0.000   | 0.000  |
| 2         | 1.0550  | 0.0476          | 86.723    | -4.210  | 108.423    | 8.490  | 21.700  | 12.700 |
| 3         | 1.0100  | -5.8385         | -94.200   | -11.238 | -0.000     | 7.762  | 94.200  | 19.000 |
| 4         | 1.0396  | -2.4060         | -47.800   | 3.900   | -0.000     | -0.000 | 47.800  | -3.900 |
| 5         | 1.0555  | -0.2211         | 144.474   | 34.951  | 152.074    | 36.551 | 7.600   | 1.600  |
| 6         | 1.0700  | -5.8122         | -11.200   | -7.624  | 0.000      | -0.124 | 11.200  | 7.500  |
| 7         | 1.0614  | -5.2080         | 0.000     | -0.000  | 0.000      | -0.000 | 0.000   | 0.000  |
| 8         | 1.0900  | -5.2080         | -0.000    | 17.668  | -0.000     | 17.668 | 0.000   | 0.000  |
| 9         | 1.0438  | -6.7085         | -29.500   | -16.600 | -0.000     | -0.000 | 29.500  | 16.600 |
| 10        | 1.0409  | -6.8337         | -9.000    | -5.800  | -0.000     | -0.000 | 9.000   | 5.800  |
| 11        | 1.0517  | -6.4488         | -3.500    | -1.800  | -0.000     | -0.000 | 3.500   | 1.800  |
| 12        | 1.0543  | -6.6881         | -6.100    | -1.600  | -0.000     | -0.000 | 6.100   | 1.600  |
| 13        | 1.0485  | -6.7710         | -13.500   | -5.800  | -0.000     | -0.000 | 13.500  | 5.800  |
| 14        | 1.0277  | -7.7490         | -14.900   | -5.000  | -0.000     | -0.000 | 14.900  | 5.000  |
| Total     |         |                 | 4.720     | 0.315   | 263.720    | 73.815 | 259.000 | 73.500 |

Table C- 13: Line flows and line losses of IEEE 14-bus system with IPFC and SA

| From<br>Bus | To<br>Bus | P<br>MW | Q<br>MVar | From<br>Bus | To<br>Bus | P<br>MW | Q<br>MVar | Line Loss    |        |
|-------------|-----------|---------|-----------|-------------|-----------|---------|-----------|--------------|--------|
|             |           |         |           |             |           |         |           | MW           | MVar   |
| 1           | 2         | -10.484 | -4.686    | 2           | 1         | 10.509  | 4.762     | <b>0.025</b> | 0.076  |
| 1           | 5         | 1.053   | -2.338    | 5           | 1         | -1.049  | 2.352     | <b>0.003</b> | 0.014  |
| 2           | 3         | 59.209  | 13.031    | 3           | 2         | -57.686 | -6.616    | 1.523        | 6.415  |
| 2           | 4         | 28.858  | 1.279     | 4           | 2         | -28.430 | 0.018     | 0.427        | 1.297  |
| 2           | 5         | 5.151   | -1.557    | 5           | 2         | -5.136  | 1.601     | 0.015        | 0.044  |
| 3           | 4         | -36.514 | -1.475    | 4           | 3         | 37.374  | 3.670     | 0.860        | 2.195  |
| 4           | 5         | -98.713 | -8.366    | 5           | 4         | 99.906  | 12.128    | 1.192        | 3.761  |
| 4           | 7         | 26.670  | -8.144    | 7           | 4         | -26.670 | 9.591     | -0.000       | 1.448  |
| 4           | 9         | 15.299  | 0.686     | 9           | 4         | -15.299 | 0.464     | -0.000       | 1.150  |
| 5           | 6         | 46.333  | -0.127    | 6           | 5         | -46.333 | 4.574     | 0.000        | 4.447  |
| 6           | 11        | 8.676   | 4.882     | 11          | 6         | -8.594  | -4.710    | 0.082        | 0.172  |
| 6           | 12        | 7.998   | 2.649     | 12          | 6         | -7.921  | -2.491    | 0.076        | 0.159  |
| 6           | 13        | 18.459  | 7.914     | 13          | 6         | -18.226 | -7.455    | 0.233        | 0.459  |
| 7           | 8         | 0.000   | -14.905   | 8           | 7         | -0.000  | 15.249    | -0.000       | 0.345  |
| 7           | 9         | 26.670  | 17.522    | 9           | 7         | -26.670 | -16.535   | 0.000        | 0.987  |
| 9           | 10        | 3.938   | 2.968     | 10          | 9         | -3.931  | -2.949    | 0.007        | 0.019  |
| 9           | 14        | 8.531   | 2.816     | 14          | 9         | -8.437  | -2.617    | 0.093        | 0.199  |
| 10          | 11        | -5.069  | -2.851    | 11          | 10        | 5.094   | 2.910     | 0.025        | 0.060  |
| 12          | 13        | 1.821   | 0.891     | 13          | 12        | -1.813  | -0.883    | 0.008        | 0.007  |
| 13          | 14        | 6.539   | 2.539     | 14          | 13        | -6.463  | -2.383    | 0.076        | 0.156  |
| Total loss  |           |         |           |             |           |         |           | <b>4.648</b> | 23.411 |

Table C- 14 : Newton-Raphson load flow analysis of IEEE 14-bus system with IPFC  
and SA

| Bus<br>No | V<br>pu | Angle<br>Degree | Injection |         | Generation |         | Load    |        |
|-----------|---------|-----------------|-----------|---------|------------|---------|---------|--------|
|           |         |                 | MW        | MVar    | MW         | Mvar    | MW      | MVar   |
| 1         | 1.0600  | 0.0000          | -9.431    | -12.754 | -9.431     | -12.754 | 0.000   | 0.000  |
| 2         | 1.0650  | 0.2956          | 103.726   | 8.148   | 125.426    | 20.848  | 21.700  | 12.700 |
| 3         | 1.0200  | -5.5741         | -94.200   | -11.035 | -0.000     | 7.965   | 94.200  | 19.000 |
| 4         | 1.0482  | -2.2786         | -47.800   | 3.900   | -0.000     | -0.000  | 47.800  | -3.900 |
| 5         | 1.0648  | -0.2017         | 140.053   | 46.424  | 147.653    | 48.024  | 7.600   | 1.600  |
| 6         | 1.0700  | -5.6827         | -11.200   | -13.125 | 0.000      | -5.625  | 11.200  | 7.500  |
| 7         | 1.0654  | -5.0784         | 0.000     | -0.000  | 0.000      | -0.000  | 0.000   | 0.000  |
| 8         | 1.0900  | -5.0784         | -0.000    | 15.249  | -0.000     | 15.249  | 0.000   | 0.000  |
| 9         | 1.0476  | -6.5847         | -29.500   | -16.600 | -0.000     | -0.000  | 29.500  | 16.600 |
| 10        | 1.0440  | -6.7096         | -9.000    | -5.800  | -0.000     | -0.000  | 9.000   | 5.800  |
| 11        | 1.0533  | -6.3242         | -3.500    | -1.800  | -0.000     | -0.000  | 3.500   | 1.800  |
| 12        | 1.0546  | -6.5562         | -6.100    | -1.600  | -0.000     | -0.000  | 6.100   | 1.600  |
| 13        | 1.0491  | -6.6428         | -13.500   | -5.800  | -0.000     | -0.000  | 13.500  | 5.800  |
| 14        | 1.0302  | -7.6193         | -14.900   | -5.000  | -0.000     | -0.000  | 14.900  | 5.000  |
| Total     |         |                 | 4.648     | 0.206   | 263.648    | 73.706  | 259.000 | 73.500 |

*Appendix D:*

*Line flows, line losses and Newton-Raphson load flow analysis of IEEE 30-bus system*

Table D- 1: Line flows and line losses of IEEE 30-bus system without IPFC

| From Bus   | To Bus | P MW    | Q MVar  | From Bus | To Bus | P MW     | Q MVar  | Line Loss     |        |
|------------|--------|---------|---------|----------|--------|----------|---------|---------------|--------|
|            |        |         |         |          |        |          |         | MW            | Mvar   |
| 1          | 2      | 173.143 | -18.108 | 2        | 1      | -167.964 | 33.617  | <b>5.179</b>  | 15.509 |
| 1          | 3      | 87.785  | 6.248   | 3        | 1      | -84.669  | 5.140   | <b>3.116</b>  | 11.388 |
| 2          | 4      | 43.618  | 5.194   | 4        | 2      | -42.607  | -2.113  | 1.011         | 3.081  |
| 3          | 4      | 82.269  | -3.772  | 4        | 3      | -81.411  | 6.235   | 0.858         | 2.463  |
| 2          | 5      | 82.293  | 4.033   | 5        | 2      | -79.347  | 8.342   | 2.945         | 12.374 |
| 2          | 6      | 60.353  | 1.403   | 6        | 2      | -58.406  | 4.503   | 1.946         | 5.906  |
| 4          | 6      | 72.272  | -17.521 | 6        | 4      | -71.630  | 19.753  | 0.641         | 2.231  |
| 5          | 7      | -14.853 | 11.796  | 7        | 5      | 15.015   | -11.387 | 0.162         | 0.409  |
| 6          | 7      | 38.195  | -1.201  | 7        | 6      | -37.815  | 2.370   | 0.381         | 1.169  |
| 6          | 8      | 29.490  | -3.213  | 8        | 6      | -29.387  | 3.574   | 0.103         | 0.361  |
| 6          | 9      | 27.799  | -18.485 | 9        | 6      | -27.799  | 20.698  | 0.000         | 2.213  |
| 6          | 10     | 15.882  | -5.306  | 10       | 6      | -15.882  | 6.781   | 0.000         | 1.475  |
| 9          | 11     | -0.000  | -15.799 | 11       | 9      | 0.000    | 16.269  | 0.000         | 0.470  |
| 9          | 10     | 27.799  | 7.041   | 10       | 9      | -27.799  | -6.221  | 0.000         | 0.819  |
| 4          | 12     | 44.147  | -16.795 | 12       | 4      | -44.147  | 21.983  | 0.000         | 5.188  |
| 12         | 13     | 0.000   | -10.119 | 13       | 12     | -0.000   | 10.247  | 0.000         | 0.128  |
| 12         | 14     | 7.790   | 2.390   | 14       | 12     | -7.717   | -2.238  | 0.073         | 0.152  |
| 12         | 15     | 17.639  | 6.705   | 15       | 12     | -17.429  | -6.290  | 0.211         | 0.415  |
| 12         | 16     | 7.518   | 3.420   | 16       | 12     | -7.460   | -3.299  | 0.058         | 0.121  |
| 14         | 15     | 1.517   | 0.638   | 15       | 14     | -1.511   | -0.633  | 0.006         | 0.005  |
| 16         | 17     | 3.960   | 1.499   | 17       | 16     | -3.946   | -1.468  | 0.014         | 0.032  |
| 15         | 18     | 6.291   | 1.829   | 18       | 15     | -6.249   | -1.742  | 0.043         | 0.087  |
| 18         | 19     | 3.049   | 0.842   | 19       | 18     | -3.042   | -0.830  | 0.006         | 0.012  |
| 19         | 20     | -6.457  | -2.570  | 20       | 19     | 6.473    | 2.601   | 0.016         | 0.031  |
| 10         | 20     | 8.749   | 3.471   | 20       | 10     | -8.673   | -3.301  | 0.076         | 0.170  |
| 10         | 17     | 5.067   | 4.367   | 17       | 10     | -5.054   | -4.332  | 0.013         | 0.035  |
| 10         | 21     | 18.285  | 11.764  | 21       | 10     | -18.134  | -11.439 | 0.151         | 0.325  |
| 10         | 22     | 5.780   | 3.107   | 22       | 10     | -5.751   | -3.048  | 0.029         | 0.059  |
| 21         | 23     | 0.635   | 0.239   | 23       | 21     | -0.635   | -0.239  | 0.000         | 0.000  |
| 15         | 23     | 4.449   | 2.593   | 23       | 15     | -4.424   | -2.544  | 0.025         | 0.050  |
| 22         | 24     | 5.751   | 3.048   | 24       | 22     | -5.706   | -2.977  | 0.045         | 0.071  |
| 23         | 24     | 1.859   | 1.183   | 24       | 23     | -1.853   | -1.171  | 0.006         | 0.012  |
| 24         | 25     | -1.141  | 1.748   | 25       | 24     | 1.149    | -1.734  | 0.008         | 0.066  |
| 25         | 26     | 3.544   | 2.366   | 26       | 25     | -3.500   | -2.300  | 0.044         | 0.066  |
| 25         | 27     | -4.694  | -0.632  | 27       | 25     | 4.717    | 0.677   | 0.024         | 0.045  |
| 28         | 27     | 17.997  | -3.529  | 27       | 28     | -17.997  | 4.791   | 0.000         | 1.262  |
| 27         | 29     | 6.189   | 1.667   | 29       | 27     | -6.103   | -1.505  | 0.086         | 0.162  |
| 27         | 30     | 7.091   | 1.661   | 30       | 27     | -6.930   | -1.358  | 0.161         | 0.303  |
| 29         | 30     | 3.703   | 0.605   | 30       | 29     | -3.670   | -0.542  | 0.033         | 0.063  |
| 8          | 28     | -0.613  | -0.241  | 28       | 8      | 0.614    | 0.242   | 0.007         | 0.001  |
| 6          | 28     | 18.670  | -3.094  | 28       | 6      | -18.611  | 3.304   | 0.059         | 0.209  |
| Total loss |        |         |         |          |        |          |         | <b>17.528</b> | 68.888 |

Table D- 2: Newton-Raphson load flow analysis of IEEE 30-bus system without IPFC

| Bus No | V pu   | Angle Degree | Injection |         | Generation |         | Load    |         |
|--------|--------|--------------|-----------|---------|------------|---------|---------|---------|
|        |        |              | MW        | MVar    | MW         | Mvar    | MW      | MVar    |
| 1      | 1.0600 | 0.0000       | 260.927   | -17.118 | 260.927    | -17.118 | 0.000   | 0.000   |
| 2      | 1.0430 | -5.3474      | 18.300    | 35.065  | 40.000     | 47.765  | 21.700  | 12.700  |
| 3      | 1.0217 | -7.5448      | -2.400    | -1.200  | 0.000      | 0.000   | 2.400   | 1.200   |
| 4      | 1.0129 | -9.2989      | -7.600    | -1.600  | 0.000      | 0.000   | 7.600   | 1.600   |
| 5      | 1.0100 | -14.1542     | -94.200   | 16.965  | -0.000     | 35.965  | 94.200  | 19.000  |
| 6      | 1.0121 | -11.0880     | 0.000     | 0.000   | 0.000      | 0.000   | 0.000   | 0.000   |
| 7      | 1.0035 | -12.8733     | -22.800   | -10.900 | 0.000      | 0.000   | 22.800  | 10.900  |
| 8      | 1.0100 | -11.8039     | -30.000   | 0.691   | 0.000      | 30.691  | 30.000  | 30.000  |
| 9      | 1.0507 | -14.1363     | -0.000    | 0.000   | -0.000     | 0.000   | 0.000   | 0.000   |
| 10     | 1.0438 | -15.7341     | -5.800    | 17.000  | 0.000      | 19.000  | 5.800   | 2.000   |
| 11     | 1.0820 | -14.1363     | 0.000     | 16.269  | 0.000      | 16.269  | 0.000   | 0.000   |
| 12     | 1.0576 | -14.9415     | -11.200   | -7.500  | 0.000      | 0.000   | 11.200  | 7.500   |
| 13     | 1.0710 | -14.9415     | -0.000    | 10.247  | -0.000     | 10.247  | 0.000   | 0.000   |
| 14     | 1.0429 | -15.8243     | -6.200    | -1.600  | 0.000      | 0.000   | 6.200   | 1.600   |
| 15     | 1.0384 | -15.9100     | -8.200    | -2.500  | 0.000      | 0.000   | 8.200   | 2.500   |
| 16     | 1.0445 | -15.5487     | -3.500    | -1.800  | 0.000      | 0.000   | 3.500   | 1.800   |
| 17     | 1.0387 | -15.8856     | -9.000    | -5.800  | 0.000      | 0.000   | 9.000   | 5.800   |
| 18     | 1.0282 | -16.5424     | -3.200    | -0.900  | 0.000      | 0.000   | 3.200   | 0.900   |
| 19     | 1.0252 | -16.7272     | -9.500    | -3.400  | 0.000      | 0.000   | 9.500   | 3.400   |
| 20     | 1.0291 | -16.5362     | -2.200    | -0.700  | 0.000      | 0.000   | 2.200   | 0.700   |
| 21     | 1.0293 | -16.2462     | -17.500   | -11.200 | 0.000      | 0.000   | 17.500  | 11.200  |
| 22     | 1.0353 | -16.0737     | 0.000     | 0.000   | 0.000      | 0.000   | 0.000   | 0.000   |
| 23     | 1.0291 | -16.2528     | -3.200    | -1.600  | 0.000      | 0.000   | 3.200   | 1.600   |
| 24     | 1.0237 | -16.4408     | -8.700    | -2.400  | 0.000      | 4.300   | 8.700   | 6.700   |
| 25     | 1.0202 | -16.0539     | 0.000     | 0.000   | 0.000      | 0.000   | 0.000   | 0.000   |
| 26     | 1.0025 | -16.4712     | -3.500    | -2.300  | 0.000      | 0.000   | 3.500   | 2.300   |
| 27     | 1.0265 | -15.5557     | 0.000     | 0.000   | 0.000      | 0.000   | 0.000   | 0.000   |
| 28     | 1.0109 | -11.7436     | 0.000     | 0.000   | 0.000      | 0.000   | 0.000   | 0.000   |
| 29     | 1.0067 | -16.7777     | -2.400    | -0.900  | 0.000      | 0.000   | 2.400   | 0.900   |
| 30     | 0.9953 | -17.6546     | -10.600   | -1.900  | -0.000     | -0.000  | 10.600  | 1.900   |
| Total  |        |              | 17.528    | 20.921  | 300.928    | 147.121 | 283.400 | 126.200 |

Table D- 3: Line flows and line losses of IEEE 30-bus system with IPFC

| From Bus   | To Bus | P MW    | Q MVar  | From Bus | To Bus | P MW     | Q MVar  | Line Loss    |        |
|------------|--------|---------|---------|----------|--------|----------|---------|--------------|--------|
|            |        |         |         |          |        |          |         | MW           | Mvar   |
| 1          | 2      | 50.661  | 12.195  | 2        | 1      | -50.151  | -10.666 | <b>0.510</b> | 1.528  |
| 1          | 3      | 12.013  | 14.576  | 3        | 1      | -11.855  | -13.999 | <b>0.158</b> | 0.577  |
| 2          | 4      | 22.919  | 8.735   | 4        | 2      | -22.603  | -7.775  | 0.315        | 0.961  |
| 3          | 4      | 125.478 | -5.471  | 4        | 3      | -123.514 | 11.113  | 1.965        | 5.641  |
| 2          | 5      | 75.214  | 4.649   | 5        | 2      | -72.750  | 5.703   | 2.464        | 10.352 |
| 2          | 6      | 44.669  | 4.191   | 6        | 2      | -43.594  | -0.929  | 1.075        | 3.262  |
| 4          | 6      | 92.857  | -17.888 | 6        | 4      | -91.827  | 21.471  | 1.030        | 3.583  |
| 5          | 7      | -21.450 | 13.773  | 7        | 5      | 21.743   | -13.034 | 0.293        | 0.739  |
| 6          | 7      | 45.072  | -2.394  | 7        | 6      | 21.743   | 4.020   | 0.529        | 1.626  |
| 6          | 8      | 29.432  | 0.640   | 8        | 6      | -29.331  | -0.286  | 0.101        | 0.354  |
| 6          | 9      | 26.977  | -18.199 | 9        | 6      | -26.977  | 20.295  | 0.000        | 2.096  |
| 6          | 10     | 15.417  | -5.215  | 10       | 6      | -15.417  | 6.604   | 0.000        | 1.389  |
| 9          | 11     | 0.000   | -15.373 | 11       | 9      | -0.000   | 15.818  | -0.000       | 0.445  |
| 9          | 10     | 26.977  | 7.037   | 10       | 9      | -26.977  | -6.264  | 0.000        | 0.773  |
| 4          | 12     | 45.660  | -15.846 | 12       | 4      | -45.660  | 21.240  | -0.000       | 5.394  |
| 12         | 13     | 0.000   | -8.997  | 13       | 12     | -0.000   | 9.098   | 0.000        | 0.101  |
| 12         | 14     | 7.971   | 2.325   | 14       | 12     | -7.895   | -2.168  | 0.076        | 0.157  |
| 12         | 15     | 18.382  | 6.576   | 15       | 12     | -18.157  | -6.133  | 0.225        | 0.443  |
| 12         | 16     | 8.107   | 3.325   | 16       | 12     | -8.043   | -3.189  | 0.065        | 0.136  |
| 14         | 15     | 1.695   | 0.568   | 15       | 14     | -1.689   | -0.562  | 0.006        | 0.006  |
| 16         | 17     | 4.543   | 1.389   | 17       | 16     | -4.526   | -1.349  | 0.017        | 0.040  |
| 15         | 18     | 6.568   | 1.766   | 18       | 15     | -6.522   | -1.672  | 0.046        | 0.093  |
| 18         | 19     | 3.322   | 0.772   | 19       | 18     | -3.315   | -0.758  | 0.007        | 0.014  |
| 19         | 20     | -6.185  | -2.642  | 20       | 19     | 6.200    | 2.671   | 0.015        | 0.029  |
| 10         | 20     | 8.472   | 3.532   | 20       | 10     | -8.400   | -3.371  | 0.072        | 0.161  |
| 10         | 17     | 4.486   | 4.482   | 17       | 10     | -4.474   | -4.451  | 0.012        | 0.031  |
| 10         | 21     | 17.838  | 11.852  | 21       | 10     | -17.692  | -11.538 | 0.146        | 0.315  |
| 10         | 22     | 5.797   | 3.073   | 22       | 10     | -5.768   | -3.013  | 0.029        | 0.059  |
| 21         | 23     | 0.192   | 0.338   | 23       | 21     | -0.192   | -0.337  | 0.000        | 0.000  |
| 15         | 23     | 5.078   | 2.429   | 23       | 15     | -5.049   | -2.369  | 0.029        | 0.059  |
| 22         | 24     | 5.768   | 3.013   | 24       | 22     | -5.723   | -2.943  | 0.045        | 0.071  |
| 23         | 24     | 2.041   | 1.107   | 24       | 23     | -2.034   | -1.093  | 0.007        | 0.014  |
| 24         | 25     | -0.943  | 1.636   | 25       | 24     | 0.950    | -1.625  | 0.006        | 0.011  |
| 25         | 26     | 3.544   | 2.366   | 26       | 25     | -3.500   | -2.300  | 0.044        | 0.066  |
| 25         | 27     | -4.494  | -0.741  | 27       | 25     | 4.516    | 0.783   | 0.022        | 0.042  |
| 28         | 27     | 17.795  | -3.472  | 27       | 28     | -17.795  | 4.703   | -0.000       | 1.230  |
| 27         | 29     | 6.189   | 1.667   | 29       | 27     | -6.103   | -1.505  | 0.086        | 0.162  |
| 27         | 30     | 7.091   | 1.660   | 30       | 27     | -6.930   | -1.358  | 0.161        | 0.303  |
| 29         | 30     | 3.703   | 0.605   | 30       | 29     | -3.670   | -0.542  | 0.033        | 0.063  |
| 8          | 28     | -0.669  | -0.844  | 28       | 8      | 0.669    | 0.847   | 0.001        | 0.002  |
| 6          | 28     | 18.522  | -2.439  | 28       | 6      | -18.465  | 2.642   | 0.057        | 0.203  |
| Total loss |        |         |         |          |        |          |         | <b>9.648</b> | 42.532 |

Table D- 4: Newton-Raphson load flow analysis of IEEE 30-bus system IPFC

| Bus No | V pu   | Angle Degree | Injection |         | Generation |         | Load    |         |
|--------|--------|--------------|-----------|---------|------------|---------|---------|---------|
|        |        |              | MW        | MVar    | MW         | Mvar    | MW      | MVar    |
| 1      | 1.0600 | 0.0000       | 62.674    | 21.512  | 62.674     | 21.512  | 0.000   | 0.000   |
| 2      | 1.0430 | -1.5273      | 92.650    | -2.272  | 114.350    | 10.428  | 21.700  | 12.700  |
| 3      | 1.0295 | -0.7657      | 113.623   | -22.078 | 116.023    | -20.878 | 2.400   | 1.200   |
| 4      | 1.0165 | -3.4100      | -7.600    | -1.600  | 0.000      | -0.000  | 7.600   | 1.600   |
| 5      | 1.0100 | -9.5463      | -94.200   | 16.303  | -0.000     | 35.303  | 94.200  | 19.000  |
| 6      | 1.0137 | -5.6667      | 0.000     | 0.000   | 0.000      | 0.000   | 0.000   | 0.000   |
| 7      | 1.0044 | -7.7829      | -22.800   | -10.900 | 0.000      | 0.000   | 22.800  | 10.900  |
| 8      | 1.0100 | -6.3542      | -30.000   | -3.773  | 0.000      | 26.227  | 30.000  | 30.000  |
| 9      | 1.0516 | -8.6176      | -0.000    | 0.000   | -0.000     | 0.000   | 0.000   | 0.000   |
| 10     | 1.0446 | -10.1655     | -5.800    | 17.000  | 0.000      | 19.000  | 5.800   | 2.000   |
| 11     | 1.0820 | -8.6176      | -0.000    | 15.818  | -0.000     | 15.818  | 0.000   | 0.000   |
| 12     | 1.0591 | -9.2180      | -11.200   | -7.500  | 0.000      | 0.000   | 11.200  | 7.500   |
| 13     | 1.0710 | 9.2180       | 0.000     | 9.098   | 0.000      | 9.098   | 0.000   | 0.000   |
| 14     | 1.0444 | -10.1263     | -6.200    | -1.600  | 0.000      | 0.000   | 6.200   | 1.600   |
| 15     | 1.0397 | -10.2388     | -8.200    | -2.500  | 0.000      | 0.000   | 8.200   | 2.500   |
| 16     | 1.0457 | -9.8888      | -3.500    | -1.800  | 0.000      | 0.000   | 3.500   | 1.800   |
| 17     | 1.0396 | -10.2889     | -9.000    | -5.800  | 0.000      | 0.000   | 9.000   | 5.800   |
| 18     | 1.0293 | -10.9057     | -3.200    | -0.900  | 0.000      | 0.000   | 3.200   | 0.900   |
| 19     | 1.0262 | -11.1117     | -9.500    | -3.400  | 0.000      | 0.000   | 9.500   | 3.400   |
| 20     | 1.0300 | -10.9324     | -2.200    | -0.700  | 0.000      | 0.000   | 2.200   | 0.700   |
| 21     | 1.0302 | -10.6573     | -17.500   | -11.200 | 0.000      | 0.000   | 17.500  | 11.200  |
| 22     | 1.0362 | -10.5072     | 0.000     | 0.000   | 0.000      | 0.000   | 0.000   | 0.000   |
| 23     | 1.0301 | -10.6576     | -3.200    | -1.600  | 0.000      | 0.000   | 3.200   | 1.600   |
| 24     | 1.0246 | -10.8774     | -8.700    | -2.400  | 0.000      | 4.300   | 8.700   | 6.700   |
| 25     | 1.0211 | -10.5385     | 0.000     | 0.000   | 0.000      | 0.000   | 0.000   | 0.000   |
| 26     | 1.0035 | -10.9550     | -3.500    | -2.300  | 0.000      | 0.000   | 3.500   | 2.300   |
| 27     | 1.0275 | -10.0705     | 0.000     | 0.000   | 0.000      | 0.000   | 0.000   | 0.000   |
| 28     | 1.0121 | -6.3093      | 0.000     | 0.000   | 0.000      | 0.000   | 0.000   | 0.000   |
| 29     | 1.0077 | -11.2902     | -2.400    | -0.900  | 0.000      | 0.000   | 2.400   | 0.900   |
| 30     | 0.9963 | -12.1654     | -10.600   | -1.900  | -0.000     | -0.000  | 10.600  | 1.900   |
| Total  |        |              | 9.648     | -5.392  | 293.048    | 120.808 | 283.400 | 126.200 |

Table D- 5: Line flows and line losses of IEEE 30-bus system with IPFC and PSO

| From Bus   | To Bus | P MW    | Q MVar  | From Bus | To Bus | P MW     | Q MVar  | Line Loss    |         |
|------------|--------|---------|---------|----------|--------|----------|---------|--------------|---------|
|            |        |         |         |          |        |          |         | MW           | Mvar    |
| 1          | 2      | 2.024   | 12.230  | 2        | 1      | -1.998   | -12.151 | <b>0.026</b> | 0.079   |
| 1          | 3      | 3.584   | 4.155   | 3        | 1      | -3.572   | -4.111  | <b>0.012</b> | 0.044   |
| 2          | 4      | 28.021  | 5.102   | 4        | 2      | -27.604  | -3.831  | 0.417        | 1.271   |
| 3          | 4      | 114.947 | 22.123  | 4        | 3      | -113.313 | -17.431 | 1.634        | 4.692   |
| 2          | 5      | 76.547  | 9.774   | 5        | 2      | -74.012  | 0.876   | 2.535        | 10.650  |
| 2          | 6      | 48.535  | 5.651   | 6        | 2      | -47.284  | -1.855  | 1.251        | 3.796   |
| 4          | 6      | 88.274  | 2.459   | 6        | 4      | -87.400  | 0.583   | 0.874        | 3.041   |
| 5          | 7      | -20.188 | 10.024  | 7        | 5      | 20.417   | -9.446  | 0.229        | 0.578   |
| 6          | 7      | 43.708  | 1.061   | 7        | 6      | 0.446    | 0.446   | 1.507        | 1.507   |
| 6          | 8      | 29.421  | 15.413  | 8        | 6      | -29.294  | -14.968 | 0.127        | 0.446   |
| 6          | 9      | 27.269  | -17.205 | 9        | 6      | -27.269  | 19.239  | 0.000        | 2.034   |
| 6          | 10     | 27.269  | -4.985  | 10       | 6      | -15.605  | 6.375   | 0.000        | 1.390   |
| 9          | 11     | -0.000  | -13.45  | 11       | 9      | 0.000    | 13.795  | 0.000        | 0.338   |
| 9          | 10     | 27.269  | 6.266   | 10       | 9      | -27.269  | -5.493  | 0.000        | 0.773   |
| 4          | 12     | 27.269  | 12.00   | 12       | 4      | -45.042  | 17.288  | 0.000        | 4.904   |
| 12         | 13     | 0.000   | -5.219  | 13       | 12     | -0.000   | 5.252   | 0.000        | 0.034   |
| 12         | 14     | 7.904   | 2.394   | 14       | 12     | -7.830   | -2.240  | 0.074        | -17.858 |
| 12         | 15     | 18.076  | 6.802   | 15       | 12     | -17.858  | -6.372  | 0.218        | 0.430   |
| 12         | 16     | 7.863   | 3.508   | 16       | 12     | -7.801   | -3.378  | 0.062        | 0.130   |
| 14         | 15     | 1.630   | 0.640   | 15       | 14     | -1.624   | -0.635  | 0.006        | 0.006   |
| 16         | 17     | 4.301   | 1.578   | 17       | 16     | -4.285   | -1.541  | 0.016        | 0.037   |
| 15         | 18     | 6.458   | 1.861   | 18       | 15     | -6.414   | -1.771  | 0.044        | 0.090   |
| 18         | 19     | 3.214   | 0.871   | 19       | 18     | -3.207   | -0.857  | 0.007        | 0.013   |
| 19         | 20     | -6.293  | -2.543  | 20       | 19     | 6.308    | 2.572   | 0.015        | 0.029   |
| 10         | 20     | 8.580   | 3.434   | 20       | 10     | -8.508   | -3.272  | 0.073        | 0.162   |
| 10         | 17     | 8.580   | 4.290   | 17       | 10     | -4.715   | -4.259  | 0.012        | 0.031   |
| 10         | 21     | 18.000  | 11.673  | 21       | 10     | -17.854  | -11.360 | 0.145        | 0.031   |
| 10         | 22     | 5.767   | 3.056   | 22       | 10     | -17.854  | -11.360 | 0.145        | 0.313   |
| 21         | 23     | 0.354   | 0.160   | 23       | 21     | 0.000    | 0.000   | 0.000        | 0.000   |
| 15         | 23     | 4.823   | 2.646   | 23       | 15     | -4.796   | -2.590  | 0.028        | 0.056   |
| 22         | 24     | 5.739   | 2.998   | 24       | 22     | -5.695   | 0.044   | 0.044        | 0.069   |
| 23         | 24     | 5.739   | 1.150   | 24       | 23     | -1.943   | -1.137  | 0.006        | 0.013   |
| 24         | 25     | -1.062  | 1.666   | 25       | 24     | 1.069    | -1.654  | 0.007        | 0.012   |
| 25         | 26     | 3.544   | 2.366   | 26       | 25     | -3.500   | -2.300  | 0.044        | 0.066   |
| 25         | 27     | -4.613  | -0.711  | 27       | 25     | 4.635    | 0.755   | 0.023        | 0.043   |
| 28         | 27     | 17.912  | -3.587  | 27       | 28     | -17.912  | 4.824   | 0.000        | 1.237   |
| 27         | 29     | 6.188   | 1.664   | 29       | 27     | -6.103   | -1.504  | 0.085        | 0.160   |
| 27         | 30     | 7.089   | 1.657   | 30       | 27     | -6.930   | -1.358  | 0.159        | 0.300   |
| 29         | 30     | 3.703   | 0.604   | 30       | 29     | -3.670   | -0.542  | 0.033        | 0.062   |
| 8          | 28     | -0.706  | -3.218  | 28       | 8      | 0.713    | 3.239   | 0.007        | 0.021   |
| 6          | 28     | 18.682  | -0.163  | 28       | 6      | -18.625  | 0.364   | 0.057        | 0.201   |
| Total loss |        |         |         |          |        |          |         | <b>8.789</b> | 39.271  |



Table D- 6: Newton-Raphson load flow analysis of IEEE 30-bus system IPFC and  
PSO

| Bus<br>No | V<br>pu | Angle<br>Degree | Injection |         | Generation |         | Load    |         |
|-----------|---------|-----------------|-----------|---------|------------|---------|---------|---------|
|           |         |                 | MW        | MVar    | MW         | Mvar    | MW      | MVar    |
| 1         | 1.0600  | 0.0000          | 5.609     | 11.126  | 5.609      | 11.126  | 0.000   | 0.000   |
| 2         | 1.0530  | 0.0608          | 151.105   | -0.983  | 172.805    | 11.717  | 21.700  | 12.700  |
| 3         | 1.0520  | -0.2077         | 111.375   | 15.290  | 113.775    | 16.490  | 2.400   | 1.200   |
| 4         | 1.0303  | -2.3567         | -7.600    | -1.600  | 0.000      | 0.000   | 7.600   | 1.600   |
| 5         | 1.0100  | -7.8938         | -94.200   | 7.727   | -0.000     | 26.727  | 94.200  | 19.000  |
| 6         | 1.0198  | -4.3341         | 0.000     | 0.000   | 0.000      | 0.000   | 0.000   | 0.000   |
| 7         | 1.0081  | -6.3163         | -22.800   | -10.900 | 0.000      | 0.000   | 22.800  | 10.900  |
| 8         | 1.0100  | -4.9186         | -30.000   | -20.828 | -0.000     | 9.172   | 30.000  | 30.000  |
| 9         | 1.0555  | -7.2883         | -0.000    | 0.000   | -0.000     | 0.000   | 0.000   | 0.000   |
| 10        | 1.0493  | -8.8403         | -5.800    | 17.000  | 0.000      | 19.000  | 5.800   | 2.000   |
| 11        | 1.0820  | -7.2883         | 0.000     | 13.795  | 0.000      | 13.795  | 0.000   | 0.000   |
| 12        | 1.0641  | -7.9818         | -11.200   | -7.500  | 0.000      | 0.000   | 11.200  | 7.500   |
| 13        | 1.0710  | -7.9818         | 0.000     | 5.252   | 0.000      | 5.252   | 0.000   | 0.000   |
| 14        | 1.0494  | -8.8684         | -6.200    | -1.600  | 0.000      | 0.000   | 6.200   | 1.600   |
| 15        | 1.0447  | -8.9645         | -8.200    | -2.500  | 0.000      | 0.000   | 8.200   | 2.500   |
| 16        | 1.0507  | -8.6125         | -3.500    | -1.800  | 0.000      | 0.000   | 3.500   | 1.800   |
| 17        | 1.0444  | -8.9764         | -9.000    | -5.800  | 0.000      | 0.000   | 9.000   | 5.800   |
| 18        | 1.0342  | -9.6069         | -3.200    | -0.900  | 0.000      | 0.000   | 3.200   | 0.900   |
| 19        | 1.0312  | -9.8001         | -9.500    | -3.400  | 0.000      | 0.000   | 9.500   | 3.400   |
| 20        | 1.0349  | -9.6168         | -2.200    | -0.700  | 0.000      | 0.000   | 2.200   | 0.700   |
| 21        | 1.0351  | -9.3372         | -17.500   | -11.200 | 0.000      | 0.000   | 17.500  | 11.200  |
| 22        | 1.0410  | -9.1772         | 0.000     | 0.000   | 0.000      | 0.000   | 0.000   | 0.000   |
| 23        | 1.0350  | -9.3406         | -3.200    | -1.600  | 0.000      | 0.000   | 3.200   | 1.600   |
| 24        | 1.0295  | -9.5421         | -8.700    | -2.400  | 0.000      | 4.300   | 8.700   | 6.700   |
| 25        | 1.0262  | -9.1821         | 0.000     | 0.000   | 0.000      | 0.000   | 0.000   | 0.000   |
| 26        | 1.0086  | -9.5945         | -3.500    | -2.300  | 0.000      | 0.000   | 3.500   | 2.300   |
| 27        | 1.0325  | -8.7036         | 0.000     | 0.000   | 0.000      | 0.000   | 0.000   | 0.000   |
| 28        | 1.0168  | -4.9539         | 0.000     | 0.000   | 0.000      | 0.000   | 0.000   | 0.000   |
| 29        | 1.0129  | -9.9111         | -2.400    | -0.900  | 0.000      | 0.000   | 2.400   | 0.900   |
| 30        | 1.0015  | -10.7772        | -10.600   | -1.900  | 0.000      | 0.000   | 10.600  | 1.900   |
| Total     |         |                 | 8.789     | -8.620  | 292.189    | 117.580 | 283.400 | 126.200 |

Table D- 7: Line flows and line losses of IEEE 30-bus system with IPFC and GA

| From Bus   | To Bus | P MW    | Q MVar  | From Bus | To Bus | P MW     | Q MVar  | Line Loss    |        |
|------------|--------|---------|---------|----------|--------|----------|---------|--------------|--------|
|            |        |         |         |          |        |          |         | MW           | Mvar   |
| 1          | 2      | 2.015   | 12.233  | 2        | 1      | -1.989   | -12.154 | <b>0.026</b> | 0.079  |
| 1          | 3      | 3.572   | 4.159   | 3        | 1      | -3.560   | -4.115  | <b>0.012</b> | 0.044  |
| 2          | 4      | 28.015  | 5.104   | 4        | 2      | -27.598  | -3.833  | 0.417        | 1.270  |
| 3          | 4      | 114.959 | 22.119  | 4        | 3      | -113.324 | -17.425 | 1.635        | 4.693  |
| 2          | 5      | 76.545  | 9.774   | 5        | 2      | -74.011  | 0.875   | 2.535        | 10.649 |
| 2          | 6      | 48.531  | 5.652   | 6        | 2      | -47.281  | -1.856  | 1.251        | 3.796  |
| 4          | 6      | 88.280  | 2.456   | 6        | 4      | -87.405  | 0.586   | 0.874        | 3.042  |
| 5          | 7      | -20.189 | 10.025  | 7        | 5      | 20.419   | -9.447  | 0.229        | 0.578  |
| 6          | 7      | 43.709  | 1.060   | 7        | 6      | -43.219  | 0.447   | 0.491        | 1.507  |
| 6          | 8      | 29.421  | 15.413  | 8        | 6      | -29.294  | -14.967 | 0.127        | 0.446  |
| 6          | 9      | 27.269  | -17.205 | 9        | 6      | -27.269  | 19.239  | 0.000        | 2.034  |
| 6          | 10     | 15.605  | -4.985  | 10       | 6      | -15.605  | 6.375   | 0.000        | 1.390  |
| 9          | 11     | -0.000  | -13.457 | 11       | 9      | 0.000    | 13.795  | 0.000        | 0.338  |
| 9          | 10     | 27.269  | 6.266   | 10       | 9      | -27.269  | -5.493  | -0.000       | 0.773  |
| 4          | 12     | 45.043  | -12.384 | 12       | 4      | -45.043  | 17.288  | 0.000        | 4.905  |
| 12         | 13     | -0.000  | -5.219  | 13       | 12     | 0.000    | 5.253   | 0.000        | 0.034  |
| 12         | 14     | 7.904   | 2.394   | 14       | 12     | -7.830   | -2.240  | 0.074        | 0.154  |
| 12         | 15     | 18.076  | 6.802   | 15       | 12     | -17.858  | -6.372  | 0.218        | 0.430  |
| 12         | 16     | 7.863   | 3.508   | 16       | 12     | -7.801   | -3.378  | 0.062        | 0.130  |
| 14         | 15     | 1.630   | 0.640   | 15       | 14     | -1.624   | -0.635  | 0.006        | 0.006  |
| 16         | 17     | 4.301   | 1.578   | 17       | 16     | -4.285   | -1.541  | 0.016        | 0.037  |
| 15         | 18     | 6.458   | 1.861   | 18       | 15     | -6.414   | -1.771  | 0.044        | 0.090  |
| 18         | 19     | 3.214   | 0.871   | 19       | 18     | -3.207   | -0.857  | 0.007        | 0.013  |
| 19         | 20     | -6.293  | -2.543  | 20       | 19     | 6.308    | 2.572   | 0.015        | 0.029  |
| 10         | 20     | 8.580   | 3.434   | 20       | 10     | -8.508   | -3.272  | 0.073        | 0.162  |
| 10         | 17     | 4.727   | 4.290   | 17       | 10     | -4.715   | -4.259  | 0.012        | 0.031  |
| 10         | 21     | 17.999  | 11.673  | 21       | 10     | -17.854  | -11.360 | 0.145        | 0.313  |
| 10         | 22     | 5.767   | 3.056   | 22       | 10     | -5.739   | -2.998  | 0.028        | 0.058  |
| 21         | 23     | 0.354   | 0.160   | 23       | 21     | -0.354   | -0.160  | 0.000        | 0.000  |
| 15         | 23     | 4.824   | 2.646   | 23       | 15     | -4.796   | -2.590  | 0.028        | 0.056  |
| 22         | 24     | 5.739   | 2.998   | 24       | 22     | -5.695   | -2.929  | 0.044        | 0.069  |
| 23         | 24     | 1.950   | 1.150   | 24       | 23     | -1.943   | -1.137  | 0.006        | 0.013  |
| 24         | 25     | -1.062  | 1.666   | 25       | 24     | 1.069    | -1.654  | 0.007        | 0.012  |
| 25         | 26     | 3.544   | 2.366   | 26       | 25     | -3.500   | -2.300  | 0.044        | 0.066  |
| 25         | 27     | -4.613  | -0.711  | 27       | 25     | 4.635    | 0.755   | 0.023        | 0.043  |
| 28         | 27     | 17.912  | -3.587  | 27       | 28     | -17.912  | 4.824   | 0.000        | 1.237  |
| 27         | 29     | 6.188   | 1.664   | 29       | 27     | -6.103   | -1.504  | 0.085        | 0.160  |
| 27         | 30     | 7.089   | 1.657   | 30       | 27     | -6.930   | -1.358  | 0.159        | 0.300  |
| 29         | 30     | 3.703   | 0.604   | 30       | 29     | -3.670   | -0.542  | 0.033        | 0.062  |
| 8          | 28     | -0.706  | -3.218  | 28       | 8      | 0.713    | 3.239   | 0.007        | 0.021  |
| 6          | 28     | 18.682  | -0.163  | 28       | 6      | -18.625  | 0.364   | 0.057        | 0.201  |
| Total loss |        |         |         |          |        |          |         | <b>8.789</b> | 39.271 |

Table D- 8: Newton-Raphson load flow analysis of IEEE 30-bus system IPFC and  
GA

| Bus<br>No | V<br>pu | Angle<br>Degree | Injection |         | Generation |         | Load    |         |
|-----------|---------|-----------------|-----------|---------|------------|---------|---------|---------|
|           |         |                 | MW        | MVar    | MW         | Mvar    | MW      | MVar    |
| 1         | 1.0600  | 0.0000          | 5.587     | 11.134  | 5.587      | 11.134  | 0.000   | 0.000   |
| 2         | 1.0530  | 0.0611          | 151.104   | -0.983  | 172.804    | 11.717  | 21.700  | 12.700  |
| 3         | 1.0520  | -0.2066         | 111.398   | 15.281  | 113.798    | 16.481  | 2.400   | 1.200   |
| 4         | 1.0303  | -2.3559         | -7.600    | -1.600  | 0.000      | 0.000   | 7.600   | 1.600   |
| 5         | 1.0100  | -7.8933         | -94.200   | 7.727   | -0.000     | 26.727  | 94.200  | 19.000  |
| 6         | 1.0198  | -4.3333         | 0.000     | 0.000   | 0.000      | 0.000   | 0.000   | 0.000   |
| 7         | 1.0081  | -6.3156         | -22.800   | -10.900 | 0.000      | 0.000   | 22.800  | 10.900  |
| 8         | 1.0100  | -4.9179         | -30.000   | -20.827 | -0.000     | 9.173   | 30.000  | 30.000  |
| 9         | 1.0555  | -7.2876         | 0.000     | 0.000   | 0.000      | 0.000   | 0.000   | 0.000   |
| 10        | 1.0493  | -8.8395         | -5.800    | 17.000  | 0.000      | 19.000  | 5.800   | 2.000   |
| 11        | 1.0820  | -7.2876         | 0.000     | 13.795  | 0.000      | 13.795  | 0.000   | 0.000   |
| 12        | 1.0641  | -7.9810         | -11.200   | -7.500  | 0.000      | 0.000   | 11.200  | 7.500   |
| 13        | 1.0710  | -7.9810         | 0.000     | 5.253   | 0.000      | 5.253   | 0.000   | 0.000   |
| 14        | 1.0494  | -8.8676         | -6.200    | -1.600  | 0.000      | 0.000   | 6.200   | 1.600   |
| 15        | 1.0447  | -8.9638         | -8.200    | -2.500  | 0.000      | 0.000   | 8.200   | 2.500   |
| 16        | 1.0507  | -8.6117         | -3.500    | -1.800  | 0.000      | 0.000   | 3.500   | 1.800   |
| 17        | 1.0444  | -8.9757         | -9.000    | -5.800  | 0.000      | 0.000   | 9.000   | 5.800   |
| 18        | 1.0342  | -9.6062         | -3.200    | -0.900  | 0.000      | 0.000   | 3.200   | 0.900   |
| 19        | 1.0312  | -9.7994         | -9.500    | -3.400  | 0.000      | 0.000   | 9.500   | 3.400   |
| 20        | 1.0349  | -9.6160         | -2.200    | -0.700  | 0.000      | 0.000   | 2.200   | 0.700   |
| 21        | 1.0351  | -9.3364         | -17.500   | -11.200 | 0.000      | 0.000   | 17.500  | 11.200  |
| 22        | 1.0410  | -9.1764         | 0.000     | 0.000   | 0.000      | 0.000   | 0.000   | 0.000   |
| 23        | 1.0350  | -9.3399         | -3.200    | -1.600  | 0.000      | 0.000   | 3.200   | 1.600   |
| 24        | 1.0295  | -9.5413         | -8.700    | -2.400  | 0.000      | 4.300   | 8.700   | 6.700   |
| 25        | 1.0262  | -9.1814         | 0.000     | 0.000   | 0.000      | 0.000   | 0.000   | 0.000   |
| 26        | 1.0086  | -9.5937         | -3.500    | -2.300  | 0.000      | 0.000   | 3.500   | 0.000   |
| 27        | 1.0325  | -8.7029         | 0.000     | 0.000   | 0.000      | 0.000   | 0.000   | 0.000   |
| 28        | 1.0168  | -4.9532         | 0.000     | 0.000   | 0.000      | 0.000   | 0.000   | 0.000   |
| 29        | 1.0129  | -9.9103         | -2.400    | -0.900  | 0.000      | 0.000   | 2.400   | 0.900   |
| 30        | 1.0015  | -10.7765        | -10.600   | -1.900  | 0.000      | 0.000   | 10.600  | 1.900   |
| Total     |         |                 | 8.789     | -8.620  | 292.189    | 117.580 | 283.400 | 126.200 |

Table D- 9: Line flows and line losses of IEEE 30-bus system with IPFC and SA

| From Bus   | To Bus | P MW    | Q MVar  | From Bus | To Bus | P MW     | Q MVar  | Line Loss    |        |
|------------|--------|---------|---------|----------|--------|----------|---------|--------------|--------|
|            |        |         |         |          |        |          |         | MW           | Mvar   |
| 1          | 2      | 2.278   | 12.144  | 2        | 1      | -2.252   | -12.066 | <b>0.026</b> | 0.078  |
| 1          | 3      | 3.347   | 5.542   | 3        | 1      | -3.330   | -5.480  | <b>0.017</b> | 0.062  |
| 2          | 4      | 27.896  | 5.799   | 4        | 2      | -27.479  | -4.528  | 0.417        | 1.272  |
| 3          | 4      | 115.167 | 19.334  | 4        | 3      | -113.534 | -14.645 | 1.633        | 4.688  |
| 2          | 5      | 76.532  | 9.775   | 5        | 2      | -73.998  | 0.870   | 2.534        | 10.646 |
| 2          | 6      | 48.454  | 5.915   | 6        | 2      | -47.205  | -2.126  | 1.249        | 3.789  |
| 4          | 6      | 88.343  | 0.720   | 6        | 4      | -87.466  | 2.331   | 0.877        | 3.050  |
| 5          | 7      | -20.202 | 10.250  | 7        | 5      | 20.433   | -9.666  | 0.231        | 0.584  |
| 6          | 7      | 43.725  | 0.844   | 7        | 6      | -43.233  | 0.665   | 0.491        | 1.509  |
| 6          | 8      | 29.421  | 14.393  | 8        | 6      | -29.297  | -13.959 | 0.124        | 0.434  |
| 6          | 9      | 27.257  | -17.269 | 9        | 6      | -27.257  | 19.308  | 0.000        | 2.038  |
| 6          | 10     | 15.596  | -4.997  | 10       | 6      | -15.596  | 6.388   | 0.000        | 1.391  |
| 9          | 11     | 0.000   | -13.593 | 11       | 9      | -0.000   | 13.938  | 0.000        | 0.345  |
| 9          | 10     | 27.257  | 6.327   | 10       | 9      | -27.257  | -5.554  | 0.000        | 0.774  |
| 4          | 12     | 45.069  | -12.670 | 12       | 4      | -45.069  | 17.606  | 0.000        | 4.937  |
| 12         | 13     | -0.000  | -5.516  | 13       | 12     | 0.000    | 5.554   | 0.000        | 0.038  |
| 12         | 14     | 7.906   | 2.389   | 14       | 12     | -7.832   | -2.234  | 0.074        | 0.154  |
| 12         | 15     | 18.089  | 6.780   | 15       | 12     | -17.871  | -6.350  | 0.218        | 0.430  |
| 12         | 16     | 7.874   | 3.491   | 16       | 12     | -7.812   | -3.360  | 0.062        | 0.130  |
| 14         | 15     | 1.632   | 0.634   | 15       | 14     | -1.626   | -0.629  | 0.006        | 0.006  |
| 16         | 17     | 4.312   | 1.560   | 17       | 16     | -4.296   | -1.524  | 0.016        | 0.037  |
| 15         | 18     | 6.463   | 1.852   | 18       | 15     | -6.418   | -1.762  | 0.044        | 0.091  |
| 18         | 19     | 3.218   | 0.862   | 19       | 18     | -3.212   | -0.848  | 0.007        | 0.013  |
| 19         | 20     | -6.288  | -2.552  | 20       | 19     | 6.303    | 2.581   | 0.015        | 0.029  |
| 10         | 20     | 8.576   | 3.443   | 20       | 10     | -8.503   | -3.281  | 0.073        | 0.162  |
| 10         | 17     | 4.716   | 4.308   | 17       | 10     | -4.704   | -4.276  | 0.012        | 0.031  |
| 10         | 21     | 17.993  | 11.689  | 21       | 10     | -17.847  | -11.376 | 0.146        | 0.313  |
| 10         | 22     | 5.769   | 3.058   | 22       | 10     | -5.741   | -3.000  | 0.028        | 0.058  |
| 21         | 23     | 0.347   | 0.176   | 23       | 21     | -0.347   | -0.176  | 0.000        | 0.000  |
| 15         | 23     | 4.834   | 2.626   | 23       | 15     | -4.806   | -2.570  | 0.028        | 0.056  |
| 22         | 24     | 5.741   | 3.000   | 24       | 22     | -5.696   | -2.930  | 0.045        | 0.069  |
| 23         | 24     | 1.954   | 1.146   | 24       | 23     | -1.947   | -1.133  | 0.006        | 0.013  |
| 24         | 25     | -1.056  | 1.663   | 25       | 24     | 1.063    | -1.651  | 0.007        | 0.012  |
| 25         | 26     | 3.544   | 2.366   | 26       | 25     | -3.500   | -2.300  | 0.044        | 0.066  |
| 25         | 27     | -4.607  | -0.714  | 27       | 25     | 4.630    | 0.757   | 0.023        | 0.043  |
| 28         | 27     | 17.907  | -3.578  | 27       | 28     | -17.907  | 4.815   | 0.000        | 1.237  |
| 27         | 29     | 6.188   | 1.665   | 29       | 27     | -6.103   | -1.504  | 0.085        | 0.160  |
| 27         | 30     | 7.089   | 1.658   | 30       | 27     | -6.930   | -1.358  | 0.159        | 0.300  |
| 29         | 30     | 3.703   | 0.604   | 30       | 29     | -3.670   | -0.542  | 0.033        | 0.062  |
| 8          | 28     | -0.703  | -3.055  | 28       | 8      | 0.709    | 3.074   | 0.006        | 0.019  |
| 6          | 28     | 18.673  | -0.319  | 28       | 6      | -18.616  | 0.520   | 0.057        | 0.201  |
| Total loss |        |         |         |          |        |          |         | <b>8.792</b> | 39.327 |

Table D- 10: Newton-Raphson load flow analysis of IEEE 30-bus system IPFC and  
SA

| Bus<br>No | V<br>pu | Angle<br>Degree | Injection |         | Generation |         | Load    |         |
|-----------|---------|-----------------|-----------|---------|------------|---------|---------|---------|
|           |         |                 | MW        | MVar    | MW         | Mvar    | MW      | MVar    |
| 1         | 1.0600  | 0.0000          | 5.625     | 12.428  | 5.625      | 12.428  | 0.000   | 0.000   |
| 2         | 1.0530  | 0.0524          | 150.630   | 0.065   | 172.330    | 12.765  | 21.700  | 12.700  |
| 3         | 1.0499  | -0.1557         | 111.837   | 11.142  | 114.237    | 12.342  | 2.400   | 1.200   |
| 4         | 1.0292  | -2.3352         | -7.600    | -1.600  | 0.000      | 0.000   | 7.600   | 1.600   |
| 5         | 1.0100  | -7.9005         | -94.200   | 7.948   | 0.000      | 26.948  | 94.200  | 19.000  |
| 6         | 1.0193  | -4.3283         | 0.000     | 0.000   | 0.000      | 0.000   | 0.000   | 0.000   |
| 7         | 1.0078  | -6.3158         | -22.800   | -10.900 | 0.000      | 0.000   | 22.800  | 10.900  |
| 8         | 1.0100  | -4.9199         | -30.000   | -19.655 | -0.000     | 10.345  | 30.000  | 30.000  |
| 9         | 1.0552  | -7.2832         | -0.000    | 0.000   | -0.000     | 0.000   | 0.000   | 0.000   |
| 10        | 1.0490  | -8.8354         | -5.800    | 17.000  | 0.000      | 19.000  | 5.800   | 2.000   |
| 11        | 1.0820  | -7.2832         | -0.000    | 13.938  | -0.000     | 13.938  | 0.000   | 0.000   |
| 12        | 1.0637  | -7.9717         | -11.200   | -7.500  | 0.000      | 0.000   | 11.200  | 7.500   |
| 13        | 1.0710  | -7.9717         | 0.000     | 5.554   | 0.000      | 5.554   | 0.000   | 0.000   |
| 14        | 1.0490  | -8.8597         | -6.200    | -1.600  | 0.000      | 0.000   | 6.200   | 1.600   |
| 15        | 1.0443  | -8.9568         | -8.200    | -2.500  | 0.000      | 0.000   | 8.200   | 2.500   |
| 16        | 1.0503  | -8.6048         | -3.500    | -1.800  | 0.000      | 0.000   | 3.500   | 1.800   |
| 17        | 1.0441  | -8.9709         | -9.000    | -5.800  | 0.000      | 0.000   | 9.000   | 5.800   |
| 18        | 1.0339  | -9.6007         | -3.200    | -0.900  | 0.000      | 0.000   | 3.200   | 0.900   |
| 19        | 1.0308  | -9.7947         | -9.500    | -3.400  | 0.000      | 0.000   | 9.500   | 3.400   |
| 20        | 1.0346  | -9.6115         | -2.200    | -0.700  | 0.000      | 0.000   | 2.200   | 0.700   |
| 21        | 1.0347  | -9.3321         | -17.500   | -11.200 | 0.000      | 0.000   | 17.500  | 11.200  |
| 22        | 1.0406  | -9.1726         | 0.000     | 0.000   | 0.000      | 0.000   | 0.000   | 0.000   |
| 23        | 1.0346  | -9.3354         | -3.200    | -1.600  | 0.000      | 0.000   | 3.200   | 1.600   |
| 24        | 1.0292  | -9.5378         | -8.700    | -2.400  | 0.000      | 4.300   | 8.700   | 6.700   |
| 25        | 1.0258  | -9.1789         | 0.000     | 0.000   | 0.000      | 0.000   | 0.000   | 0.000   |
| 26        | 1.0083  | -9.5915         | -3.500    | -2.300  | 0.000      | 0.000   | 3.500   | 2.300   |
| 27        | 1.0322  | -8.7008         | 0.000     | 0.000   | 0.000      | 0.000   | 0.000   | 0.000   |
| 28        | 1.0165  | -4.9498         | 0.000     | 0.000   | 0.000      | 0.000   | 0.000   | 0.000   |
| 29        | 1.0125  | -9.9091         | -2.400    | -0.900  | 0.000      | 0.000   | 2.400   | 0.900   |
| 30        | 1.0012  | -10.7759        | -10.600   | -1.900  | 0.000      | 0.000   | 10.600  | 1.900   |
| Total     |         |                 | 8.792     | -8.581  | 292.192    | 117.619 | 283.400 | 126.200 |

### *Appendix E: Particle Swarm Optimization MATLAB code*

```
%Simulates the movements of a swarm to minimize the transmission
line losses of IEEE 14-bus 30-bus system incoorporating with IPFC

%The swarm matrix is swarm(index, [location, velocity, best position,
best value], [x, y , z , h ,components or the value component])
tic
clc
clear all
format short

%===== initial Parameters of PSO =====

Iterations =100;           % Iterations number
SwarmSize = 35 ;          % Where S is the swarm size
W = 1.2 ;                 % W is the inertia weight is set as constant in
BPSO
C1 = 2.;                  % C1 and C2 are the acceleration constants
C2 = 2;
ValMat = [];
PBestx = [];
PBesty = [];
PBestz = [];
PBesth = [];
GBest =[];

% ---initial swarm position for the first transmission line system---

for index = 1 :SwarmSize
    swarm(index, 1, 1) = 0.1*rand;
    swarm(index, 1, 2) = 1.6*rand;
    swarm(index, 1, 3) = 0.1*rand;
    swarm(index, 1, 4) = 1.6*rand;
end

swarm(:, 4, 1)= 6.4;      % intial best value for the objective function
swarm(:, 4, 2) = 6.4;     % best value so far
swarm(:, 4, 3) = 6.4;     % intial best value for the objective
function
swarm(:, 4, 4) = 6.4;     % best value so far
swarm(:, 2, :) = 0;       % initial velocity

%=====Iterations=====

for iter = 1:Iterations

%-- evaluating position & quality-----

for i = 1 : SwarmSize
    swarm(i, 1, 1) = swarm(i, 1, 1) + swarm(i, 2, 1)/1.3; %update x
position
    swarm(i, 1, 2) = swarm(i, 1, 2) + swarm(i, 2, 2)/1.3; %update y
position
    swarm(i, 1, 3) = swarm(i, 1, 3) + swarm(i, 2, 3)/1.3; %update z
position
```

```

        swarm(i, 1, 4) = swarm(i, 1, 4) + swarm(i, 2, 4)/1.3; %update h
position
        x = swarm(i, 1, 1);
        y = swarm(i, 1, 2);
        z = swarm(i, 1, 3);
        h = swarm(i, 1, 4);

%===== set the variable x and y constraints=====
        if x < 0.0
            x = 0.0;
        elseif x > 0.15
            x = 0.15;
        end

        if y < -1.57
            y = -1.57;
        elseif y > 1.57
            y = 1.57;
        end
        if z < 0.0
            z = 0.0;
        elseif z > 0.15
            z = 0.15;
        end

        if h < -1.57
            h = -1.57;
        elseif h > 1.57
            h = 1.57;
        end

%===== fitness evaluation =====

        [val,nbus,V,del,BMva]= LFnalysis(x,y,z,h);
        ValMat = [ValMat ; val];

%===== calculate the Pbest =====

        if val < swarm(i, 4, 1)                                % if new position is
better                                                         better
            swarm(i, 3, 1) = swarm(i, 1, 1);                  % update best x,
            swarm(i, 3, 2) = swarm(i, 1, 2);                  % best y postions
            swarm(i, 3, 3) = swarm(i, 1, 3);                  % update best z,
            swarm(i, 3, 4) = swarm(i, 1, 4);                  % best h postions
            swarm(i, 4, 1) = val;                               % and best value

        end
        PBestx = [PBestx; swarm(i, 1, 1)];
        PBesty = [PBesty; swarm(i, 1, 2)];
        PBestz = [PBestz; swarm(i, 1, 3)];
        PBesth = [PBesth; swarm(i, 1, 4)];
    end

%===== calculate the Gbest =====

```

```

[temp, gbest] = min(swarm(:,4, 1));           % global best position

GBest = [GBest; min(swarm(i,4,1))];

%===== updating velocity vectors=====

for i = 1 : SwarmSize
    swarm(i, 2, 1) =W*swarm(i, 2, 1) + C1*rand*(swarm(i, 3, 1) -
swarm(i, 1, 1))...
    + C2*rand*(swarm(gbest, 3, 1) - swarm(i, 1, 1));    %X
velocity component
    swarm(i, 2, 2) =W*swarm(i, 2, 2) + C1*rand*(swarm(i, 3, 2) -
swarm(i, 1, 2))...
    + C2*rand*(swarm(gbest, 3, 2) - swarm(i, 1, 2));    %y
velocity component

    swarm(i, 2, 3) =W*swarm(i, 2, 3) + C1*rand*(swarm(i, 3, 3) -
swarm(i, 1, 3))...
    + C2*rand*(swarm(gbest, 3, 3) - swarm(i, 1, 3));    %z
velocity component
    swarm(i, 2, 4) =W*swarm(i, 2, 4) + C1*rand*(swarm(i, 3, 4) -
swarm(i, 1, 4))...
    + C2*rand*(swarm(gbest, 3, 4) - swarm(i, 1, 4));    %h
velocity component
end

%===== velocity constraints=====

for i=1:SwarmSize
    if swarm(i, 2 ,1)> 0.5*swarm(i,3,1)
        swarm(i,2,1)= 0.5*swarm(i,3,1);
    end
    if swarm(i,2,1)<-0.5*swarm(i,3,1)
        swarm(i,2,1)= -0.5*swarm(i,3,1);
    end

    if swarm(i, 2 ,2)>0.5*swarm(i,3,2)
        swarm(i,2,2)= 0.5*swarm(i,3,2);
    end

    if swarm(i,2,2)<- 0.5*swarm(i,3,2)
        swarm(i,2,2)= - 0.5*swarm(i,3,2);
    end
    if swarm(i, 2 ,3)> 0.5*swarm(i,3,3)
        swarm(i,2,3)= 0.5*swarm(i,3,3);
    end
    if swarm(i,2,3)<-0.5*swarm(i,3,3)
        swarm(i,2,3)= -0.5*swarm(i,3,3);
    end

    if swarm(i, 2 ,4)>0.5*swarm(i,3,4)
        swarm(i,2,4)= 0.5*swarm(i,3,4);
    end

    if swarm(i,2,4)<- 0.5*swarm(i,3,4)

```



```

        swarm(i,2,4)= - 0.5*swarm(i,3,4);
    end
end
%===== Plotting the swarm =====

clf
%     subplot(4,1,1)
%     plot(PBestx, 'x') ; % drawing swarm movements
%     xlabel('Number of Generation');
%     ylabel('Voltage');
%     title('Voltage movements');
% %     axis([0 100 0.005 0.12]);
%
%     subplot(4,1,2)
%     plot(PBesty, 'x') ; % drawing swarm movements
%     xlabel('Number of Generation');
%     ylabel('angle');
%     title('Angle movements');
% %     axis([0 100 -1.6 1.6]);
%
%     subplot(2,1,1)
%     plot(swarm(:, 1, 1),swarm(:, 1, 2),'x')
%     xlabel('Number of Generation')
%     ylabel('Losses')
% %     axis([0 2.50 -15 15]);
%
%     subplot(1,1,1)
%     plot(GBest)
%     xlabel('Number of Iteration');
%     ylabel(' PLoss (MW) ');
%     axis([0 100 0 20]);

    pause(.01)
end

loadflow(nbus,V,del,BMva);          % Calling Loadflow.m..
toc

```